DOCTOR OF PHILOSOPHY

Fault detection and diagnosis and unknown input reconstruction based on parity equations concept

Sumislawska, Malgorzata

Award date:
2012

Awarding institution:
Coventry University

Fault detection and diagnosis and unknown input reconstruction based on parity equations concept

Małgorzata Sumisławska

MSc Teleinformatics, MSc Control Engineering

October 2012

A thesis submitted in partial fulfilment of the University's requirements for the degree of Doctor of Philosophy.

Control Theory and Applications Centre

Coventry University

Abstract

There are two main threads of this thesis, namely, an unknown (unmeasurable) input reconstruction and fault detection and diagnosis. The developed methods are in the form of parity equations, i.e. finite impulse response filters of the available input and output measurements.

In the first thread the design of parity equations for the purpose of an unknown input reconstruction of linear, time-invariant, discrete-time, stochastic systems is taken into consideration. An underlying assumption is that both measurable system inputs as well as the outputs can be subjected to noise, which leads to an errors-in-variables framework. The main contribution of the scheme is accommodation of the Lagrange multiplier method in order to minimise the influence of the noise on the unknown input estimate. Two potential applications of the novel input reconstruction method are proposed, which are a control enhancement of a hot strip steel rolling mill and an estimation of a pollutant level in a river.

Furthermore, initial research is conducted in the field of the unknown input reconstruction for a class of nonlinear systems, namely, Hammerstein-Wiener systems, where a linear dynamic block is preceded and followed by a static nonlinear function. Many man-made as well as naturally occurring systems can be accurately described using Hammerstein-Wiener models. However, it is considered that not much attention has been paid to Hammerstein-Wiener systems in the errors-in-variables framework and in this thesis it is aimed to narrow this gap.

The second thread considers a problem of robust (disturbance decoupled) fault detection as well as fault isolation and identification. Unmeasurable external stimuli, parameter variations or discrepancies between the system and the model act as disturbances, which can obstruct the fault detection process and lead to false alarms. Thus, a fault detection filter needs to be decoupled from the disturbances. In this thesis the right eigenstructure assignment method used for the robust fault detection filter design is extended to systems with unstable invariant zeros. Another contribution regards the design of robust parity equations of any arbitrary order using both left and right eigenstructure assignment. Furthermore, a parity equation-based fault isolation and identification filter is designed which provides an estimate of the fault. A simple method for the calculation of thresholds whose violation indicates a fault occurrence is also proposed for the errors-in-variables framework.

Acknowledgements

Firstly, I would like to express my gratitude towards my Director of Studies, Prof Keith J. Burnham and my supervisor Dr Tomasz Larkowski for their support and encouragement during this project. I would like to acknowledge Dr Leszek Koszałka and Dr Iwona Poźniak-Koszałka for enabling me the initial opportunity to study at the Control Theory and Applications Centre. I would also like to give my special thanks to Ivan Zajíc, Prof Peter Young, Dr Gerald Hearns, Dr Peter Reeve, and Prof Ron J. Patton for inspiring discussions and their valuable comments.

Contents

Nomenclature

Abbreviations

AO-PE-UIO-HW	adaptive order parity equations-based unknown input observer for Hammerstein-Wiener systems
ARMAX	autoregressive model with moving average and exogenous input
ARX	autoregressive model with exogenous input
cf.	confer (compare)
DC	direct current
DRFDF	deadbeat robust fault detection filter
e.g.	exempli gratia (for example)
EIV	errors-in-variables
INPEST	input estimation (input reconstruction method)
LMI	linear matrix inequalities
MIMO	multiple-input multiple-output
MVU	minimum variance unbiased (MVU) state and input estimator
NMSS	non-minimum state-space
OE	output error model
PE	parity equations
PE-UIO	parity equations-based unknown input observer
PE-UIO-HW	parity equations-based unknown input observer for Hammerstein-Wiener systems
PIP	proportional integral plus
PIP-LQ	proportional integral plus linear quadratic
RFDF	robust fault detection filter
SISO	single-input single-output
SVF	state variable feedback

Notation

Latin variables

a_i	autoregressive parameter in polynomial model
A	state transition matrix in state-space model
A_{c_1}, A_{c_2}	filter state transition matrices
A_p	piston area (in steel rolling mill model)
$A_\lambda, A_e^*, A_e^{*(i)}, A_w$	auxiliary matrices
$\tilde{\tilde{A}}, \tilde{A}, A'$	auxiliary matrices
$b(t)$	auxiliary vector

b_i	exogenous parameter in polynomial model
B	input matrix of known input in state-space model
$\tilde{\tilde{B}}$	auxiliary matrix
c_i	moving average parameter in ARMAX model
C	output matrix in state-space model or compensation variable in steel rolling mill model
C'	auxiliary matrix
$d(t)$	disturbance signal
d_1, d_2, d_2	damping coefficients (in steel rolling mill model)
$d_i(t)$	i^{th} element of $d(t)$
$d^*(t)$	$d(t)$, whose elements, $d_i(t)$, are delayed, respectively by δ_i
D	feedforward matrix of known input in state-space model
$e(t)$	noise term
e	matrix of directions of elements of $d(t)$
e_i	direction of $d_i(t)$
$\bar{e}$	matrix built from matrices $\bar{e}_i$
$\bar{e}_i$	matrix whose image is sum of image of e_i and images of invariant zero directions of (A, e_i, C)
E	input matrix of disturbance signal in state-space model
E_i	i^{th} column of input matrix of disturbance signal in state-space model
$f(\cdot)$	function to be minimised by the Lagrange multiplier method
f	matrix of directions of elements of $\mu(t)$
f_i	direction of μ_i
$\bar{f}$	matrix built from matrices $\bar{f}_i$
$\bar{f}_i$	matrix whose image is sum of image of f_i and images of invariant zero directions of (A, f_i, C)
F	input matrix of fault signal in state-space model
$F_c(t)$	Coulomb friction (in steel rolling mill model)
$F_{fric}(t)$	total friction force (in steel rolling mill model)
$F_h(t)$	hydraulic force (in steel rolling mill model)
F_i	i^{th} column of F
$F_r(t)$	roll force (in steel rolling mill model)
$F_s(t)$	Stribeck friction (stiction) in steel rolling mill model
$F_v(t)$	viscous friction (in steel rolling mill model)
$g(\cdot)$	constraint function in the Lagrange multiplier method
g, g_i	auxiliary scalar
G	input matrix of unknown input in state-space model
G_1, G_2	controller gains (in steel rolling mill model)
G'	auxiliary matrix
$G_u(z)$	z-domain transfer function between $u_0(t)$ and $y(t)$
$G_v(z)$	z-domain transfer function between $v(t)$ and $y(t)$
$G'_v(z)$	auxiliary transfer function
$h(t)$	exit gauge (in steel rolling mill model)
$\hat{h}(t)$	estimate of exit gauge (in steel rolling mill model)

$h_{ref}(t)$	exit gauge reference signal (in steel rolling mill model)
$H(t)$	input gauge (in steel rolling mill model)
H	feedforward matrix of unknown input in state-space model
H'	auxiliary matrix
J, J_1, J_2	gain matrices
k_1, k_2	spring constants (in steel rolling mill model)
k_3	steel strip spring constant (in steel rolling mill model)
$K(t)$	gain matrix (used by MVU)
K, K_1, K_2, K' ...	gain matrices
K_c	hydraulic oil compressibility coefficient (in steel rolling mill model)
K_p	proportional gain of hydraulic piston controller (in steel rolling mill model)
l	stroke length of the piston (in steel rolling mill model)
l_j, l_j^*	transposes of left eigenvectors of filter state transition matrix
m	number of system outputs
m_1	mass of hydraulic piston (in steel rolling mill model)
m_2	mass of backup roll (in steel rolling mill model)
m_3	mass of work roll (in steel rolling mill model)
M	mill modulus (spring constant) in steel rolling mill model
$\hat{M}$	estimated mill modulus (in steel rolling mill model)
$M_v(z)$	auxiliary transfer function
$M(t)$	auxiliary matrix (used by MVU) or stacked vector of last $\tau + 1$ values of $\mu(t)$ (depending on context)
n	order of the system
n_a	order of autoregressive polynomial
n_b	order of exogenous polynomial
n_c	order of moving average polynomial
$N_v(z)$	auxiliary transfer function
p	number of known inputs to a system
$p(t)$	hydraulic pressure (in steel rolling mill model)
p_i	element of vector P
P	auxiliary vector or matrix
$P(\lambda_i)$	auxiliary function of eigenvalue λ_i
$P_{l,k}$	auxiliary term
$P^x(t)$,$P^d(t)$.....	submatrices of state and input estimation error covariance matrix
$P^{dx}(t)$,$P^{xd}(t)$...	submatrices of state and input estimation error covariance matrix
q	number of disturbance signals
$q_f(t)$	fluid flow to hydraulic capsule (in steel rolling mill model)
Q	block Toeplitz matrix or gain matrix (depending on context)
$\tilde{Q}$	covariance matrix of $\xi(t)$
r	number of fault signals
$r(t)$	residual
$r_i(t)$	i^{th} element of $r(t)$

r_q	number of rows of Q
R	covariance matrix of $\zeta(t)$ or an auxiliary matrix (depending on context)
$\tilde{R}$	covariance matrix (used in MVU)
s	parity space order
S	auxiliary matrix
T	block Toeplitz matrix or similarity transformation matrix (depending on context)
T_1, T_2	submatrices of the similarity transformation matrix T
T'	auxiliary matrix
$u_0(t)$	noise-free known input
$u(t)$	measured input
$\tilde{u}(t)$	input measurement noise
$\tilde{u}^*(t)$	auxiliary variable
$\bar{u}_0(t)$	input to linear dynamic block in Hammerstein-Wiener system
$\tilde{\bar{u}}(t)$	estimation error of $\bar{u}_0(t)$
$U_0(t)$	stacked vector of last $s+1$ values of $u_0(t)$ (used in parity equations)
$U_0(z)$	$u_0(t)$ in z-domain
$U(t)$	stacked vector of last $s+1$ values of $u(t)$ (used in parity equations)
$U(z)$	$u(t)$ in z-domain
$\tilde{U}(t)$	stacked vector of last $s+1$ values of $\tilde{u}(t)$ (used in parity equations)
$\tilde{U}(z)$	$\tilde{u}(t)$ in z-domain
$\tilde{U}^*(t)$	stacked vector of last $s+1$ values of $\tilde{u}^*(t)$ (used in parity equations)
$\tilde{U}^*(z)$	$\tilde{u}^*(t)$ in z-domain
$\tilde{\bar{U}}(t)$	stacked vector of last $s+1$ values of $\tilde{\bar{u}}(t)$
$v(t)$	unknown (unmeasurable) input
v_c, v_1, v_2	auxiliary friction coefficients (in steel rolling mill model)
$v, v_j, v_j^{(i)}$	auxiliary vectors
V_e	matrix whose columns are eigenvectors of filter state transition matrix
$V(t)$	stacked vector of last $s+1$ values of unknown input (used in parity equations)
$V(z)$	$v(t)$ in z-domain
$\hat{v}(t)$	unknown input estimate
$\hat{V}(z)$	$\hat{v}(t)$ in z-domain
$v'(t)$	auxiliary variable
$V'(t)$	stacked vector of last $s+1$ values of $v'(t)$ (used in parity equations)
$V'(z)$	$v'(t)$ in z-domain
w_{q_i}, w_{ξ_i}	auxiliary polynomial parameters
$w_j, w_j^{(i)}, w_j'^{(i)}$ ...	right eigenvectors of filter state transition matrix
w_j^*	auxiliary vector
W	vector, which belongs to $\Gamma^\perp$ or auxiliary matrix (depensing on context)
W_u, W_y	parity matrices
$W(z)$	polynomial of z-variable defined by appropriate elements of W
$W_Q(z)$	polynomial of z-variable defined by appropriate elements of WQ
$W_T(z)$	polynomial of z-variable defined by appropriate elements of WT
$W_{T'}(z)$	polynomial of z-variable defined by appropriate elements of WT'
$W_\Xi(z)$	polynomial of z-variable defined by appropriate elements of $W\Xi$

$x(t)$	state vector instate space model
$\hat{x}(t)$	state estimate
$x_{i,j}$	auxiliary scalars
X	auxiliary matrix
$y_0(t)$	noise-free output in output-error case
$y(t)$	measured output
$\tilde{y}(t)$	output measurement noise
$\bar{y}_0(t)$	output of linear dynamic block
$\tilde{\bar{y}}(t)$	estimation error of $\bar{y}_0(t)$
$\bar{Y}_0(t)$	stacked vector of last $s+1$ values of $\bar{y}_0(t)$
$Y(t)$	stacked vector of last $s+1$ values of measured output (used in parity equations)
$\tilde{\bar{Y}}(t)$	stacked vector of last $s+1$ values of $\tilde{\bar{y}}(t)$
$Y_0(t)$	stacked vector of last $s+1$ values of noise-free output (used in parity equations)
$\tilde{Y}(t)$	stacked vector of last $s+1$ values of $\tilde{y}(t)$
$Y(z)$	$y(t)$ in z-domain
$z(t)$	position of the hydraulic piston (in steel rolling mill model)
z_i	system zero
$z_i(t)$	state estimate
$z_{ref}(t)$	hydraulic piston position reference signal (in steel rolling mill model)

Greek variables

α_i, α_i'	auxiliary parameters
β_i	i^{th} diagonal element of Σ in multiple output OE case or auxiliary parameter
χ	auxiliary vector
δ	system delay
δ_i	auxiliary term
$\epsilon(t)$	auxiliary noise term
$\epsilon^*(t)$	auxiliary noise term
$\phi_u(t), \phi_y(t)$	auxiliary variance terms
$\varphi(\cdot)$	Hammerstein nonlinearity
γ	row vector of $\Gamma^\perp$
Γ	extended observability matrix
$\Gamma^\perp$	left nullspace of Γ
$\eta(\cdot)$	Wiener nonlinearity
$\eta^{-1}(\cdot)$	inverse of $\eta(\cdots)$
κ	auxiliary scalar
λ	Lagrange multiplier
$\lambda_j, \lambda_j^{(i)}$	eigenvalue of filter state transition matrix
Λ_e	diagonal matrix whose diagonal elements are eigenvalues of filter state transition matrix
$\mu(t)$	fault signal
μ_c	Coulomb friction level (in steel rolling mill model)
$\mu_i(t)$	i^{th} element of fault signal
μ_s	Stribeck friction coefficient (in steel rolling mill model)
μ_v	viscous friction coefficient (in steel rolling mill model)
$\hat{\mu}(t)$	estimate of fault signal

ν	input derivative weighting
$\Theta^{(i)}, \bar{\Theta}^{(i)}$	auxiliary matrices
Π	input matrix of noise term in state-space model
Ω	feedforward matrix of noise term in state-space model or set of all invariant zeros of (A, e, C) depending on context
Ω_i	set of all invariant zeros of (A, e_i, C)
Σ,Σ_e, $\Sigma_{\tilde{u}}$, $\Sigma_{\tilde{u}e}$	covariance matrices
$\Sigma_{\tilde{u}}, \Sigma_{\bar{\mu}}$	covariance matrices
τ	unknown input estimation lag, convergence time of finite time-convergent state observer
$\xi(t)$	process noise vector in state space model
Ξ	block Toeplitz matrix
ψ	auxiliary vector
Ψ	auxiliary matrix
$\Xi(t)$	auxiliary matrix
$\zeta(t)$	output noise vector in state space model

Operators and symbols

$\in$	element in
$\cup$	union of two sets or subspaces
$\setminus$	difference of two sets or subspaces
$\cap$	intersection of two sets or subspaces
$\subset$	a subset of
$\subseteq$	a subset or equal to
$\oplus$	direct sum
$\mathbb{R}^{m\times n}$	$m \times n$ dimensional space of real numbers
$\arg\min f(x)$	value of x that minimises $f(x)$
$\text{rank}(M)$	rank of matrix M
$\text{E}\{\cdot\}$	expected value operator
M^T	transpose of matrix M
M^{-1}	inverse of matrix M
$M^{}$	Moore-Penrose pseudo inverse of matrix M
$M^{\perp}$	nullspace of matrix M
$\mathcal{V}^{\perp}$	orthogonal completion of subspace $\mathcal{V}$
$\text{Im}\{A\}$	image of A
$\text{Ker}\{A\}$	kernel of A
$\text{round}(q)$	rounding of the scalar q to the nearest natural number
$\text{span}\{A\}$	subspace spanned by A
$\text{sum}_{\text{row}}(A)$	column vector whose elements are sums of the appropriate rows A
$\text{var}(e(t))$	variance of $e(t)$
z^{-1}	backward shift operator

List of Algorithms

Chapter 1

Introduction, motivation and outline of approach

1.1 Introduction and motivation

Safety considerations provided an essential objective for motivating the research on fault detection and diagnosis. As air travel became popular, and plans of the first manned space missions were made, it became crucial to ensure safety of the people on board in the case of malfunction. It was important to isolate a fault and handle it accurately. Early analogue methods for fault detection in DC power systems for aircrafts have been presented in (Kaufmann & Finison 1952). Then, a decade later an automated take-off monitoring system for an aircraft was patented by Craddock (1962). 1960s were times of the first space missions, which boosted research on methods for fault detection and location of faults (Janis 1963, Mast, Mayper & Pilnick 1966). In the 1970s fault accommodation in a spacecraft (i.e. reconfiguration of the control system such that safety of operation can be achieved in the presence of a fault) has been proposed (Kennedy 1970).

Another field where fault diagnosis is crucial for the safety of operators is a nuclear reactor, for which safety control apparatus has been developed, among others, in (Dever 1960). Garrick, Gekler, Goldfisher, Karcher, Shimizu & Wilson (1967) proposed a fault detection method using logic gates for a nuclear reactor. Gradually, as computational power became more available, application of fault diagnosis to other industrial processes has been considered. Lee (1962) proposed a method that can locate faults in a 555-transistor digital system. Halton (1963) proposed an automated checkout of a drone. (In the 1960's the term 'checkout' has been widely used for fault diagnosis.) A design of software for an automated checkout has been summarised in (Jirauch 1967).

A breakthrough in the fault detection and diagnosis field, which formed a basis for the modern fault detection and diagnosis, was use of the Luenberger state observer (Luenberger 1964) for the purpose of fault diagnosis by Beard (1971) and Jones (1973).

Fault diagnosis schemes based on the so-called Beard-Jones fault detection filter have been in use up to this day in various industrial processes, e.g. chemical batch reactors (Pierria, Paviglianiti, Caccavale & Mattei 2008), satellite attitude control systems (Wang, Jiang & Shi 2008), or gas turbines (Gao, Breikin & Wang 2007).

Another important method which is used up to this day are parity equations (PE), developed independently by Mironovski (1979) and Chow & Willsky (1984). Chan, Hua & Hong-Yue (2006) applied PE for fault diagnosis of DC motors. A recent work of Berriri, Naouar & Slama-Belkhodja (2011) presents a parity space approach for diagnosis of a current sensor electrical system.

Fault detection and diagnosis algorithms are used practically in every industry (Isermann 2005). They are not only used to detect abrupt malfunctions, but also to signal wear and tear of machine parts, hence indicating when particular parts should be replaced and facilitate the maintenance process.

The other topic, which is explored in this thesis, is an unknown (unmeasurable) input reconstruction. Early contributions to this subject can be found in (Dorato 1969, Sain & Massey 1969, Moylan 1977). Approximate input reconstruction has been used in (Fu, Yan, Santillo, Palanthandalam-Madapusi & Bernstein 2009, Fu, Kirtikar, Zattoni, Palanthandalam-Madapusi & Bernstein 2009) for diagnosing aircraft control surfaces. Rocha-Cozatl, Moreno & Vande Wouwer (2012) utilised a continuous-discrete unknown input observer in order estimate unknown variables in phytoplanktonic cultures. Recent work of Czop (2011) presents reconstruction of the passenger vehicle wheel vertical movement under ride conditions.

1.2 Problem statement

1.2.1 Unknown input reconstruction

A system is a real world entity, which can be represented using a mathematical model that describes relationships between system inputs and outputs. Inputs may not only represent external stimuli, but also discrepancies between the model and the real system. Some of the input signals can be measured, some, however, are inaccessible for measurement. A representation of a system with unknown (unmeasurable) inputs is depicted in Fig. 1.1. The aim of the unknown input reconstruction problem is to estimate the unmeasurable inputs to the system based on the known accessible measurements. Methods considered in this thesis assume that the mathematical model of the system is known.

1.2.2 Fault detection and diagnosis

A fault means a malfunction of a system and/or component. A fault detection and diagnosis process can be divided into three stages, which are defined by answers to the following questions:

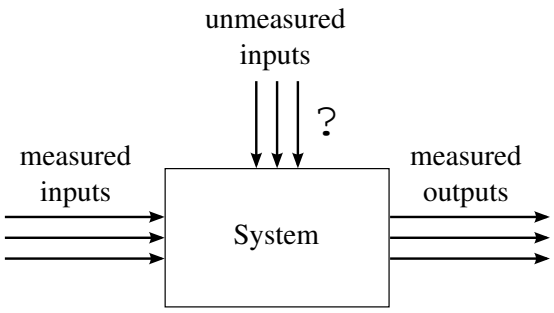

Figure 1.1: Representation of a system with unknown inputs

1. *Is there a malfunction in the system?* If the answer is 'yes', a fault has been detected. Thus, the first stage of the process is called *fault detection*.

2. *Which component is faulty?* Determining, which component is malfunctioning, is referred to as *fault isolation*.

3. *By how much the component is faulty?* Determining the magnitude of the fault is denoted as *fault identification*, i.e. defining the quantity by which the particular system parameter deviated from its acceptable/nominal value.

In the literature fault isolation and identification are often denoted as fault diagnosis. Faults are usually modelled as extra inputs to the system. Thus, a fault diagnosis process can be understood as unknown input estimation.

1.3 Outline of approach

1.3.1 Methodology

Algorithms developed in this thesis are built on existing schemes, by extending/adapting them, by combining two (or more) different methods or by applying a well known scheme for different purposes than originally designed. Proposed algorithms are described in details in a form that allows their straightforward implementation using computer software, e.g. Matlab. For a better understanding of the devised schemes tutorial examples are presented and care is taken to ensure reproducibility of the results. A benchmark comparison of some of the proposed algorithms with examples from the literature is also provided where possible.

A review of well known methods existing in the literature, on which the schemes proposed in this thesis are built, is given in the review Chapter 2. Furthermore, Chapters 3–6 start with a short literature review on the particular topic that each of the chapters explores. All abbreviations and nomenclature used throughout this thesis are given in a separate section at the beginning of the thesis. Some of the terms have different meanings depending on the context in which they are used. Therefore, for

completeness, at the beginning of Chapters 2–7 the nomenclature used in the particular chapter is provided. Additionally, Chapters 3–7 start with an indication of a preliminary reading from specific sections of this thesis. Outlines of following chapters are provided in Subsection 1.3.2.

1.3.2 Outlines of chapters

Chapter 2: The aim of this chapter is to review available methods for unknown input reconstruction and fault detection and diagnosis, which are the bases for algorithms developed in further chapters. Firstly, the notation for the system representation used throughout this thesis is provided. Then, unknown input reconstruction methods are reviewed and two schemes are presented, which are further used as benchmarks for the novel scheme developed in Chapter 3. Furthermore, the nomenclature used for fault detection and diagnosis is provided and well known methods for robust fault detection and isolation are presented, which forms a basis for development of algorithms in Chapters 5–6.

Chapter 3: In this chapter a method for unknown (unmeasurable) input reconstruction is proposed, i.e. parity equation-based unknown input observer (PE-UIO). The algorithm is devised for systems that are subjected to process and measurement noise in the errors-in-variables (EIV) framework, i.e. the known input is affected by white, Gaussian, zero-mean independent and identically distributed (i.i.d.) noise sequences, whereas the output is subjected to coloured noise. PE are used for the purpose of an unknown input reconstruction with a Lagrange multiplier method utilised to find an optimal solution minimising the effect of noise on the unknown input estimate. The order of the parity space is a tuning parameter which allows adjustment of the bandwidth and, hence, noise filtering properties of the filter. The efficacy of the novel scheme is compared with those of two known methods, namely, minimum variance unbiased (MVU) state and input estimator, see (Gillijns & De Moor 2007*b*), and input estimation (INPEST), see (Young & Sumisławska 2012).

Chapter 4: This chapter builds on the algorithm developed in Chapter 3. The unknown input reconstruction method is extended to a class of nonlinear systems, namely Wiener-Hammerstein systems, where a linear dynamic block is preceded and followed by a memoryless nonlinear function. Similarly, as in Chapter 3, an EIV framework is considered. Due to nonlinearities, the impact of the noise on the unknown input estimate depends on the values of the known input and output themselves, and is changing over time. Therefore, an adaptation scheme is devised, which allows adjustment of the order of the parity space (and, consequently, the filter bandwidth) based on the change of the measured input and output.

Chapter 5: There are two main outcomes of this chapter: firstly, the robust fault detection filter based on right eigenstructure is extended to systems with unstable invariant zeros, which extends the applicability of the aforementioned scheme. It is also demonstrated that the devised algorithm is computationally simpler than that of Chen & Speyer (2006*a*). Then, a robust PE of user-defined order is designed using right and left eigenstructure assignment. In order to obtain an open-loop solution (i.e. equivalent to PE) a finite time convergent state observer is utilised. The disturbance decoupling property of the novel scheme is proven algebraically and its efficacy is shown using a numerical example.

Chapter 6: This chapter builds on Chapter 5. Decoupling properties of the robust PE designed in Chapter 5 are used to devise a fault isolation and identification filter, which generates an estimate of the fault signal.

Chapter 7: Practical applications of the algorithms developed in Chapter 3 are proposed. The PE-based unknown input reconstruction scheme is used to improve control performance of a simulated single stand of a steel rolling mill. Furthermore, it is proposed to apply the unknown input reconstruction algorithm to a hydrological application.

Chapter 8: In this chapter concluding remarks are given and proposals for further work are stated.

A structural representation of the flow of developments carried out in this thesis is depicted in Fig. 1.2.

1.4 Contributions

Contributions of the author are listed in descending order with respect to their considered relative significance.

1. *Parity equation-based unknown input reconstruction for linear stochastic systems:* The main contribution of the scheme is use of the Lagrange multiplier method to find optimal filter parameters such that the effect of noise on the unknown input estimate is minimised. The parity equation-based unknown input observer (PE-UIO) has been originally developed in [1][1] for systems with a single output in an output error (OE) case (i.e. when the output of the system is subjected to white, Gaussian, zero-mean noise). Then, in [2] and [3], the method has been extended for systems in the EIV framework, i.e. when both input and output are affected by white, Gaussian, zero-mean, and mutually uncorrelated noise sequences. Then, in [4], the scheme has been extended to a multivariable case.

[1]Note that the references in square brackets are the publications of the author.

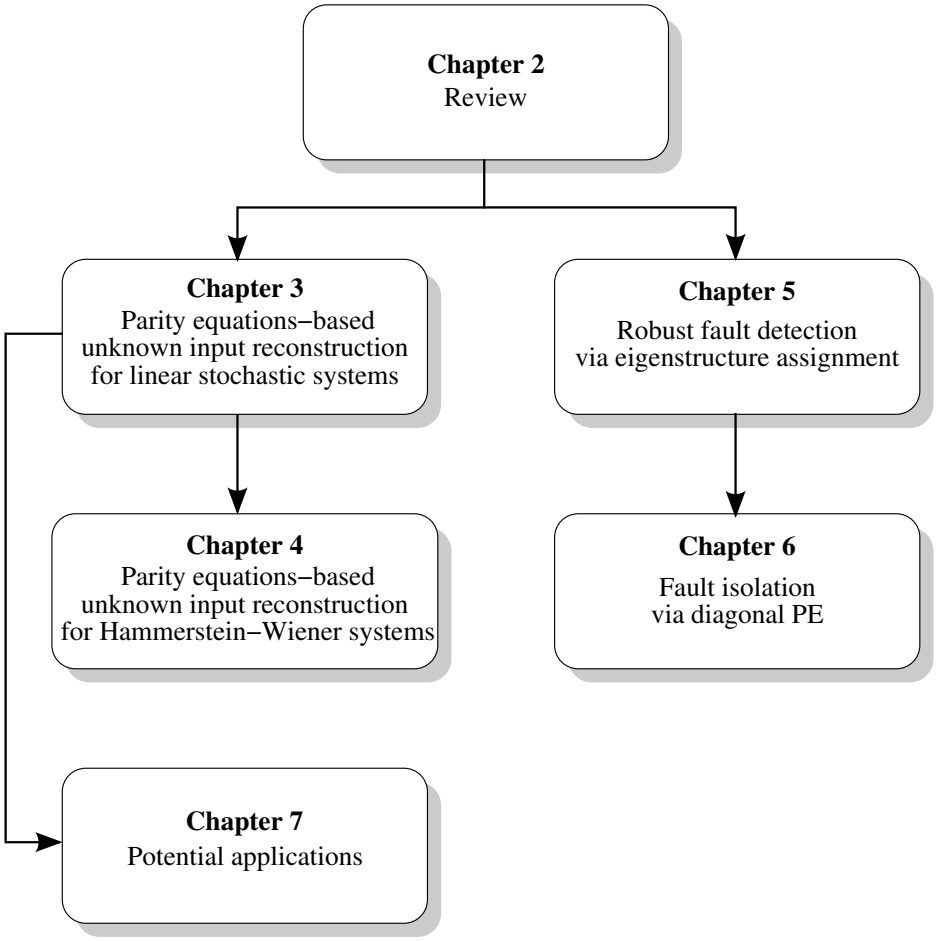

Figure 1.2: Structural representation of a logical flow of developments of this thesis

[1] Sumisławska, M., Burnham, K. J., Larkowski, T., Design of unknown input estimator of a linear system based on parity equations. In *Proc. of the 17th International Conference on Systems Science*, pages 81–90, Wroclaw, Poland, September 2010

[2] Sumisławska, M., Larkowski, T., Burnham, K. J., Design of unknown input reconstruction algorithm in presence of measurement noise. In *Proc. of the 8th European ACD2010 Workshop on Advanced Control and Diagnosis*, pages 213–216, Ferrara, Italy, November 2010

[3] Sumisławska, M., Larkowski, T., Burnham, K. J., Design of unknown input reconstruction filter based on parity equations for EIV case. In *Proc. of the 18th IFAC World Congress*, pages 4272–4277, Milan, Italy, 2011

[4] Sumisławska, M., Larkowski, T., Burnham, K. J., Parity equations-based unknown input estimator for multiple-input multiple-output linear systems. *Systems Science*, 36(3):49–56, 2010

2. *Extension to of the PE-UIO to Wiener-Hammerstein systems:* The PE-UIO has

been extended to a class of nonlinear systems, where the system consists of a linear dynamic block preceded and followed by nonlinear static functions.

[5] Sumisławska, M., Larkowski, T. and Burnham, K. J., Unknown input reconstruction observer for Hammerstein-Wiener systems in the errors-in-variables framework. In *Proc. of the 16th IFAC Symposium on System Identification*, pages 1377–1382, Brussels, Belgium, 2012.

3. *Enhancement of the control performance of a steel rolling mill:* The control of a single finishing stand in a steel rolling mill is affected by a friction force. Strongly nonlinear properties of the friction force and its positive feedback in the control loop lead to oscillations which affect the quality of the final product. It is proposed here to estimate the friction force using PE and feed it back to the controller. As a result of the compensation, significant reduction of the amplitude of oscillations has been demonstrated in a simulation study.

[6] Sumisławska, M., Burnham, K. J., Hearns, G., Larkowski, T., Reeve, P. J., Parity equation-based friction compensation applied to a rolling mill. In *Proc. of the UKACC International Conference on Control*, pages 1043–1048, Coventry, UK, September 2010

4. *Robust fault detection based on eigenstructure assignment:* Chen & Patton (1999) have shown that a special case of the robust fault detection filter based on left eigenstructure assignment is equivalent to first order PE. Also up to date the link between the right eigenstructure assignment-based robust fault detection filter and PE has not been derived. The main contribution of [7] and [8] is the design of robust PE of an arbitrary order using, respectively, right and left eigenstructure assignment.

[7] Sumisławska, M., Larkowski, T., Burnham, K. J., Design of parity equations using right eigenstructure assignment. In *Proc. of the 21st International Conference on Systems Engineering*, pages 367–370, Las Vegas, USA, August 2011

[8] Sumisławska, M., Larkowski, T. and Burnham, K. J., Design of robust parity equations of user-defined order using left eigenstructure assignment. In *Proc. of the 9th European Workshop on Advanced Control and Diagnosis*, Budapest, Hungary, November 2011

5. *Extension of the right eigenstructure assignment method to systems with unstable invariant zeros:* Invariant zeros of the residual response to disturbances are unobservable modes of the robust fault detection filter via right eigenstructure assignment, i.e. the invariant zeros of the system become poles of the fault detection filter. Therefore, design of a stable filter becomes impossible when those

zeros are unstable. A solution is proposed in this thesis which allows the design of stable robust fault detection filters for systems with unstable invariant zeros.

6. *Fault isolation and identification based on diagonal PE using right eigenstructure assignment:* This development builds on contributions 4 and 5 above. The right eigenstructure is used to design a PE, whose output is an estimate of the fault vector. A system with multiple faults is considered. The scheme is applicable to systems, whose response to faults contains unstable invariant zeros.

Chapter 2

Review

2.1 Introduction

The purpose of this chapter is to familiarise the reader with the notation and the background knowledge used to develop algorithms in the next chapters. Firstly, the notation of a linear discrete-time time-invariant stochastic system representation and a class of nonlinear systems, namely, block-oriented systems, is provided in, respectively, Section 2.2 and Section 2.3. In Section 2.4 the problem of an unknown input reconstruction is presented. Two methods for a reconstruction of the unknown input signal are presented, which are further used for a benchmark comparison with the algorithms developed in Chapter 3. Section 2.5 provides the nomenclature used in the subject of fault diagnosis as well as describes open- and closed-loop fault detection. Furthermore, in Section 2.6 the problem of a robust (disturbance decoupled) fault detection is reviewed. A closely related fault isolation and identification is presented in Section 2.7. Concluding remarks are given in Section 2.8.

2.2 Linear system representation

The algorithms presented in this thesis are designed for discrete-time time-invariant systems. The schemes proposed in Chapters 3, 5, and 6 are derived for linear systems, whilst the algorithms developed in Chapter 4 are devised for a class of nonlinear systems. The algorithms presented in this thesis utilise a state-space representation of a linear system, see Subsection 2.2.2. The unknown input reconstruction schemes developed in Chapters 3 and 4 are designed for stochastic systems, i.e. those which are subjected to random noise. The notation of a stochastic linear discrete-time time-invariant model is defined in Subsection 2.2.3. State-space representations of known polynomial noise models, see (Ljung 1999), are presented as well. For completeness, a polynomial representation of a linear system is defined in Subsection 2.2.1.

2.2.1 Polynomial representation

Assume that a linear dynamic discrete-time time-invariant multiple-input multiple-output (MIMO) system with p inputs and m outputs is represented by an n^{th} order state-space equation of the following form (Ljung 1999):

$$y(t) = -\sum_{i=1}^{n_a} a_i y(t-i) + \sum_{j=0}^{n_b} b_j u(t-j) \tag{2.1}$$

The terms $u(t) \in \mathbb{R}^p$ and $y(t) \in \mathbb{R}^m$ refer to, respectively, the input and output vectors, whilst n_a and n_b, with $n_a \geq n_b$, are the orders of the auto-regressive and exogenous parameters, respectively, and $a_i \in \mathbb{R}^{m \times m}$ and $b_i \in \mathbb{R}^{m \times p}$ are coefficient matrices.

2.2.2 State-space representation

The algorithms, which are developed within the framework of this thesis utilise the state-space form of a linear system, which is given by:

$$\begin{aligned} x(t+1) &= Ax(t) + Bu(t) \\ y(t) &= Cx(t) + Du(t) \end{aligned} \tag{2.2}$$

where $x(t) \in \mathbb{R}^n$ is the state vector, whilst $A \in \mathbb{R}^{n \times n}$, $B \in \mathbb{R}^{n \times p}$, $C \in \mathbb{R}^{m \times n}$, and $D \in \mathbb{R}^{m \times p}$. A notation (A, B, C, D) is used to refer to the system (2.2). In the case when $D = 0$, the system (2.2) is denoted as (A, B, C). System (2.1) can be described by an observer canonical form of a state-space model (Ljung 1999, Yiua & Wang 2007), where matrices A, B, C, and D are:

$$A = \begin{bmatrix} -a_1 & I & 0 & \cdots & 0 \\ -a_2 & 0 & I & \cdots & 0 \\ \vdots & \vdots & \vdots & \ddots & \vdots \\ -a_{n_a-1} & 0 & 0 & \cdots & I \\ -a_{n_a} & 0 & 0 & \cdots & 0 \end{bmatrix} \quad B = \begin{bmatrix} b_1 - a_1 b_0 \\ b_2 - a_2 b_0 \\ \vdots \\ b_{n_b} - a_{n_b} b_0 \\ -a_{n_b+1} b_0 \\ \vdots \\ -a_{n_a} b_0 \end{bmatrix} \quad C = \begin{bmatrix} I & 0 & \cdots & 0 \end{bmatrix} \quad D = b_0 \tag{2.3}$$

2.2.3 Polynomial and state-space representations of stochastic systems

Consider system (2.2) affected by stochastic noise. A general representation of the system is given by the following set of equations:

$$\begin{aligned} x(t+1) &= Ax(t) + Bu_0(t) + \Pi e(t) \\ y(t) &= Cx(t) + Du_0(t) + \Omega e(t) \\ u(t) &= u_0(t) + \tilde{u}(t) \end{aligned} \tag{2.4}$$

where $\Pi \in \mathbb{R}^{n\times m}$, $\Omega \in \mathbb{R}^{m\times m}$. The terms $u_0(t) \in \mathbb{R}^p$ and $y(t) \in \mathbb{R}^m$ refer to, respectively, the input and output vectors. The term $e(t) \in \mathbb{R}^m$ is a column vector of m zero-mean, white, Gaussian, independent and identically distributed (i.i.d.) noise sequences. The term $\tilde{u}(t) \in \mathbb{R}^p$ is a vector of white, zero-mean, Gaussian i.i.d. noise sequences, which is uncorrelated with $e(t)$. Equation (2.4) is a generalised representation of a linear system and can be simplified in more specific cases, some of which are given below.

Auto-regressive model with moving average and exogenous input (ARMAX)

A MIMO auto-regressive model with a moving average and exogenous input (ARMAX) is given by, see (Ljung 1999, Yiua & Wang 2007):

$$y(t) = -\sum_{i=1}^{n_a} a_i y(t-i) + \sum_{j=0}^{n_b} b_j u(t-j) + \sum_{k=0}^{n_c} c_k e(t-k) \tag{2.5}$$

where $u(t)$ and $y(t)$ are, respectively, the input and output vectors of the system and $e(t)$ is a vector of white, zero-mean, Gaussian, i.i.d. noise sequences. The terms n_a, n_b, n_c, with $n_a \geq n_b$ and $n_a \geq n_c$, are the orders of the auto-regressive, exogenous and moving average parameters, respectively, and $a_i \in \mathbb{R}^{m\times m}$, $b_i \in \mathbb{R}^{m\times p}$ and $c_i \in \mathbb{R}^{m\times m}$ are coefficient matrices. The last component of the right-hand side of (2.5) refers to the moving average (coloured) process noise of the system.

The state-space system matrices (2.2) for the ARMAX model (2.5) in the observer canonical form are given by:

$$A = \begin{bmatrix} -a_1 & I & 0 & \cdots & 0 \\ -a_2 & 0 & I & \cdots & 0 \\ \vdots & \vdots & \vdots & \ddots & \vdots \\ -a_{n_a-1} & 0 & 0 & \cdots & I \\ -a_{n_a} & 0 & 0 & \cdots & 0 \end{bmatrix} \quad B = \begin{bmatrix} b_1 - a_1 b_0 \\ b_2 - a_2 b_0 \\ \vdots \\ b_{n_b} - a_{n_b} b_0 \\ -a_{n_b+1} b_0 \\ \vdots \\ -a_{n_a} b_0 \end{bmatrix} \quad \Pi = \begin{bmatrix} c_1 - a_1 c_0 \\ c_2 - a_2 c_0 \\ \vdots \\ c_{n_c} - a_{n_c} c_0 \\ -a_{n_c+1} c_0 \\ \vdots \\ -a_{n_a} c_0 \end{bmatrix}$$
$$C = \begin{bmatrix} I & 0 & \cdots & 0 \end{bmatrix} \qquad D = b_0 \qquad \Omega = c_0 \tag{2.6}$$

The ARMAX model assumes that the input $u(t)$ is known exactly (there is no noise present on the input variable), hence $\tilde{u}(t) = 0$ and $u(t) = u_0(t)$. Note that an autoregressive model with an exogenous input (ARX) is obtained from an ARMAX model by setting c_i, $i = 1, \cdots, n_c$, to zero.

Output error (OE) model

An OE model assumes, that there is no process noise present in the system, however the noise-free output $y_0(t)$ is subjected to zero-mean, white, Gaussian measurement

noise $e(t)$, see (Ljung 1999):

$$\begin{aligned} y_0(t) &= -\sum_{i=1}^{n_a} a_i y_0(t-i) + \sum_{j=0}^{n_b} b_j u(t-j) \\ y(t) &= y_0(t) + e(t) \end{aligned} \tag{2.7}$$

This case can be modelled by the system representation (2.2), where matrices A, B, C, and D are all given as in the ARMAX case. The matrix Π is null, and Ω is diagonal. Also, there is no noise present on the input variable, hence $\tilde{u}(t) = 0$.

Errors-in-variables (EIV) framework

In the EIV framework, see, for example, (Söderström 2007), all measured variables, i.e. the inputs and outputs of the system, are affected by zero-mean, white, Gaussian, i.i.d. measurement noise sequences. This can be represented by (2.2), where $\tilde{u}(t) \neq 0$, $\Pi = 0$, and Ω is diagonal.

2.2.4 Invariant zeros

An invariant zero of the system (A, B, C, D) is such a value z_i for which the Rosenbrock system matrix, defined as:

$$P(z_i) = \begin{bmatrix} z_i I - A & -B \\ C & -D \end{bmatrix} \tag{2.8}$$

loses its rank (MacFarlane & Karcanias 1976). Two vectors are associated with an invariant zero: the invariant zero state direction $v \in \mathbb{R}^n$ and the invariant zero input direction $g \in \mathbb{R}^p$, which conform the following equation (El-Ghezawi, Billings & Zinober 1983, Patel 1985, Patel & Munro 1982):

$$\begin{bmatrix} z_i I - A & -B \\ C & -D \end{bmatrix} \begin{bmatrix} v \\ g \end{bmatrix} = 0 \tag{2.9}$$

2.2.5 Properties of a linear system in geometric theory

Robust fault detection and fault isolation may be easier to understand if the reader is familiar with the basics of a geometric approach. The aim of this subsection is to demonstrate some geometric properties of linear systems.

Consider a matrix $A \in \mathbb{R}^{n \times m}$. An image of A is defined as a set of all vectors Ax for any arbitrary $x \in \mathbb{R}^m$:

$$\mathrm{Im}\{A\} = \{Ax : \ x \in \mathbb{R}^m\} \tag{2.10}$$

An image of A is sometimes defined as $\mathrm{span}\{A\}$, i.e. the subspace spanned by A, which

is a set of all possible linear combinations of columns of A, i.e.

$$\text{span}\{A\} = \left\{ \sum_{i=1}^{m} \alpha_i A_i : \ \alpha_i \in \mathbb{R} \right\} \tag{2.11}$$

where $A_i, i = 1, \cdots, m$ are columns of A and α_i are arbitrary scalars. The kernel of A is a set of all $x \in \mathbb{R}^m$ for which $Ax = 0$, i.e.

$$\text{Ker}\{A\} = \{x \in \mathbb{R}^m : \ Ax = 0\} \tag{2.12}$$

Denote an n-dimensional space over the field of real numbers as $\mathcal{X}$. Consider a matrix $V \in \mathbb{R}^{n \times k}$, where $k \leq n$. Denote $\mathcal{V} = \text{Im}\{V\}$; then $\mathcal{V}$ is a k-dimensional subspace of the space $\mathcal{X}$. (Note that $\mathcal{X} = \text{Im}\{I\}$.) Consider the following subspaces $\mathcal{V}$, $\mathcal{Y}$, and $\mathcal{Z}$ of vector spaces $\mathbb{R}^n$ and $\mathbb{R}^m$ and a matrix $A \in \mathbb{R}^{m \times n}$. For completeness, basic operations on subspaces are given below (Halmos 1958, Basile & Marro 2002):

1. Sum:
$$\mathcal{Z} = \mathcal{V} + \mathcal{Y} := \{z : z = v + y, v \in \mathcal{V}, y \in \mathcal{Y}\} \tag{2.13}$$

2. Intersection:
$$\mathcal{Z} = \mathcal{V} \cap \mathcal{Y} := \{z : z \in \mathcal{V}, z \in \mathcal{Y}\} \tag{2.14}$$

3. Direct sum:
$$\mathcal{Z} = \mathcal{V} \oplus \mathcal{Y} := \{z : z = v + y, v \in \mathcal{V}, y \in \mathcal{Y}, \mathcal{V} \cap \mathcal{Y} = 0\} \tag{2.15}$$

4. Linear transformation:
$$\mathcal{Y} = A\mathcal{V} := \{y : y = Av, v \in \mathcal{V}\} \tag{2.16}$$

5. Inverse linear transformation:
$$\mathcal{V} = A^{-1}\mathcal{Y} := \{v : y = Av, y \in \mathcal{Y}\} \tag{2.17}$$

6. Orthogonal completion[1]:
$$\mathcal{Y} = \mathcal{V}^{\perp} := \{y : \langle v, y \rangle = 0, v \in \mathcal{V}\} \tag{2.18}$$

[1] In the coordinate-free subspace algebra a product of vectors v and y is usually denoted as $\langle v, y \rangle$. Note that this refers to $v^T y$ in the linear matrix algebra.

Invariant subspaces

Consider a linear transformation matrix $A \in \mathbb{R}^{n \times n}$. A subspace $\mathcal{V}$ is A-invariant if and only if $A\mathcal{V} \subseteq \mathcal{V}$. In other words, there exists such a matrix X that (Halmos 1958):

$$AV = VX \tag{2.19}$$

Note that if X is diagonal, then columns of V are the eigenvectors of A. The invariance has a physical meaning in the linear systems theory. Consider an autoregressive system described by the following equation:

$$x(t+1) = Ax(t) \tag{2.20}$$

It holds that if $x(t) \in \mathcal{V}$, where $\mathcal{V}$ is A-invariant, then $x(t+1) \in \mathcal{V}$. This means that if the system is initialised with $x(0) \in \mathcal{V}$, then the state vector will remain within $\mathcal{V}$.

Reachability and controllability

Reachability and controllability can be defined by means of geometric tools. Consider an autoregressive system with an exogenous input:

$$x(t+1) = Ax(t) + Bu(t) \tag{2.21}$$

Using the notation $\mathcal{B} = \mathrm{Im}\{B\}$, the term $\langle A|\mathcal{B}\rangle = \mathcal{B} + A\mathcal{B} + \cdots + A^{n-1}\mathcal{B}$ is the infimal A-invariant subspace containing $\mathcal{B}$, i.e. the reachable subspace of (A, B). This means that the state trajectory of the system (2.21) driven by the input $u(t)$ can be anywhere within the reachable subspace of (A, B). Furthermore, because $\langle A|\mathcal{B}\rangle$ is A-invariant, the state driven by $u(t)$ cannot leave the reachable subspace of (A, B). Note that, the reachable subspace of (A, B) can be defined as:

$$\langle A|\mathcal{B}\rangle = \mathrm{Im}\{\mathcal{R}\} \tag{2.22}$$

where:

$$\mathcal{R} = \begin{bmatrix} B & AB & \cdots & A^{n-1}B \end{bmatrix} \tag{2.23}$$

is the reachability matrix of the system.

Analogously, observability can be defined using the geometric theory. Consider the following autoregressive system:

$$\begin{aligned} x(t+1) &= Ax(t) \\ y(t) &= Cx(t) \end{aligned} \tag{2.24}$$

Denote the kernel of the matrix C as $\mathcal{K} = \mathrm{Ker}\{C\}$, i.e. $C\mathcal{K} = 0$. Then the unobservable subspace of the system (2.24) is defined as the supremal A-invariant subspace contained

in $\mathcal{K}$ (Massoumnia 1986):

$$\langle \mathcal{K}|A\rangle = \mathcal{K} \cap A^{-1}\mathcal{K} \cap \cdots \cap \mathcal{K}A^{-n+1} \tag{2.25}$$

Note that if the state vector $x(t) \in \mathcal{K}$ then $y(t) = Cx(t) = 0$. Because $\langle \mathcal{K}|A\rangle \subseteq \mathcal{K}$, it holds that $y(t) = Cx(t) = 0$ for any $x(t) \in \langle \mathcal{K}|A\rangle$. Furthermore, due to the fact that $\langle \mathcal{K}|A\rangle$ is A-invariant it holds that $x(t+1) \in \langle \mathcal{K}|A\rangle$ if $x(t) \in \langle \mathcal{K}|A\rangle$, i.e. the state vector stays within $\langle \mathcal{K}|A\rangle$. Thus, if the system (2.24) is initialised with $x(0) \in \langle \mathcal{K}|A\rangle$, then the state vector remains within the unobservable subspace of (A, C) and the output $y(t)$ remains zero.

Now consider the relation between $\langle \mathcal{K}|A\rangle$ and the system observability matrix $\mathcal{O}$:

$$\mathcal{O} = \begin{bmatrix} C \\ CA \\ \vdots \\ CA^{n-1} \end{bmatrix} \tag{2.26}$$

The subspace which is an orthogonal completion of $\langle \mathcal{K}|A\rangle$ is the observable subspace of system (2.24). An orthogonal completion of an intersection of two subspaces, $\mathcal{V}$ and $\mathcal{Z}$, is defined as, cf. Equation (3.1.10) in (Basile & Marro 2002):

$$(\mathcal{V} \cap \mathcal{Z})^{\perp} = \mathcal{V}^{\perp} + \mathcal{Z}^{\perp} \tag{2.27}$$

Hence:

$$\langle \mathcal{K}|A\rangle^{\perp} = \mathcal{K}^{\perp} + \left(A^{-1}\mathcal{K}\right)^{\perp} + \cdots + \left(A^{-n+1}\mathcal{K}\right)^{\perp} \tag{2.28}$$

Note that the orthogonal subspace of $\mathcal{K}$ is $\mathrm{Im}\{C^T\}$. An orthogonal completion of an inverse transformation of a subspace is defined as, see Property 3.1.3 in (Basile & Marro 2002):

$$(A^{-1}\mathcal{V})^{\perp} = A^T\mathcal{V}^{\perp} \tag{2.29}$$

Therefore, it holds that:

$$\begin{aligned} \langle \mathcal{K}|A\rangle^{\perp} = \mathcal{K}^{\perp} + \left(A^{-1}\mathcal{K}\right)^{\perp} + \cdots + \left(A^{-n+1}\mathcal{K}\right)^{\perp} = \mathrm{Im}\{C^T\} + \mathrm{Im}\{A^TC^T\} + \cdots + \\ + \mathrm{Im}\{(A^{n-1})^TC^T\} = \mathrm{Im}\{\begin{bmatrix} C^T & A^TC^T & \cdots & (A^{n-1})^TC^T \end{bmatrix}\} \end{aligned} \tag{2.30}$$

which is an image of the transposed observability matrix $\mathcal{O}$. Consequently, the unobservable subspace of (A,C) is given by:

$$\langle \mathcal{K}|A\rangle = \mathrm{Ker}\,\{\mathcal{O}\} \tag{2.31}$$

Controlled and conditioned invariants

The concept of controlled invariants was introduced in (Basile & Marro 1969, Wohnam & Morse 1970), whilst the concept of conditioned invariance was introduced in (Basile & Marro 1969). Consider a pair (A, B). A subspace $\mathcal{V}$ is an (A, B)-controlled invariant if:

$$A\mathcal{V} \subseteq \mathcal{V} + \mathcal{B} \tag{2.32}$$

This means that there exists such a matrix K that the input $u(t) = Kx(t)$ keeps the state of the system (2.21) within $\mathcal{V}$, i.e. there exists such a K that $(A + BK)\mathcal{V} \subseteq \mathcal{V}$. A dual of the controlled invariant is a conditioned invariant. Consider a pair (A, C). A subspace $\mathcal{S}$ is said to be an (A, C)-conditioned invariant if:

$$A(\mathcal{S} \cap \mathcal{K}) \subseteq \mathcal{S} \tag{2.33}$$

The (A, C)-conditioned invariance means that there exists such a matrix K that $(A - KC)\mathcal{S} \subseteq \mathcal{S}$. For more properties of controlled and conditioned invariants the reader is referred to (Basile & Marro 2002).

Invariant zeros

Consider the following system:

$$\begin{aligned} x(t+1) &= Ax(t) + Bu(t) \\ y(t) &= Cx(t) \end{aligned} \tag{2.34}$$

Denote the minimal (A, C)-conditioned invariant containing $\mathrm{Im}\{B\}$ as $\mathcal{S}_0$ and use the notation $\mathcal{V}_0$ for the maximal (A, B)-controlled invariant contained in $\ker\{C\}$. Consider a matrix V_1 such that $\mathrm{Im}\{V_1\} \cap \mathcal{V}_0 = \mathrm{Im}\{V_1\}$, $\mathrm{Im}\{V_1\} + \mathcal{V}_0 = \mathcal{V}_0$, and $\mathrm{Im}\{V_1\} \cap \mathcal{S}_0 = 0$. Invariant zeros of (A, B, C) are the eigenvalues of the matrix M_1, which fulfils the following equation, see (Basile & Marro 2010):

$$\begin{bmatrix} V_1 & -B \end{bmatrix} \begin{bmatrix} M_1 \\ M_2 \end{bmatrix} = AV_1 \tag{2.35}$$

Using a similarity transformation V_{m_1}, the matrix M_1 can be decomposed as:

$$M_1 = V_{m_1}^{-1} J V_{m_1} \tag{2.36}$$

Equation (2.36) can be, in particular, a Jordan normal decomposition. Consequently, equation (2.35) can be reformulated as:

$$V_1 V_{m_1}^{-1} J V_{m_1} - BM_2 = AV_1 \tag{2.37}$$

By postmultiplying both sides of (2.37) by $V_{m_1}^{-1}$ the following formula is obtained:

$$V_1 V_{m_1}^{-1} J - B M_2 V_{m_1}^{-1} = A V_1 V_{m_1}^{-1} \tag{2.38}$$

Note that if the invariant zeros of (A, B, C) are distinct, the matrix M_1 is diagonalisable, and J is diagonal, equation (2.38) is equivalent to (2.9), where the diagonal elements of J are the invariant zeros of (A, B, C), whilst columns of $V_1 V_{m_1}^{-1}$ and columns of $M_2 V_{m_1}^{-1}$ are, respectively, invariant zeros state and input directions. Therefore, if the invariant zeros of (A, B, C) are distinct, (2.9) is equivalent to (2.35), where $D = 0$. Nevertheless, as opposed to (2.9), Equation (2.35) can be used to determine the number of all of the invariant zeros of the system, including the repeated ones.

In the case when the system contains a feedthrough term, i.e. $D \neq 0$ Basile & Marro (2002) proposed some manipulations to represent the quadruple (A, B, C, D) with a triple. However, the geometric approach is used in this thesis to analyse/design fault detection and isolation filters, where the considered transfer functions between disturbances or faults and the output of the system do not contain any feedthrough term. Thus, for more details on invariant zeros of systems with a feedthrough term the reader is referred to (Basile & Marro 2002).

2.3 Block oriented models

Block-oriented model structures consist of static nonlinearities interconnected with linear dynamic blocks. In the case of a Hammerstein model, see Fig. 2.1(a), a linear block is preceded by a static nonlinear function, whereas in the case of a Wiener model, see Fig. 2.1(c), the order of these elements is reversed (Pearson 1995, Pearson & Pottmann 2000). In the case of a Hammerstein-Wiener model structure, cf. Fig. 2.1(b), a linear dynamic block is preceded and followed by static nonlinearities. A Wiener-Hammerstein model, cf. Fig. 2.1(d), is characterised by two linear dynamic blocks connected via a nonlinear static function (Crama & Schoukens 2004). Furthermore, block-oriented systems can be cascaded creating more complicated structures. Dobrowiecki & Schoukens (2002) studied cascaded Wiener-Hammerstein systems as the one presented in Fig. 2.2.

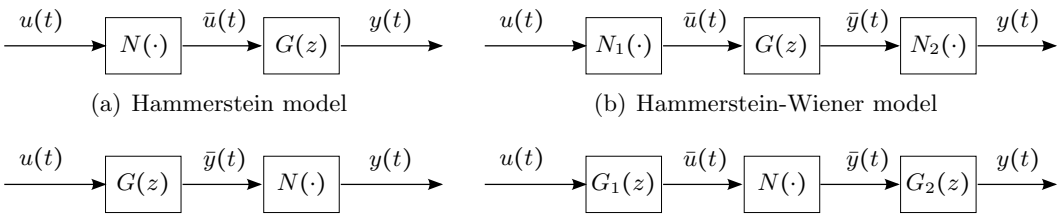

(a) Hammerstein model (b) Hammerstein-Wiener model

(c) Wiener model (d) Wiener-Hammerstein model

Figure 2.1: Block oriented models

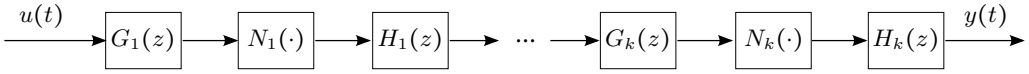

Figure 2.2: Cascade of k Wiener-Hammerstein systems

In order to capture system nonlinearities more accurately, a feedback block-oriented model can be used, see, for example, (Pearson & Pottmann 2000). Different variations of feedback block oriented models (e.g. a sandwich feedback block-oriented model as in Fig. 2.3(b), have been studied in (Pottmann & Pearson 2006).

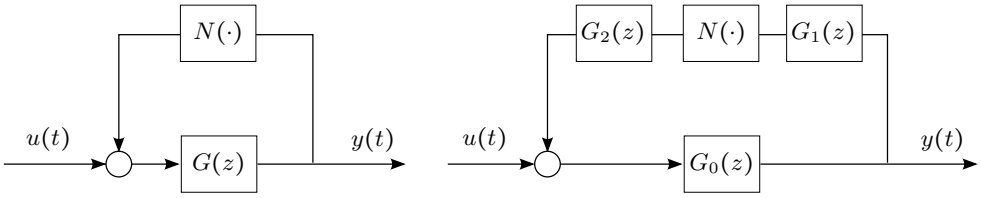

(a) Feedback block-oriented model

(b) Feedback block-oriented model – a sandwich structure

Figure 2.3: Feedback block oriented models

2.4 Unknown input reconstruction

It is assumed that the model of a linear system is known and its output is measurable, however the system is affected by noise. The aim of the unknown input reconstruction process is to estimate the unknown (unmeasurable) input to the system. The most trivial solution to this problem, a naive inversion, is not applicable when any system zero lies outside the unit circle, i.e. the system in nonminimum-phase. Also, due to highpass properties of a naive inversion, it is not preferable when the system is subjected to noise. In this Section two input reconstruction algorithms are presented, which are used as benchmarks for the assessment of the schemes developed in Chapter 3. In Subsection 2.4.1 a minimum variance unbiased (MVU) state and input estimator based on the Kalman filter, see (Gillijns & De Moor 2007*b*), is described. The second method used as a benchmark is the input estimation (INPEST) method presented in Subsection 2.4.2.

2.4.1 MVU state estimator

A Kalman filter-based MVU state and input estimator for systems with a direct feedtrough has been developed by Gillijns & De Moor (2007*b*). The scheme, for completeness, is presented in Algorithm 2.1. The system, for which the MVU has been

designed, is described by (Gillijns & De Moor 2007*b*):

$$\begin{aligned} x(t+1) &= Ax(t) + Gu(t) + \xi(t) \\ y(t) &= Cx(t) + Hu(t) + \zeta(t) \end{aligned} \tag{2.39}$$

where $u(t)$ is a vector of unknown inputs (the number of unknown inputs is lower or equal to the number of outputs), whilst $\xi(t)$ and $\zeta(t)$ are vectors of white, zero-mean, Gaussian, i.i.d. noise sequences.

It is assumed throughout this thesis that the noise distribution is Gaussian (i.e. normally distributed) and zero-mean. Whilst in practice it is known that noise is not necessary Gaussian, it is commonly accepted that a Gaussian assumption is appropriate; offering an approach which, although may no longer be optimal, would be consistent and generalisable, and is applicable to a wide range of situations.

Algorithm 2.1 (MVU).

1. Initialisation

$$\hat{x}(0) = \mathrm{E}\{x(0)\} \tag{2.40a}$$
$$P^x(0) = \mathrm{E}\{(\hat{x}(0) - x(0))\,(\hat{x}(0) - x(0))^T\} \tag{2.40b}$$
$$R = \mathrm{E}\{\zeta(t)\zeta^T(t)\} \tag{2.40c}$$
$$\tilde{Q} = \mathrm{E}\{\xi(t)\xi^T(t)\} \tag{2.40d}$$

2. Estimation of unknown input

$$\tilde{R}(t) = CP^x(t|t-1)C^T + R(t) \tag{2.40e}$$
$$M(t) = \left(H^T\tilde{R}^{-1}H\right)^{-1}H^T\tilde{R}^{-1} \tag{2.40f}$$
$$\hat{u}(t) = M(t)\,(y(t) - C\hat{x}(t|t-1)) \tag{2.40g}$$
$$P^u(t) = \left(H^T\tilde{R}^{-1}H\right)^{-1} \tag{2.40h}$$

3. Measurement update

$$K(t) = P^x(t|t-1)C^T\tilde{R}^{-1} \tag{2.40i}$$
$$\hat{x}(t|t) = \hat{x}(t|t-1) + K(t)\,(y(t) - C\hat{x}(t|t-1) - H\hat{u}(t)) \tag{2.40j}$$
$$P^x(t|t) = P^x(t|t-1) - K(t)\left(\tilde{R}(t) - HP^u(t)H^T\right)K^T(t) \tag{2.40k}$$
$$P^{xu}(t) = \left(P^{ux}(t)\right)^T = -K(t)HP^u(t) \tag{2.40l}$$

4. Time update

$$\hat{x}(t+1|t) = A\hat{x}(t|t) + G\hat{u}(t) \tag{2.40m}$$

$$P^x(t+1|t) = \begin{bmatrix} A & G \end{bmatrix} \begin{bmatrix} P^x(t|t) & P^{xu}(t) \\ P^{ux}(t) & P^v(t) \end{bmatrix} \begin{bmatrix} A^T \\ G^T \end{bmatrix} + \tilde{Q} \tag{2.40n}$$

The MVU requires the knowledge of the covariance matrices of the noise sequences, $\tilde{Q}$ and R, which are the tuning parameters for the algorithm.

Remark 2.1. If the system (2.39) is SISO, the MVU is equivalent to a naive system inversion.

Demonstration. If (2.39) is a SISO system, H and M are scalars and, therefore, $M = H^{-1}$. Incorporating (2.40g) into (2.40j) it follows that:

$$\hat{x}(t|t) = \hat{x}(t|t-1) \tag{2.41}$$

Hence, incorporating (2.40g) into (2.40m):

$$\hat{x}(t+1|t) = (A - MGC)\hat{x}(t|t-1) + MGy(t) \tag{2.42}$$

Consequently, in the SISO case Algorithm 2.1 is equivalent to:

$$\hat{x}(t+1|t) = (A - MGC)\hat{x}(t|t-1) + MGy(t) \tag{2.43a}$$

$$\hat{u}(t) = -MC\hat{x}(t|t-1) + My(t) \tag{2.43b}$$

The gain of the filter (2.43) is equal to the reciprocal of the gain of the system, see (Gillijns & De Moor 2007*b*). Denote any arbitrary zero of the filter (2.43) as z_{mvu}, then the following formula holds, cf. (2.9):

$$\left[\begin{array}{c|c} z_{\text{mvu}}I - A + MGC & -MG \\ \hline -MC & -M \end{array}\right] \begin{bmatrix} \chi \\ \kappa \end{bmatrix} = \begin{bmatrix} 0 \\ 0 \end{bmatrix} \tag{2.44}$$

where a column vector χ denotes the zero state direction and a scalar κ refers to the input zero direction of z_{mvu} (El-Ghezawi et al. 1983). Consequently:

$$(z_{\text{mvu}}I - A)\chi = 0 \tag{2.45}$$

■

which means that z_{mvu} is an eigenvalue of A, whereas χ is its corresponding eigenvector. This means that the zeros of the filter (2.43) are equal to the poles of the system (2.39).

Analogously, it can be demonstrated that the poles of (2.43) are equivalent to the zeros the the system (2.39). Thus, the MVU behaves as a naive inversion in the case when (2.39) is a SISO system.

2.4.2 Input estimation (INPEST) method

The INPEST algorithm has been designed for the input reconstruction of SISO linear systems (Young & Sumisławska 2012). A schematic diagram of the INPEST method is presented in Fig. 2.4. The basic idea of the method is to create a control loop, where the model of the system is controlled in such a way that its output tracks the measured output of the real system (which acts as a reference for the control loop). The output of the controller (i.e. the input to the controlled model) renders the unknown input estimate. The time delay τ is introduced in order to recognise, that the control system

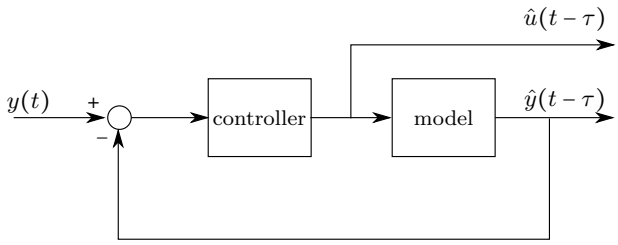

Figure 2.4: Schematic diagram of INPEST method

does not respond instantaneously to the changes in $y(t)$.

The control system utilises the proportional integral plus (PIP) controller design that exploits a non-minimum state-space (NMSS) model of the system (Young, Behzadi, Wang & Chotai 1987). The state vector of the controlled model of the system in the NMSS representation is defined by:

$$x(t) = \begin{bmatrix} \hat{y}(t) & \hat{y}(t-1) & \cdots & \hat{y}(t-n_a+1) & \hat{u}(t) & \hat{u}(t-1) & \cdots & \hat{u}(t-n_b+1) & z(t) \end{bmatrix}^T \tag{2.46}$$

where $z(t)$ is an integral of the tracking error:

$$z(k) = z(k-1) + (y(k) - \hat{y}(k)) \tag{2.47}$$

The PIP controller utilises a state variable feedback (SVF), i.e.

$$\hat{u}(t) = -gx(t) \tag{2.48}$$

where g is the controller gain. The INPEST method makes use of the PIP linear quadratic (PIP-LQ) design, which minimises the cost function defined as:

$$J = \sum_{t=0}^{\infty} \left\{ x^T(t) Q x(t) + r\hat{u}^2(t) \right\} \tag{2.49}$$

where:

$$Q = \mathrm{diag}(\begin{bmatrix} q_y & \cdots & q_y & q_u & \cdots & q_u & q_e \end{bmatrix}) \tag{2.50}$$

and $r = q_u = q_y = 1$, whilst q_e is optimised. In order to find the optimal value of the q_e parameter, denoted $\mathring{q}_e$, and the corresponding estimation delay, $\mathring{\tau}$, the following cost function $\mathcal{J}$ is optimised:

$$\begin{aligned} \{\mathring{q}_e, \mathring{\tau}\} &= \arg\min \mathcal{J}(q_e, \tau) \\ \mathcal{J}(q_e, \tau) &= \sum_{t=\tau+1}^{N} \eta^2(t) + \nu(\Delta\hat{u}(t))^2 \\ \eta(t) &= y(t) - \hat{y}(t-\tau) \\ \Delta\hat{u}(t) &= \hat{u}(t) - \hat{u}(t-1) \end{aligned} \tag{2.51}$$

where ν is a tuning parameter. The reason for penalising the derivative of the reconstructed input signal is that in the case of noisy measurements of $y(t)$ the algorithm would tend to amplify the effects of the disturbance if the rate of change on $\hat{u}(t)$ was not penalised. Note that the only tuning parameter of the INPEST method is the reconstructed input derivative weighting ν.

2.4.3 Efficacy measure of compared algorithms

An efficay index used to assess the ability of the examined algorithms to reconstruct the unmeasurable signal (unknown input) allows one to determine how much of the original signal can be explained by the reconstruction algorithm. For this purpose the following variation of a widely used *coefficient of determination*, denoted R_T^2, see, for example, (Ljung 1999, Young 2011), is utilised:

$$\mathrm{R}_T^2 = \frac{\sum_t (\hat{u}(t) - u(t))^2}{\sum_t u^2(t)} \times 100\% \tag{2.52}$$

where $u(t)$ and $\hat{u}(t)$ refer to, respectively, the unknown input and its estimate. Note that in an ideal case, i.e. when $\hat{u}(t) = u(t)$, $\mathrm{R}_T^2 = 0$ and it increases as the discrepancy between the original and the estimated input increases.

2.5 Introduction to fault detection and diagnosis

In many industrial processes fault detection and diagnosis cannot be spared as it is crucial to maintain smooth operation and safety. Undiagnosed or improperly handled faults can lead to serious consequences, starting from a damage to the product on a production line (financial loss) up to catastrophic events, which can cost lives. Therefore, measures should be taken and algorithms implemented, which can isolate and then deal with (accommodate) the faults. Furthermore, automation and availability of high computational power increases complexity of industrial systems, which become more

vulnerable to faults and hence require a complex monitoring.

An interest in the model-based fault diagnosis started in the early 1970's with observer based fault detection (Beard 1971, Jones 1973). Initially, the terminology in the early fault diagnosis literature was not consistent. In 1991 the SAFEPROCESS (fault detection, supervision, and safety for technical processes) Steering Committee was established (in 1993 it became the Technical Committee), which discussed that matter and formed commonly accepted definitions. Some of the definitions can be found in (*Reliability, Availability, and Maintainability Dictionary* 1988) and (Isermann & Balle 1997). The definitions used throughout this thesis are given in Subsection 2.5.1. Then, the fault detection problem is discussed in Subsection 2.5.2.

2.5.1 Nomenclature

The fault detection and diagnosis terminology used throughout this thesis is given below (Isermann & Balle 1997):

Fault: A deviation of at least one characteristic property or parameter of the system from the acceptable/usual/standard conditions.

Residual: An output of the fault detection/isolation/identification filter. In a fault-free condition the residual is close to zero and it significantly deviates from zero, when a fault occurs.

Fault detection: A binary decision, whether a fault is present in the system. Due to the fact that there is always a certain level of noise in the system a need arises to distinguish, whether the residual deviates from zero due to the noise or due to presence of a fault. This is achieved by setting a threshold whose violation indicates the presence of a fault.

Robust fault detection: A fault detection process which is insensitive to unmeasured disturbances. A robust fault detection filter is designed in such a way that the residuals are insensitive to (decoupled from) disturbances, whilst they are sensitive to faults.

Fault isolation: Determination of the component which deviates from the acceptable/usual/standard condition.

Fault identification: Determination of the magnitude of the fault.

Fault diagnosis: Includes fault isolation and identification, i.e. determination of the source of the fault and the fault magnitude.

2.5.2 Fault detection

Consider a process, which can be described by a linear discrete-time time-invariant model:

$$\begin{aligned} x(t+1) &= Ax(t) + Bu(t) + F\mu(t) \\ y(t) &= Cx(t) + Du(t) \end{aligned} \tag{2.53}$$

where $x(t) \in \mathbb{R}^n$ is the system state vector, $u(t) \in \mathbb{R}^p$ and $y(t) \in \mathbb{R}^m$ are, respectively, the system input and output, and $\mu(t) \in \mathbb{R}^k$ is a fault signal. Matrices A, B, C, D, and F are constant and have appropriate dimensions. The aim of fault detection is to define the time instances t, when $\mu(t) \neq 0$. When both the input and output measurements are available, so-called process-model-based fault detection methods are used for the purpose of residual generation (Isermann & Balle 1997, Simani, Fantuzzi & Patton 2002). These, in particular, are:

1. State and output observers
2. PE
3. Identification and parameter estimation

In this thesis two fault detection methods are considered, which are the state observers and the PE.

State observer (closed-loop fault detection filter)

A schematic illustration of a state observer is presented in Fig. 2.5 and given by the following set of equations (Patton 1997, Chen & Patton 1999, Simani et al. 2002):

$$\begin{aligned} \hat{x}(t+1) &= A\hat{x}(t) + (B - KD)u(t) + K(y(t) - \hat{y}(t)) \\ \hat{y}(t) &= C\hat{x}(t) + Du(t) \\ r(t) &= Q(y(t) - \hat{y}(t)) \end{aligned} \tag{2.54}$$

where K is the observer gain matrix, whilst Q is an arbitrary matrix. (The matrix Q plays an important role in robust fault detection which is described in Section 2.6; in this section, however, without loss of generality it is assumed that Q is an identity matrix.) Consider the state estimation error $\xi(t) = \hat{x}(t) - x(t)$. Then the residual is governed by:

$$\begin{aligned} \xi(t+1) &= (A - KC)\xi(t) + F\mu(t) \\ r(t) &= QC\xi(t) \end{aligned} \tag{2.55}$$

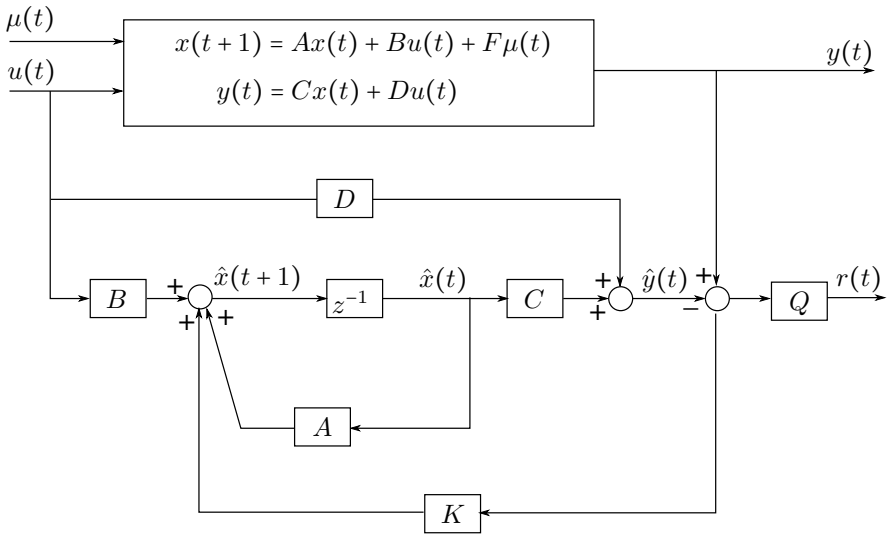

Figure 2.5: State observer-based (closed-loop) fault detection filter

Therefore, in order to detect an occurrence of a fault, the z-transform transfer function of the residual response to the fault, denoted as $G_{\mu r}(z)$ must be non-zero, i.e.

$$G_{\mu r}(z) = QC(Iz - A + KC)^{-1}F \neq 0 \tag{2.56}$$

Parity equations (open-loop fault detection filter)

PE are widely used for the purpose of fault detection and isolation, see, for example, (Chow & Willsky 1984, Gertler & Singer 1990, Li & Shah 2002). A schematic illustration of PE is presented in Fig. 2.6. As opposed to the observer-based (closed-loop) fault detection filters, PE have an open-loop structure.

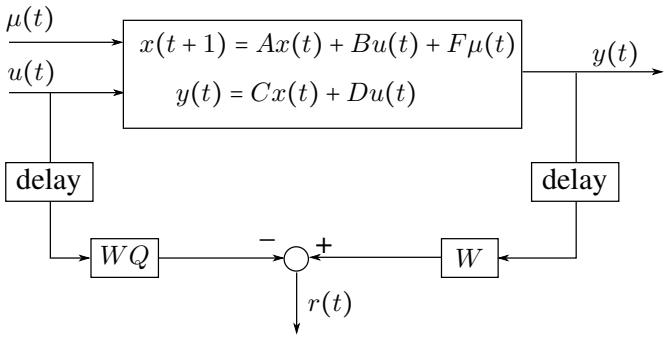

Figure 2.6: Open-loop fault detection filter (PE)

Consider a state-space representation of the system (2.2). The stacked vector of the system output $y(t)$ is defined as:

$$Y(t) = \begin{bmatrix} y^T(t-s) & y^T(t-s+1) & \cdots & y^T(t) \end{bmatrix}^T \tag{2.57}$$

where the term s denotes the order of the parity space. Analogously, one can construct a stacked vector of $u(t)$, which is denoted as $U(t)$. Using this notation the system defined by (2.53) in a fault-free case can be expressed in the form of:

$$Y(t) = \Gamma x(t-s) + QU(t) \tag{2.58}$$

where Γ is an extended observability matrix:

$$\Gamma = \begin{bmatrix} C \\ CA \\ \vdots \\ CA^s \end{bmatrix} \in \mathbb{R}^{(s+1)m \times n} \tag{2.59}$$

and Q is the following block Toeplitz matrix:

$$Q = \begin{bmatrix} D & 0 & \cdots & 0 \\ CB & D & \cdots & 0 \\ CAB & CB & \cdots & 0 \\ \vdots & \vdots & \ddots & \vdots \\ CA^{s-1}B & CA^{s-2}B & \cdots & D \end{bmatrix} \in \mathbb{R}^{(s+1)m \times (s+1)p} \tag{2.60}$$

For the purpose of elimination of the unknown state vector from (2.58), a matrix $W \in \mathbb{R}^{l \times (s+1)m}$, $l \geq 1$, is defined, which belongs to the left nullspace of Γ, i.e.

$$W\Gamma = 0 \tag{2.61}$$

Note that W can always be found by choosing s to be sufficiently large. Therefore, by premultiplying (2.58) by W the following expression is obtained:

$$WY(t) = WQU(t) \tag{2.62}$$

Consequently, the residual defined as:

$$r(t) = WY(t) - WQU(t) \tag{2.63}$$

deviates from zero if a fault occurs in the system. It is worth noting that, because the residual response to fault is open-loop, the residual is correlated only with the last $s+1$ samples of the fault signal.

2.6 Robust fault detection

Unmodelled dynamics, process noise, parameter variations, or unmeasurable external stimuli act as disturbances and may affect the fault detection process leading to false

alarms. Therefore, it is required to construct such a fault detection filter, which is sensitive to faults but insensitive to disturbances. Disturbances are often represented by an extra input to the system, $d(t) \in \mathbb{R}^q$, with a known distribution matrix $E \in \mathbb{R}^{n\times q}$. Thus, the system (2.53) with disturbances is represented by the following set of equations:

$$\begin{aligned} x(t+1) &= Ax(t) + Bu(t) + Ed(t) + F\mu(t) \\ y(t) &= Cx(t) + Du(t) \end{aligned} \tag{2.64}$$

A complete disturbance decoupling is achieved if the residual is sensitive to a fault, i.e. $r(t) \neq 0$ if $\mu(t) \neq 0$, but it is insensitive to disturbances, i.e. if $\mu = 0$ then $r(t) = 0$ for any $d(t) \in \mathbb{R}$. A robust fault detection filter may be either open-loop (equivalent to PE) or closed-loop (observer-based). In Subsections 2.6.1 and 2.6.3 the design of robust, observer-based fault detection filters using, respectively, right and left eigenstructure assignment (Patton & Chen 1991*a*, Chen & Patton 1999) is presented. In Subsection 2.6.2 a geometric insight into a robust fault detection filter via right eigenstructure assignment is given. It has been shown in (Patton & Chen 1991*a*) that a special case of a robust fault detection filter via left eigenstructure assignment is equivalent to the first order PE, which is shown in Subsection 2.6.4.

2.6.1 Robust fault detection via right eigenstructure assignment

In this subsection a design of a robust fault detection filter using right eigenstructure assignment is presented. Consider the filter (2.54). The sufficient conditions for the decoupling of the disturbances from the residual are, see (Chen & Patton 1999):

1. All columns of the matrix E are right eigenvectors of $(A-KC)$ corresponding to any eigenvalues
2. $QCE = 0$

It is assumed that E is full column rank. Denote the i^{th} column of E as E_i, which is also a right eigenvector of $(A-KC)$ corresponding to the desired eigenvalue λ_i. In order to satisfy the decoupling condition 1, it should hold that:

$$(\lambda_i I - A + KC)E_i = 0 \text{ for } i = 1, \cdots, q \tag{2.65}$$

which is equivalent to:

$$KCE_i = (A - \lambda_i)E_i \text{ for } i = 1, \cdots, q \tag{2.66}$$

The procedure for finding such a gain matrix K, for which the decoupling conditions are fulfilled, has been proposed by Chen & Patton (1999). Using the notation:

$$A_\lambda = \begin{bmatrix} (A-\lambda_1 I)E_1 & (A-\lambda_2 I)E_2 & \cdots & (A-\lambda_q I)E_q \end{bmatrix} \tag{2.67}$$

equation (2.66) can be reformulated as:

$$KCE = A_\lambda \tag{2.68}$$

The sufficient conditions to assign all columns of E as right eigenvectors of $(A - KC)$ are, see (Chen & Patton 1999):

(i) $\text{rank}(CE) = \text{rank}(\begin{bmatrix} A_\lambda \\ CE \end{bmatrix})$

(ii) (C', A') is a detectable pair, where:

$$\begin{aligned} A' &= A - A_\lambda (CE)^{+} C \\ C' &= (I - CE(CE)^{+})C \end{aligned} \tag{2.69}$$

The matrix K is subsequently calculated as:

$$K = A_\lambda (CE)^{+} + K'(I - CE(CE)^{+}) \tag{2.70}$$

where K' is an arbitrary matrix (Chen & Patton 1999). Note that:

$$A - KC = A - A_\lambda (CE)^{+} C - K'(I - CE(CE)^{+})C = A' - K'C' \tag{2.71}$$

Consequently, the columns of E are the right eigenvectors of $(A' - K'C') = (A - KC)$ corresponding to the desired eigenvectors λ_i, $i = 1, 2, ..., q$. Hence, one can allocate remaining $(n-q)$ eigenvalues by choosing an appropriate gain matrix K' and subsequently compute the gain matrix K using (2.70). Note that the eigenvalues λ_i, $i = 1, 2, ..., q$ are the unobservable modes of the pair (C', A'), which means that only remaining $n - q$ eigenvalues can be allocated by K'. The proof of this statement is provided in (Chen & Patton 1999).

2.6.2 Disturbance decoupling in geometric approach

Consider the robust fault detection filter described in Subsection 2.6.1. Each column of E is a right eigenvector of $(A - KC)$. Therefore, $\text{Im}\{E_i\}$, for $i = 1, \cdots, q$ is an $(A - KC)$-invariant subspace. Furthermore, $\text{Im}\{E_i\}$, for $i = 1, \cdots, q$ is an infimal $(A - KC)$-invariant subspace containing $\text{Im}\{E_i\}$, i.e. the reachability subspace of $(A - KC, E_i)$. This means that the state trajectory driven by the i^{th} disturbance signal, $d_i(t)$, will remain within $\text{Im}\{E_i\}$. Due to the fact that $QCE = 0$, $\text{Im}\{E_i\} \subseteq \text{Ker}\{QC\}$ and, because $\text{Im}\{E_i\}$ is $(A-KC)$-invariant, it belongs to the supremal $(A-KC)$-invariant contained in $\text{Ker}\{QC\}$, i.e. the unobservable subspace of $(A-KC, E, QC)$. Thus, the state vector driven by the disturbance remains in the unobservable space of the fault detection filter $(A - KC, E, QC)$ and, hence, the residual is insensitive to disturbances.

2.6.3 Robust fault detection via left eigenstructure assignment

A tutorial paper for the left eigenstructure assignment technique has been written by (Patton & Chen 1991*b*). Subsequently, these results have been revisited in (Chen & Patton 1999). Patton & Chen (1992) utilised the left eigenstructure assignment technique for a jet engine sensor fault detection.

Any transfer function matrix can be written as:

$$(zI - A + KC)^{-1} = \frac{v_1 l_1^T}{z - \lambda_1} + \frac{v_2 l_2^T}{z - \lambda_2} + \cdots + \frac{v_n l_n^T}{z - \lambda_n} \tag{2.72}$$

where v_i and l_i^T are, respectively, the right and left eigenvectors of $(A - KC)$ corresponding to the eigenvalue λ_i, see (Patton & Chen 1991*b*, Patton & Chen 1992, Chen & Patton 1999). Denote left and right eigenvector matrices, respectively, as:

$$L = \begin{bmatrix} l_1^T \\ l_2^T \\ \vdots \\ l_n^T \end{bmatrix} \qquad V = \begin{bmatrix} v_1 & v_2 & \cdots & v_n \end{bmatrix} \tag{2.73}$$

It is known that the left eigenvector l_i^T is orthogonal to the right eigenvector v_j if $i \neq j$, cf. (Patton & Chen 1991*b*, Chen & Patton 1999). Therefore, if the vectors l_i^T and v_i are appropriately scaled:

$$LV = I \tag{2.74}$$

and hence:

$$L = V^{-1} \tag{2.75}$$

The transfer function between the disturbance and the residual can be expressed as:

$$G_{rd}(z) = \sum_{i=1}^{n} \frac{QCv_i l_i^T E}{z - \lambda_i} \tag{2.76}$$

Hence, $G_{rd}(z)$ vanishes if and only if for $i = 1, \cdots, n$:

$$QCv_i l_i^T E = 0 \tag{2.77}$$

which implies that:

$$\sum_{i=1}^{n} QCv_i l_i^T E = QCVLE = QCE = 0 \tag{2.78}$$

Therefore, the first step for the disturbance decoupling is to find the matrix Q, such that $QCE = 0$, see (Patton & Chen 1991*b*, Chen & Patton 1999). Consequently, sufficient conditions for the disturbance decoupling using the left eigenstructure assignment are:

1. $QCE = 0$

2. All rows of QC are left eigenvectors of $(A-KC)$ corresponding to any eigenvalues

The proof of the above conditions can be found in (Chen & Patton 1999).

Assignability condition

Rows of QC should be the first r_q eigenvectors of $(A - KC)$, where r_q denotes the number of column of QC, i.e.

$$l_i^T(A - KC) = \lambda_i l_i^T \tag{2.79}$$

where l_i^T is the i^{th} row of QC. The above expression can be reformulated as:

$$l_i^T(A - \lambda_i I) = l_i^T KC \tag{2.80}$$

Consequently:

$$l_i^T = -l_i^T KC(A - \lambda_i I)^{-1} \tag{2.81}$$

Note that $l_i^T \in \mathbb{R}^{1\times n}$ and $K \in \mathbb{R}^{n\times m}$. Therefore, $l_i^T K \in \mathbb{R}^{1\times m}$, whilst the matrix $C(A - \lambda_i I)^{-1} \in \mathbb{R}^{m\times n}$. This means that by premultiplying the matrix $C(A - \lambda_i I)^{-1}$ by a row vector $l_i^T K$ a linear combination of rows of $C(A - \lambda_i I)^{-1}$ is obtained. Consequently, a solution to (2.79) exists for the desired λ_i if and only if the vector l_i^T lies in a row subspace spanned by $C(\lambda_i I - A)^{-1}$, i.e. l_i lies in a column subspace spanned by $(\lambda_i I - A^T)^{-1}C^T$, see (Chen & Patton 1999). Therefore, l_i must be equal to its projection on the subspace $\mathrm{Im}\{(\lambda_i I - A^T)^{-1}C^T\}$. Denote $(\lambda_i I - A^T)^{-1}C^T$ as $P(\lambda_i)$. The projection of l_i onto $\mathrm{Im}\{(\lambda_i I - A^T)^{-1}C^T\}$ is given by:

$$l_i^* = P(\lambda_i)w_i^* \quad \text{for } i = 1, \cdots, r_q \tag{2.82}$$

where:

$$w_i^* = [P(\lambda_i)^T P(\lambda_i)]^{-1} P(\lambda_i)^T l_i \quad \text{for } i = 1, \cdots, r_q \tag{2.83}$$

In the case when $l_i^* = l_i$, the left eigenvector l_i is assignable. Otherwise a complete disturbance decoupling using the left eigenstructure assignment is not possible. Consider the following equation:

$$(l_i^*)^T(A - KC) = \lambda_i (l_i^*)^T \tag{2.84}$$

it holds that:

$$l_i^* = -(\lambda_i I - A^T)^{-1} C^T K^T l_i^* \tag{2.85}$$

Therefore, one can note that, cf. (2.82):

$$w_i^* = -K^T l_i^* \tag{2.86}$$

The disturbance decoupling conditions require only r_q eigenvectors to be specified (i.e. rows of QC). The remaining $n - r_q$ eigenvectors may be selected freely from the assignable subspace $\mathrm{Im}\{(\lambda_i I - A^T)C^T\}$, i.e.:

$$l_i = -(\lambda_i I - A^T)^{-1} C^T w_i \quad \text{for } i = r_q + 1, \cdots, n \tag{2.87}$$

for any arbitrary w_i, $i = q+1, \cdots, n$. Subsequently, the gain matrix K is calculated via (see (Chen & Patton 1999)):

$$K = -[W L^{-1}]^T \tag{2.88}$$

where:

$$L = \begin{bmatrix} l_1^* & \cdots & l_{r_q}^* & l_{r_q+1} & \cdots & l_n \end{bmatrix} \tag{2.89}$$

and:

$$W = \begin{bmatrix} w_1^* & \cdots & w_{r_q}^* & w_{r_q+1} & \cdots & w_n \end{bmatrix} \tag{2.90}$$

2.6.4 Design of first order PE using left eigenstructure assignment

Consider a fault detection filter via left eigenstructure assignment, where (Chen & Patton 1999):

$$QC(A - KC) = 0 \tag{2.91}$$

This occurs when eigenvalues of $(A - KC)$ assigned to the columns of QC are equal zero. Then, the z-form of the residual is, cf. (2.54):

$$\begin{aligned} r(z) = &\left(Q - QC(zI - A + KC)^{-1}K\right) y(z) - \\ &\left(QD - QC(zI - A + KC)^{-1}(B - QD)\right) u(z) \end{aligned} \tag{2.92}$$

where $u(z)$, $y(z)$, and $r(z)$ are the z-transform forms of, respectively, $u(t)$, $y(t)$, and $z(t)$. Note that:

$$\begin{aligned} QC(zI - A + KC)^{-1} = z^{-1}QC(I + (A - KC)z^{-1} + (A - KC)^2 z^{-2} + \\ (A - KC)^3 z^{-3} + \cdots) \end{aligned} \tag{2.93}$$

Hence, $QC(zI - A + KC)^{-1} = z^{-1}QC$. Therefore, the computational form of the residual vector $r(z)$ can be rewritten as:

$$r(z) = \left(Q - z^{-1}QCK\right) y(z) - \left(QD - z^{-1}QC(B - QD)\right) u(z) \tag{2.94}$$

which is equivalent to a first order PE:

$$r(t) = \begin{bmatrix} Q & -QCK \end{bmatrix} \begin{bmatrix} y(t) \\ y(t-1) \end{bmatrix} - \begin{bmatrix} QD & -QC(B - QD) \end{bmatrix} \begin{bmatrix} u(t) \\ u(t-1) \end{bmatrix} \tag{2.95}$$

The above scheme is also referred as a deadbeat robust fault detection filter (DRFDF), see (Chen & Patton 1999).

2.7 Fault isolation and identification

Isermann & Balle (1997) listed various statistical methods, as well as neural networks and fuzzy logic for fault isolation. This thesis, however, deals with deterministic methods, which generate residuals of the following properties (Gertler & Kunver 1995):

Structured residual set: Each fault yields certain residuals deviate from zero, whereas other residuals remain zero. This can be interpreted as the fault $\mu_i(t)$ causing the residual vector to lie in a certain subspace of the residual space, see Fig 2.7(a). An example of a structured residual set is presented in Table 2.1.

Fixed direction residuals: Presence of the fault $\mu_i(t)$ yields the residual to lie in a fixed direction, see Fig 2.7(b). Residual directions do not need to be linearly independent. However, multiple faults cannot be detected unless residual directions are linearly independent.

Diagonal residual set: A combination of the two above, i.e. the fault $\mu_i(t)$ causes the residual $r_i(t)$ to deviate from zero, whilst the remaining residuals are equal to zero. A diagonal residual set can be used to isolate multiple faults. Note that a diagonal residual set can be obtained from a set of linearly independent fixed direction residuals by a similarity transformation (change of basis).

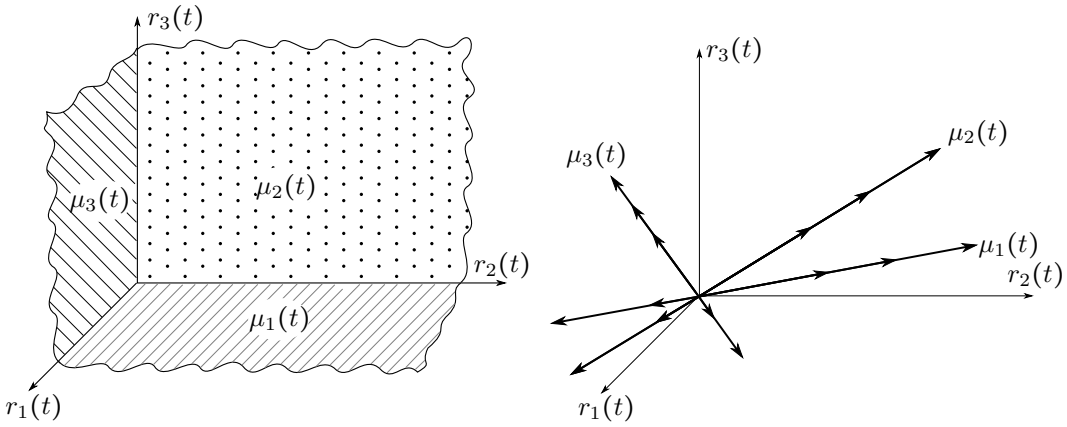

(a) Structured residual set (b) Directional residual set

Figure 2.7: Graphical illustration of structured and directional residual set

2.7.1 Fault isolation via diagnostic observers

Diagnostic observers are state observers which are used for diagnostic purposes. The pioneers of model-based fault isolation filters are Beard (1971) and Jones (1973). Note

Table 2.1: Example of a structured residual set. The entry 1 in the i^{th} row (corresponding to the fault $\mu_i(t)$) and the j^{th} column (corresponding to the residual $r_j(t)$) denotes that $\mu_i(t)$ yields the residual $r_j(t)$ deviate from zero. Note that multiple faults cannot be isolated using this residual set.

	$r_1(t)$	$r_2(t)$	$r_3(t)$	$r_4(t)$
$\mu_1(t)$	1	0	1	0
$\mu_2(t)$	0	1	1	0
$\mu_3(t)$	1	0	1	1
$\mu_4(t)$	0	1	0	1

that the fault isolation schemes developed by them are often referred to as 'Beard-Jones fault detection filters'. In this thesis the term 'fault detection' refers to the process of determining a fault occurrence, whereas the schemes proposed by Beard (1971) and Jones (1973) are, for sake of consistency, referred to as 'fault isolation filters'.

Consider the system described by equation (2.53). Denote each column of the matrix F as F_i and each corresponding fault signal as $\mu_i(t)$. Let δ_i be the smallest non-negative integer such that $CA^{\delta_i}F_i \neq 0$. Then the term $f_i = A^{\delta_i}F_i$ is further referred to as the fault direction (Massoumnia 1986, Chen & Speyer 2006*a*). Consider the following fault isolation filter:

$$\hat{x}(t+1) = (A - KC)\hat{x}(t) + (B - KD)u(t) + Ky(t) \tag{2.96a}$$

$$r(t) = y(t) - C\hat{x}(t) - Du(t) \tag{2.96b}$$

The objectives of the filter design are:

> The residual lies in the direction Cf_i when the fault μ_i occurs
>
> Eigenvalues of $(A-KC)$ can be arbitrarily specified (with constraint of conjugate symmetry and no repeated eigenvalues[2])

In order for the filter design to be feasible, the following conditions must be fulfilled (Chow & Willsky 1984, Massoumnia 1986, Chen & Speyer 2006*b*):

1. (C, A) is observable pair
2. $\text{rank}(\begin{bmatrix} Cf_1 & Cf_2 & \cdots & Cf_k \end{bmatrix}) = k$

Assumption 1. ensures that all the filter eigenvalues can be arbitrarily specified, whereas Assumption 2. allows for the faults to be isolated, i.e. yields residuals caused by different faults lie in different directions.

[2]Constraint of no repeated eigenvalues is often imposed for clarity of analysis and derivation processes (Chen & Patton 1999, Chen & Speyer 2006*a*)

Different solutions have been proposed to design a fault diagnostic observer. Massoumnia (1986) represented the Beard-Jones fault isolation filter in a geometric domain and, furthermore, added a solution for the filter design when the output response to fault has invariant zeros. White & Speyer (1986) reformulated the Beard-Jones fault isolation filter to an eigenstructure assignment problem. Then, Chen & Speyer (2006*b*) used the spectral theory to design a Beard-Jones fault isolation filter. Furthermore, a design of the filter has been presented using eigenstructure assignment (Chen & Speyer 2006*a*) and linear matrix inequalities (LMI), see e.g. (Chen & Nagarajaiah 2007).

Design of fault isolation filter

A fault isolation filter design using the right eigenstructure assignment developed by Chen & Speyer (2006*a*) is presented here. Eigenvalues of $(A - KC)$ can be arbitrarily specified and for each column of F n_i eigenvalues, denoted $\lambda_j^{(i)}$, are allocated to $(A - KC)$, corresponding to the eigenvectors $w_j^{(i)}$, $j = 1, 2, \cdots, n_i$:

$$(A - KC)w_j^{(i)} = \lambda_j^{(i)} w_j^{(i)} \tag{2.97}$$

It is demonstrated in (Chen & Speyer 2006*a*) that the number of assignable eigenvalues, n_i, depends on the rank of the observability matrix of (C_i, A_i):

$$\mathcal{O}_i = \begin{bmatrix} C_i \\ C_i A_i \\ \vdots \\ C_i A_i^{n-1} \end{bmatrix} \tag{2.98}$$

where $A_i = A - Af_i(Cf_i)\ C$ and $C_i = \left(I - Cf_i(Cf_i)\ \right)C$ and:

$$n_i = n - \text{rank}(\mathcal{O}_i) \tag{2.99}$$

It is also shown that the unobservable subspace of (A_i, C_i), i.e. $\ker\{\mathcal{O}_i\}$, is $\text{Im}\{\begin{bmatrix} F_i & AF_i & \cdots & A^{\delta_i}F_i \end{bmatrix}\} \oplus \mathcal{V}_i$, where $\mathcal{V}_i$ is the subspace spanned by the invariant zero state directions of (A, F_i, C). Therefore, $n_i = \delta_i + \dim\{\mathcal{V}_i\} + 1$. It is pointed out that Cf_i and $Cw_j^{(i)}$ are colinear and, for convenience, it is assumed that (Chen & Speyer 2006*a*):

$$Cf_i = Cw_j^{(i)} \tag{2.100}$$

Incorporating (2.100) into (2.97) the following relation is obtained:

$$KCf_i = (A - \lambda_j^{(i)})w_j^{(i)} \tag{2.101}$$

The eigenvectors of $(A - KC)$ are defined as:

$$w_j^{(i)} = \Theta_i \beta_j^{(i)} \tag{2.102}$$

where $\mathrm{Im}\{\Theta_i\} = \ker\{\mathcal{O}_i\}$ and $\beta_j^{(i)}$ is a coefficient vector (Chen & Speyer 2006*a*). From (2.100) if follows that the last element of $\beta_j^{(i)}$ is unity, hence (2.102) is reformulated as:

$$w_j^{(i)} = \begin{bmatrix} \bar{\Theta}_i & f_i \end{bmatrix} \begin{bmatrix} \bar{\beta}_j^{(i)} \\ 1 \end{bmatrix} = \bar{\Theta}_i \bar{\beta}_j^{(i)} + f_i \tag{2.103}$$

where:

$$\mathrm{Im}\{\bar{\Theta}_i\} = \mathrm{Im}\{\begin{bmatrix} F_i & AF_i & \cdots & A^{\delta_i - 1} F_i \end{bmatrix}\} \oplus \mathcal{V}_i \tag{2.104}$$

Substituting (2.103) into (2.101):

$$(A - \lambda_j^{(i)}) \bar{\Theta}_i \bar{\beta}_j^{(i)} = KCf_i - (A - \lambda_j^{(i)}) f_i \tag{2.105}$$

and repeating (2.105) n_i times:

$$\begin{bmatrix} (A - \lambda_1^{(i)})\bar{\Theta}_i & 0 & \cdots & 0 \\ 0 & (A - \lambda_2^{(i)})\bar{\Theta}_i & \cdots & 0 \\ \vdots & \vdots & \ddots & \vdots \\ 0 & 0 & \cdots & (A - \lambda_{n_i}^{(i)})\bar{\Theta}_i \end{bmatrix} \begin{bmatrix} \bar{\beta}_1^{(i)} \\ \bar{\beta}_2^{(i)} \\ \vdots \\ \bar{\beta}_{q_1+1}^{(i)} \end{bmatrix} = \begin{bmatrix} KCf_i - \lambda_1^{(i)} f_i \\ KCf_i - \lambda_2^{(i)} f_i \\ \cdots \\ KCf_i - \lambda_{n_i}^{(i)} f_i \end{bmatrix} \tag{2.106}$$

After subtracting the last row of (2.106) from the others, the following expression is obtained:

$$\begin{bmatrix} (A - \lambda_1^{(i)})\bar{\Theta}_i & 0 & \cdots & -(A - \lambda_{n_i}^{(i)})\bar{\Theta}_i \\ 0 & (A - \lambda_2^{(i)})\bar{\Theta}_i & \cdots & -(A - \lambda_{n_i}^{(i)})\bar{\Theta}_i \\ \vdots & \vdots & \ddots & \vdots \\ 0 & 0 & \cdots & (A - \lambda_{n_i-1}^{(i)})\bar{\Theta}_i - (A - \lambda_{n_i}^{(i)})\bar{\Theta}_i \end{bmatrix}$$
$$\begin{bmatrix} \bar{\beta}_1^{(i)} \\ \bar{\beta}_2^{(i)} \\ \vdots \\ \bar{\beta}_{q_1+1}^{(i)} \end{bmatrix} = \begin{bmatrix} (\lambda_1^{(i)} - \lambda_{n_i}^{(i)}) f_i \\ (\lambda_2^{(i)} - \lambda_{n_i}^{(i)}) f_i \\ \cdots \\ (\lambda_{n_i-1}^{(i)} - \lambda_{n_i}^{(i)}) f_i \end{bmatrix} \tag{2.107}$$

Denote the matrix at the left hand side of (2.107) as $\tilde{A}_i$. Then the coefficient vectors $\bar{\beta}_j^{(i)}$, $j = 1, 2, \cdots, n_i$ are calculated using a pseudoinverse of $\tilde{A}_i$:

$$\begin{bmatrix} \bar{\beta}_1^{(i)} \\ \bar{\beta}_2^{(i)} \\ \cdots \\ \bar{\beta}_{q_1+1}^{(i)} \end{bmatrix} = \tilde{A}_i \begin{bmatrix} (\lambda_1^{(i)} - \lambda_{n_i}^{(i)}) f_i \\ (\lambda_2^{(i)} - \lambda_{n_i}^{(i)}) f_i \\ \cdots \\ (\lambda_{n_i-1}^{(i)} - \lambda_{n_i}^{(i)}) f_i \end{bmatrix} \tag{2.108}$$

From (2.100) it follows that (Chen & Speyer 2006*a*):

$$KCf_i = (A - \lambda_1^{(i)} I) w_1^{(i)} = \cdots = (A - \lambda_{n_i}^{(i)} I) w_{n_i}^{(i)} \tag{2.109}$$

Combining the above for $i = 1, 2, \cdots, q$:

$$KCf = \begin{bmatrix} \lambda_1^{(1)} w_1^{(1)} & \lambda_1^{(2)} w_1^{(2)} & \cdots & \lambda_1^{(q)} w_1^{(q)} \end{bmatrix} \tag{2.110}$$

Consequently, the gain matrix K is calculated as:

$$K = \begin{bmatrix} \lambda_1^{(1)} w_1^{(1)} & \lambda_1^{(2)} w_1^{(2)} & \cdots & \lambda_1^{(q)} w_1^{(q)} \end{bmatrix} (Cf) + K_0 \left(I - (Cf)(Cf) \right) \tag{2.111}$$

where K_0 is an arbitrary matrix.

2.7.2 Geometric properties of fault isolation filter

A Beard-Jones fault isolation filter has been derived using a geometric approach in (Massoumnia 1986). For each fault direction f_i it holds that $\mathrm{Im}\{\Theta_i\} = \mathrm{Im}\{\begin{bmatrix} F_i & AF_i & \cdots & A^{\delta_i} F_i \end{bmatrix}\} \oplus \mathcal{V}_i$ is an $(A - KC)$-invariant subspace. Consequently, the state trajectory driven by the fault $\mu_i(t)$ remains within $\mathrm{Im}\{\Theta_i\}$. This yields the residual to lie in the direction $\mathrm{Im}\{C\Theta_i\} = Cf_i$. Due to the fact that $Cf_i \neq Cf_j, i \neq j$, i.e. different faults yield different residual directions, faults can be isolated.

2.7.3 Fault identification

In order to identify the magnitude of the fault fault, a fault identification filter is designed in such a way that the residual approximates the fault signal, i.e. (Ding 2008):

$$r(t) \approx \mu(t) \tag{2.112}$$

This is an unmeasurable input reconstruction problem. In the case of multiple faults a diagonal fault isolation filter can be utilised. It is, however, important that the steady state gain of the residual response to fault is non-zero (Ding 2008).

2.8 Concluding remarks

In this chapter a background knowledge which is used to develop the algorithms proposed in this thesis has been provided. The reader has been familiarised with the representation of a dynamic, discrete-time, time-invariant stochastic system in both polynomial and state-space forms, and an insight into the geometric theory of linear systems has been given. The problem of an unknown (unmeasurable) input reconstruction has been introduced and two methods known from the literature have been presented. Furthermore, the reader has been familiarised with the basics of fault detec-

tion and diagnosis. Both closed-loop (observer-based) and open-loop (PE-based) fault detection/isolation filters have been discussed and appropriate algorithms selected from the literature have been presented.

Chapter 3

Parity equations-based unknown input reconstruction for linear stochastic systems

Nomenclature

a_i	autoregressive parameter in polynomial model
A	state transition matrix in state-space model
$b(t)$	auxiliary vector
b_i	exogenous parameter in polynomial model
B	input matrix of known input in state-space model
c_i	moving average parameter in ARMAX model
C	output matrix in a state-space model
D	feedforward matrix of known input in state-space model
$e(t)$	noise term
$f(\cdot)$	function to be minimised by Lagrange multiplier method
$g(\cdot)$	constraint function in Lagrange multiplier method
G	input matrix of unknown input in state-space model
G'	auxiliary matrix
$G_u(z)$	z-domain transfer function between $u_0(t)$ and $y(t)$
$G_v(z)$	z-domain transfer function between $v(t)$ and $y(t)$
$G'_v(z)$	auxiliary z-domain transfer function
H	feedforward matrix of unknown input in state-space model
H'	auxiliary matrix
k	number of rows of the matrix spanning the left nullspace of Γ
$K(t)$	gain matrix (used by MVU)
m	number of system outputs
$M(t)$	auxiliary matrix (used by MVU)
$M_v(z)$	auxiliary transfer function
n	order of system
n_a	order of autoregressive polynomial
n_b	order of exogenous polynomial
n_c	order of moving average polynomial

$N_v(z)$	auxiliary transfer function
p	number of known inputs to the system
p_i	element of P
P	auxiliary vector
$P^x(t), P^d(t)$.....	submatrices of state and input estimation error covariance matrix
$P^{dx}(t), P^{xd}(t)$...	submatrices of state and input estimation error covariance matrix
Q	block Toeplitz matrix
$\tilde{Q}$	covariance matrix of $\xi(t)$
R	covariance matrix of $\zeta(t)$
$\tilde{R}$	covariance matrix (used in MVU)
s	parity space order
S	auxiliary matrix
T	block Toeplitz matrix
T'	auxiliary matrix
$u(t)$	measured input
$\tilde{u}(t)$	input measurement noise
$\tilde{u}^*(t)$	auxiliary variable
$u_0(t)$	noise-free known input
$U(t)$	stacked vector of last $s+1$ values of $u(t)$
$U(z)$	$u(t)$ in z-domain
$\tilde{U}(t)$	stacked vector of last $s+1$ values of $\tilde{u}(t)$
$\tilde{U}(z)$	$\tilde{u}(t)$ in z-domain
$\tilde{U}^*(t)$	stacked vector of last $s+1$ values of $\tilde{u}^*(t)$
$\tilde{U}^*(z)$	$\tilde{u}^*(t)$ in z-domain
$U_0(t)$	stacked vector of last $s+1$ values of $u_0(t)$
$U_0(z)$	$u_0(t)$ in z-domain
$v(t)$	unknown (unmeasurable) input
$\hat{v}(t)$	unknown input estimate
$v'(t)$	auxiliary variable
$V(t)$	stacked vector of last $s+1$ values of unknown input
$V(z)$	$v(t)$ in z-domain
$\hat{V}(z)$	$\hat{v}(t)$ in z-domain
$V'(t)$	stacked vector of last $s+1$ values of $v'(t)$
$V'(z)$	$v'(t)$ in z-domain
w_{q_i}, w_{ξ_i}	auxiliary polynomial parameters
W	vector, which belongs to $\Gamma^\perp$
$W(z)$	polynomial of z-variable defined by appropriate elements of W
$W_Q(z)$	polynomial of z-variable defined by appropriate elements of WQ
$W_T(z)$	polynomial of z-variable defined by appropriate elements of WT
$W_{T'}(z)$	polynomial of z-variable defined by appropriate elements of WT'
$W_\Xi(z)$	polynomial of z-variable defined by appropriate elements of $W\Xi$
$x(t)$	state vector instate space model
$y(t)$	measured output
$y_0(t)$	noise-free output in output-error case
$Y(t)$	stacked vector of last $s+1$ values of measured output
$Y(z)$	$y(t)$ in z-domain
$Y_0(t)$	stacked vector of last $s+1$ values of noise-free output
z_i	system zero
α_i, α_i'	auxiliary parameters
β_i	i^{th} diagonal element of Σ in multiple output OE case

χ	auxiliary vector
δ	system delay
$\epsilon(t)$	auxiliary noise term
$\epsilon^*(t)$	auxiliary noise term
γ	row vector of $\Gamma^\perp$
Γ	extended observability matrix
$\Gamma^\perp$	left nullspace of Γ
κ	auxiliary scalar
λ	Lagrange multiplier
ν	input derivative weighting
Π	input matrix of noise term in the state-space model
Ω	feedforward matrix of noise term in the state-space model
$\Sigma, \Sigma_e, \Sigma_{\tilde{u}}, \Sigma_{\tilde{u}e}$ ..	covariance matrices
τ	unknown input estimation lag
Ξ	block Toeplitz matrix
ψ	auxiliary vector
$\xi(t)$	process noise vector in state space model
$\zeta(t)$	output noise vector in state space model

Preliminary reading: Sections 2.2, 2.4, and Subsection 2.5.2.

3.1 Introduction

In the literature the problem of the unknown (unmeasurable) input estimation is solved either by a system inversion or by a joint state and input estimation. Early contributions to the inversion of multiple-input multiple-output (MIMO) deterministic systems have been presented by Dorato (1969) and Sain & Massey (1969), however their approaches did not ensure stability of the inverted systems. Moylan (1977) provided a stable inversion algorithm for minimum-phase systems, whilst Antsaklis (1978) developed a straightforward state feedback-based method, which allows to assign poles of the inverted system. This latter method is however limited to the systems with stable zeros.

Over the last decade a geometric approach to an unknown input reconstruction has gained considerable interest, see e.g. (Edelmayer 2005). Kirtikar, Palanthandalam-Madapusi, Zattoni & Bernstein (2009) proposed an unknown input reconstruction scheme for minimum phase systems. An exhaustive solution to an unknown-state unknown-input reconstruction for both minimum-phase and nonminimum-phase systems has relatively recently been developed by Marro & Zattoni (2010). Nevertheless, this approach does not consider the effects of measurement noise.

Another approach to the unknown input estimation for deterministic systems is based on state observers. The Luenberger state observer, see (Luenberger 1964), has been extended to the class of systems with both, known and unknown system inputs, see for example (Hou & Müller 1992, Darouach & Zasadzinski 1997). The work of Fernando & Trinh (2006) presents a joint input and state observer based on a descriptor approach.

When dealing with stochastic systems Kalman filter-based approaches have gained an interest, see, for example, (Hsieh 2000, Floquet & Barbot 2006). Gillijns & De Moor (2007*a*) combined the state observer proposed by Darouach & Zasadzinski (1997) and the unknown input estimator of Hsieh (2000) creating a joint state and unknown input observer, which is optimal in the minimum variance sense. This approach has subsequently been extended to the case of a linear system with a direct feedthrough term, see (Gillijns & De Moor 2007*b*). Palanthandalam-Madapusi & Bernstein (2007) introduced concept of a state and input observability, i.e. they provided a scheme, which allows to determine, if both the unknown input and the state can be derived from the output measurements. Keller & Sauter (2010) proposed a variable geometric Kalman filter, where the statistical effect of each unknown input is tested before deriving the state estimate. In the recent work of Ghahremani & Kamwa (2011) an extended Kalman filter with unknown inputs has been developed and applied to state estimation of a synchronous machine in a power system.

In this chapter a novel approach to the unknown input reconstruction for MIMO discrete-time stochastic systems is presented. The parity equation-based unknown input observer (PE-UIO) utilises a parity equations (PE) concept for the unknown input reconstruction. The design freedom is used to minimise the effect of stochastic disturbances on the unknown input estimate. For this purpose a Lagrange multiplier method is utilised. The proposed method is suitable for both minimum and nonminimum-phase systems, which is an important result, because unstable zeros may result from a discretisation of a continuous-time system. The PE-UIO has been originally developed for single-input single-output (SISO) output error (OE) systems in (Sumisławska, Burnham & Larkowski 2010). The algorithm has been subsequently extended to the errors-in-variables (EIV) framework in (Sumisławska, Larkowski & Burnham 2010*b*). The analysis of the PE-UIO in frequency domain has been provided in (Sumisławska, Larkowski & Burnham 2011*a*). In (Sumisławska, Larkowski & Burnham 2010*a*) the scheme has been extended to a MIMO case and a potential application to a steel rolling mill has been described. In this chapter the PE-UIO is extended to a coloured process noise case. A generalised form of the algorithm is provided, where the output is subjected to coloured noise (accounting for measurement and process noise), whilst the input is affected by white measurement noise. An extension of the PE-UIO algorithm for the cases when systems zero is close or equal to unity is also provided.

This chapter is organised as follows: in Section 3.2 the problem of the unknown input reconstruction is stated. Subsequently, in Section 3.3 the PE-UIO is presented. Then, in Section 3.5, the limitation of the scheme in the case when the system has zeros close or equal to unity is discussed and an extension, which tackles this problem, is provided. The proposed algorithms are demonstrated on tutorial examples in Section 3.7. Finally, in Section 3.8, the efficacy of the proposed methods is compared with two existing methods, namely, the minimum variance unbiased (MVU) joint state and

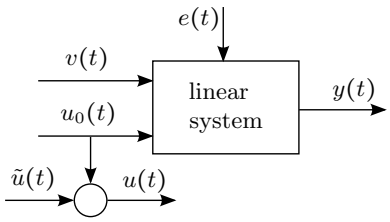

Figure 3.1: Schematic view of a linear system

input estimator, see (Gillijns & De Moor 2007*b*), and the input estimation (INPEST) method of Young & Sumisławska (2012).

3.2 Linear system representation

Assume that a linear dynamic discrete-time time-invariant multiple-input multiple-output (MIMO) system with p known inputs, m outputs and a single unknown input is represented by an n^{th} order state-space equation of the following form:

$$\begin{aligned} x(t+1) &= Ax(t) + Bu_0(t) + Gv(t) + \Pi e(t) \\ y(t) &= Cx(t) + Du_0(t) + Hv(t) + \Omega e(t) \\ u(t) &= u_0(t) + \tilde{u}(t) \end{aligned} \tag{3.1}$$

where $A \in \mathbb{R}^{n\times n}$, $B \in \mathbb{R}^{n\times p}$, $C \in \mathbb{R}^{m\times n}$, $D \in \mathbb{R}^{m\times p}$, $G \in \mathbb{R}^{n\times 1}$, $H \in \mathbb{R}^{m\times 1}$, $\Pi \in \mathbb{R}^{n\times m}$, $\Omega \in \mathbb{R}^{m\times m}$. The terms $u_0(t)$ and $y(t)$ refer to, respectively, the known input and output vectors, whereas $v(t)$ denotes the scalar unknown (unmeasurable) input. The term $e(t)$ is a column vector of m zero-mean, white Gaussian, i.i.d. noise sequences. The term $\tilde{u}(t)$ is a vector of white, Gaussian, zero-mean, i.i.d. noise sequences, which is uncorrelated with $e(t)$. The aim of the proposed approach is to reconstruct the unknown input $v(t)$, minimising at the same time the influence of the disturbances $e(t)$ and $\tilde{u}(t)$ on the estimate. A schematic picture of the considered system is presented in Fig. 3.1.

Equation (3.1) is a generalised representation of a linear stochastic system and can be simplified in more specific cases, see Subsection 2.2.3, which, for completeness, are given below.

ARMAX: The state-space system matrices A, B, C, D, Π, and Ω for the ARMAX model, cf. (2.5), in the observer canonical form are given by equation (2.6). The matrices G and H are built by replacing b_i in, respectively, matrices B and D with exogenous matrix parameters related to the unknown input $v(t)$. Note, the ARMAX model assumes that the input $u(t)$ is known exactly (there is no noise present on the input variable), hence $\tilde{u}(t) = 0$.

ARX: An ARX model is obtained from the ARMAX model by setting c_i, $i = 1, \cdots, n_c$, to zero.

OE: An OE case can be modelled by the system representation (3.1), where matrices A, B, C, D and also G and H are all given as in the ARMAX case. The matrix Π is null and Ω is diagonal. Also there is no noise present on the input variable, hence $\tilde{u}(t) = 0$. The PE-UIO algorithm for a SISO OE case has been developed in (Sumisławska, Burnham & Larkowski 2010).

EIV framework: The EIV framework, see, for example, (Söderström 2007), can be represented by (3.1), where $\tilde{u}(t) \neq 0$, $\Pi = 0$, and Ω is diagonal. The PE-UIO algorithm for a SISO case in the EIV framework has been presented in (Sumisławska, Larkowski & Burnham 2010*b*, Sumisławska et al. 2011*a*).

3.3 Design of unknown input reconstructor

In this section the PE-UIO algorithm is derived. Firstly, for completeness, the PE for the state-space model (3.1) are described in Subsection 3.3.1. This is followed by a development of a new unknown input observer based on PE in Subsections 3.3.2 and 3.3.3. Finally, in Subsection 3.3.4, simplified PE-UIO design algorithms for special cases of a stochastic linear system, such as SISO OE and MIMO OE, are presented.

3.3.1 Parity equations

The approach presented in this chapter utilises the PE to design an unknown input reconstructor. Recall the stacked vector of the system output $y(t)$, cf. (2.58):

$$Y(t) = \begin{bmatrix} y^T(t-s) & y^T(t-s+1) & \cdots & y^T(t) \end{bmatrix}^T \tag{3.2}$$

where the term s denotes the order of the parity space. Analogously, one can construct stacked vectors of $v(t)$, $u(t)$, $u_0(t)$, $\tilde{u}(t)$ and $e(t)$ which are denoted, respectively, as $V(t)$, $U(t)$, $U_0(t)$, $\tilde{U}(t)$ and $E(t)$. Using this notation the system defined by (3.1) can be expressed in the form of:

$$Y(t) = \Gamma x(t-s) + QU_0(t) + TV(t) + \Xi E(t) \tag{3.3}$$

where Γ is an extended observability matrix, cf. (2.59), and Q is given by (2.60). Analogously, one can build the matrix $T \in \mathbb{R}^{(s+1)m \times (s+1)}$ by replacing B and D in Q by, respectively, G and H, and the matrix $\Xi \in \mathbb{R}^{(s+1)m \times (s+1)m}$ is obtained by replacing B and D in Q by, respectively Π and Ω. The term $W \in \mathbb{R}^{1 \times (s+1)m}$ is considered to be a row vector, which belongs to the left nullspace of Γ, cf. (2.61). Consequently, (3.3) can

be reformulated as, cf. (2.62):

$$WY(t) = WQU(t) - WQ\tilde{U}(t) + WTV(t) + W\Xi E(t) \tag{3.4}$$

By rearranging the measured (known) variables to the right-hand side of (3.4) and the unknowns to the left-hand side, the following parity relation is obtained, cf. (Li & Shah 2002):

$$WTV(t) + W\Xi E(t) - WQ\tilde{U}(t) = WY(t) - WQU(t) \tag{3.5}$$

In the next subsection the PE are used in order to derive the PE-UIO.

3.3.2 Unknown input estimation

Denote the matrix spanning the left nullspace of Γ as $\Gamma^{\perp}$. Consequently, the row vector W is a linear combination of rows of $\Gamma^{\perp}$. In the disturbance-free case, i.e. when $U(t) = U_0(t)$ and $E(t) = 0$, the following equation holds, cf. (3.5):

$$\Gamma^{\perp}TV(t) = b(t) \tag{3.6}$$

where $b(t)$ is a column vector given by:

$$b(t) = \Gamma^{\perp}Y(t) - \Gamma^{\perp}QU(t) \tag{3.7}$$

Selection of a sufficiently large s would lead (3.6) to be a set of equations with an explicit solution or an overdetermined set of equations. Nevertheless, in practice, precision of the solution to (3.6) can still be seriously affected by noise. The algorithm proposed here provides an on-line approximation of the unknown input, simultaneously minimising unwanted effects of noise.

It is proposed to calculate the value of the unknown input as:

$$\hat{v}(t-\tau) = WY(t) - WQU(t) \tag{3.8}$$

where τ is an estimation lag (estimation delay) and it accounts for the fact that the unknown input may not be reconstructed instantenously. Therefore, at the time instance t the estimate of $v(t-\tau)$ is obtained. The estimation delay τ is defined further in this section. In the noise-free case, $\hat{v}(t-\tau)$ is simply:

$$\hat{v}(t-\tau) = WTV(t) \tag{3.9}$$

Therefore, based on the assumption that the unknown input is varying relatively slowly (see Subsection 3.5.1), its estimate can be calculated as a linear combination of the sequence $v(t-s)$, $v(t-s+1), \cdots, v(t)$, i.e.

$$\hat{v}(t-\tau) = \alpha_0 v(t) + \alpha_1 v(t-1) + \cdots + \alpha_s v(t-s) \tag{3.10}$$

where the α parameters are dependent on the choice of the vector W, such that:

$$WT = \begin{bmatrix} \alpha_s & \alpha_{s-1} & \cdots & \alpha_0 \end{bmatrix}^T \tag{3.11}$$

One can note that (3.10) represents a moving average finite impulse response filter with the gain being given by the sum of the α parameters, i.e. the sum of elements of the vector WT. Thus, it is suggested that W should be selected in such a way, that the sum of elements of the vector WT is equal unity. Furthermore, it is anticipated that the choice of the order of the parity space s, as well as the vector W, both influence the estimation lag τ in the estimate of the unknown input (due to the moving average filtering property of the unknown input estimator). The estimation lag is defined as the centre of gravity of the moving average filter rounded to the nearest natural number and is calculated via:

$$\tau = \text{round}\left(\frac{\sum \alpha_i i}{\sum \alpha_i}\right) \tag{3.12}$$

In the following subsection an algorithm for the selection of the optimal vector W is derived based on the Lagrange multiplier method.

3.3.3 Selection of optimal W

In the case of noisy input and output measurements, equation (3.9) becomes:

$$\hat{v}(t-\tau) = WTV(t) + W\Xi E(t) - WQ\tilde{U}(t) \tag{3.13}$$

which can be expanded to give:

$$\begin{aligned} \hat{v}(t-\tau) = {} & \alpha_0 v(t) + \alpha_1 v(t-1) + \cdots + \alpha_s v(t-s) + w_{\xi_{s+1}} e(t) + w_{\xi_s} e(t-1) + \cdots + \\ & + w_{\xi_1} e(t-s) - w_{q_{s+1}} \tilde{u}(t) - w_{q_s} \tilde{u}(t-1) - \cdots - w_{q_1} \tilde{u}(t-s) \end{aligned} \tag{3.14}$$

where the vector coefficients w_{ξ_i} and w_{q_i}, $i = 1, 2, \cdots, s+1$, are constructed from the appropriate elements of the vectors $W\Xi$ and WQ, respectively. (In the case when $p = m = 1$, i.e. $u(t)$ and $y(t)$ are scalars, w_{ξ_i} and w_{q_i} refer to the i^{th} elements of vectors $W\Xi$ and WQ, respectively.) Note, that in (3.14) the estimate of the unknown input is affected by two coloured noise sequences. However, by a careful choice of W, the degrading effect of these disturbances can be minimised.

Furthermore, the influence of measurement noise on the unknown input estimate can be reduced by minimising the variance of the term $W\Xi E(t) - WQ\tilde{U}(t)$, i.e.:

$$\begin{aligned} & \mathrm{E}\{(W\Xi E(t) - WQ\tilde{U}(t))(W\Xi E(t) - WQ\tilde{U}(t))^T\} = \\ & = W\Xi\Sigma_e\Xi^T W^T + WQ\Sigma_{\tilde{u}}Q^T W^T - W\Xi\Sigma_{\tilde{u}e}^T Q^T W^T - WQ\Sigma_{\tilde{u}e}\Xi^T W^T \end{aligned} \tag{3.15}$$

where $\Sigma_{\tilde{u}} = \mathrm{E}\{\tilde{U}(t)\tilde{U}^T(t)\}$, $\Sigma_e = \mathrm{E}\{E(t)E^T(t)\}$, and $\Sigma_{\tilde{u}e} = \mathrm{E}\{\tilde{U}(t)E^T(t)\} = 0$. Conse-

quently, the vector W should be selected to minimise the cost function $f(W)$:

$$f(W) = W\Xi\Sigma_e\Xi^T W^T + WQ\Sigma_{\tilde{u}}Q^T W^T \tag{3.16}$$

subject to the following constraints:

1. Sum of elements of WT is equal to 1.
2. $W\Gamma = 0$.

Note, that the condition 1 is sufficient to ensure unity gain, because $\mathrm{E}\{e(t)\} = 0$ and $\mathrm{E}\{\tilde{u}(t)\} = 0$.

The cost function (3.16) can be minimised by making use of the Lagrange multiplier method, see, for example, (Bertsekas 1982). Denote the rows of $\Gamma^\perp$ by γ_1, γ_2, ..., γ_k, where:

$$\Gamma^\perp = \begin{bmatrix} \gamma_1^T & \gamma_2^T & \cdots & \gamma_k^T \end{bmatrix}^T \tag{3.17}$$

The vector W is a linear combination of rows of $\Gamma^\perp$, which ensures that the constraint 2 is satisfied, i.e.

$$W = \sum_{i=1}^{k} p_i\gamma_i \tag{3.18}$$

Hence, the cost function (3.16) can be reformulated as a function of the parameter vector $P = \begin{bmatrix} p_1 & p_2 & \cdots & p_k \end{bmatrix}^T$:

$$f(P) = \left(\sum_{i=1}^{k} p_i\gamma_i\right)\Sigma\left(\sum_{j=1}^{k} p_j\gamma_j^T\right) \tag{3.19}$$

where

$$\Sigma = \Xi\Sigma_e\Xi^T + Q\Sigma_{\tilde{u}}Q^T \tag{3.20}$$

The cost function $f(P)$ is required to be minimised subject to the constraint:

$$g(P) = \mathrm{sum}_{\mathrm{row}}(WT) - 1 = 0 \tag{3.21}$$

where the operator $\mathrm{sum}_{\mathrm{row}}(A)$ denotes a column vector whose elements are sums of the appropriate rows of an arbitrary matrix A. (In the case of a row vector q, the term $\mathrm{sum}_{\mathrm{row}}(q)$ is simply a scalar being a sum of elements of the vector q, whilst, if q is a column vector, $\mathrm{sum}_{\mathrm{row}}(q) = q$.)

The solution to the Lagrange minimisation problem is given by, see (Bertsekas 1982):

$$\nabla f(P) = \lambda\nabla g(P) \tag{3.22}$$

The cost function (3.19) can be expanded as:

$$\begin{aligned} f(P) = \quad & p_1^2\gamma_1\Sigma\gamma_1^T + p_1p_2\gamma_1\Sigma\gamma_2^T + \cdots + p_1p_k\gamma_1\Sigma\gamma_k^T + \\ & p_1p_2\gamma_2\Sigma\gamma_1^T + p_2^2\gamma_2\Sigma\gamma_2^T + \cdots + p_2p_k\gamma_2\Sigma\gamma_k^T + \\ & \vdots \\ & p_1p_k\gamma_k\Sigma\gamma_1^T + p_2p_k\gamma_k\Sigma\gamma_2^T + \cdots + p_k^2\gamma_k\Sigma\gamma_k^T \end{aligned} \tag{3.23}$$

Hence, the partial derivative of $f(P)$ with respect to the i^{th} element of the vector P (denoted as p_i) is given by:

$$\begin{aligned} \frac{\partial f(P)}{\partial p_i} = & p_1\gamma_i\Sigma\gamma_1^T + p_2\gamma_i\Sigma\gamma_2^T + \cdots + p_i\gamma_i\Sigma\gamma_i^T + \cdots + p_k\gamma_i\Sigma\gamma_k^T + \\ & p_1\gamma_1\Sigma\gamma_i^T + p_2\gamma_2\Sigma\gamma_i^T + \cdots + p_i\gamma_i\Sigma\gamma_i^T + \cdots + p_k\gamma_k\Sigma\gamma_i^T \end{aligned} \tag{3.24}$$

Consequently, the gradient of $f(P)$ can be written as:

$$\begin{aligned} \begin{bmatrix} \frac{\partial f(P)}{\partial p_1} \\ \frac{\partial f(P)}{\partial p_2} \\ \vdots \\ \frac{\partial f(P)}{\partial p_k} \end{bmatrix} = & \begin{bmatrix} \gamma_1\Sigma\gamma_1^T & \gamma_1\Sigma\gamma_2^T & \cdots & \gamma_1\Sigma\gamma_k^T \\ \gamma_2\Sigma\gamma_1^T & \gamma_2\Sigma\gamma_2^T & \cdots & \gamma_2\Sigma\gamma_k^T \\ \vdots & \vdots & \ddots & \vdots \\ \gamma_k\Sigma\gamma_1^T & \gamma_k\Sigma\gamma_2^T & \cdots & \gamma_k\Sigma\gamma_k^T \end{bmatrix} P + \\ & \begin{bmatrix} \gamma_1\Sigma\gamma_1^T & \gamma_2\Sigma\gamma_1^T & \cdots & \gamma_k\Sigma\gamma_1^T \\ \gamma_1\Sigma\gamma_2^T & \gamma_2\Sigma\gamma_2^T & \cdots & \gamma_k\Sigma\gamma_2^T \\ \vdots & \vdots & \ddots & \vdots \\ \gamma_1\Sigma\gamma_k^T & \gamma_2\Sigma\gamma_k^T & \cdots & \gamma_k\Sigma\gamma_k^T \end{bmatrix} P = (\nabla f(P))^T \end{aligned} \tag{3.25}$$

Thus, recalling that Σ is symmetric, expression (3.25) can be reformulated as:

$$(\nabla f(P))^T = \left(\Gamma^{\perp}\Sigma\left(\Gamma^{\perp}\right)^T + \left(\Gamma^{\perp}\Sigma\left(\Gamma^{\perp}\right)^T\right)^T\right)P \tag{3.26}$$

The constraint function $g(P)$ is:

$$g(P) = \mathrm{sum}_{\mathrm{row}}(WT) - 1 = \sum_{i=1}^{k}\mathrm{sum}_{\mathrm{row}}(p_i\gamma_iT) - 1 \tag{3.27}$$

Hence the partial derivative of $g(P)$ with respect to p_i is calculated via:

$$\frac{\partial g(P)}{\partial p_i} = \mathrm{sum}_{\mathrm{row}}(\gamma_iT) \tag{3.28}$$

Thus, the gradient of $g(P)$ can be reformulated as:

$$(\nabla g(P))^T = \mathrm{sum}_{\mathrm{row}}(\Gamma^{\perp}T) \tag{3.29}$$

Using the notation:

$$S = \Gamma^{\perp}\Sigma(\Gamma^{\perp})^T + \left(\Gamma^{\perp}\Sigma\left(\Gamma^{\perp}\right)^T\right)^T \tag{3.30}$$

and

$$\psi = \mathrm{sum}_{\mathrm{row}}(\Gamma^{\perp}T) \tag{3.31}$$

the solution to the Lagrange optimisation problem (3.22) can be rewritten as:

$$SP = \lambda\psi \tag{3.32}$$

Hence, the optimal parameter vector P is given by:

$$P = \lambda S^{-1}\psi \tag{3.33}$$

The constraint function $g(P) = 0$ can be rewritten as:

$$P^T\psi - 1 = 0 \tag{3.34}$$

Incorporating (3.33) into (3.34) yields:

$$\lambda\left(S^{-1}\psi\right)^T\psi - 1 = 0 \tag{3.35}$$

Finally, the Lagrange multiplier is given by:

$$\lambda = \left(\left(S^{-1}\psi\right)^T\psi\right)^{-1} \tag{3.36}$$

Consequently, the algorithm for calculating the optimal vector W and estimation of the unknown input is summarised as follows:

Algorithm 3.1 (PE-UIO).

1. Select the order of the parity space $s \geq n$ and build matrices Γ, Q, T, and Ξ.
2. Obtain $\Gamma^{\perp}$.
3. Compute Σ as:

$$\Sigma = \Xi\Sigma_e\Xi^T + Q\Sigma_{\tilde{u}}Q^T \tag{3.37a}$$

4. Calculate the column vector S via:

$$S = \Gamma^{\perp}\Sigma(\Gamma^{\perp})^T + \left(\Gamma^{\perp}\Sigma\left(\Gamma^{\perp}\right)^T\right)^T \tag{3.37b}$$

5. Compute the matrix ψ by making use of:

$$\psi = \mathrm{sum}_{\mathrm{row}}(\Gamma^{\perp} T) \tag{3.37c}$$

6. Obtain the Lagrange multiplier λ:

$$\lambda = \left(\left(S^{-1} \psi \right)^T \psi \right)^{-1} \tag{3.37d}$$

7. Calculate the parameter vector P by:

$$P = \lambda S^{-1} \psi \tag{3.37e}$$

8. Compute the vector W using:

$$W = P^T \Gamma^{\perp} \tag{3.37f}$$

9. Calculate the estimation lag as:

$$\tau = \mathrm{round}\left(\frac{\sum \alpha_i i}{\sum \alpha_i} \right) \tag{3.37g}$$

where:

$$WT = \begin{bmatrix} \alpha_s & \alpha_{s-1} & \cdots & \alpha_0 \end{bmatrix}^T$$

10. Obtain the estimate of $v(t-\tau)$ via:

$$\hat{v}(t-\tau) = WY(t) - WQU(t) \tag{3.37h}$$

It should be noted that, due to the fact that the $\arg\min f(P)$ needs to be found, cf. (3.19), the function $f(P)$ can be scaled by an arbitrary number. Therefore, the covariance matrices of $\tilde{u}(t)$ and $e(t)$ do not require to be known explicitly. It is sufficient to know only the ratio between the variances of the noise sequences and scale $\Sigma_{\tilde{u}}$ and Σ_e accordingly.

3.3.4 Design of PE-UIO for OE systems

In the case when the system input measurements are noise-free and there is no process noise, whilst the output vector is affected by a white, Gaussian, zero-mean, i.i.d. noise sequences (OE case), the procedure of finding the optimal vector W can be simplified, which is presented in this subsection.

Single-output OE

Consider a single-output OE system described by (3.1). Without loss of generality it is assumed that $\Omega = 1$ and $e(t)$ is a white, zero-mean, Gaussian sequence with the variance of $\text{var}(e(t))$. Since there is no process noise and Ξ is an identity matrix, the term Σ, cf. (3.20), is given by:

$$\Sigma = \Sigma_e = \text{var}(e(t))I \tag{3.38}$$

Since the objective is to find the minimum of the cost function $f(P)$, it can be scaled by any arbitrary number. Therefore, for sake of simplicity, the term $\text{var}(e(t))$ can be omitted. Consequently, the cost function $f(P)$ becomes, cf. (3.19):

$$f(P) = \left(\sum_{i=1}^{k} p_i \gamma_i\right)\left(\sum_{j=1}^{k} p_j \gamma_j^T\right) \tag{3.39}$$

One can select $\Gamma^\perp$ such that its rows are orthonormal, i.e. $\Gamma^\perp \left(\Gamma^\perp\right)^T = I$. Therefore, the cost function can be reformulated as:

$$f(P) = \sum_{i=1}^{k} p_i^2 \tag{3.40}$$

This gives a partial derivative if $f(P)$ equal to:

$$\frac{\partial f(P)}{\partial p_i} = 2p_i \tag{3.41}$$

Consequently:

$$\left(\nabla f(P)\right)^T = 2P \tag{3.42}$$

Incorporating (3.29) and (3.42) into (3.22) the solution to the Lagrange optimisation problem is calculated as:

$$P = \lambda \text{sum}_{\text{row}}\left(\Gamma^\perp\right) \tag{3.43}$$

The constraint equation (3.27) can be reformulated as:

$$P^T \text{sum}_{\text{row}}\left(\Gamma^\perp\right) = 1 \tag{3.44}$$

Incorporating (3.43) into (3.44) yields:

$$\lambda \left(\text{sum}_{\text{row}}\left(\Gamma^\perp\right)\right)^T \text{sum}_{\text{row}}\left(\Gamma^\perp\right) = 1 \tag{3.45}$$

Consequently, the Lagrange multiplier is calculated as:

$$\lambda = \left[\left(\text{sum}_{\text{row}}\left(\Gamma^\perp\right)\right)^T \text{sum}_{\text{row}}\left(\Gamma^\perp\right)\right]^{-1} \tag{3.46}$$

A simplified version of Algorithm 3.1 for single-output OE systems is given below:

Algorithm 3.2 (PE-UIO for single-output OE).

1. Select the order of the parity space $s \geq n$ and build matrices Γ, Q, T, and Ξ.
2. Obtain $\Gamma^{\perp}$ such that $\Gamma^{\perp}\left(\Gamma^{\perp}\right)^{T} = I$.
3. Obtain the Lagrange multiplier λ using (3.46).
4. Calculate the parameter vector P by (3.43).
5. Compute the vector W using (3.18).
6. Compute τ using (3.12).
7. Obtain the estimate of $v(t-\tau)$ via equation (3.8).

Multiple output OE

Consider the system (3.1), where $m > 1$, $\tilde{u}(t) = 0$, $\Pi = 0$ and Ω is diagonal. In such a case Ξ and consequently Σ, cf. (3.20), are diagonal matrices. Assume that $\Gamma^{\perp}$ is selected, such that its rows are orthonormal vectors, i.e. $\Gamma^{\perp}\left(\Gamma^{\perp}\right)^{T} = I$. Then the cost function $f(P)$ can be simplified to, cf. (3.40):

$$f(P) = \sum_{i=1}^{k} \beta_i p_i^2 \tag{3.47}$$

where β_i denotes the i^{th} element of the diagonal of Σ. Therefore, the partial derivative of $f(P)$ is calculated as:

$$\frac{\partial f(P)}{\partial p_i} = 2\beta_i p_i \tag{3.48}$$

Consequently, the gradient of $f(P)$ is:

$$\left(\nabla f(P)\right)^{T} = 2\Sigma P \tag{3.49}$$

Therefore, the Lagrange optimisation problem can be reformulated as, cf. (3.43):

$$\Sigma P = \lambda \mathrm{sum}_{\mathrm{row}}\left(\Gamma^{\perp}\right) \tag{3.50}$$

Incorporating (3.50) into (3.44) yields:

$$\lambda \left(\mathrm{sum}_{\mathrm{row}}\left(\Gamma^{\perp}\right)\right)^{T} \Sigma^{-1} \mathrm{sum}_{\mathrm{row}}\left(\Gamma^{\perp}\right) = 1 \tag{3.51}$$

Consequently, the Lagrange multiplier is calculated as:

$$\lambda = \left(\left(\text{sum}_{\text{row}}\left(\Gamma^{\perp}\right)\right)^{T} \Sigma^{-1} \text{sum}_{\text{row}}\left(\Gamma^{\perp}\right)\right)^{-1} \tag{3.52}$$

A simplified version of Algorithm 3.1 for multiple-output OE systems is given below:

Algorithm 3.3 (PE-UIO for multiple-output OE).

1. Select the order of the parity space $s \geq n$ and build matrices Γ, Q, T, and Ξ.
2. Obtain $\Gamma^{\perp}$ such that $\Gamma^{\perp}\left(\Gamma^{\perp}\right)^{T} = I$.
3. Obtain the Lagrange multiplier λ using (3.52).
4. Calculate the parameter vector P by:

$$P = \lambda \Sigma^{-1} \text{sum}_{\text{row}}\left(\Gamma^{\perp}\right) \tag{3.53}$$

5. Compute the vector W using (3.18).
6. Compute the estimation lag τ using (3.12).
7. Obtain the estimate of $v(t-\tau)$ via equation (3.8).

3.4 Analysis in frequency domain

The two relationships between each system input (both known and unknown) and the output can be described by discrete-time transfer functions of the z-variable of the following form, cf. (3.1):

$$\begin{aligned} G_u(z) &= C(zI - A)^{-1}B + D \\ G_v(z) &= C(zI - A)^{-1}G + H \end{aligned} \tag{3.54}$$

Denote $y(t)$, $u_0(t)$, and $v(t)$ in the z-domain, respectively, as $Y(z)$, $U_0(z)$, and $V(z)$. Consequently, equation (3.4) in the noise-free case can be reformulated as the following relation:

$$W(z)Y(z) = W_Q(z)U_0(z) + W_T(z)V(z) \tag{3.55}$$

where terms $W(z)$, $W_Q(z)$ and $W_T(z)$ are appropriate polynomial vectors of the z-variable with parameters defined by vectors W, WQ, and WT, respectively. Therefore, in the noise-free case, the relationship between the unknown input and its estimate in

the z-domain is given by, cf. (3.10) and (3.11):

$$\hat{V}(z) = W(z)Y(z) - W_Q(z)U_0(z) = W_T(z)V(z) \tag{3.56}$$

In the case when noise is present in the system, equation (3.56) becomes:

$$\hat{V}(z) = W_T(z)V(z) + W_\Xi(z)E(z) - W_Q(z)\tilde{U}(z) \tag{3.57}$$

where $W_\Xi(z)$ and $E(z)$ refer to, respectively, the appropriate polynomial vector of the z-variable with parameters defined by the vector $W\Xi$ and the variable $e(t)$ in z-domain, whilst $\tilde{U}(z)$ denotes the z-domain representation of $\tilde{u}(t)$.

In the case when $p = m = 1$ the transfer functions corresponding to $u_0(t)$ and $v(t)$ are given, respectively, by:

$$\begin{aligned} G_u(z) &= \frac{W_Q(z)}{W(z)} \\ G_v(z) &= \frac{W_T(z)}{W(z)} \end{aligned} \tag{3.58}$$

where $G_u(z)$ defines the relationship between $U_0(z)$ and the output, whereas $G_v(z)$ describes the relationship between $V(z)$ and $Y(z)$, cf. (3.54). In the case when $s = n$, the left nullspace of Γ is a row vector $\Gamma^\perp = W$ (it is assumed here that the system (3.1) is observable) and the degree of the polynomial $W(z)$ is equal to the order of the system. Hence, one can deduce from (3.58) that the roots of the polynomial $W(z)$ are eigenvalues of the matrix A (i.e. poles of both $G_v(z)$ and $G_u(z)$). Denote the set of poles and zeros of $G_v(z)$ by P_v and Z_v, respectively. Analogously, refer to P_u and Z_u as, respectively, poles and zeros of $G_u(z)$. Then, it is true that the roots of $W(z)$ are $P_v \cup P_u$, the roots of $W_Q(z)$ are defined by the set $Z_u \cup (P_v \backslash P_u)$, whilst roots of $W_T(z)$ are $Z_v \cup (P_u \backslash P_v)$.

If the order of the parity space is higher than that of the system, i.e. $s > n$, then the set of equations (3.58) must still be fulfilled. This means, that $W(z)$, $W_Q(z)$ and $W_T(z)$ have common $s - n$ roots (a zero-pole cancellation occurs, hence both $\frac{W_Q(z)}{W(z)}$ and $\frac{W_T(z)}{W(z)}$ remain unaltered). The choice of those additional $s - n$ zeros influences the properties of the noise filtration of the filter (3.13). Hence, the problem of finding the optimal vector W can be reformulated as a filter zeros assignment problem. The unknown input reconstruction is possible when the bandwidth of the unknown input is narrower than that of $W_T(z)$, whilst the ability of the PE-UIO to filter $\tilde{u}(t)$ and $e(t)$ depends on the frequency response of both, i.e. $W_Q(z)$ and $W(z)$.

3.5 Two stage PE-UIO

The previous section explains, why the PE-UIO cannot be used when the $G_v(z)$ contains a derivative term, i.e. a zero equal to unity. In such a case the polynomial $W_T(z)$ also contains the derivative term and its steady state gain is zero. Therefore, use of the standard PE-UIO for the purpose of the unknown input estimation is infeasible. Furthermore, if $G_v(z)$ contains a zero close to unity, the step response of $W_T(z)$ is characterised by a large overshoot (characteristic for systems whose zeros lie close to unity), hence the unknown input estimate becomes seriously affected. The overshoot of $W_T(z)$ can be minimised by a significant increase of the order of the parity space, however this results in a reduction of the bandwidth of the filter. Therefore, a modification of the PE-UIO is needed, and it is provided in the next subsection. Note that this problem will occur also for multiple input systems as long as the system has a single output. Thus, during the derivation of the modified PE-UIO filter in Subsection 3.5.1 it is assumed that the single output system may have an arbitrary number of measured inputs, i.e. $m = 1$ and $p \in \mathbb{N}$. The algorithm developed in the following section is applicable to systems, whose 'problematic' zero lies on the real axis and is lower or equal to unity. This result is extended in Section 3.6 to the cases with multiple zeros which lie on or within the unit circle and are relatively close to unity.

3.5.1 Two stage filter design

Consider a single output system, whose transfer function between the unknown input and the output, denoted as $G_v(z)$, contains a zero, denoted as z_0, which is close or equal to unity. Such a transfer function can be represented by:

$$G_v(z) = G'_v(z)\frac{z - z_0}{z} \tag{3.59}$$

Therefore, the input-output relationship in a z-domain can be represented as:

$$\begin{aligned} Y(z) &= G_v(z)V(z) + G_u(z)U_0(z) = G'_v(z)\frac{z - z_0}{z}V(z) + G_u(z)U_0(z) = \\ &= G'_v(z)V'(z) + G_u(z)U_0(z) \end{aligned} \tag{3.60}$$

where $V'(z) = \frac{z-z_0}{z}V(z)$ is the z-domain representation of the variable $v'(t)$, whose relation with the unknown input is defined as:

$$v'(t) = v(t) - z_0 v(t-1) \tag{3.61}$$

The transfer function $G'_v(z)$ can be represented by:

$$G'_v(z) = C(zI - A)^{-1}G' + H' \tag{3.62}$$

where H' and G' are the appropriately modified matrices H and G, respectively. The matrix T' is calculated by replacing G and H in T by, respectively, G' and H'. Subsequently, (3.5) can be reformulated as:

$$WT'V'(t) + W\Xi E(t) - WQ\tilde{U}(t) = WY(t) - WQU(t) \tag{3.63}$$

Analogously to the algorithm described in Section 3.3, it is proposed to estimate the variable $v'(t-\tau)$ as:

$$\hat{v}'(t-\tau) = WY(t) - WQU(t) \tag{3.64}$$

which in the noise-free case is equal to:

$$\hat{v}'(t-\tau) = WT'V'(t) \tag{3.65}$$

Subsequently, the unknown input estimate can be calculated via, cf. (3.61):

$$\hat{v}(t) = z_0\hat{v}(t-1) + \hat{v}'(t) \tag{3.66}$$

Note that this scheme is applicable only to systems with $|z_0| \leq 1$. Otherwise, (3.66) becomes unstable.

In the noisy case the term $\hat{v}'(t)$ is given by:

$$\hat{v}'(t-\tau) = WT'V'(t) + \epsilon(t) \tag{3.67}$$

where $\epsilon(t)$ accounts for the disturbance introduced by $e(t)$ and $\tilde{u}(t)$, i.e.:

$$\epsilon(t) = W\Xi E(t) - WQ\tilde{U}(t) \tag{3.68}$$

Hence, it follows from equations (3.66) and (3.67), that the estimate of $v(t-\tau)$ is affected by the error term $\epsilon^*(t)$, whose relation to $\epsilon(t)$ is given by:

$$\epsilon^*(t) = \epsilon(t) + z_0\epsilon^*(t-1) \tag{3.69}$$

For convenience, the following notation is introduced:

$$\begin{aligned} \tilde{u}^*(t) &= \tilde{u}(t) + z_0\tilde{u}^*(t-1) \\ e^*(t) &= e(t) + z_0 e^*(t-1) \end{aligned} \tag{3.70}$$

Thus, the term $\epsilon^*(t)$ is given by:

$$\epsilon^*(t) = W\Xi E^*(t) - WQ\tilde{U}^*(t) \tag{3.71}$$

where terms $E^*(t)$ and $\tilde{U}^*(t)$ are built from the current and previous values of $e^*(t)$ and $\tilde{u}^*(t)$, respectively, cf. (3.2). It is required to minimise the variance of the term

$\epsilon^*(t)$, which is given by:

$$\begin{aligned}\operatorname{var}(\epsilon^*(t)) &= \mathrm{E}\{(W\Xi E^*(t) - WQ\tilde{U}^*(t))(W\Xi E^*(t) - WQ\tilde{U}^*(t))^T\} = \\ &= W\Xi\Sigma_{e^*}\Xi^T W^T + WQ\Sigma_{\tilde{u}^*}Q^T W^T - W\Xi\left(\Sigma_{\tilde{u}^*e^*}\right)^T Q^T W^T - WQ\Sigma_{\tilde{u}^*e^*}\Xi^T W^T\end{aligned} \tag{3.72}$$

where $\Sigma_{\tilde{u}^*} = \mathrm{E}\{\tilde{U}^*(t)(\tilde{U}^*(t))^T\}$, $\Sigma_{e^*} = \mathrm{E}\{E^*(t)E^{*T}(t)\}$ and $\Sigma_{\tilde{u}^*e^*} = \mathrm{E}\{\tilde{U}^*(t)E^{*T}(t)\} = 0$. Hence, the function to be minimised is given by:

$$f(W) = W\Xi\Sigma_{e^*}\Xi^T W^T + WQ\Sigma_{\tilde{u}^*}Q^T W^T \tag{3.73}$$

In order to calculate (3.73), first, the terms Σ_{e^*} and $\Sigma_{\tilde{u}^*}$ need to be obtained. The signal $e^*(t)$ can be described by a function of its previous values, cf. (3.70):

$$e^*(t) = e(t) + z_0 e(t-1) + z_0^2 e(t-2) + \cdots \tag{3.74}$$

Therefore, by recalling that $e(t)$ is assumed white, the expected value of $e^*(t)e^*(t-i)$ is calculated as:

$$\begin{aligned}\mathrm{E}\{e^*(t)e^*(t-i)\} &= \mathrm{E}\{z_0^i e^2(t-i) + z_0^{i+2}e^2(t-i-1) + z_0^{i+4}e^2(t-i-2) + \cdots\} \\ &= \mathrm{E}\{e^2(t)\}z_0^i\left(1 + z_0^2 + z_0^4 + \cdots\right)\end{aligned} \tag{3.75}$$

which is a sum of a geometric series and in the case when $|z_0| < 1$ it can be simplified to:

$$\mathrm{E}\{e^*(t)e^*(t-i)\} = \mathrm{E}\{e^2(t)\}\frac{z_0^i}{1-z_0^2} \tag{3.76}$$

Analogously, by recalling that $\tilde{u}(t)$ is assumed white, the expected value of $\tilde{u}^*(t)\tilde{u}^*(t-1)$ can be derived as:

$$\mathrm{E}\{\tilde{u}^*(t)(\tilde{u}^*(t-i))^T\} = \mathrm{E}\{\tilde{u}(t)\tilde{u}^T(t)\}\frac{z_0^i}{1-z_0^2} \tag{3.77}$$

(Note that $e(t)$ is a scalar, whilst $\tilde{u}(t)$ is, in general, a vector.) In the case when $|z| = 1$ the sum of the geometric series (3.75) is infinite. Therefore, to cope with such a case it is proposed to replace z_0 in (3.76) and (3.77) by a value smaller than unity in order to indicate that $e^*(t)$ and $\tilde{u}^*(t)$ are not white.

The matrices Σ_{e^*} and $\Sigma_{\tilde{u}^*}$ are built by filling their entries by the appropriate values of, respectively, $\mathrm{E}\{e^*(t)e^*(t-i)\}$ and $\mathrm{E}\{\tilde{u}^*(t)\tilde{u}^*(t-i)\}$. For convenience, a new term is introduced, cf. (3.20):

$$\Sigma^* = \Xi\Sigma_{e^*}\Xi^T + Q\Sigma_{\tilde{u}^*}Q^T \tag{3.78}$$

Hence, the cost function (3.73) becomes:

$$f(P) = \left(\sum_{i=1}^{s-n+1} p_i \gamma_i^T \right) \Sigma^* \left(\sum_{j=1}^{s-n+1} p_j \gamma_j \right) \tag{3.79}$$

which is required to be minimised subject to the constraint:

$$g(P) = \mathrm{sum}_{\mathrm{row}}(WT') - 1 = 0 \tag{3.80}$$

The solution to this constrained optimisation problem is solved analogously to the one in Section 3.3. Therefore, the algorithm for calculating the unknown input is summarised as follows:

Algorithm 3.4 (Two stage PE-UIO).

1. Select the order of the parity space $s \geq n$ and build matrices Γ, Q, T', and Ξ.
2. Obtain $\Gamma^{\perp}$.
3. Calculate Σ_{e^*} and $\Sigma_{\tilde{u}^*}$ using (3.76) and (3.77), respectively.
4. Compute Σ^* using (3.78).
5. Calculate the matrix S by:

$$S = \Gamma^{\perp} \Sigma^* (\Gamma^{\perp})^T + (\Gamma^{\perp} \Sigma^* (\Gamma^{\perp})^T)^T \tag{3.81a}$$

6. Calculate the column vector ψ via:

$$\psi = \mathrm{sum}_{\mathrm{row}}(\Gamma^{\perp} T') \tag{3.81b}$$

7. Obtain the Lagrange multiplier λ via:

$$\lambda = \left(\left(S^{-1} \psi \right)^T \psi \right)^{-1} \tag{3.81c}$$

8. Calculate the parameter vector P by:

$$P = \lambda S^{-1} \psi \tag{3.81d}$$

9. Compute the vector W, cf. (3.18), as:

$$W = P^T \Gamma^{\perp} \tag{3.81e}$$

10. Calculate the estimation lag as:

$$\tau = \text{round}\left(\frac{\sum \alpha_i' i}{\sum \alpha_i'}\right), \text{ for } i = 0, \cdots, s \tag{3.81f}$$

where α_i parameters are defined by the equation:

$$WT' = \begin{bmatrix} \alpha_s' & \alpha_{s-1}' & \cdots & \alpha_0' \end{bmatrix}^T \tag{3.81g}$$

11. Obtain $\hat{v}'(t-\tau)$ via:

$$\hat{v}'(t-\tau) = WT'V'(t) \tag{3.81h}$$

12. Obtain the estimate of $v(t-\tau)$ as:

$$\hat{v}(t-\tau) = z_0\hat{v}(t-\tau-1) + \hat{v}'(t-\tau) \tag{3.81i}$$

3.5.2 Analysis in frequency domain

The variable $v'(t-\tau)$ in the z-domain is given by, cf. (3.64):

$$V'(z) = W_{T'}(z)V'(z) - W_Q(z)\tilde{U}(z) + W_\Xi(z)E(z) \tag{3.82}$$

where the coefficients of the polynomial $W_{T'}(z)$ are appropriate elements of the vector WT'. Consequently, the unknown input estimate in the z-domain is, see (3.57):

$$\hat{V}(z) = W_{T'}(z)V(z) - \frac{z}{z-z_0}W_Q(z)\tilde{U}(z) + \frac{z}{z-z_0}W_\Xi(z)E(z) \tag{3.83}$$

It can be deduced that the use of the two stage PE-UIO is advisable if z_0 is a positive real number lower or equal unity. Firstly, if the single stage PE-UIO is used in such a case, the presence of z_0 in $W_T(z)$ will cause an overshoot in the step response of the input estimation filter, which may me undesirable. Secondly, the factor $\frac{z}{z-z_0}$, for $0 \leq z_0 \leq 1$, reduces the bandwidth of the noise affecting the input estimate, cf. (3.83). On the other hand the use of the single stage PE-UIO may be preferred over its two stage version if $z_0 > 0$ is relatively close to zero, and the phase lead caused by the presence of z_0 is desirable, e.g. in an on-line application, when the fast response of the filter is required. It is not recommended to use the two stage PE-UIO in noisy systems when z_0 is lower than zero, due to highpass properties of $\frac{z}{z-z_0}$, which would cause an amplification of noise effect on the unknown input estimate.

3.6 Generalised two stage PE-UIO

The two stage PE-UIO presented in Section 3.5 is used to cope with a single 'problematic' zero. It is worth exploring a generalised form of the-two stage PE-UIO, which can eliminate more than one 'inconvenient' zero. Therefore, the transfer function $G_v(z)$ can be formulated as, cf. (3.59):

$$G_v(z) = M_v(z)N_v(z) \tag{3.84}$$

where $N_v(z)$ is in a form of:

$$N_v(z) = \frac{\sum_{i=1}^{k}(z - z_i)}{z^k} \tag{3.85}$$

and k denotes the number of zeros which need to be eliminated from the unknown input reconstruction filter. In general it is assumed that zeros $z_1, \cdots, z_k$ are complex (with the constraint of conjugate symmetry). Similarly, as in Section 3.5, zeros $z_1, \cdots, z_k$ must be stable or marginally stable. Consider a variable $v'(t)$, cf.(3.61), which in z-domain is given by:

$$V'(z) = N_v(z)V(z) \tag{3.86}$$

Consequently:

$$G_v(z)V(z) = M_v(z)V'(z) \tag{3.87}$$

The transfer function $M_v(z)$ is defined as:

$$M_v(z) = C(zI - A)^{-1}G' + H' \tag{3.88}$$

where H' and G' are the appropriately modified matrices H and G, respectively. The matrix T' is calculated by replacing G and H in T by, respectively, G' and H'. Subsequently, in the first stage of the algorithm, the term $V'(z)$ is estimated as:

$$\hat{V}'(z) = W(z)Y(z) - W_Q(z)U(z) \tag{3.89}$$

The unknown input is calculated in the second stage of the algorithm as:

$$V(z) = N_v^{-1}(z)V'(z) \tag{3.90}$$

where $N_v^{-1}(z)$ is defined as:

$$N_v^{-1}(z) = \frac{z^k}{\sum_{i=1}^{k}(z - z_i)} \tag{3.91}$$

In the case when noise is present in the system, the variable $V'(z)$ is given by, cf. (3.64), (3.67) and (3.68):

$$\hat{V}'(z) = W_T'(z)V'(z) + W_\Xi(z)E(z) - W_Q(z)\tilde{U}(z) \tag{3.92}$$

Therefore, the unknown input estimate is, cf. (3.90):

$$\hat{V}(z) = W_T'(z)V(z) + W(z)_{\Xi}N_v^{-1}(z)E(z) - W_Q(z)N_v^{-1}(z)\tilde{U}(z) \tag{3.93}$$

The following notation is used:

$$E^*(z) = N_v^{-1}(z)E(z) \tag{3.94}$$

The term $E^*(z)$ is denoted in time domain as $e^*(t)$ and, subsequently, the stacked vector of $e^*(t)$ is $E^*(t)$. Analogous notation is used for $N_v^{-1}\tilde{U}(z)$, i.e. $\tilde{U}^*(z)$, $\tilde{u}^*(t)$, and $\tilde{U}^*(t)$.

Analogously to (3.72), the variance of the following term must be minimised:

$$\begin{aligned}&\mathrm{E}\{(W\Xi E^*(t) - WQ\tilde{U}^*(t))(W\Xi E^*(t) - WQ\tilde{U}^*(t))^T\} = \\ &= W\Xi\Sigma_{e^*}\Xi^T W^T + WQ\Sigma_{\tilde{u}^*}Q^T W^T - W\Xi\left(\Sigma_{\tilde{u}^*e^*}\right)^T Q^T W^T - WQ\Sigma_{\tilde{u}^*e^*}\Xi^T W^T\end{aligned} \tag{3.95}$$

where $\Sigma_{\tilde{u}^*} = \mathrm{E}\{\tilde{U}^*(t)(\tilde{U}^*(t))^T\}$, $\Sigma_{e^*} = \mathrm{E}\{E^*(t){E^*}^T(t)\}$ and $\Sigma_{\tilde{u}^*e^*} = \mathrm{E}\{\tilde{U}^*(t){E^*}^T(t)\} = 0$. Hence, the function to be minimised is given by:

$$f(W) = W\Sigma^* W^T \tag{3.96}$$

where:

$$\Sigma^* = \Xi\Sigma_{e^*}\Xi^T + Q\Sigma_{\tilde{u}^*}Q^T \tag{3.97}$$

The covariance matrices Σ_{e^*} and $\Sigma_{\tilde{u}^*}$ depend on $z_i, i = 1, \cdots, k$ and variances of $e(t)$ and $\tilde{u}(t)$ and should be calculated for each case individually. Finally, the generalised two stage PE-UIO is summarised as follows:

Algorithm 3.5 (Generalised two stage PE-UIO).

1. Select zeros, $z_1, \cdots, z_k$, which need to be eliminated from the PE.
2. Calculate $N_v(z)$ using (3.85).
3. Select the order of the parity space $s \geq n$ and build matrices Γ, Q, T', and Ξ.
4. Obtain $\Gamma^{\perp}$.
5. Calculate Σ_{e^*} and $\Sigma_{\tilde{u}^*}$.
6. Compute Σ^* using (3.97).
7. Calculate the matrix S by:

$$S = \Gamma^{\perp}\Sigma^*(\Gamma^{\perp})^T + (\Gamma^{\perp}\Sigma^*(\Gamma^{\perp})^T)^T \tag{3.98a}$$

8. Calculate the column vector ψ via:

$$\psi = \text{sum}_{\text{row}}(\Gamma^{\perp} T') \tag{3.98b}$$

9. Obtain the Lagrange multiplier λ as:

$$\lambda = \left(\left(S^{-1} \psi \right)^T \psi \right)^{-1} \tag{3.98c}$$

10. Calculate the parameter vector P by:

$$P = \lambda S^{-1} \psi \tag{3.98d}$$

11. Compute the vector W as:

$$W = P^T \Gamma^{\perp} \tag{3.98e}$$

12. Calculate the estimation lag using (3.81f).

13. Obtain $\hat{v}'(t-\tau)$ as:

$$v'(t-\tau) = WY(t) - WQU(t) \tag{3.98f}$$

14. Obtain the estimate of the unknown input using (3.90).

3.7 Tutorial examples

In this section the design of the proposed approaches is demonstrated on numerical examples. In Subsection 3.7.1 the design of the PE-UIO is demonstrated on two examples, namely, an OE case as well as an ARMAX system in the EIV framework. The influence of the choice of the tuning parameter s on the frequency response of the filter is also presented. In Subsection 3.7.2 the design of the two stage PE-UIO is demonstrated and compared with the standard PE-UIO.

Although the examples presented here are described by feedtrough models, it should be noted that the causality of physical systems assumes that there is a delay on the system input, denoted as δ, which results in the transfer function defined by:

$$G(z^{-1}) = \frac{b_n z^{-\delta} + b_{n-1} z^{-1-\delta} + \cdots + b_0 z^{-n-\delta}}{a_n + a_{n-1} z^{-1} + \cdots + a_0 z^{-n}} \tag{3.99}$$

where z^{-1} is a backwards shift operator, i.e. $z^{-1} y(t) = y(t-1)$, $G(z^{-1})$ denotes the transfer function between any of the system input (either $v(t)$ or $u(t)$) and the output,

a_i and b_i, $i = 1, \cdots, n$, are transfer function polynomial coefficients, and n refers to the order of the system. Without loss of generality, the delay term δ can be omitted and therefore, the transfer function $G(z^{-1})$ can be represented by:

$$G(z^{-1}) = \frac{b_n + b_{n-1}z^{-1} + \cdots + b_0 z^{-n}}{a_n + a_{n-1}z^{-1} + \cdots + a_0 z^{-n}} \tag{3.100}$$

which corresponds to the following z-domain transfer fuction:

$$G(z) = \frac{b_n z^n + b_{n-1}z^{n-1} + \cdots + b_0}{a_n z_n + a_{n-1}z^{n-1} + \cdots + a_0} \tag{3.101}$$

3.7.1 PE-UIO

This subsection presents a step-by-step design of the PE-UIO algorithm for two different cases, namely, an OE and an ARMAX case in the EIV framework. The importance of the tuning parameter s on the frequency response of the filter is also explained.

Example 3.1. Design of the PE-UIO in the OE case
Consider a linear system, whose transfer functions, $G_u(z)$ and $G_v(z)$, cf. (3.54) are given by:

$$\begin{aligned} G_u(z) &= \frac{z + 0.01}{(z - 0.9)(z - 0.85)} \\ G_v(z) &= \frac{(z + 1.95)(z - 0.2)}{(z - 0.9)(z - 0.85)} \end{aligned} \tag{3.102}$$

It can be represented by equation (3.1), whose matrices are given by:

$$\begin{aligned} A &= \begin{bmatrix} 1.750 & 1 \\ -0.765 & 0 \end{bmatrix} \quad B = \begin{bmatrix} 1.00 \\ 0.01 \end{bmatrix} \quad G = \begin{bmatrix} 3.500 \\ -1.155 \end{bmatrix} \\ C &= \begin{bmatrix} 1 & 0 \end{bmatrix} \qquad D = 0 \qquad H = 1 \end{aligned} \tag{3.103}$$

It is assumed that the output of the system is affected by a white, zero-mean, Gaussian noise sequence of the variance $\mathrm{var}(e(t)) = 1$. Since the considered case is single-output OE, Algorithm 3.3 is used for the unknown input reconstruction.

The parity space order is chosen to be $s = 4$, hence the extended observability matrix is:

$$\Gamma = \begin{bmatrix} 1.0000 & 0 \\ 1.7500 & 1 \\ 2.2975 & 1.7500 \\ 2.6819 & 2.2975 \\ 2.9357 & 2.6819 \end{bmatrix} \tag{3.104}$$

The left nullspace of Γ is calculated as:

$$\Gamma^{\perp} = \begin{bmatrix} -0.3578 & 0.1454 & 0.8094 & -0.2794 & -0.3431 \\ -0.3118 & 0.4635 & -0.2389 & 0.5947 & -0.5264 \\ -0.2720 & 0.6999 & -0.2723 & -0.4955 & 0.3412 \end{bmatrix} \tag{3.105}$$

Note that $\Gamma^{\perp}$ is orthonormal, i.e. $\Gamma^{\perp}(\Gamma^{\perp})^T = I$. The matrix Q is given by:

$$Q = \begin{bmatrix} 0 & 0 & 0 & 0 & 0 \\ 1 & 0 & 0 & 0 & 0 \\ 1.7600 & 1 & 0 & 0 & 0 \\ 2.3150 & 1.7600 & 1 & 0 & 0 \\ 2.7049 & 2.3150 & 1.7600 & 1 & 0 \end{bmatrix} \tag{3.106}$$

whereas the matrix T is:

$$T = \begin{bmatrix} 1.0000 & 0 & 0 & 0 & 0 \\ 3.5000 & 1.0000 & 0 & 0 & 0 \\ 4.9700 & 3.5000 & 1.0000 & 0 & 0 \\ 6.0200 & 4.9700 & 3.5000 & 1.0000 & 0 \\ 6.7330 & 6.0200 & 4.9700 & 3.5000 & 1.0000 \end{bmatrix} \tag{3.107}$$

Using (3.46) the Lagrange multiplier λ is calculated to be 0.0403. Subsequently, the parameter vector P is obtained using (3.43):

$$P = \begin{bmatrix} -0.1608 \\ -0.1199 \\ 0.0083 \end{bmatrix} \tag{3.108}$$

The vector W is calculated as, cf. (3.18):

$$W = \begin{bmatrix} 0.0927 & -0.0732 & -0.1038 & -0.0305 & 0.1211 \end{bmatrix} \tag{3.109}$$

Consequently, the vector WT is :

$$W = \begin{bmatrix} -0.0480 & 0.1463 & 0.3856 & 0.3929 & 0.1232 \end{bmatrix} \tag{3.110}$$

which corresponds to $\tau = 1$, cf. (3.12). Therefore, $\hat{v}(t-1)$ is calculated via:

$$\begin{aligned} \hat{v}(t-1) = {} & 0.1211y(t) - 0.0305y(t-1) - 0.1038y(t-2) - 0.0732y(t-3) + \\ & 0.0927y(t) + 0.1211u(t) + 0.1827u(t-1) + 0.1229u(t-2) + 0.0012u(t-3) \end{aligned} \tag{3.111}$$

Example 3.2. Design of the PE-UIO for an ARMAX system in the EIV framework

Consider an ARMAX system, whose A, B, C, D, G, and H matrices are the same as in Example 3.1. The moving average coloured noise parameters are $c_0 = 1$, $c_1 = 0.3$, and $c_2 = 0.1$. It is assumed that the input measurement is affected by a white, zero-mean, Gaussian noise $\tilde{u}(t)$ of the variance equal to the variance of $e(t)$. Thus the noise distribution matrix is given by:

$$\Pi = \begin{bmatrix} 2.050 \\ -0.665 \end{bmatrix} \tag{3.112}$$

whereas $\Omega = 1$. The parity space order is selected as $s = 4$. Matrices Q, T, Γ, and $\Gamma^{\perp}$ are the same as in Example 3.1. Then, one can compute the matrix Ξ as:

$$\Xi = \begin{bmatrix} 1 & 0 & 0 & 0 & 0 \\ 2.0500 & 1 & 0 & 0 & 0 \\ 2.9225 & 2.0500 & 1 & 0 & 0 \\ 3.5461 & 2.9225 & 2.0500 & 1 & 0 \\ 3.9700 & 3.5461 & 2.9225 & 2.05 & 1 \end{bmatrix} \tag{3.113}$$

Note that the variances of $\tilde{u}(t)$ and $e(t)$ are unknown, however for the purpose of finding the optimal filter parameters only the ratio between those variances is needed, which is equal to one. Substituting unity for the variances of both $\tilde{u}(t)$ and $e(t)$, the term Σ is calculated using (3.37a):

$$\Sigma = \begin{bmatrix} 1.0000 & 2.0500 & 2.9225 & 3.5461 & 3.9700 \\ 2.0500 & 6.2025 & 9.8011 & 12.5071 & 14.3895 \\ 2.9225 & 9.8011 & 17.8411 & 24.2391 & 28.8699 \\ 3.5461 & 12.5071 & 24.2391 & 35.7753 & 44.5789 \\ 3.9700 & 14.3895 & 28.8699 & 44.5789 & 58.8525 \end{bmatrix} \tag{3.114}$$

whereas S is equal to, cf. (3.37b):

$$S = \begin{bmatrix} 5.6976 & 3.5814 & -0.2238 \\ 3.5814 & 2.8100 & -0.3369 \\ -0.2238 & -0.3369 & 1.0128 \end{bmatrix} \tag{3.115}$$

Consequently, the vector ψ is given by, cf. (3.37c):

$$\psi = \begin{bmatrix} -3.9894 \\ -2.9748 \\ 0.2060 \end{bmatrix} \tag{3.116}$$

Using (3.37d), the Lagrange multiplier is calculated as $\lambda = 3.1271$ and the parameter vector P is computed from (3.37e) as:

$$P = \begin{bmatrix} -0.0477 \\ -0.2749 \\ -0.0383 \end{bmatrix} \tag{3.117}$$

Finally, the vector W is obtained using (3.37f):

$$W = \begin{bmatrix} 0.1132 & -0.1612 & 0.0375 & -0.1312 & 0.1480 \end{bmatrix} \tag{3.118}$$

The estimation lag is equal to 1. Therefore, the unknown input estimate $\hat{v}(t-1)$ is calculated via:

$$\begin{aligned} \hat{v}(t-1) = {} & 0.1480y(t) - 0.1312y(t-1) + 0.0375y(t-2) - 0.1612y(t-3) + \\ & 0.1132y(t-4) + 0.1480u(t-1) + 0.1293u(t-2) + \\ & 0.1492u(t-3) + 0.0015u(t-4) \end{aligned} \tag{3.119}$$

Importance of the tuning parameter s

The order of the parity space s is a tuning parameter of the PE-UIO algorithm. It is anticipated that an increase of s will lead to a reduction of the impact of disturbances on the unknown input estimate. At the same time it is expected that an increase of the order of parity space will yield a reduction of the filter bandwidth, which will result in the input reconstruction filter being sluggish. This phenomenon can be seen in Fig. 3.2, where the frequency responses of the polynomial filters $W_T(z)$, $W_Q(z)$, and $W(z)$, cf. (3.55), for three different cases of s are compared. This effect is also visible in Fig. 3.3, where the reconstructed input signals are compared for different values of parity space orders. The system from Example 3.1 is considered in this experiment. Whilst for $s = 4$ the unknown input estimate is noisy (i.e. the noise filtering is rather poor in this case), for $s = 15$ the filter does not reproduce high frequency oscillations of the input. The PE-UIO with $s = 7$ seems to be the optimal setting for the given example.

3.7.2 Two stage PE-UIO

In this subsection a design of the two stage PE-UIO is presented on a numerical example. Furthermore, using different scenarios, the efficacy of the algorithm is compared with that of the standard PE-UIO.

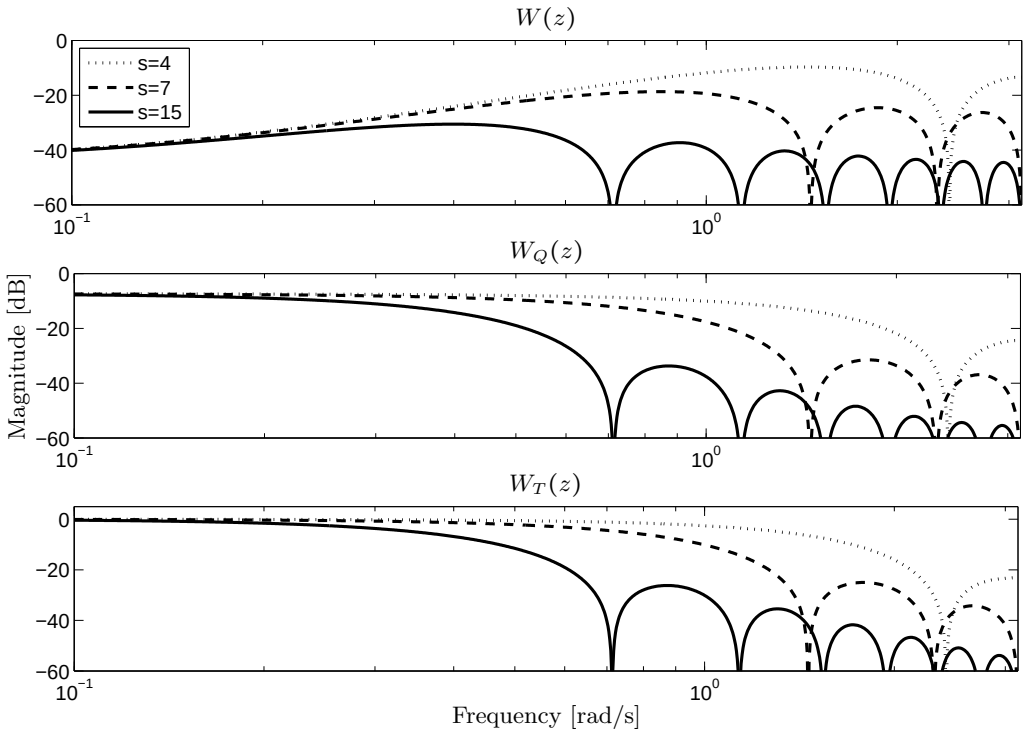

Figure 3.2: Frequency responses of $W(z)$, $W_Q(z)$ and $W_T(z)$ for different values of the parity space order s

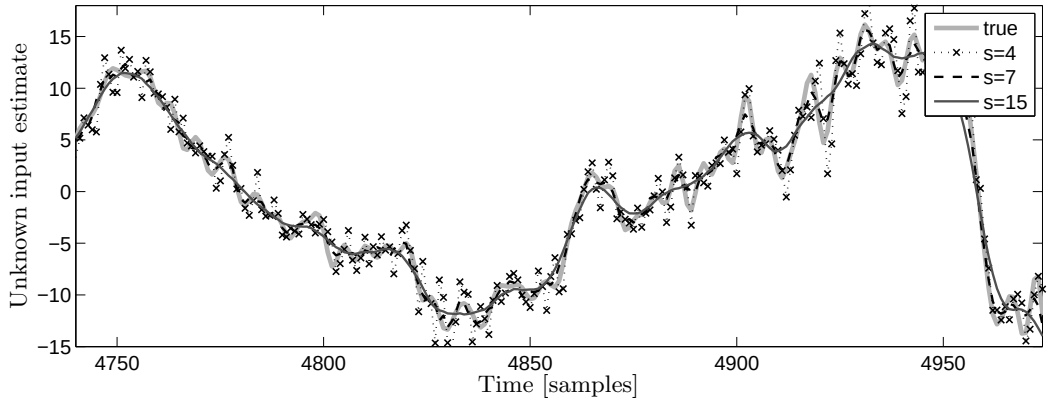

Figure 3.3: Comparison of unknown input estimates for different values of s

Example 3.3. Design of the two stage PE-UIO for an OE model

Consider a linear system, whose transfer functions, $G_u(z)$ and $G_v(z)$ are given by:

$$\begin{aligned} G_u(z) &= \frac{z-0.1}{(z-0.9)(z-0.8)} \\ G_v(z) &= \frac{(z+1.2)(z-0.95)}{(z-0.9)(z-0.8)} \end{aligned} \tag{3.120}$$

It can be represented by the state-space model (3.1), whose matrices are:

$$A = \begin{bmatrix} 1.70 & 1 \\ -0.72 & 0 \end{bmatrix} \quad B = \begin{bmatrix} 1 \\ -0.1 \end{bmatrix} \quad G = \begin{bmatrix} 1.95 \\ -1.86 \end{bmatrix}$$
$$C = \begin{bmatrix} 1 & 0 \end{bmatrix} \qquad D = 0 \qquad H = 1 \tag{3.121}$$

It is assumed that the output of the system is subjected to white, zero-mean, Gaussian measurement noise (OE case) of the variance $\mathrm{var}(e(t)) = 2.7$. After elimination of the zero at 0.95, the corresponding modified matrices H' and G' are built such that $H' = 1$ and:

$$G' = \begin{bmatrix} 2.90 \\ -0.72 \end{bmatrix} \tag{3.122}$$

The covariance of $e^*(t)$ is calculated as, cf. (3.76):

$$\mathrm{E}\{e^*(t)e^*(t-i)\} = \mathrm{var}(e(t))\frac{0.95^i}{1-0.95^2} \tag{3.123}$$

Consequently:

$$\Sigma_{e^*} = 2.7 \begin{bmatrix} 1.0000 & 0.9500 & 0.9025 & 0.8574 & 0.8145 & 0.7738 \\ 0.9500 & 1.0000 & 0.9500 & 0.9025 & 0.8574 & 0.8145 \\ 0.9025 & 0.9500 & 1.0000 & 0.9500 & 0.9025 & 0.8574 \\ 0.8574 & 0.9025 & 0.9500 & 1.0000 & 0.9500 & 0.9025 \\ 0.8145 & 0.8574 & 0.9025 & 0.9500 & 1.0000 & 0.9500 \\ 0.7738 & 0.8145 & 0.8574 & 0.9025 & 0.9500 & 1.0000 \end{bmatrix} \frac{1}{1-0.95^2} \tag{3.124}$$

The vector W is calculated to be:

$$W = \begin{bmatrix} 0.0658 & -0.0576 & -0.0417 & -0.0292 & -0.0196 & 0.0914 \end{bmatrix} \tag{3.125}$$

which corresponds to $\tau = 3$. Therefore, the unknown input is computed via:

$$\begin{aligned} v'(t-3) = {} & 0.0914y(t) - 0.0196y(t-1) - 0.0292y(t-2) - 0.0417y(t-3) - \\ & 0.0576y(t-4) + 0.0658y(t-5) + 0.0914u(t-1) + 0.1267u(t-2) + \\ & 0.1223u(t-3) + 0.0779u(t-4) - 0.0091u(t-5) \\ v(t) = {} & v'(t) + 0.95v(t-1) \end{aligned} \tag{3.126}$$

Fig. 3.4 compares step responses of $W_{T'}(t)$ for the two stage PE-UIO with $s = 5$ and $W_T(t)$ for two cases of the standard PE-UIO ($s = 5$ and $s = 15$). It can be noted that the system zero at 0.95 causes a large overshoot in the case when the standard PE-UIO is used (for both $s = 5$ and $s = 15$). This results in a significant distortion of the unknown input estimate, which can be seen in Fig. 3.5, where the time-domain result of

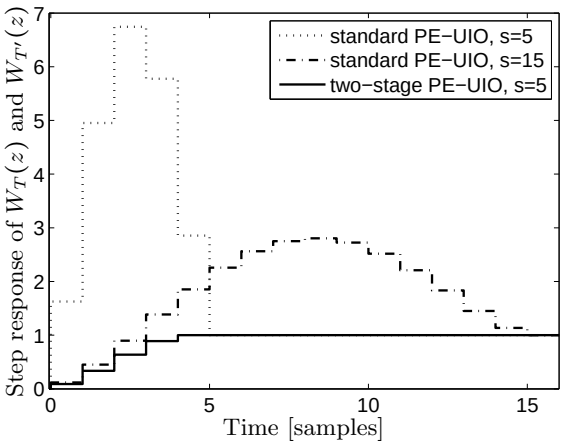

Figure 3.4: Step responses of $W_{T'}(t)$ for the two stage PE-UIO and $W_T(t)$ for two cases of the standard PE-UIO

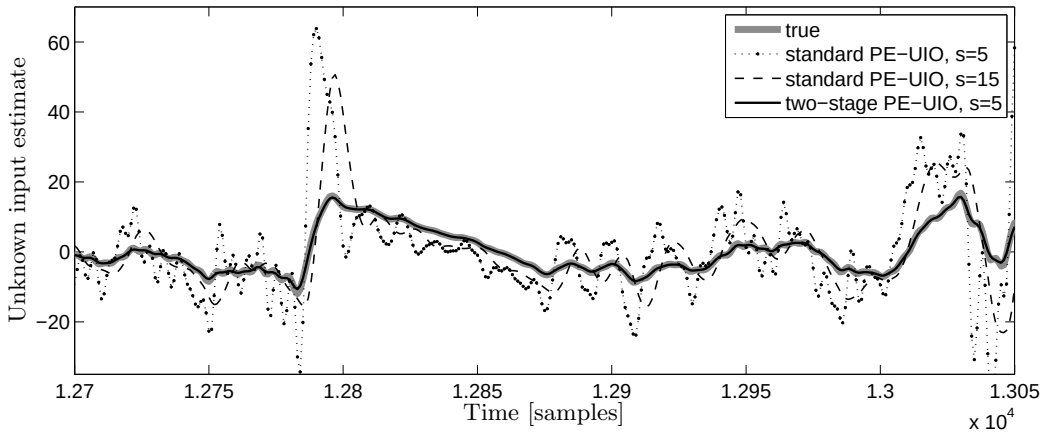

Figure 3.5: Comparison of the unknown input estimate using the two stage PE-UIO and the standard PE-UIO, z_0 = 0.95. Distortion of the unknown input estimate caused by the phase lead can be seen in the case of the standard PE-UIO.

the unknown input reconstruction in a noise-free case is shown. The advantage of the two stage PE-UIO in this particular case can be also seen in Fig. 3.6, where frequency responses of $W(z)$, $W_Q(z)$, $W_T(t)$, and $W_{T'}(t)$ are presented.

Example 3.4. Comparison of the standard and the two stage PE-UIO in an on-line application

In this example a situation is presented, where the phase lead introduced by the PE-UIO is advantageous. Consider an on-line application, where an estimation delay is crucial for the system performance, e.g. where the reconstructed input is utilised by a feedback controller. Bearing in mind that at the time instance t the delayed input

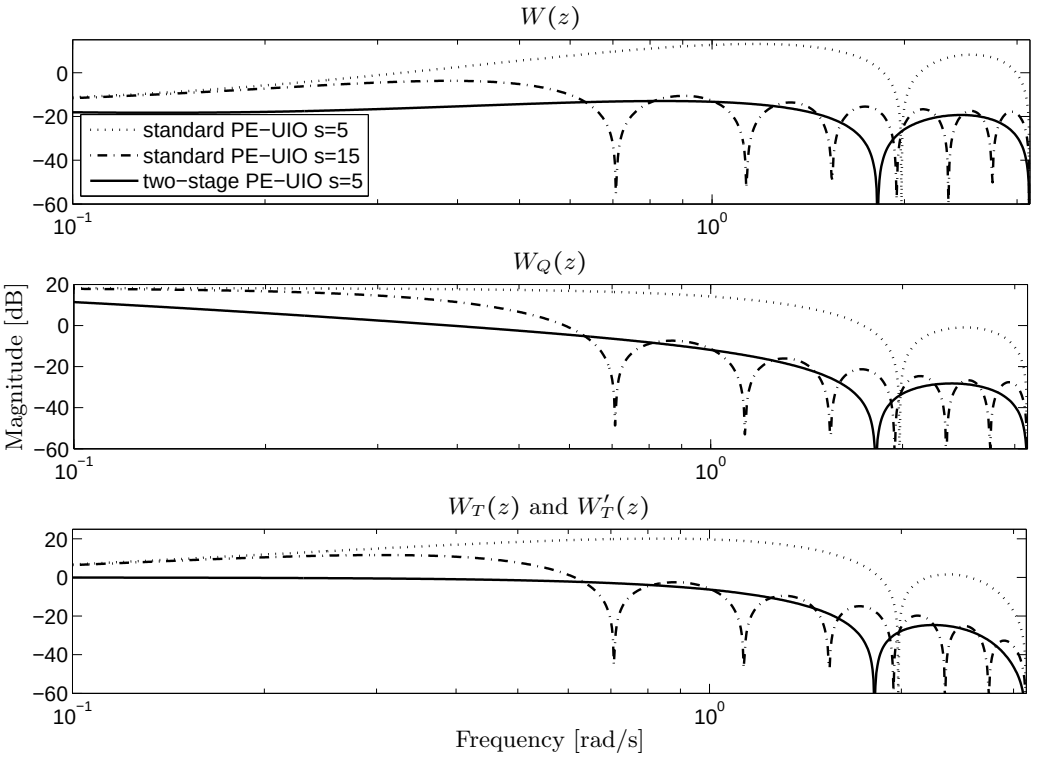

Figure 3.6: Frequency responses of $W_{T'}(t)$ for the two stage PE-UIO and $W_T(t)$ for two cases of the standard PE-UIO

estimate $\hat{v}(t-\tau)$ is obtained, the on-line estimation error is defined as:

$$\epsilon_{\text{on-line}}(t) = \hat{v}(t-\tau) - v(t) \tag{3.127}$$

(In contrary, in an off-line situation or when the estimation delay is not crucial the difference between $\hat{v}(t-\tau)$ and $v(t-\tau)$ is taken into consideration.)

The system used in this example is given by the equation:

$$G_v(z) = \frac{(z-0.3)(z+1.8)}{(z-0.8)(z-0.9)} \tag{3.128}$$

The zero at $z_0 = 0.3$ causes a phase lead (and consequently an overshoot of the step response) of $W_T(z)$ when the standard PE-UIO is used. However, it is expected that the zero at 0.3 will reduce the impact of the estimation lag caused by the zero at −1.8. (Due for the fact that 0.3 lies relatively far from unity, it is not expected to cause such as damaging distortion in the step response of $W_T(z)$ as shown in Example 3.3.) Consequently, a faster response is anticipated when using the PE-UIO instead of the two stage PE-UIO with $z_0 = 0.3$, which may be particularly desired in on-line applications.

In Fig. 3.7, for completeness, step responses of $W_T(z)$, for the standard PE-UIO,

and $W_{T'}(z)$, for the two stage PE-UIO, are compared (the parity space order is in both cases $s = 2$).

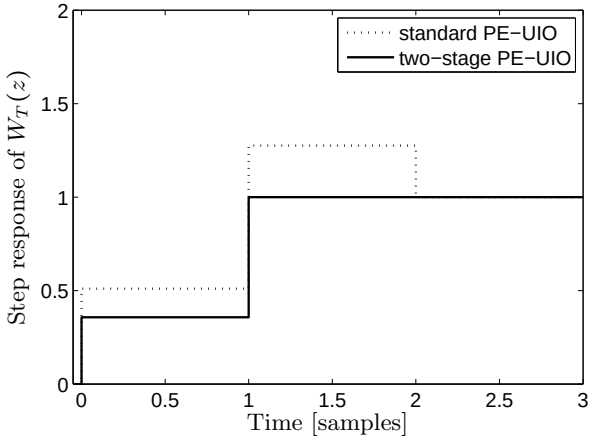

Figure 3.7: Step responses of $W_T(z)$ and $W_{T'}(z)$, $s = 2$, $z_0 = 0.3$

Sample time responses of the unknown input estimates using the two algorithms are presented in Fig. 3.8. It is assumed that the output of the system is subjected

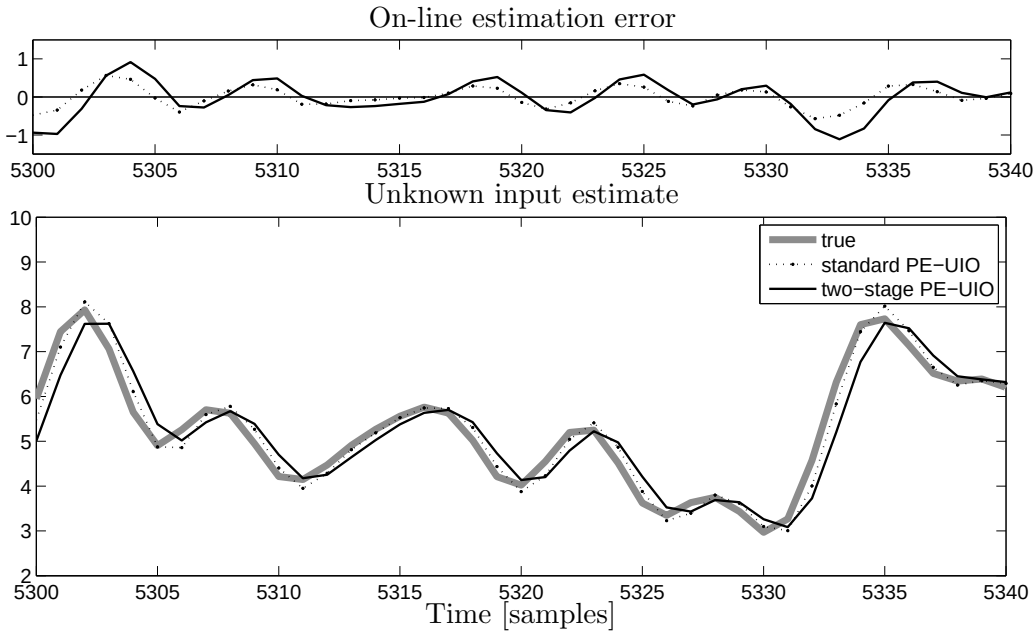

Figure 3.8: On-line unknown input estimation using the standard PE-UIO and the two stage PE-UIO. In both cases order of parity space $s = 2$, variance of noise $\mathrm{var}(e(t))$ = 14e-4.

to low level OE noise ($\mathrm{var}(e(t))$ = 14e-4). It can be noted that the input estimate, when using the standard PE-UIO, yields a smaller estimation delay compared to the

two stage PE-UIO (τ = 0 in the case of the PE-UIO and τ = 1 for the two stage PE-UIO), which is due to the fact that, when the standard PE-UIO is used, the lead caused by the zero at 0.3 partially compensates for the lag caused by the zero at −1.8. Nevertheless, the two stage PE-UIO has superior noise filtering properties (in terms of the bandwidth of $W(z)$), what can be observed in Fig. 3.9. The efficacy of the

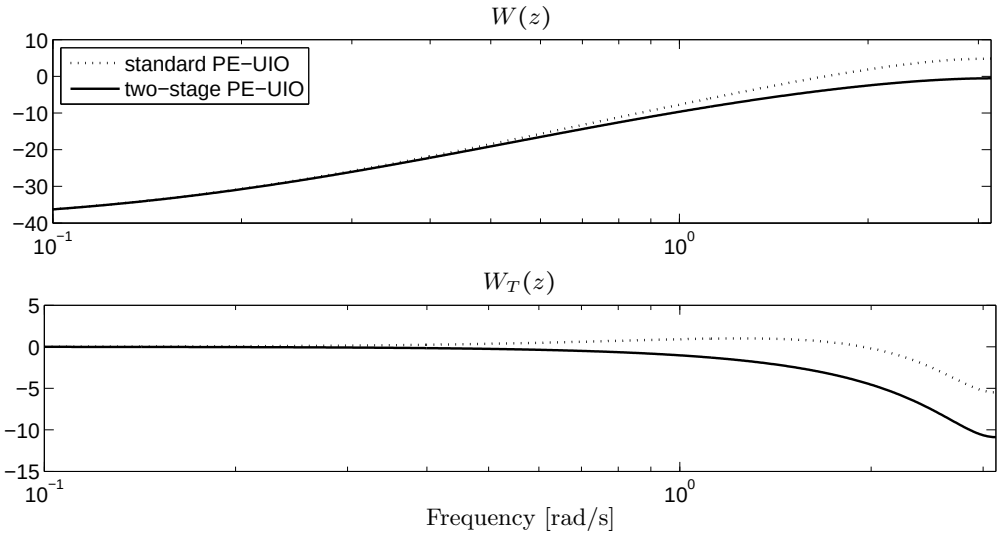

Figure 3.9: Frequency responses of $W_T(z)$ and $W_{T'}(z)$, s = 2, z_0 = 0.3

two algorithms for different levels of noise and different orders of the parity space s are compared in Table 3.1. It can be noted that for relatively low levels of noise the standard PE-UIO preforms better in terms of the on-line input estimation error (3.127) than the two stage PE-UIO, due to the lag compensation. However, as the noise level increases, the on-line input estimation error variance increases more slowly when the two stage PE-UIO is utilised, which is due to superior noise filtering properties of the two stage PE-UIO. As the order of the parity space, i.e. s, is increased, the level of the OE noise, for which both the standard PE-UIO and the two stage PE-UIO perform the same in terms of the variance of the on-line input estimation error, is also increased.

3.8 Comparison with other methods

In this section the efficacy of the PE-UIO is compared with two other algorithms, namely, the minimum variance unbiased (MVU) state and input estimator, see (Gillijns & De Moor 2007*b*), and the INPEST (input estimation), see (Young & Sumisławska 2012). In order to assess the efficacy of the considered algorithms, the R_T^2, cf. Section 2.4.3, is used.

Example 3.5. Comparison of efficacy of the PE-UIO and the MVU
In this example the efficacy of the unknown input reconstruction using two methods,

Table 3.1: Comparison the standard PE-UIO and the two stage PE-UIO in terms of the variance of the on-line unknown input reconstruction error, i.e. $\epsilon_{\text{on-line}}(t)$, for different levels of noise and different orders of the parity space. The term '% std dev' refers to the percentage value of the ratio between the output meausrement noise $e(t)$ and the system output $y_0(t)$ in terms of the standard deviation.

s	var($e(t)$)	% std dev	1-stage PE-UIO	2-stage PE-UIO
2	14e-4	0.0099	0.0855	0.2994
2	2.8e-1	0.1407	0.4056	0.4082
2	14	0.99	16.1863	5.7649
4	14e-1	0.3145	1.1337	1.5725
4	14	0.9947	1.8377	1.9169
4	14e1	3.1455	8.8554	5.3312
6	14	0.9947	2.5897	3.0861
6	14e1	3.1455	3.8324	3.8192
6	14e2	9.9469	16.1160	11.0143

namely, the PE-UIO the MVU is compared. The following single-input two-output ARX model is considered:

$$\begin{aligned} y(t) = &\begin{bmatrix} -1.75 & 0 \\ 0 & -1.75 \end{bmatrix} y(t-1) + \begin{bmatrix} 0.76 & 0 \\ 0 & 0.765 \end{bmatrix} y(t-2) + \\ &\begin{bmatrix} 1 \\ 1 \end{bmatrix} v(t) + \begin{bmatrix} 1.3 \\ -0.3 \end{bmatrix} v(t-1) + \begin{bmatrix} 2.4 & 0 \\ 0 & 0.7 \end{bmatrix} e(t-1) \end{aligned} \tag{3.129}$$

which corresponds to the system (3.1), whose matrices are given by:

$$\begin{aligned} A &= \begin{bmatrix} 1.75 & 0 & 1 & 0 \\ 0 & 1.75 & 0 & 1 \\ -0.76 & 0 & 0 & 0 \\ 0 & -0.765 & 0 & 0 \end{bmatrix} \quad G = \begin{bmatrix} 3.05 \\ 1.45 \\ -0.76 \\ -0.765 \end{bmatrix} \quad \Pi = \begin{bmatrix} 2.4 & 0 \\ 0 & 0.7 \\ 0 & 0 \\ 0 & 0 \end{bmatrix} \\ C &= \begin{bmatrix} 1 & 0 & 0 & 0 \\ 0 & 1 & 0 & 0 \end{bmatrix} \qquad H = \begin{bmatrix} 1 \\ 1 \end{bmatrix} \qquad \Omega = \begin{bmatrix} 0 & 0 \\ 0 & 0 \end{bmatrix} \end{aligned} \tag{3.130}$$

Note, that the model (3.129) corresponds to the model (2.39), whose A, B, G, and H matrices are as in (3.130), whilst $\zeta(t) = 0$ and:

$$\xi(t) = \begin{bmatrix} 2.4 & 0 \\ 0 & 0.7 \\ 0 & 0 \\ 0 & 0 \end{bmatrix} e(t) \tag{3.131}$$

Consequently, the noise covariance matrices used by the MVU are $R = 0$ and:

$$\tilde{Q} = \mathrm{var}(e(t)) \begin{bmatrix} 5.76 & 0 & 0 & 0 \\ 0 & 0.49 & 0 & 0 \\ 0 & 0 & 0 & 0 \\ 0 & 0 & 0 & 0 \end{bmatrix} \tag{3.132}$$

The algorithms are compared for tree different levels of $\mathrm{var}(e(t))$, namely, 1, 8, and 0.001, which correspond to, respectively, 4.8 %, 13.6 %, and 0.152 % of noise on each output by means of the standard deviation. In the experiment the MVU is compared with the PE-UIO designed with different values of s. A Monte-Carlo simulation with 100 runs is carried-out in order to provide reliable results, which are presented in Table 3.2. The MVU ensures the minimum variance of the estimation error resulting from

Table 3.2: Comparison of efficacy of PE-UIO and MVU

$\mathrm{var}(e(t))$	1		8		0.001	
s	τ	R_T^2 [%]	τ	R_T^2 [%]	τ	R_T^2 [%]
2	0	2.2153	0	17.6747	0	**0.0091202**
3	1	1.7598	1	9.4901	1	0.6559958
4	1	**0.9371**	1	6.0884	1	0.2019992
5	2	1.5533	2	5.4152	2	1.0017866
6	2	1.5191	2	**4.6083**	2	1.0776268
7	3	2.4092	3	4.9843	3	2.0409051
MVU	0	1.9986	0	15.7028	0	0.0019627

the disturbances. Therefore, achieving lower R_T^2 than that of MVU and ensuring at the same time $\tau = 0$ is not feasible, what can be seen in the simulation results. However, the major advantage of the PE-UIO is the ability to adjust the filter bandwidth by selecting the tuning parameter s. By choice of an optimal s, the R_T^2 is reduced approximately 2 and 4 times for, respectively, $\mathrm{var}(e(t)) = 1$ and $\mathrm{var}(e(t)) = 8$ compared to the MVU. The results show that for a low level of noise ($\mathrm{var}(e(t)) = 0.001$) the MVU performs better than the PE-UIO. This is due to the fact that the PE-UIO provides an estimate of the unknown input, cf. (3.10) and (3.11).

Example 3.6. Comparison of the INPEST, MVU, standard PE-UIO, and two stage PE-UIO

In this example four methods are compared, namely, the standard PE-UIO, the two stage PE-UIO, the INPEST and the MVU. Due to the fact that the INPEST method has been designed for SISO systems, the considered model has only one unknown input and no known inputs:

$$G_v(z) = \frac{z^2 + 0.55z - 0.38}{z^2 + 0.05z - 0.756} \tag{3.133}$$

The output of the system is subjected to white, zero-mean, Gaussian noise of unity variance. Note that in the SISO case, the MVU resembles a naive inversion, cf. Remark 2.1. Results of 100-run Monte-Carlo simulation are presented in Table 3.3, whilst samples of the estimated input signals are presented in Fig. 3.10. It can be noted

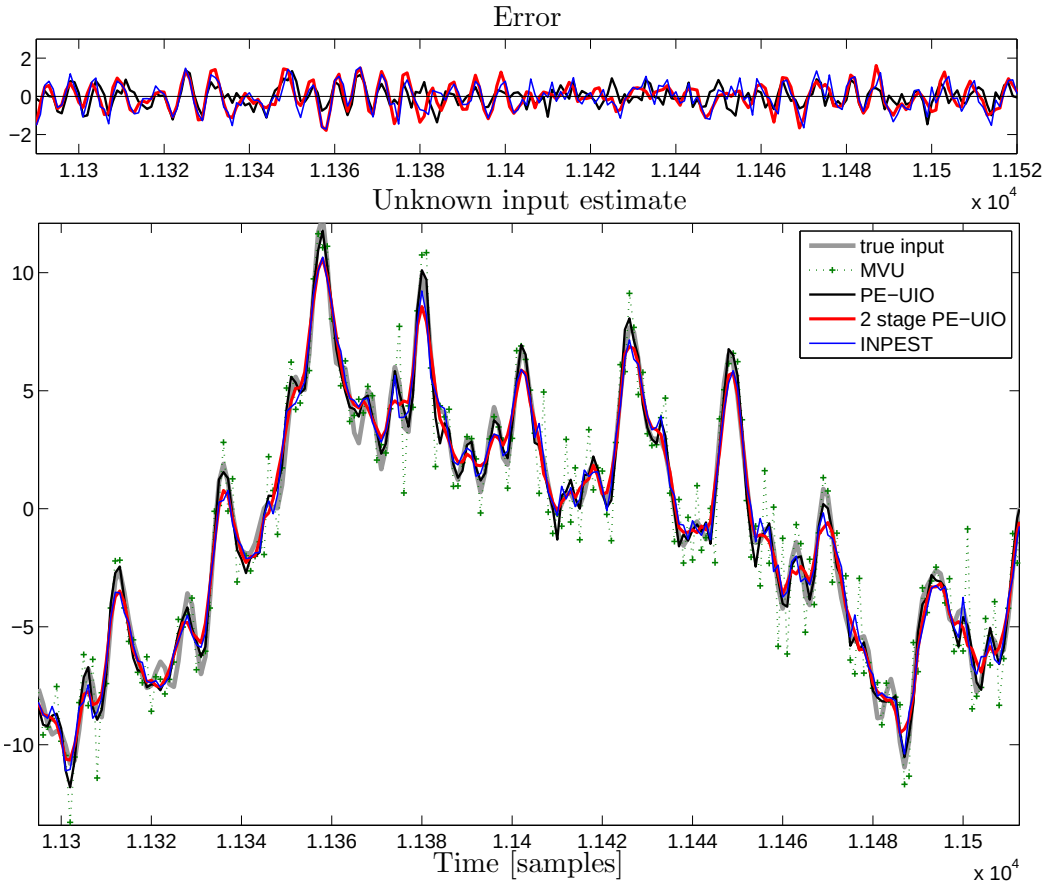

Figure 3.10: Comparison of unknown input reconstruction efficacy of standard PE-UIO, two stage PE-UIO, INPEST, and MVU

that the standard PE-UIO, the two stage PE-UIO, and the INPEST provide comparable results, whereas the MVU seems to give inferior results in terms of R_T^2. This is due to the relatively high bandwidth of the MVU, which results in the lowest possible estimation lag (in this case $\tau = 0$). The other examined algorithms can be tuned to reduce the reconstruction filter bandwidth (by increasing ν in the case of the INPEST method and s in the case of the standard and the two stage PE-UIO), which also yields an inherent estimation delay ($\tau > 0$).

Example 3.7. Comparison of the INPEST and the two stage PE-UIO

In this example the efficacy of the two stage PE-UIO and the INPEST is compared in the case when the output response to unknown input contains a zero close to unity.

Table 3.3: Results of comparison of various input reconstruction methods. Noise variance $\mathrm{var}(e(t)) = 1$

Method	R_T^2 [%]	τ
PE-UIO ($s = 4$)	1.1538	1
2-stage PE-UIO ($s = 5$)	1.1395	2
INPEST	1.3557	1
MVU	5.5980	0

The considered system is described by the following transfer function:

$$G_v(z) = \frac{0.01759z^2 + 0.05856z - 0.07367}{z^2 - 1.868z + 0.8706} \tag{3.134}$$

The system has two zeros at: -4.3023 and 0.9735. Note, that (3.134) is non-minimum phase, however both the two stage PE-UIO and the INPEST methods can cope with the zero at -4.3023. The zero at $z_0 = 0.9735$ needs to be eliminated from the parity equation in the two stage PE-UIO. The output of the system is subjected to white, zero-mean, Gaussian noise of the variance 0.003, which means that the standard deviation of the output measurement noise is equal to approximately 6% of the standard deviation of the output. The INPEST method is optimised for $\nu = 0.004$, which results in $\mathring{q}_e = 0.2635$ and $\mathring{\tau} = 7$. The results of the input reconstruction are presented in Fig. 3.11, whereas the efficacy in terms of R_T^2 and τ is compared in Table 3.4. It can be noted that both

Table 3.4: Comparison of INPEST and two stage PE-UIO. System has zero at 0.9735

Method	R_T^2 [%]	τ
INPEST	0.3423	7
2-stage PE-UIO ($s = 13$)	0.2946	6
2-stage PE-UIO ($s = 14$)	0.2667	7
2-stage PE-UIO ($s = 15$)	0.2721	7

algorithms yield comparable results for $\tau = 7$.

3.9 Concluding remarks

An approach to the unknown input reconstruction problem has been proposed. The scheme is applicable to MIMO systems with a single unmeasurable input, whereas the number of outputs and known inputs may be arbitrary. The generalised scheme is suitable for OE and ARMAX linear systems. It is also applicable in the EIV case. An extension to the standard PE-UIO, namely, the two stage PE-UIO, has been also proposed. The latter copes with systems which contain a derivative term or whose zeros lie close to unity (these are cases when the standard PE-UIO is not applicable). In the numerical study the developed algorithms have been compared with two other

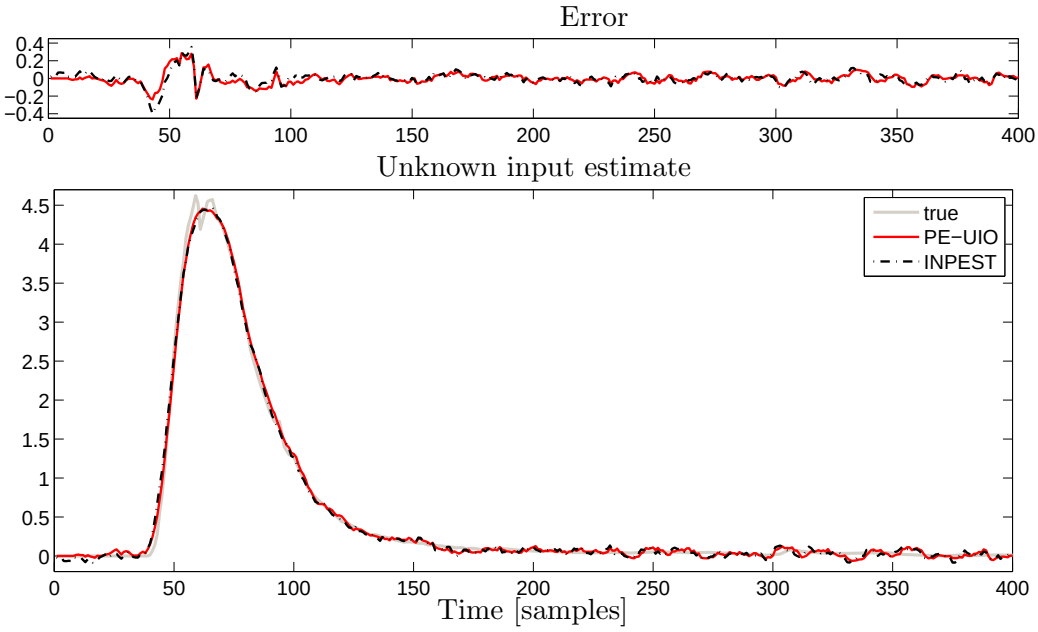

Figure 3.11: Comparison of unknown input reconstruction efficacy of the two stage PE-UIO and the INPEST; in both cases $\tau = 7$. The system has zeros at −4.3023 and 0.9735.

methods, namely, the Kalman filter-based MVU and the INPEST method which is based on a closed loop control concept.

The main advantage of the PE-UIO is its simplicity; the filter parameters are calculated once at the beginning of the reconstruction process. The method is fast as it utilises two moving average filters. The only tuning parameter of the PE-UIO is the order of the parity space s. By altering it, the bandwidth of the input reconstruction filter is shaped. This property allows the designer to tune the algorithm for different levels of noise. It should be noted that by reduction of the filter bandwidth (hence improvement of the noise filtering properties of the scheme) an estimation lag is introduced. Similar property has been observed in the INPEST method, whereas the MVU does not allow for introduction of an estimation lag in order to reduce the impact of the noise (in terms of a bandwidth reduction). Furthermore, the PE-UIO is suitable for non-minimum phase systems.

The two versions of the PE-UIO algorithm have been compared. The two stage PE-UIO allows to eliminate selected system zeros from the PE, which changes the response of the input reconstruction filter. This is particularly desirable, when the system zeros lie close to unity, which results in a large overshoot in the step response of the standard PE-UIO. The design of the two stage PE-UIO allows the elimination of this overshoot and hence a distortion of the unknown input estimate. Furthermore, the two stage PE-UIO provides better (in terms of bandwidth) noise filtering properties. On the

other hand it has been shown using a numerical example that the phase lead caused by the system zero when using the standard PE-UIO may be desirable. This might be the case in an on-line application when the estimation delay is crucial. The phase lead, when using the standard PE-UIO, result in a reduced estimation delay compared to the two stage PE-UIO.

The comparison of both PE-UIO methods, the INPEST, and the MVU revealed comparable efficacy of the PE-UIO and the INPEST. Both algorithms have the possibility to shape the filter bandwidth (by introducing an inherent delay) by selection of a single tuning parameter (ν in the case of the INPEST and s in the case of the PE-UIO). The MVU does not have such a possibility of shaping the bandwidth of the filter to this extent as in the case of the PE-UIO or the INPEST.

Further work aims towards an extension of the algorithms to systems with multiple unmeasurable inputs. Although the proposed algorithms are generally applicable for nonminimum-phase systems, a solution for systems, whose nonmiminum-phase zero is close to unity, still remains an open question.

Chapter 4

Parity equations-based unknown input reconstruction for Hammerstein-Wiener systems

Nomenclature

a_i	autoregressive parameter in polynomial model
A	state transition matrix in state-space model
b_i	exogenous parameter in polynomial model
B	input matrix of known input in state-space model
c_i	moving average parameter in ARMAX model
C	output matrix in state-space model
D	feedforward matrix of known input in state-space model
$e(t)$	noise term
$f(\cdot)$	function to be minimised by Lagrange multiplier method
$g(\cdot)$	constraint function in Lagrange multiplier method
G	input matrix of unknown input in state-space model
$G_u(z)$	z-domain transfer function between $u_0(t)$ and $y(t)$
$G_v(z)$	z-domain transfer function between $v(t)$ and $y(t)$
H	feedforward matrix of unknown input in state-space model
m	number of system outputs
n	order of the system
n_a	order of autoregressive polynomial
n_b	order of exogenous polynomial
n_c	order of moving average polynomial
p	number of known inputs to a system
p_i	element of P
P	auxiliary vector
Q	block Toeplitz matrix
s	parity space order
S	auxiliary matrix
T	block Toeplitz matrix
$u_0(t)$	noise-free known input

$u(t)$	measured input
$\tilde{u}(t)$	input measurement noise
$\bar{u}_0(t)$	input to linear dynamic block
$\tilde{u}^*(t)$	auxiliary variable
$\tilde{\bar{u}}(t)$	estimation error of $\bar{u}_0(t)$
$U_0(t)$	stacked vector of last $s+1$ values of $u_0(t)$
$U_0(z)$	$u_0(t)$ in z-domain
$\tilde{U}(t)$	stacked vector of last $s+1$ values of $\tilde{\bar{u}}(t)$
$U(t)$	stacked vector of last $s+1$ values of $u(t)$
$U(z)$	$u(t)$ in z-domain
$\tilde{U}(t)$	stacked vector of last $s+1$ values of $\tilde{u}(t)$
$\tilde{U}(z)$	$\tilde{u}(t)$ in z-domain
$\tilde{U}^*(t)$	stacked vector of last $s+1$ values of $\tilde{u}^*(t)$
$\tilde{U}^*(z)$	$\tilde{u}^*(t)$ in z-domain
$\hat{v}(t)$	unknown input estimate
$v(t)$	unknown (unmeasurable) input
$V(t)$	stacked vector of last $s+1$ values of unknown input
$V(z)$	$v(t)$ in z-domain
$\hat{V}(z)$	$\hat{v}(t)$ in z-domain
w_{q_i}	auxiliary polynomial parameter
w_{ξ_i}	auxiliary polynomial parameter
W	vector, which belongs to $\Gamma^\perp$
$W(z)$	polynomial of z-variable defined by appropriate elements of W
$W_Q(z)$	polynomial of z-variable defined by appropriate elements of WQ
$W_T(z)$	polynomial of z-variable defined by appropriate elements of WT
$W_{T'}(z)$	polynomial of z-variable defined by appropriate elements of WT'
$W_\Xi(z)$	polynomial of z-variable defined by appropriate elements of $W\Xi$
$x(t)$	state vector instate space model
$y_0(t)$	noise-free system output
$\bar{y}_0(t)$	output of linear dynamic block
$\tilde{\bar{y}}(t)$	estimation error of $\bar{y}_0(t)$
$y(t)$	measured output
$\tilde{y}(t)$	output measurement noise
$Y_0(t)$	stacked vector of last $s+1$ values of noise-free output
$\bar{Y}_0(t)$	stacked vector of last $s+1$ values of $\bar{y}_0(t)$
$Y(t)$	stacked vector of last $s+1$ values of measured output
$\tilde{\bar{Y}}(t)$	stacked vector of last $s+1$ values of $\tilde{\bar{y}}(t)$
$Y(z)$	$y(t)$ in z-domain
z_i	system zero
α_i	auxiliary parameter
α_i	auxiliary parameter
δ	system delay
$\epsilon(t)$	auxiliary noise term
$\epsilon^*(t)$	auxiliary noise term
$\phi_u(t), \phi_y(t)$	auxiliary variance terms
$\varphi(\cdot)$	Hammerstein nonlinearity
γ	row vector of $\Gamma^\perp$
Γ	extended observability matrix
$\Gamma^\perp$	left nullspace of Γ
$\eta(\cdot)$	Wiener nonlinearity

$\eta^{-1}(\cdot)$	inverse of $\eta(\cdots)$
λ	Lagrange multiplier
Π	input matrix of noise term in state-space model
Ω	feedforward matrix of noise term in state-space model
$\Sigma, \Sigma_e, \Sigma_{\tilde{u}}, \Sigma_{\tilde{u}e}$ ..	covariance matrices
τ	unknown input estimation lag
Ξ	block Toeplitz matrix
ψ	auxiliary vector

Preliminary reading: Sections 2.2, 2.3, 2.4, Subsection 2.5.2, Sections 3.2 and 3.3.

4.1 Introduction

Block oriented models are convenient for modelling nonlinear systems. Their relatively simple structure of a linear dynamic block interconnected with nonlinear memoryless function(s) provides a powerful tool for an approximation of a large class of nonlinear systems, see (Pearson & Pottmann 2000, Pearson 2003). Block oriented models have been used for modelling such phenomena as, for instance: infant EEG (electroencephalogram) seizures (Celka & Colditz 2002), a radio frequency amplifier (Crama & Rolain 2002), a glucose-insulin process in diabetes type I patient (Bhattacharjee, Sengupta & Sutradhar 2010), ionospheric dynamics (Palanthandalam-Madapusi, Ridley & Bernstein 2005) or human operator dynamics (Tervo & Manninen 2010). Furthermore, such models are also used for control purposes, see, for example, (Anbumani, Patnaik & Sarma 1981, Fruzzetti, Palazoglu & McDonald 1997, De-Feng, Li & Guo-Shi 2010), and fault detection (Korbicz, Koscielny, Kowalczuk & Cholewa 2003, Lajic, Blanke & Nielsen 2009).

A two-input single-output Hammerstein-Wiener model is considered, i.e. the linear dynamic block is preceded and followed by nonlinear static functions. (In the case of a Hammerstein model a linear block is preceded by a static nonlinear function, whereas in the case of a Wiener model the order of these elements is reversed.) A problem of the reconstruction of the unknown/unmeasurable input to the system is taken into consideration. Up to date, only a limited number of publications are available on this subject. Szabo, Gaspar & Bokor (2005) proposed an inversion of Wiener systems using a geometric method based on the assumption that the static nonlinearity transforming the output is invertible, whilst Ibnkahla (2002) used neural networks for Hammerstein system inversion.

The algorithm presented here extends the approach developed in Chapter 3 to a Hammerstein-Wiener case. An EIV framework, see (Söderström 2007), is considered, i.e. all the measured signals are affected by white, Gaussian, zero-mean and mutually uncorrelated measurement noise sequences. The theory described in Sections 4.2–4.3 has been presented in (Sumisławska, Larkowski & Burnham 2012).

This chapter is organised as follows: in Section 4.2, for completeness, the idea of

block oriented models is presented and the Hammerstein-Wiener model, for which the unknown input reconstruction algorithm is designed, is defined. Then, the PE-UIO method for Hammerstein-Wiener systems (PE-UIO-HW) is described in Section 4.3. Furthermore, in Section 4.4 the PE-UIO-HW is extended to an adaptive version, which accounts for changes in noise levels. Finally, conclusions are provided in Section 4.5.

4.2 Problem statement

It is assumed that a two-input single-output nonlinear system can be described by a Hammerstein-Wiener model. An EIV framework is considered (Söderström 2007), see Fig. 4.1. Thus, the Hammerstein-Wiener model is given by the following state-space form:

$$\bar{u}_0(t) = \varphi\left(u_0(t)\right) \tag{4.1a}$$
$$x(t+1) = Ax(t) + B\bar{u}_0(t) + Gv(t) \tag{4.1b}$$
$$\bar{y}_0(t) = Cx(t) + D\bar{u}_0(t) + Hv(t) \tag{4.1c}$$
$$y_0(t) = \eta\left(\bar{y}_0(t)\right) \tag{4.1d}$$
$$u(t) = u_0(t) + \tilde{u}(t) \tag{4.1e}$$
$$y(t) = y_0(t) + \tilde{y}(t) \tag{4.1f}$$

where $\varphi(\cdot)$ is a static nonlinearity transforming the first system input $u_0(t)$ into an inaccessible signal $\bar{u}_0(t)$ which serves as the first input to the linear block. It is assumed that the second input $v(t)$ is fed directly (without a nonlinear transformation) to the linear block, which is described by a state-space model, where $A \in \mathbb{R}^{n\times n}$, $B \in \mathbb{R}^{n\times 1}$, $C \in \mathbb{R}^{1\times n}$, $D \in \mathbb{R}^{1\times 1}$, $G \in \mathbb{R}^{n\times 1}$ and $H \in \mathbb{R}^{1\times 1}$. The term $\bar{y}_0(t)$ refers to the output of the linear part of the system, which is then transformed by the memoryless function $\eta(\cdot)$ into the overall system output $y_0(t)$. Since the EIV case is considered, all measured variables, which are $u(t)$ and $y(t)$, are affected by white, Gaussian, zero-mean, and mutually uncorrelated measurement noise sequences denoted by $\tilde{u}(t)$ and $\tilde{y}(t)$, respectively. Noise sequences are postulated to be uncorrelated with the noise-free but unmeasured system input and output, denoted as $u_0(t)$ and $y_0(t)$, respectively. It is assumed here that $\eta(\cdot)$ is strictly monotonic, hence its inverse exists. Note that (4.1) represents a Hammerstein or a Wiener model if, respectively, $\eta(\cdot)$ or $\varphi(\cdot)$ is an identity function.

Similarly as in Chapter 3, the objective of the proposed scheme is to estimate the unknown input $v(t)$, simultaneously minimising the effect of the measurement noise on the unknown input estimate. It is assumed that the model of the system is known and that $v(t)$ is varying relatively slowly, cf. Subsection 3.5.1.

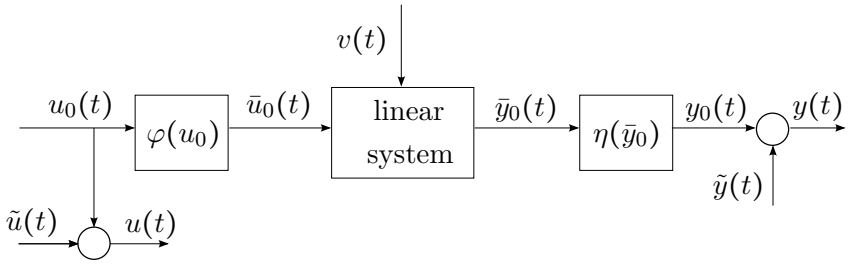

Figure 4.1: A Hammerstein-Wiener system in the EIV framework

4.3 PE-UIO for Hammerstein-Wiener systems

In this section the algorithm for estimation of the unknown input is derived. Firstly, for completeness, the PE for Hammerstein-Wiener systems are derived in Subsection 4.3.1. This is followed by a development of a PE-UIO-HW algorithm for the considered class of block oriented systems in Subsections 4.3.2 and 4.3.3.

4.3.1 Parity relations for Hammerstein-Wiener system

Consider the system described by (4.1). Analogously, as in Equation (3.2), one can build stacked vectors of $y(t)$, $y_0(t)$, $\bar{y}_0(t)$, $\tilde{y}(t)$, $\bar{u}_0(t)$, $u(t)$, $u_0(t)$ and $\tilde{u}(t)$ which are denoted, respectively, as $Y(t)$, $Y_0(t)$, $\bar{Y}_0(t)$, $\tilde{Y}(t)$, $\bar{U}_0(t)$, $U(t)$, $U_0(t)$ and $\tilde{U}(t)$. By making use of this notation the system defined by (4.1) can be expressed in the form of:

$$\bar{U}_0(t) = \varphi(U_0(t)) \tag{4.2a}$$

$$\bar{Y}_0(t) = \Gamma x(t-s) + Q\bar{U}(t)_0 + TV(t) \tag{4.2b}$$

$$Y_0(t) = \eta(\bar{Y}_0(t)) \tag{4.2c}$$

where $\varphi(U_0(t))$ is a vector whose elements are $\varphi(u_0(t-s))$, $\varphi(u_0(t-s+1))$, $\cdots$, $\varphi(u_0(t))$. Analogously, the function $\eta(\bar{Y}_0(t))$ is defined.

The linear part of the system, defined by (4.2b), can be represented by the following parity relation, cf. Subsection 3.3.1.

$$W\bar{Y}_0(t) = WTV(t) + WQ\bar{U}_0(t) \tag{4.3}$$

which, since $\eta(\cdot)$ is assumed to be invertible, can be reformulated as:

$$W\eta^{-1}(Y_0(t)) = WTV(t) + WQ\varphi(U_0(t)) \tag{4.4}$$

where $\eta^{-1}(\cdot)$ denotes an inverse of $\eta(\cdot)$. Due to the fact that $y_0(t)$ and $u_0(t)$ are inaccessible, the parity relation (4.4) can be approximated by the measured values of

the input and output:

$$W\eta^{-1}(Y(t)) = WTV(t) + WQ\varphi(U(t)) + \xi(t) \tag{4.5}$$

where $\xi(t)$ accounts for an overall error resulting from the presence of measurement noise. (Note that $\xi(t)$ depends also on the current values of $u(t)$ and $y(t)$ due to the nonlinearities in the system.) By rearranging the measured (known) variables to the right-hand side and the unknowns to the left-hand side, the following parity equation is obtained, cf. (Li & Shah 2002):

$$W\eta^{-1}(Y(t)) - WQ\varphi(U(t)) = WTV(t) + \xi(t) \tag{4.6}$$

4.3.2 Unknown input estimation

Analogously to the PE-UIO it is proposed to estimate the value of the unknown input as:

$$\hat{v}(t-\tau) = W\eta^{-1}(Y(t)) - WQ\varphi(U(t)) \tag{4.7}$$

which, in the case of noise-free input and output measurements, is:

$$\hat{v}(t-\tau) = WTV(t) \tag{4.8}$$

In the case of noisy input and output measurements the unknown input estimate is affected by an error, cf. (4.6):

$$\hat{v}(t-\tau) = WTV(t) + \xi(t) \tag{4.9}$$

resulting from both the input and output measurement uncertainties, which can be deduced to be given by:

$$\xi(t) = W\left(\eta^{-1}(Y(t)) - \eta^{-1}(Y_0(t))\right) - WQ\left(\varphi(U(t)) - \varphi(U_0(t))\right) \tag{4.10}$$

Using the notation:

$$\begin{aligned} \tilde{\tilde{Y}}(t) &= \eta^{-1}(Y(t)) - \eta^{-1}(Y_0(t)) \\ \tilde{\tilde{U}}(t) &= \varphi(U(t)) - \varphi(U_0(t)) \end{aligned} \tag{4.11}$$

Equation (4.10) can be rewritten as:

$$\xi(t) = W\tilde{\tilde{Y}}(t) - WQ\tilde{\tilde{U}}(t) \tag{4.12}$$

Since $\varphi(\cdot)$ and $\eta(\cdot)$ are memoryless, the sequences:

$$\tilde{\tilde{u}}(t) = \varphi(u(t)) - \varphi(u_0(t)) \tag{4.13}$$

and

$$\tilde{\tilde{y}}(t) = \eta^{-1}(y(t)) - \eta^{-1}(y_0(t)) \tag{4.14}$$

are white and mutually uncorrelated (as $\tilde{u}(t)$ and $\tilde{y}(t)$ are white and mutually uncorrelated), which is demonstrated further in this Section. The variance of $\tilde{\tilde{u}}(t)$, further referred to as $\mathrm{var}(\tilde{\tilde{u}}(t))$, is time varying and depends on $\varphi(u(t))$, $u(t)$ and the variance of $\tilde{u}(t)$, denoted as $\mathrm{var}(\tilde{u})$. Analogously, the variance of $\tilde{\tilde{y}}(t)$, i.e. $\mathrm{var}(\tilde{\tilde{y}}(t))$, is dependent on $\mathrm{var}(\tilde{y})$ and the current values of $\eta(y(t))$ and $y(t)$. The expression $\varphi(u_0(t))$ can be approximated using a first order Taylor expansion at $u(t)$:

$$\varphi(u_0(t)) \approx \varphi(u(t)) + \frac{\partial\varphi(u(t))}{\partial u(t)}\,(u_0(t) - u(t)) = \varphi(u(t)) - \frac{\partial\varphi(u(t))}{\partial u(t)}\tilde{u}(t) \tag{4.15}$$

Thus, incorporating (4.15) into (4.13), the dependency between the $\tilde{\tilde{u}}(t)$ and $\tilde{u}(t)$ can be approximated via:

$$\tilde{\tilde{u}}(t) = \varphi(u(t)) - \varphi(u_0(t)) \approx \frac{\partial\varphi(u(t))}{\partial u(t)}\tilde{u}(t) \tag{4.16}$$

This means that the ratio between $\tilde{\tilde{u}}(t)$ and $\tilde{u}(t)$ is approximately proportional to the tangential of $\varphi(u(t))$. Analogously, the ratio between $\tilde{\tilde{y}}(t)$ and $\tilde{y}(t)$ is approximately proportional to $\frac{\partial\eta^{-1}(y(t))}{\partial y(t)}$, i.e.

$$\tilde{\tilde{y}}(t) \approx \frac{\partial\eta^{-1}(y(t))}{\partial y(t)}\tilde{y}(t) \tag{4.17}$$

Note that:

$$\begin{aligned}
&\mathrm{E}\{\tilde{\tilde{u}}(t-i)\tilde{\tilde{u}}(t-j)\} \approx \mathrm{E}\{\frac{\partial\varphi(u(t-i))}{\partial u(t)}\tilde{u}(t-i)\frac{\partial\varphi(u(t-j))}{\partial u(t)}\tilde{u}(t-j)\}\\
&= \mathrm{E}\{\frac{\partial\varphi(u(t-i))}{\partial u(t)}\frac{\partial\varphi(u(t-j))}{\partial u(t)}\}\mathrm{E}\{\tilde{u}(t-i)\tilde{u}(t-j)\}\\
&= \mathrm{E}\{\frac{\partial\varphi(u(t-i))}{\partial u(t)}\frac{\partial\varphi(u(t-j))}{\partial u(t)}\} \times 0 = 0, \text{ for } i \neq j
\end{aligned} \tag{4.18}$$

Hence, the sequence $\tilde{\tilde{u}}(t)$ is white. Analogously, it can be demonstrated that $\tilde{\tilde{y}}(t)$ is white as well as $\tilde{\tilde{u}}(t)$ and $\tilde{\tilde{y}}(t)$ are mutually uncorrelated.

The variances of $\tilde{\tilde{u}}(t)$ and $\tilde{\tilde{y}}(t)$ can be approximated, respectively, as:

$$\begin{aligned}
\mathrm{var}(\tilde{\tilde{u}}(t)) &\approx \left(\frac{\partial\varphi(u(t))}{\partial u(t)}\right)^2 \mathrm{var}(\tilde{u})\\
\mathrm{var}(\tilde{\tilde{y}}(t)) &\approx \left(\frac{\partial\eta^{-1}(y(t))}{\partial y(t)}\right)^2 \mathrm{var}(\tilde{y})
\end{aligned} \tag{4.19}$$

It should be noted that $\mathrm{var}(\tilde{\tilde{u}}(t))$ and $\mathrm{var}(\tilde{\tilde{y}}(t))$ are, in general, time varying as they depend on the current values of the functions $\varphi(u(t))$ and $\eta^{-1}(y(t))$. Furthermore, the

ratio between $\mathrm{var}(\tilde{\bar{u}}(t))$ and $\mathrm{var}(\tilde{\bar{y}}(t))$ is not constant, i.e. the impact of either input or output measurement noise on the unknown input estimation error can be prevailing, depending on the system operating point. Therefore, the unknown input reconstruction filter should adapt to these changes.

The aim of the PE-UIO for Hammerstein-Wiener systems is to select such a vector W that the variance of the error term $\xi(t)$ is minimised, i.e.

$$\begin{aligned}\mathrm{var}(\xi(t)) &= \mathrm{E}\{(W\tilde{\bar{Y}}(t) - WQ\tilde{\bar{U}}(t))(W\tilde{\bar{Y}}(t) - WQ\tilde{\bar{U}}(t))^T\} \\ &= W\Sigma_{\tilde{\bar{y}}}W^T + WQ\Sigma_{\tilde{\bar{u}}}Q^TW^T - W\Sigma_{\tilde{\bar{u}}\tilde{\bar{y}}}^TQ^TW^T - WQ\Sigma_{\tilde{\bar{u}}\tilde{\bar{y}}}W^T\end{aligned} \tag{4.20}$$

where $\Sigma_{\tilde{\bar{u}}} = E\{\tilde{\bar{U}}(t)\tilde{\bar{U}}^T(t)\}$, $\Sigma_{\tilde{\bar{y}}} = E\{\tilde{\bar{Y}}(t)\tilde{\bar{Y}}^T(t)\}$, $\Sigma_{\tilde{\bar{u}}\tilde{\bar{y}}} = E\{\tilde{\bar{U}}(t)\tilde{\bar{Y}}^T(t)\}$. The term $\Sigma_{\tilde{\bar{u}}}$ is calculated via, cf. (4.19):

$$\Sigma_{\tilde{\bar{u}}} = \begin{bmatrix} \mathrm{var}(\tilde{\bar{u}}(t-s)) & \cdots & 0 & 0 \\ \vdots & \ddots & \vdots & \vdots \\ 0 & \cdots & \mathrm{var}(\tilde{\bar{u}}(t-1)) & 0 \\ 0 & \cdots & 0 & \mathrm{var}(\tilde{\bar{u}}(t)) \end{bmatrix} \tag{4.21}$$

Analogously, the expression $\Sigma_{\tilde{\bar{y}}}$ is obtained by replacing the terms $\mathrm{var}(\tilde{\bar{u}}(\cdot))$ in (4.21) by $\mathrm{var}(\tilde{\bar{y}}(\cdot))$. Due to the fact that $\tilde{u}(t)$ and $\tilde{y}(t)$ are mutually uncorrelated, $\Sigma_{\tilde{\bar{u}}\tilde{\bar{y}}} = 0$. For convenience, an expression Σ is introduced, which is equal to:

$$\Sigma = \Sigma_{\tilde{\bar{y}}} + Q\Sigma_{\tilde{\bar{u}}}Q^T \tag{4.22}$$

Subsequently, the vector W should be selected to minimise the cost function $f(W)$:

$$f(W) = W\Sigma W^T \tag{4.23}$$

subject to the following constraints:

1. The sum of elements of WT is equal to 1
2. $W\Gamma = 0$

The solution to the constrained optimisation problem has been solved using the Lagrange multiplier method in Chapter 3.

Note that due to the fact that the ratio of the variances $\mathrm{var}(\tilde{\bar{u}}(t))$ and $\mathrm{var}(\tilde{\bar{y}}(t))$ is changing over the time, cf. (4.19), as opposed to the linear case in Chapter 3, the vector W needs to be updated at each time step, i.e. the elements of W are time varying. This may eventually result in an unnecessary jitter of the estimation lag τ. This happens if the mantissa of $\frac{\sum \alpha_i i}{\sum \alpha_i}$, cf. (3.11) and (3.12), is close to 0.5 and in some time instances it exceeds 0.5, whilst in the other is lower than 0.5. Thus, it is suggested to calculate τ only once at the beginning of the input reconstruction process. Finally, the algorithm for calculating the optimal vector W is summarised as follows:

Algorithm 4.1 (PE-UIO-HW).

1. Select the order of the parity space $s \geq n$ and build matrices Γ, Q and T.
2. Obtain $\Gamma^{\perp}$.

for $t = 1 : N$

3. Calculate variances of $\tilde{\tilde{u}}(t)$ and $\tilde{\tilde{y}}(t)$ using (4.19)
4. Compute Σ using:

$$\Sigma = \Sigma_{\tilde{\tilde{y}}} + Q\Sigma_{\tilde{\tilde{u}}}Q^T \tag{4.24a}$$

5. Calculate the column vector S via:

$$S = \Gamma^{\perp}\Sigma(\Gamma^{\perp})^T + \left(\Gamma^{\perp}\Sigma\left(\Gamma^{\perp}\right)^T\right)^T \tag{4.24b}$$

6. Compute the matrix ψ by making use of:

$$\psi = \mathrm{sum}_{\mathrm{row}}(\Gamma^{\perp}T) \tag{4.24c}$$

7. Obtain the Lagrange multiplier λ as:

$$\lambda = \left(\left(S^{-1}\psi\right)^T\psi\right)^{-1} \tag{4.24d}$$

8. Calculate the parameter vector P by:

$$P = \lambda S^{-1}\psi \tag{4.24e}$$

9. Compute the vector W as:

$$W = P^T\Gamma^{\perp} \tag{4.24f}$$

if $t = 1$

Calculate the estimation lag as:

$$\tau = \mathrm{round}\left(\frac{\sum \alpha_i i}{\sum \alpha_i}\right) \tag{4.24g}$$

where:

$$WT = \begin{bmatrix} \alpha_s & \alpha_{s-1} & \cdots & \alpha_0 \end{bmatrix}^T$$

end

10. Obtain the estimate of $v(t-\tau)$ via:

$$\hat{v}(t-\tau) = W(t)\eta^{-1}(Y(t)) - W(t)Q(t)\varphi(U(t)) \tag{4.24h}$$

end

4.3.3 Confidence bounds

It can be seen from (4.20), that the variance of the error term $\mathrm{var}(\xi(t))$ can be represented as a sum of two terms, each of which depends solely on either the output or the input measurement noise, such as:

$$\mathrm{var}(\xi(t)) = \phi_u(t) + \phi_y(t) \tag{4.25}$$

where $\phi_u(t)$ and $\phi_y(t)$ are defined as:

$$\phi_u(t) = WQ\Sigma_{\tilde{u}}Q^TW^T \tag{4.26a}$$
$$\phi_y(t) = W\Sigma_{\tilde{y}}W^T \tag{4.26b}$$

Therefore, it can be noted that the PE-UIO-HW algorithm minimises the sum of $\phi_u(t)$ and $\phi_y(t)$.

The accuracy of the unknown input estimation alters over the time, as $\mathrm{var}(\xi(t))$ is changing. Based on the assumption of a Gaussian distribution of $\tilde{u}(t)$ and $\tilde{y}(t)$ it can be assumed that the distribution of $\xi(t)$ can be approximated with a Gaussian curve with the variance of $\mathrm{var}(\xi(t))$. Consequently, confidence bounds of the unknown input estimate can be approximated using Gaussian distribution tables as multiplicities of the standard deviation of $\xi(t)$.

4.3.4 Numerical examples

Example 4.1. Design of the PE-UIO-HW

Consider an examplary system, whose matrices of the linear block are given by:

$$A = \begin{bmatrix} 0 & -0.56 \\ 1 & 1.5 \end{bmatrix} \quad B = \begin{bmatrix} -0.1200 \\ 0.4125 \end{bmatrix} \quad G = \begin{bmatrix} 0.0055 \\ 0.0963 \end{bmatrix} \tag{4.27}$$
$$C = \begin{bmatrix} 0 & 1 \end{bmatrix} \qquad D = 0.125 \qquad H = 0.025$$

The memoryless input and output nonlinearities are arbitrarily selected as:

$$\begin{aligned} \bar{u}_0(t) &= \exp\left(0.165 \cdot 10^{-5} u_0^3(t) + u_0(t)\right) - 1 \\ y_0(t) &= \exp\left(11 + 0.165 \cdot 10^{-5} \left(\bar{y}_0(t)\right)^3\right) - \exp(11) \end{aligned} \tag{4.28}$$

Fig. 4.2 depicts functions $\varphi(\cdot)$ and $\eta(\cdot)$ where it is observed that they are both mono-

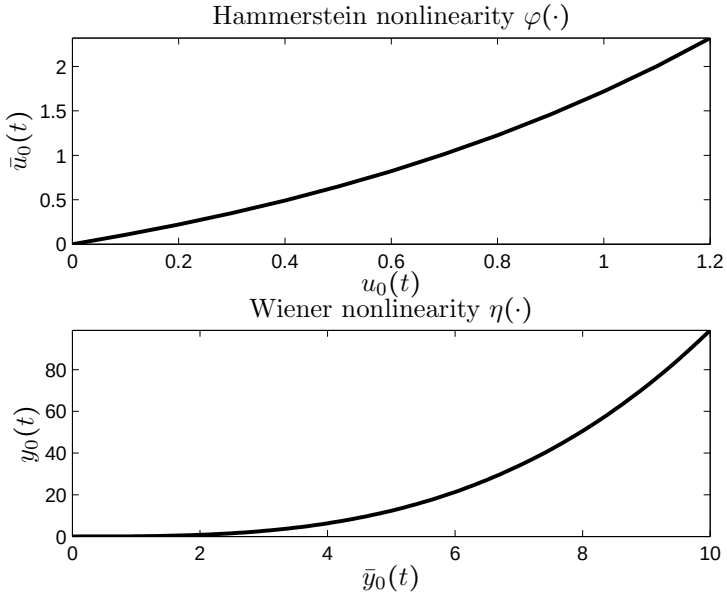

Figure 4.2: Hammerstein and Wiener nonlinearities

tonic and strictly increasing. This means that the impact of the input measurement noise on the unknown input estimate is expected to be relatively low for low values of $u(t)$ (as the gradient of $\varphi(u(t))$ is small for low values of $u(t)$). On the other hand, this impact will be relatively high for large values of $u(t)$ (as the gradient of $\varphi(u(t))$ is large for high values of $u(t)$). Due to the fact that the scheme utilises an inversion of $\eta(\cdot)$, an opposite situation is expected according to the output measurement noise. Low values of the output are expected to yield a significant impact of the output measurement error on the accuracy of the unknown input estimate.

The known input and output signals as well as $\bar{u}_0(t)$ and $\bar{y}_0(t)$ are presented in Fig. 4.3. For the first 1000 samples of the simulation $y_0(t)$ is relatively high and, as the slope of $\eta(\cdot)$ becomes steeper for higher values of $\bar{y}_0(t)$, it is anticipated that the inversion of the noisy measurement $y(t)$ for the first 1000 samples will significantly reduce the impact of the output measurement noise. After 1000 samples both $u_0(t)$ and $y_0(t)$ decrease, which results in a higher vulnerability of the input reconstruction process to the output measurement noise, cf. the slope of $\eta(\cdot)$ for the relatively low values of the output. The input and output measurements are subjected to white, Gaussian, zero-mean, and mutually uncorrelated noise sequences, whose variances are,

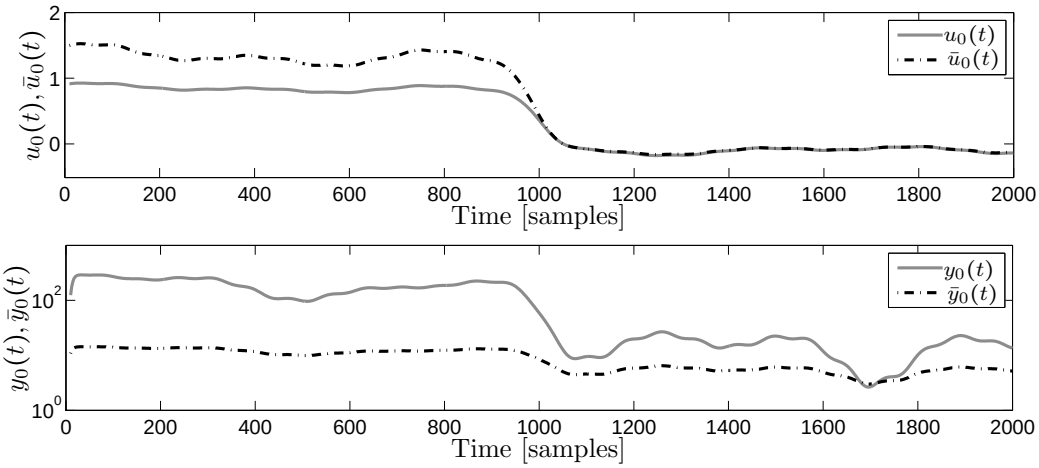

Figure 4.3: Input and output of the considered system (grey solid curve) compared with input and output of linear block (dashed-dotted curve)

respectively, $\text{var}(\tilde{u}(t)) = 0.002$ and $\text{var}(\tilde{y}(t)) = 0.5$. As a result of the inversion of $\eta(\cdot)$, needed for the calculation of $\bar{y}_0(t)$, the ratio of standard deviations of $\tilde{\bar{y}}(t)$ to $\bar{y}_0(t)$ is 2.2 %. However, as expected, the impact of the measurement noise on the accuracy of the estimate of $\bar{y}_0(t)$ changes over time. For the period between 100 and 900 samples the standard deviation of $\tilde{\bar{y}}(t)$ is equal to 1.4 % of the standard deviation of $\bar{y}_0(t)$. Whereas for the period between 1100 and 1900 samples this ratio is 12.3 %. This can be interpreted that the impact of the measurement noise decreases over 8 times after 1000 samples. The order of the parity space has been selected as 12, which gives $\tau = 6$ samples. The unknown input estimate with 95% confidence bounds is presented in Fig. 4.4. In the upper subfigure of Fig. 4.5 $\text{var}(\tilde{u}(t))$ and $\phi_u(t)$ are compared, whilst the middle subfigure of Fig. 4.5 compares $\text{var}(\tilde{\bar{y}}(t))$ and $\phi_y(t)$. The lower subfigure of Fig. 4.5 presents the optimisation effect by comparing the sum of $\text{var}(\tilde{u}(t))$ and $\text{var}(\tilde{\bar{y}}(t))$ with the sum of $\phi_u(t)$ and $\phi_y(t)$. During the first 1000 samples the input measurement noise has a larger influence on the unknown input estimation error in comparison to the output measurement noise. One can note that for the first 300 samples the effect of the output measurement noise is actually amplified (as a result of the minimisation of the joint impact of the input and output measurement noise). However, due to a relatively large $\tilde{u}(t)$, it has a negligible effect on the input estimation error. After 1000 samples of the simulation the situation changes. The effect of the input measurement noise becomes less significant, whereas the term $\tilde{\bar{y}}(t)$ increases as it depends strongly on the value of the output.

Example 4.2. Distribution of $\xi(t)$

In order to calculate confidence bounds of the unknown input estimate a Gaussian distribution of $\xi(t)$ is assumed. In this example a Monte-Carlo simulation with 10000 runs is carried out and the theoretical distribution of $\xi(t)$ is compared with an experi-

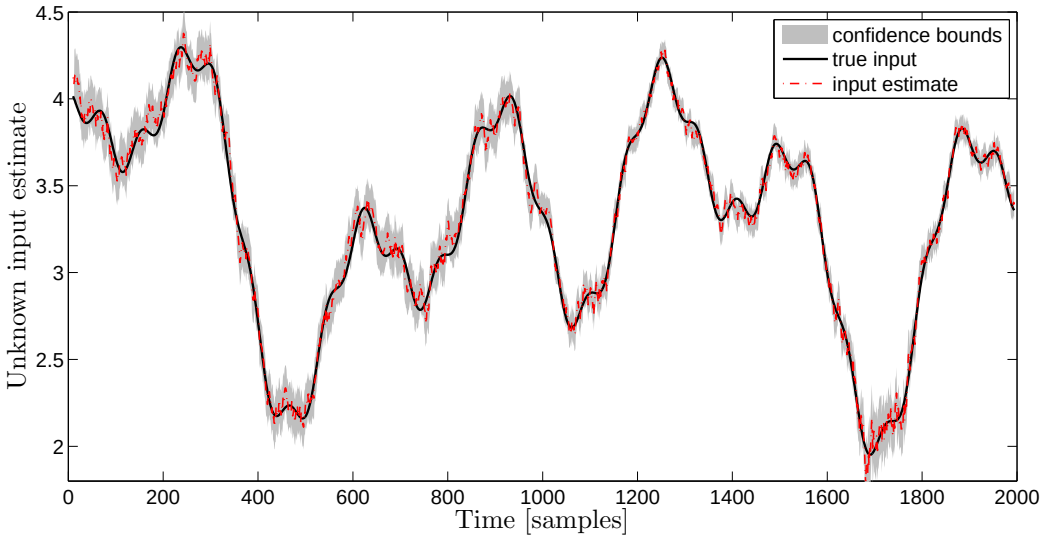

Figure 4.4: Unknown input estimation for Hammerstein-Wiener system in the EIV framework

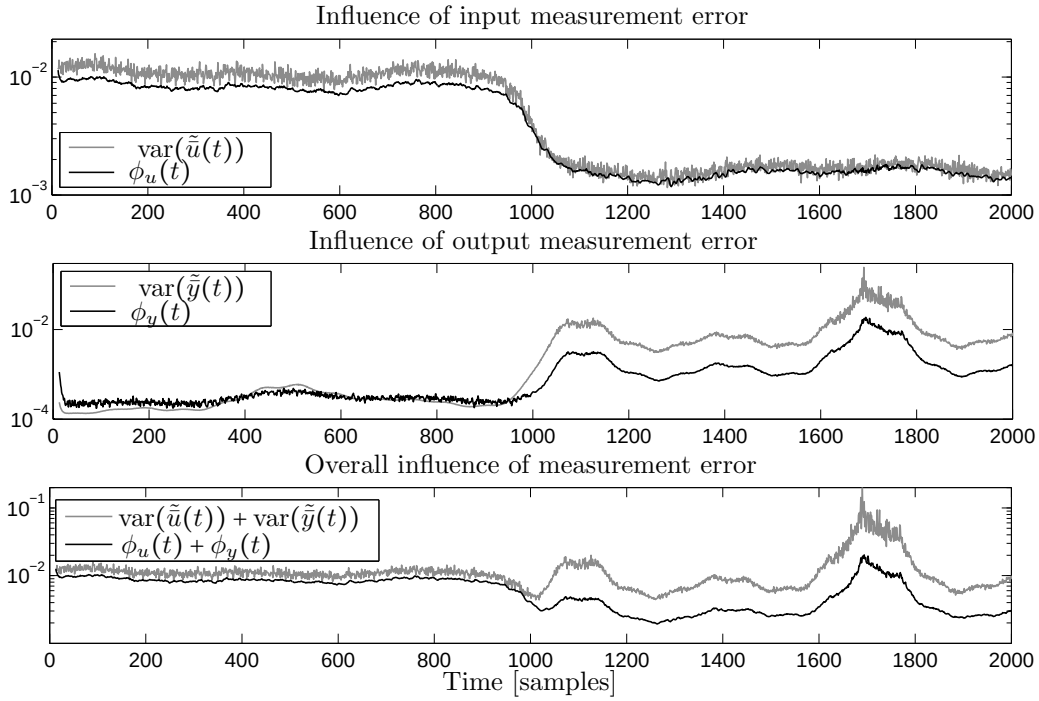

Figure 4.5: Adaptive minimisation of the effect of measurement noise on the input estimate

mentally obtained probability density function of the variable:

$$W\tilde{\tilde{Y}}(t)\tilde{\tilde{Y}}^T(t)W^T + WQ\tilde{\tilde{U}}(t)\tilde{\tilde{U}}^T(t)Q^TW^T \tag{4.29}$$

at each time sample. The system from the previous example is used for the simulation. In Fig. 4.6 those two distributions have been compared as functions of time. Further-

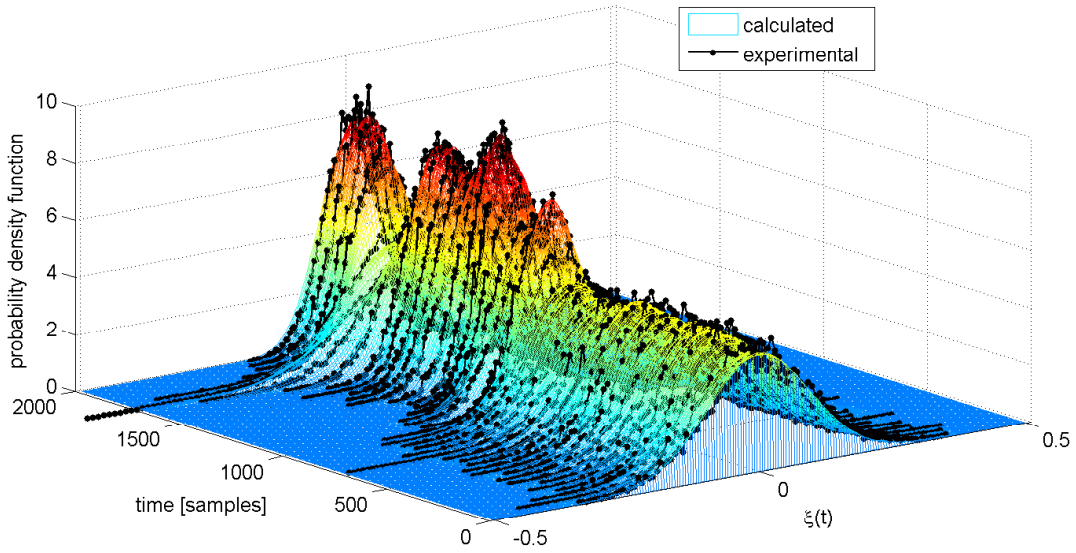

Figure 4.6: Experimental and calculated distributions of $\xi(t)$ as functions of time. The coloured surface presents the theoretical distribution of $\xi(t)$ (Gaussian curve with the variance defined by (4.20)) for a single simulation run. Black plots are experimentally obtained probability density functions of $\xi(t)$ from 10000 runs of the Monte-Carlo simulation.

more, in Fig. 4.7 both theoretical and experimental distributions of $\xi(t)$ are presented for four different time instances. It can be noted that the experimentally obtained distribution of $\xi(t)$ matches the theoretical Gaussian distribution with the variance given by equation (4.20). In Fig. 4.8 values of $\phi_u(t)$ and $\phi_y(t)$ as functions of time for a single simulation run have been compared with functions of time of mean values of, respectively, $WQ\tilde{\tilde{U}}(t)\tilde{\tilde{U}}^T(t)Q^TW^T$ and $W\tilde{\tilde{Y}}(t)\tilde{\tilde{Y}}^T(t)W^T$ from the Monte-Carlo simulation. It can be noted that the values of $\phi_u(t)$ and $\phi_y(t)$ calculated using (4.26) match the experimental data.

Example 4.3. Use of the linear PE-UIO instead of the PE-UIO-HW

As filter parameters are recalculated at each time sample, the PE-UIO-HW algorithm becomes computationally demanding. Therefore, it is worth considering to approximate the Hammerstein-Wiener system with a linear model and then use the linear PE-UIO described in Chapter 3 instead. Use of the linear PE-UIO in a Hammerstein-Wiener case is, however, feasible only if the nonlinearities are mild enough, so the error resulting from a linear approximation of the nonlinear system is relatively small. In this example use of the linear PE-UIO instead of the PE-UIO-HW is considered and a degradation of performance resulting from the use of the linear algorithm is examined.

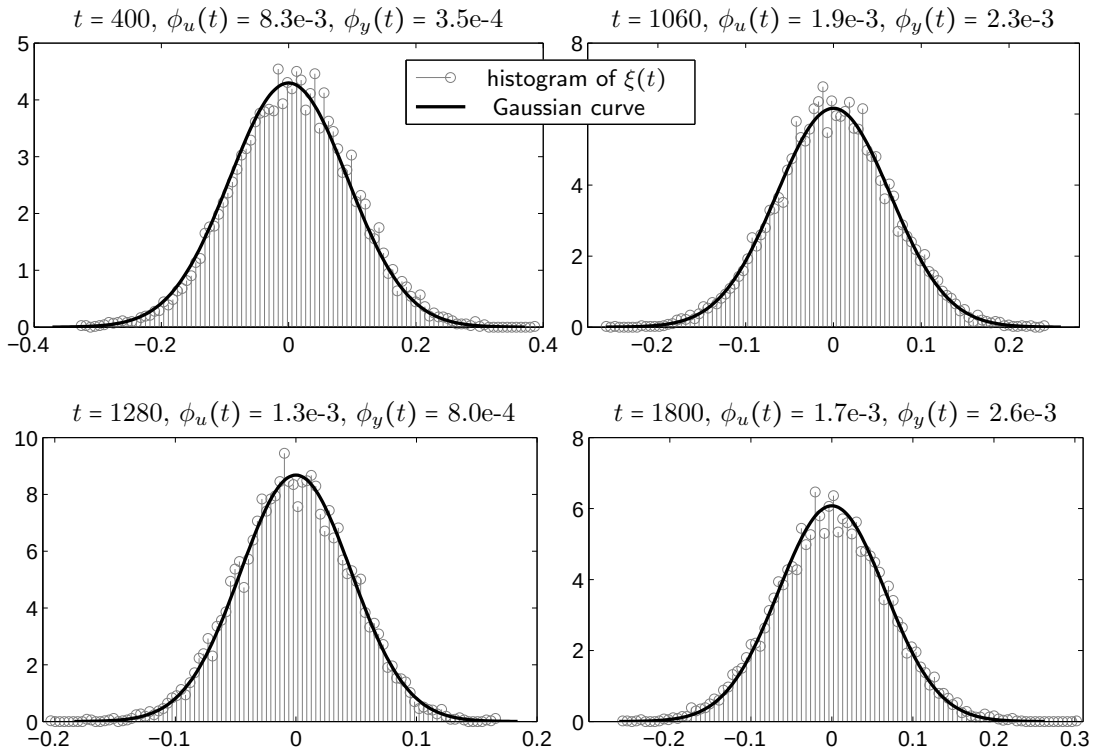

Figure 4.7: Comparison of theoretical distribution of $\xi(t)$ with experimental data. Black solid lines present theoretical distributions of $\xi(t)$ for different time instances (Gaussian curves with variance defined by (4.20)) for a single simulation run. Grey stems are experimentally obtained probability density functions of $\xi(t)$ from 10000 runs of Monte-Carlo simulation.

The linear block of the considered system is given by (4.28), whilst the Hammerstein and Wiener nonlinearities are:

$$\begin{aligned} \bar{u}_0(t) &= \frac{10}{1+e^{-0.4u_0(t)}} - 5 \\ y_0(t) &= \frac{b_i}{1+e^{-a_i\bar{y}_0(t)}} + c_i \end{aligned} \tag{4.30}$$

where a_i, b_i, and c_i are the coefficients of the Wiener nonlinearity $\eta(\cdot)$. The experiment has been performed for three different Wiener nonlinearities ($i = 1, 2, 3$), whose coefficients are given in Table 4.1. The Hammerstein nonlinearity as well as the three considered Wiener nonlinearities, denoted as $\eta_1(\cdot)$, $\eta_2(\cdot)$, and $\eta_3(\cdot)$, are presented in Fig. 4.9.

Both known and unknown inputs to the system, $u_0(t)$ and $v(t)$, are the same as in Example 4.1. The upper subfigure of Fig. 4.10 presents $u_0(t)$ and $\bar{u}_0(t)$. Due to the fact that the Hammerstein nonlinearity at the operating point is negligible $\bar{u}_0(t)$

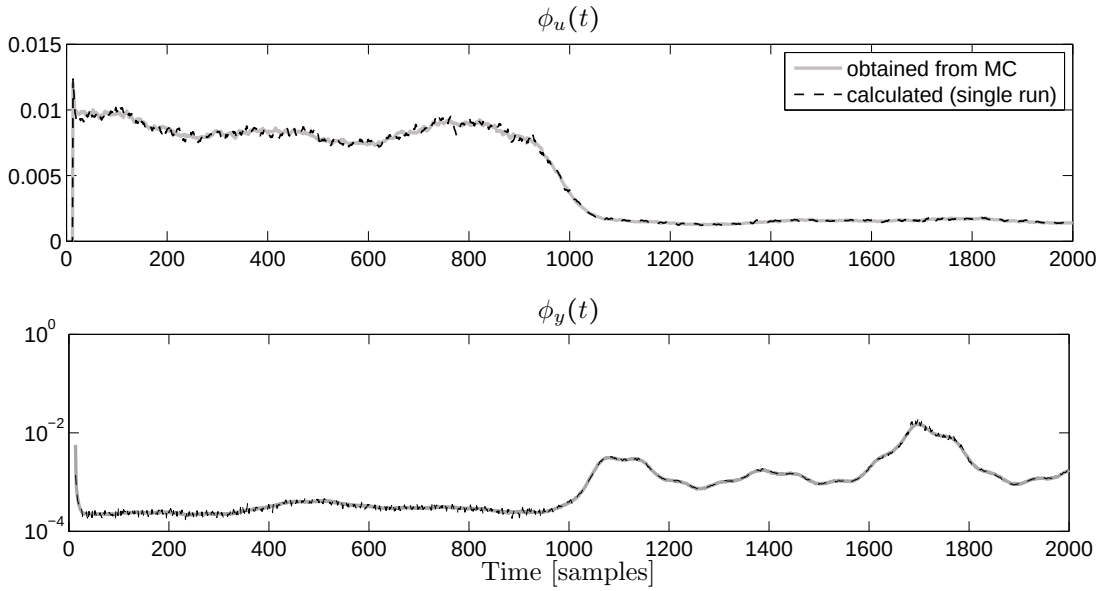

Figure 4.8: Comparison of calculated and experimental values of $\phi_u(t)$ and $\phi_y(t)$. Black dashed curves present theoretical values of $\phi_u(t)$ and $\phi_y(t)$ as functions of time (calculated using (4.26) for a single simulation run). Grey curves are experimentally obtained values of $\phi_u(t)$ and $\phi_y(t)$ from 10000 runs of Monte-Carlo simulation.

Table 4.1: Coefficients of Wiener nonlinearities $\eta_1(\cdot)$, $\eta_2(\cdot)$, and $\eta_3(\cdot)$

i	a_i	b_i	c_i
1	0.25	24	−12
2	0.2	26	−13
3	0.1	43	−21.5

is very close to $u_0(t)$ (the considered system is virtually a Wiener system). The lower subfigure of Fig. 4.10 shows $\bar{y}_0(t)$ and the corresponding $y_0(t)$ for three different Wiener nonlinearities. It is anticipated that the accuracy of the unknown input estimation using the linear PE-UIO will depend on the severity of the Wiener nonlinearity, i.e. the best accuracy is expected for $\eta_3(\cdot)$, whilst it is anticipated that $\eta_1(\cdot)$ will result is the most distorted unknown input estimate. The measured input and the output of the system are subjected to white, zero-mean, Gaussian, mutually uncorrelated sequences with the variances, respectively, $\mathrm{var}(\tilde{u}(t)) = 0.002$ and $\mathrm{var}(\tilde{y}(t)) = 0.003$.

For each case of a nonlinear system (i.e. a system with different Wiener nonlinearity) a linear model is obtained using the least squares technique in order to estimate the unknown input using the PE-UIO with $s = 12$ samples. A Monte-Carlo simulation with 100 runs is carried out, whose results in terms of R_T^2 are compared with results of the PE-UIO-HW and presented in Table 4.2 . Sample plots of the unknown input estimate

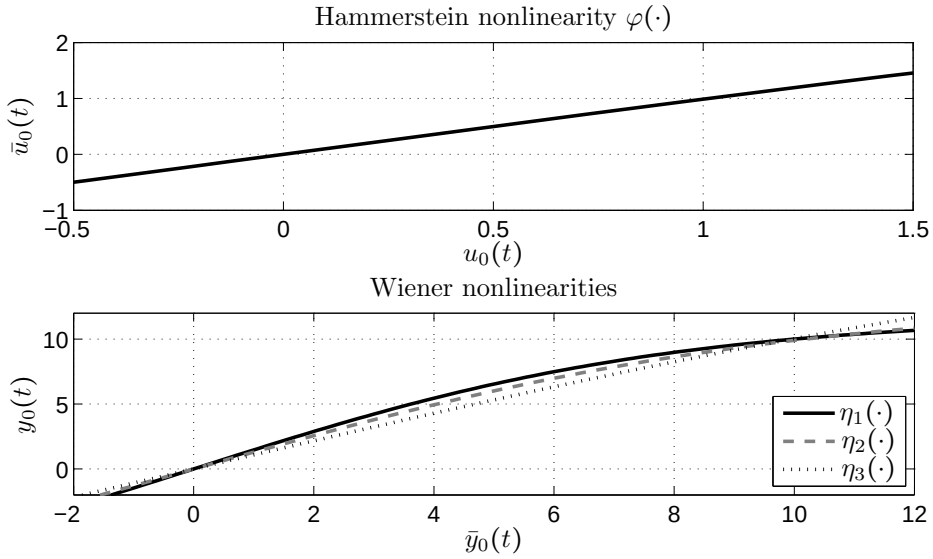

Figure 4.9: Hammerstein and Wiener nonlinearities

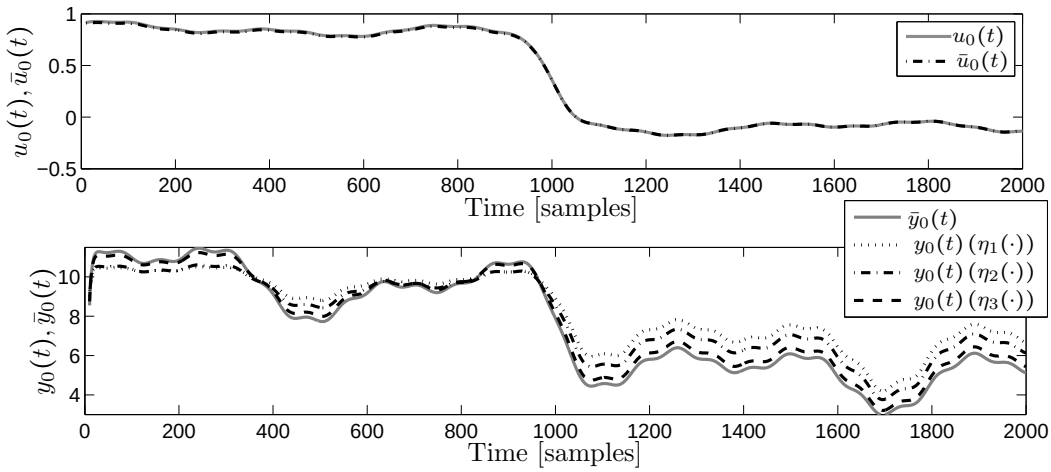

Figure 4.10: The upper subfigure shows the input of the considered system (grey solid curve) compared with the input of linear block (dashed-dotted curve). The lower subfigure presents the output of the linear dynamic block (grey solid curve) compared with the output of the system for different Wiener nonlinearities (black dashed, dashed-dotted and dotted curves).

for the considered models are plotted in Fig. 4.11. As expected the distortion in the unknown input estimate using the linear PE-UIO is least when the Wiener nonlinearity is given by $\eta_3(\cdot)$, whilst for $\eta_1(\cdot)$ the reconstructed signal is least accurate.

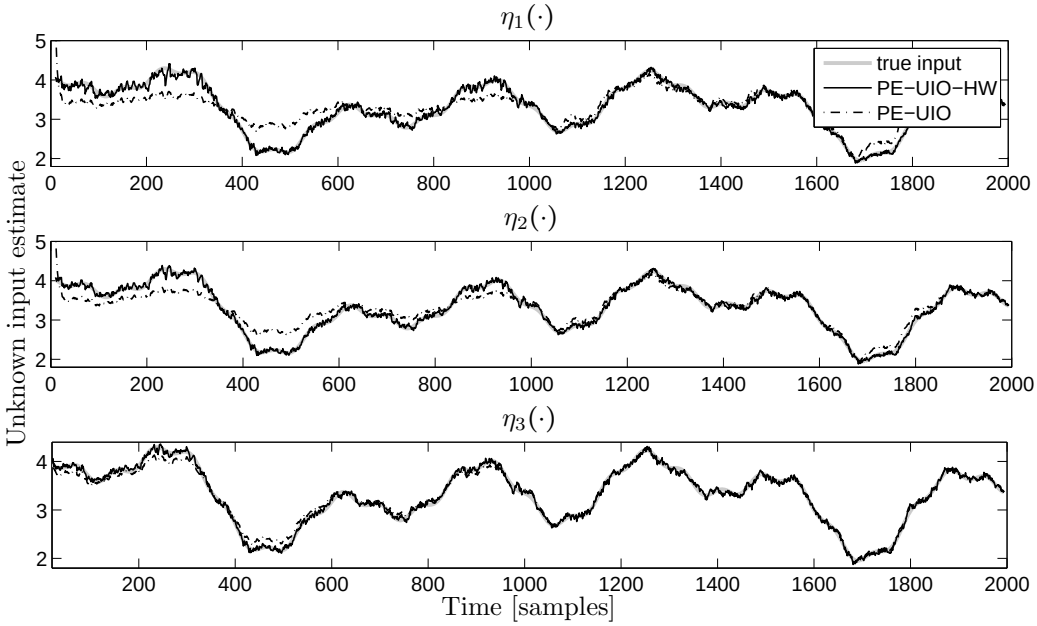

Figure 4.11: Unknown input estimation for different Wiener nonlinearities

Table 4.2: Comparison of efficacy (in terms of the mean value of R_T^2 [%] from a Monte-Carlo simulation with 100 runs) of the linear PE-UIO and the PE-UIO-HW for three different Wiener nonlinearities

$\eta_1(\cdot)$		$\eta_2(\cdot)$		$\eta_3(\cdot)$	
linear	nonlinear	linear	nonlinear	linear	nonlinear
0.7130	0.0385	0.4349	0.0270	0.0658	0.0216

4.4 Adaptive order PE-UIO for Hammerstein-Wiener systems

As it has been demonstrated in Subsection 3.7.1 an increase of the parity space order s reduces the bandwidth of the unknown input reconstructor thus improving the noise filtering properties of the filter (i.e. reducing the impact of the noise on the unknown input estimate). However, the reduction of the filter bandwidth results in the input reconstruction filter being sluggish. Due to the fact that $\mathrm{var}(\tilde{\tilde{u}}(t))$ and $\mathrm{var}(\tilde{\tilde{y}}(t))$ are time varying, the impact of the noise on the unknown input varies. Therefore, it is beneficial to vary the bandwidth of the filter (via changing the value of the parity space order s) as values of $\mathrm{var}(\tilde{\tilde{u}}(t))$ and $\mathrm{var}(\tilde{\tilde{y}}(t))$ change. In the algorithm proposed in this section the order of the parity space varies according to the changes of $\mathrm{var}(\tilde{\tilde{u}}(t))$ and $\mathrm{var}(\tilde{\tilde{y}}(t))$. In order to recognise that the order of the parity space is time varying, its value at the time instance t is further denoted as $s(t)$.

4.4.1 Choice of $s(t)$

The choice of $s(t)$ should depend on both $\mathrm{var}(\tilde{\tilde{u}}(t))$ and $\mathrm{var}(\tilde{\tilde{y}}(t))$. Considering (4.25) and (4.26) it should be noted that the input and output noise filtering indices defined as:

$$\rho_u = \frac{\phi_u}{\mathrm{var}(\tilde{\tilde{u}}(t))} \tag{4.31a}$$

$$\rho_y = \frac{\phi_y}{\mathrm{var}(\tilde{\tilde{y}}(t))} \tag{4.31b}$$

are not equal due to the presence of the matrix Q in (4.26a) and hence its influence on (4.31a). This means that the impact of the change of $s(t)$ will be different for the input and the output measurement noise. It is proposed to create a two-dimensional map, which assigns the value of $s(t)$ for each couple of $\mathrm{var}(\tilde{\tilde{u}}(t))$ and $\mathrm{var}(\tilde{\tilde{y}}(t))$. Furthermore, as the values of $\mathrm{var}(\tilde{\tilde{u}}(t))$ and $\mathrm{var}(\tilde{\tilde{y}}(t))$ are calculated based on the current values of the measured input and output signals (affected by noise), cf. (4.19), the order of the parity space $s(t)$ selected based on the current values of $\mathrm{var}(\tilde{\tilde{u}}(t))$ and $\mathrm{var}(\tilde{\tilde{y}}(t))$ may jitter unnecessarily. In order to avoid this problem, it is proposed to use local mean values of $\mathrm{var}(\tilde{\tilde{u}}(t))$ and $\mathrm{var}(\tilde{\tilde{y}}(t))$ defined as:

$$\overline{\mathrm{var}(\tilde{\tilde{u}}(t))} = \frac{1}{t_1 + t_2 + 1} \sum_{i=t-t_1}^{t+t_2} (\mathrm{var}(\tilde{\tilde{u}}(i)) \tag{4.32a}$$

$$\overline{\mathrm{var}(\tilde{\tilde{y}}(t))} = \frac{1}{t_1 + t_2 + 1} \sum_{i=t-t_1}^{t+t_2} (\mathrm{var}(\tilde{\tilde{y}}(i)) \tag{4.32b}$$

where t_1 and t_2 are arbitrarily defined by the user.

4.4.2 Variable estimation lag

At the time instance t, the following delayed unknown input estimate is calculated:

$$\hat{v}(t - \tau(t)) = W(t)\eta^{-1}(Y(t)) - W(t)Q(t)\varphi(U(t)) \tag{4.33}$$

where $\tau(t)$ is time varying, due to the alternating value of $s(t)$. (Note that the notation $\tau(t)$, $W(t)$, and $Q(t)$ has been used instead of τ, W, and Q in order to indicate that the estimation lag τ, the vector W, and the matrix Q as well as sizes of W and Q are time varying.) This would eventually lead to difficulties, such as some time instances of the unknown input would be omitted, and some of them estimated more than once. Therefore, a logic must be implemented, which copes with the variable estimation lag. A difficulty may arise in two situations:

(i) $\tau(t) > \tau(t-1)$

(ii) $\tau(t) < \tau(t-1)$

In the first case a particular time instance of the unknown input estimate is calculated twice. In such a case from the two values of the unknown input estimate sample the one should be selected, which is less affected by the noise. The fact that $\tau(t)$ increases, means an increase of the noise influence, i.e. $\mathrm{var}(\tilde{\tilde{u}}(t))$ or $\mathrm{var}(\tilde{\tilde{y}}(t))$ has increased. Therefore, the impact of the measurement noise on the unknown input estimate has also increased. Consequently, it can be deduced that the previously calculated value of the unknown input estimate is less affected by noise.

In the second case, the situation is opposite, i.e. some time instances of $\hat{v}(t)$ will be omitted. It is proposed to use $W(t-1)$ and $Q(t-1)$ to calculate the missing values of the unknown input estimate.

Incorporating this logic into Algorithm 4.1 the adaptive order PE-UIO-HW (AO-PE-UIO-HW) is obtained:

Algorithm 4.2 (AO-PE-UIO-HW).

for $t = 1 : N$

- Calculate $\overline{\mathrm{var}(\tilde{\tilde{u}}(t))}$ and $\overline{\mathrm{var}(\tilde{\tilde{y}}(t))}$
- Based on $\overline{\mathrm{var}(\tilde{\tilde{u}}(t))}$ and $\overline{\mathrm{var}(\tilde{\tilde{y}}(t))}$ select $s(t)$
- Obtain $W(t)$, $Q(t)$, and $\tau(t)$ as in Algorithm 4.1

if $\tau(t) = \tau(t-1)$

- Calculate $\hat{v}(t-\tau(t))$ as:

$$\hat{v}(t-\tau(t)) = W(t)\eta^{-1}(Y(t)) - W(t)Q(t)\varphi(U(t)) \tag{4.34}$$

elseif $\tau(t) < \tau(t-1)$

for $k = \tau(t-1) : \tau(t) - 1$

$$\hat{v}(t-k) = W(t-1)\eta^{-1}(Y(t-k)) - W(t-1)Q(t-1)\varphi(U(t-k)) \tag{4.35}$$

end

$$\hat{v}(t-\tau(t)) = W(t)\eta^{-1}(Y(t)) - W(t)Q(t)\varphi(U(t)) \tag{4.36}$$

else

- Do nothing

end

Table 4.3: The table assigns value of the parity space order $s(t)$ based on the values of $\overline{\text{var}(\tilde{\tilde{u}}(t))}$ and $\overline{\text{var}(\tilde{\tilde{y}}(t))}$. The row of the table is selected such that $u_d < \log\left\{\overline{\text{var}(\tilde{\tilde{u}}(t))}\right\} \leq u_u$, whereas the column is chosen such that $y_d < \log\left\{\overline{\text{var}(\tilde{\tilde{y}}(t))}\right\} \leq y_u$

			$\log\left\{\overline{\text{var}(\tilde{\tilde{y}}(t))}\right\}$														
		y_d	$-\infty$	-2.87	2.66	-2.52	-2.42	-2.31	-2.19	-2.10	-2.01	-1.94	-1.88	-1.83	-1.76	-1.68	-1.61
	u_d	y_u / u_u	-2.87	-2.66	-2.52	-2.42	-2.31	-2.19	-2.10	-2.01	-1.94	-1.88	-1.83	-1.76	-1.68	-1.61	∞
$\log\left\{\overline{\text{var}(\tilde{\tilde{u}}(t))}\right\}$	$-\infty$	-3.3	10	11	12	13	14	15	16	17	18	19	20	21	22	23	24
	-3.3	-3.2	11	12	13	14	15	16	17	18	19	20	21	22	23	24	25
	-3.2	-3.0	12	13	14	15	16	17	18	19	20	21	22	23	24	25	26
	-3.0	-2.9	13	14	15	16	17	18	19	20	21	22	23	24	25	26	27
	-2.9	-2.8	14	15	16	17	18	19	20	21	22	23	24	25	26	27	28
	-2.8	-2.6	15	16	17	18	19	20	21	22	23	24	25	26	27	28	29
	-2.6	-2.5	16	17	18	19	20	21	22	23	24	25	26	27	28	29	30
	-2.5	-2.3	17	18	19	20	21	22	23	24	25	26	27	28	29	30	31
	-2.3	-2.1	18	19	20	21	22	23	24	25	26	27	28	29	30	31	32
	-2.1	-2.0	19	20	21	22	23	24	25	26	27	28	29	30	31	32	33
	-2.0	-1.8	20	21	22	23	24	25	26	27	28	29	30	31	32	33	34
	-1.8	-1.7	21	22	23	24	25	26	27	28	29	30	31	32	33	34	35
	-1.7	-1.6	22	23	24	25	26	27	28	29	30	31	32	33	34	35	36
	-1.6	-1.4	23	24	25	26	27	28	29	30	31	32	33	34	35	36	37
	-1.4	-1.1	24	25	26	27	28	29	30	31	32	33	34	35	36	37	38
	-1.1	-0.7	25	26	27	28	29	30	31	32	33	34	35	36	37	38	39

4.4.3 Numerical examples

In this subsection the design of the AO-PE-UIO-HW is presented. Two examples are considered here. The first example resembles an OE case, i.e. the input measurement is noise-free whilst the output is subjected to white, Gaussian, zero-mean measurement noise. The second example is in the EIV framework, i.e. both the system input and the output are affected by white, Gaussian, zero-mean measurement noise.

Example 4.4. Design of the AO-PE-UIO-HW in an OE noise case
Consider a system defined by (4.27) and (4.28). It is assumed that the output of the system is subjected to white, Gaussian, zero-mean noise sequence of the variance $\mathrm{var}(\tilde{y}) = 0.5$, whereas $\mathrm{var}(\tilde{u}) = 0$ (OE case).

The input and output signals as well as $\bar{u}_0(t)$ and $\bar{y}_0(t)$ are presented in Fig. 4.12. Similarly as in Example 4.1, $y_0(t)$ is relatively high for the first 1000 samples of the simulation, hence it is anticipated that the inversion of the noisy measurement $y(t)$ for the first 1000 samples will reduce the impact of the output measurement noise. This is due to relatively steep slope of $\eta(\cdot)$ for high values of $y_0(t)$. After 1000 samples $y_0(t)$ decreases, which is expected to result in a higher vulnerability of the input reconstruction process to the output measurement noise, as the slope of $\eta(\cdot)$ is less steep for the relatively low values of the output.

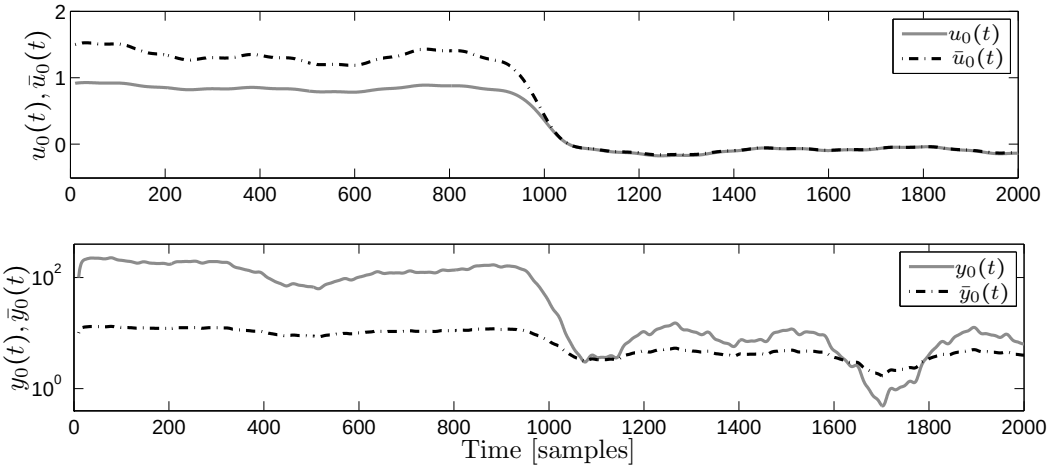

Figure 4.12: Input and output of the considered system (grey solid curve) compared with input and output of linear block (dashed-dotted curve)

The unknown input in this example is slightly lower than that in Example 4.1, which yields lower values of $y_0(t)$ compared to Example 4.1. Therefore, it is anticipated that the effect of measurement noise on the unknown input reconstruction process will be more significant than in Example 4.1 (especially when $y_0(t)$ is very low between 1600 and 1800 sample).

As a result of the inversion of $\eta(\cdot)$, needed for the calculation of $\bar{y}_0(t)$, the ratio of

standard deviations of $\tilde{\bar{y}}(t)$ to $\bar{y}_0(t)$ is 4.5 %. However, this ratio changes over the time. For the period between 100 and 800 samples the standard deviation of $\tilde{\bar{y}}(t)$ is equal to 1.7 % of the standard deviation of $\bar{y}_0(t)$. Whereas for the period between 1100 and 1600 samples this ratio is 27.0 %. In the extreme case of the period between 1600 and 1800 samples this ratio is equal to 81.1 %. Such a large deviation of the measurement noise impact requires adaptivity of the unknown input reconstruction scheme. The term $\overline{\mathrm{var}(\tilde{\bar{y}}(t))}$ has been calculated with $t_1 = 2\tau(t-1)+1$ and $t_2 = 0$, cf. (4.32).

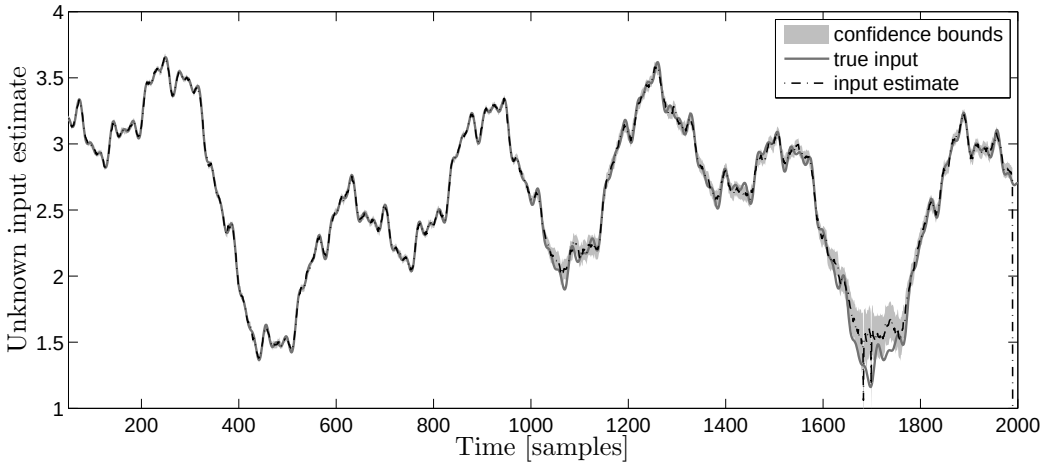

Figure 4.13: Unknown input estimation for a Hammerstein-Wiener OE system using AO-PE-UIO-HW

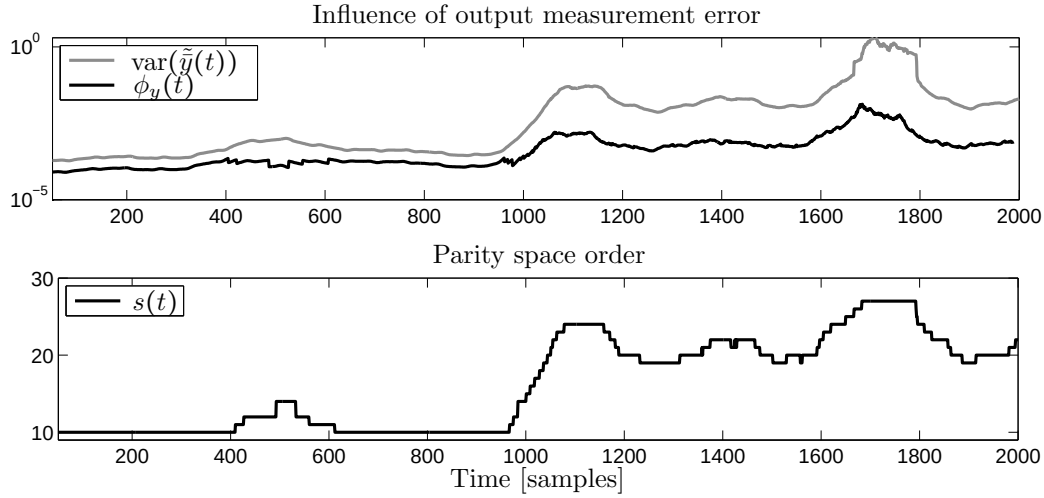

Figure 4.14: Adaptive minimisation of the effect of measurement output noise on the input estimate

The unknown input estimate with 95 % confidence bounds is presented in Fig. 4.13. The parity space order varies according to Table 4.3 and as a function of time is

presented in the lower subfigure of Fig. 4.14. The upper subfigure of Fig. 4.14 presents $\mathrm{var}(\tilde{\bar{y}}(t))$ and $\phi_y(t)$. As expected, the parity space order is low in the first half of the simulation, when the impact of the measurement noise is low. Such a small $s(t)$ ensures a high bandwidth of the filter, and therefore even high frequency components of $v(t)$ are reconstructed, cf. Fig. 4.13. In the second half of the simulation, when the impact of the measurement noise becomes more significant, the order of the parity space increases. Furthermore, a higher parity space order yields stronger noise attenuation (in terms of the ratio between $\mathrm{var}(\tilde{\bar{y}}(t))$ and $\phi_y(t)$), which can be seen in the upper subfigure of Fig. 4.14.

A Monte-Carlo simulation with 100 runs has been carried out to compare the performance of the AO-PE-UIO-HW and the PE-UIO-HW with a constant parity space order for two cases of s. The aim of this experiment is to quantify the improvement of the unknown input reconstruction process when the AO-PE-UIO-HW is used instead of the PE-UIO-HW. Results in terms of the R_T^2 are compared in Table 4.4. It can be noted that by varying the parity space order an improvement of the accuracy of the algorithm has been achieved. However, it needs to be remembered that the adaptive algorithm needs more computational power.

Table 4.4: Comparison of efficacy of the PE-UIO-HW and the A0-PE-UIO-HW in terms of R_T^2 [%]

	PE-UIO-HW			AO-PE-UIO-HW
sample	$s = 10$	$s = 23$	$s = 26$	variable s
100:1990	0.0305	0.0320	0.0438	0.0197
100:1000	6.5e-4	0.0023	0.0033	5.7e-4
1000:1990	0.0600	0.0609	0.0837	0.0378

Example 4.5. Design of the AO-PE-UIO-HW in the EIV framework
Similarly as in Example 4.4 the Hammerstein-Wiener system is defined by (4.27) and (4.28). The input and output signals as well as $\bar{u}_0(t)$ and $\bar{y}_0(t)$ are the same as in Example 4.4, cf. Fig. 4.12. Both input and output measurements are subjected to white, Gaussian, zero-mean, mutually uncorrelated noise sequences, whose variances are, respectively, $\mathrm{var}(\tilde{u}) = 0.001$ and $\mathrm{var}(\tilde{y}) = 0.5$, i.e. EIV framework. Similarly as in Example 4.5, for the first 1000 samples the output signal is relatively high, hence the output measurement error is expected to have a relatively low impact on the input reconstruction error. However, as the known input is relatively high for the first half of the simulation, whilst the slope $\varphi(\cdot)$ is relatively small, it is anticipated that the impact of the input measurement noise on the estimation error will be prevailing for the first 1000 samples of the simulation, cf. Example 4.1. In contrast, after 1000 samples, when both $u_0(t)$ and $y_0(t)$ decrease, the influence of the output measurement noise is expected to increase, whilst the impact of the input measurement noise is anticipated

to reduce. Similarly as in the previous example the parity space order has been obtained using Table 4.3, whereas terms $\overline{\text{var}(\tilde{\tilde{u}}(t))}$ and $\overline{\text{var}(\tilde{\tilde{y}}(t))}$ have been calculated using $t_1 = 2\tau(t-1)+1$ and $t_2 = 0$.

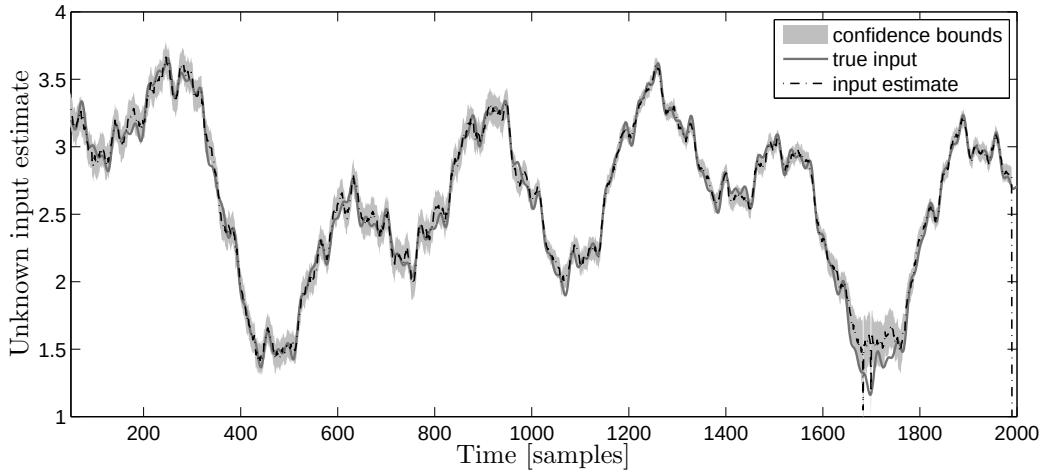

Figure 4.15: Unknown input estimation for a Hammerstein-Wiener system in the EIV framework using AO-PE-UIO-HW

The unknown input estimate is presented in Fig. 4.15. The values $\text{var}(\tilde{\tilde{u}}(t))$ and $\phi_u(t))$ are depicted in the upper subfigure of Fig. 4.16, whilst $\text{var}(\tilde{\tilde{y}}(t))$ and $\phi_y(t))$, are shown in the middle subfigure of Fig. 4.16. The lower subfigure of Fig. 4.16 presents the parity space order $s(t)$ as a function of time, which is compared with the $s(t)$ from the previous example. Note that the only difference between Examples 4.4 and 4.5 is presence of the input measurement noise. The term $\text{var}(\tilde{\tilde{u}}(t))$ is relatively large for the first half of the simulation, whereas it becomes negligible after 1000 samples. This influence of the input measurement noise can be noticed by comparing the values of $s(t)$ for the two considered examples. The presence of the input measurement noise causes an increase of $s(t)$ by approximately 5 samples compared to the OE case during the first half of the simulation. After the first 1000 samples, as the impact of the input measurement noise on the unknown input estimate becomes negligible, $s(t)$ is similar for both the OE (Example 4.4) and the EIV (Example 4.5) cases.

4.5 Concluding remarks

The algorithms presented in this chapter are extensions of the PE-UIO developed in Chapter 3. The basic idea of the unknown input reconstruction scheme for Hammerstein-Wiener systems is to, firstly, knowing the system nonlinearities calculate the known input and the output of the linear block, then use the PE-UIO to calculate the unknown input. The algorithm has been developed for the EIV framework, i.e. when both measured input and output of the system are subjected to white, Gaussian, zero-mean,

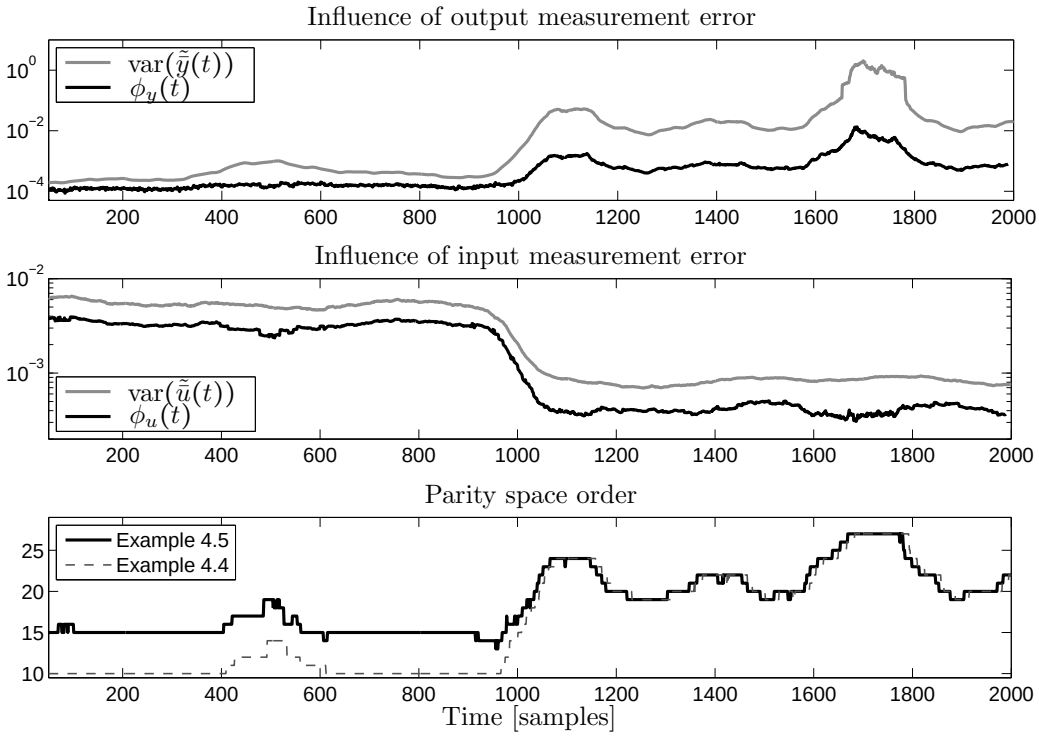

Figure 4.16: Upper and middle subfigures demonstrate adaptive minimisation of the effect of measurement output noise on the input estimate in Example 4.5. Lower subfigure compares values of parity space order $s(t)$ as functions of time in Examples 4.4 (OE) and 4.5 (EIV).

mutually uncorrelated noise sequences. The calculated values of the known input and the output of the linear block are affected by measurement noise and the impact of the EIV disturbance sequences depends on the values of the known input and output themselves. This is due to the nonlinearities preceding and following the linear block. Consequently, the impact of the measurement noise on the unknown input estimate changes over time. Therefore, the filter parameters are calculated at each time instance.

In the first of the proposed algorithms, the PE-UIO-HW, the order of the parity space, and thus the estimation delay, remains constant, whilst the filter parameters vary over time.

Due to the fact that the impact of the measurement noise on the unknown input estimate may vary significantly, a further extension to the scheme is proposed, where the order of the parity space, $s(t)$, is time varying. The parity space order is selected based on values of the input and output measurement noise impact coefficients, calculated as functions of noise variances and measured signals. The variable parity space order allows the adjustment of the bandwidth of the unknown input reconstruction filter

to the changing impact of the measurement noise on the unknown input estimate. The variation of $s(t)$ imposes a variable estimation lag, $\tau(t)$. Consequently, a logic is implemented, which resolves the problem of time varying $\tau(t)$, resulting in a smooth estimate of the unknown input.

The proposed schemes, since inherently adaptive, require at each discrete time step a non negligible computational effort. The future work, therefore, aims towards an optimisation of the computational procedure. It is also intended to extend the algorithm to the multivariable case. Furthermore, block oriented models in the EIV framework are a new topic in the literature, for which effective identification schemes are required. Although it has been assumed that the unknown input is fed directly to the linear block, the algorithm can be easily extended to the case, when the unknown input is transformed by a nonlinear memoryless function, and afterwards, the transformed unknown input is fed to the linear dynamic block (based on the assumption that the static nonlinearity is invertible).

Chapter 5

Robust fault detection via eigenstructure assignment

Nomenclature

A	state transition matrix in state-space model
A_{c_1}, A_{c_2}	filter state transition matrices
$A_\lambda, A_e^*, A_e^{*(i)}, A_w$	auxiliary matrices
$\tilde{\tilde{A}}, \tilde{A}$	auxiliary matrices
A'	auxiliary matrix
B	input matrix of the input in state-space model
$\tilde{\tilde{B}}$	auxiliary matrix
C	output matrix in state-space model
C'	auxiliary matrix
$d(t)$	disturbance signal
$d_i(t)$	i^{th} element of $d(t)$
$d^*(t)$	$d(t)$, whose elements $d_i(t)$ are delayed, respectively, by δ_i
D	feedforward matrix of known input in state-space model
e	matrix of directions of elements of $d(t)$
e_i	direction of d_i
$\bar{e}$	matrix built from matrices e_i
$\bar{e}_i$	matrix whose image is sum of image of e_i and images of invariant zero directions of (A, e_i, C)
E	input matrix of disturbance signal in state-space model
E_i	i^{th} column of input matrix of disturbance signal in state-space model
F	input matrix of fault signal in state-space model
$F(\bar{e})$	projection of F on subspace spanned by columns of $\bar{e}$
$F(\bar{e}^\perp)$	projection of F on subspace orthogonal to $\bar{e}$
g, g_i	auxiliary scalar
I	identity matrix
J, J_1, J_2	gain matrices
K, K_1, K_2, K' ...	gain matrices
l_j, l_j^*	transposes of left eigenvectors of filter state transition matrix
m	number of system outputs
n	number of states in state-space model

p	number of system inputs
$P(\lambda_i)$	auxiliary function of λ_i
P, R	auxiliary matrices
$P_{l,k}$	auxiliary term
q	number of disturbance signals
Q	gain matrix
r	number of fault signals
$r(t)$	residual
$r_i(t)$	i^{th} element of $r(t)$
r_q	number of rows of Q
T	similarity transformation matrix
T_1, T_2	submatrices of T
$u(t)$	system input
$u_0(t)$	noise-free output in output-error case
$\tilde{u}(t)$	input measurement noise
$U(t)$	stacked vector of last $\tau + 1$ values of $u(t)$
$U_0(t)$	stacked vector of last $\tau + 1$ values of $u_0(t)$
$\tilde{U}(t)$	stacked vector of last $\tau + 1$ values of $\tilde{u}(t)$
$v, v_j, v_j^{(i)}$	auxiliary vectors
V_e	matrix whose columns are eigenvectors of filter state transition matrix
$w_j, w_j^{(i)}, w_j^{\prime(i)}$ ...	right eigenvectors of filter state transition matrix
w_j^*	auxiliary vector
W	auxiliary matrix
W_u, W_y	parity matrices
$x(t)$	state vector instate space model
$\hat{x}(t)$	state estimate
$x_{i,j}$	auxiliary scalars
X	auxiliary matrix
$y(t)$	system output
$y_0(t)$	noise-free output in output-error case
$\tilde{y}(t)$	output measurement noise
$Y(t)$	stacked vector of last $\tau + 1$ values of $y(t)$
$Y_0(t)$	stacked vector of last $\tau + 1$ values of $y_0(t)$
$\tilde{Y}(t)$	stacked vector of last $\tau + 1$ values of $\tilde{y}(t)$
z_i	system zero
$z_i(t)$	state estimate
α_i	auxiliary parameter
$\beta_i, \bar{\beta}_i$	auxiliary parameter vector
δ_i	auxiliary term
$\lambda_j, \lambda_j^{(i)}$	eigenvalue of filter state transition matrix
Λ_e	diagonal matrix whose diagonal elements are eigenvalues of filter state transition matrix
$\mu(t)$	fault signal
$\mu_i(t)$	i^{th} element of fault signal
$\Theta^{(i)}, \bar{\Theta}^{(i)}$	auxiliary matrices
Ω	set of all invariant zeros of (A, e, C) or an auxiliary matrix
Ω_i	set of all invariant zeros of (A, e_i, C)
$\Sigma_{\tilde{u}}, \Sigma_{\tilde{y}}, \Sigma_{\bar{\mu}}$	covariance matrices
τ	convergence time of finite time-convergent state observer, order of parity space
$\xi(t)$	state estimation error

Ψ ..... auxiliary matrix

Preliminary reading: Sections 2.2, 2.6, and 2.7.

5.1 Introduction

Increasing complexity of industrial systems leads to a growing demand for system fault diagnosis. Furthermore, system uncertainties (disturbances), such as modelling errors, parameter variations or unmeasurable external stimuli, obstruct the fault detection process, leading to false alarms. Therefore, a need arises for robust, i.e. disturbance decoupled, fault detection schemes. In this chapter robust fault detection is considered. This means that the residual generator is sensitive to faults but insensitive to disturbances.

Frank & Wünnenberg (1989), Duan & Patton (2001), and Edelmayer (2005) presented robust fault detection schemes based on unknown input observers. LMI have been also used for the robust fault detection (Chen & Nagarajaiah 2007, Ding, Zhong, Bingyong & Zhang 2001). Zhong, Ding, Lam & Wang (2003) proposed an LMI approach to design a robust fault detection filter for uncertain linear time-invariant systems. Patton and Chen (Patton & Chen 1991*b*, Chen & Patton 1999) used the left and right eigenstructure assignment techniques for the purpose of disturbance decoupling. Furthermore, the equivalence between the left eigenstructure assignment-based robust fault detection filter and the first order PE has been demonstrated by Patton & Chen (1991*a*, 1991*b*, 1991*c*). Also the problem of the robust fault detection via eigenstructure assignment has been of the topic of the research of Park & Rizzoni (1994) and Shen & Hsu (1998). Douglas & Speyer (1995) proposed an algorithm for preventing ill-conditioning when using left eigenstructure assignment. A novel method for left eigenstructure assignment has been proposed in (Kowalczuk & Suchomski 2005). Patton & Liu (1994) presented a robust control design method using eigenstructure assignment, genetic algorithms and a gradient-based optimisation. A reconfigurable control scheme has been presented in (Ashari, Sedigh & Yazdanpanah 2005*a*, Ashari, Sedigh & Yazdanpanah 2005*b*).

Eigenstructure assignment has been used in various industrial applications. A review of applications has been presented in (Isermann & Balle 1997). Robust fault detection filters based on eigenstructure assignment have been used in a rolling mill (Gu & Poon 2003), a jet engine (Patton & Chen 1992), an automotive engine (Shen & Hsu 1998), an advanced vehicle control systems (Douglas, Speyer, Mingori, Chen, Malladi & Chung 1996), a single-shaft gas turbine (Fantuzzi, Simani & Beghelli 2001), a flexible manipulator (Tan & Habib 2006), an inverted pendulum (Tan & Habib 2004), a vehicle health monitoring system (Ng, Chen & Speyer 2006), and a longitudinal motion of an unmanned aircraft model (Siahi, Sadrnia & Darabi 2009). Luenberger state observers using a fixed-structure H_∞ optimization have been applied to fault detection of a

lane-keeping control of automated vehicles (Ibaraki, Suryanarayanan & Tomizuka 2005) and fifth order linearised dynamics of an aircraft (Ashari et al. 2005*a*).

This chapter is organised as follows: in Section 5.2 the robust fault detection filter design method via right eigenstructure assignment of Chen & Patton (1999) is extended to systems whose output response to disturbances contains invariant zeros. Then design of robust PE via right eigenstructure assignment is proposed in Section 5.3. Furthermore, in Section 5.4 the left eigenstructure assignment is utilised to design robust PE of a user defined order.

5.2 Robust fault detection via right eigenstructure assignment for systems with unstable invariant zeros

Tan, Edwards & Kuang (2006*b*) extended the work of Chen & Patton (1999) providing a right eigenstructure method for a sensor fault reconstruction. They demonstrated that the invariant zeros of the transfer function between the disturbance and the output are the unobservable modes of the robust fault detection filter. Therefore, filter stability can only be ensured provided these zeros lie inside the unit circle. Tan, Edwards & Kuang (2006*b*) used LMI to solve the filter equations. A continuation of they work has been presented in (Tan, Edwards & Kuang 2006*a*), however the problem of using the right eigenstructure assignment for the robust fault detection filter design in the presence of unstable invariant zeros has not been resolved. The problem has been solved by Chen & Speyer (2006*a*, 2006*b*, 2007) using a geometric approach. Chen & Speyer (2006*b*) used the spectral theory to design a Beard-Jones fault isolation filter, whose applicability has been extended to systems with unstable invariant zeros. Furthermore, a design of the filter has been presented using eigenstructure assignment (Chen & Speyer 2006*a*) and LMI (Chen & Nagarajaiah 2007).

This section extends the design method of a robust fault detection filter proposed in (Chen & Patton 1999) to systems whose output response to disturbances contains invariant zeros. Although the geometrical structure of the filter proposed here is similar to that of Chen and colleagues (2006*b*, 2006*a*, 2007), the design procedure is simpler. Similarities and differences between the robust fault detection filter presented in this section and a fault isolation filter of Chen & Speyer (2006*a*) are discussed in Subsection 5.2.6.

5.2.1 Problem statement

It is assumed that a linear, dynamic, discrete-time, time-invariant system can be represented by the following equations, cf. (2.64):

$$\begin{aligned} x(t+1) &= Ax(t) + Bu(t) + Ed(t) + F\mu(t) \\ y(t) &= Cx(t) + Du(t) \end{aligned} \tag{5.1}$$

where $x(t) \in \mathbb{R}^n$ is the system state vector, $u(t) \in \mathbb{R}^p$ and $y(t) \in \mathbb{R}^m$ are, respectively, the system input and output, $d(t) \in \mathbb{R}^q$ denotes a disturbance vector, whilst $\mu(t) \in \mathbb{R}^r$ is a fault signal. Matrices A, B, C, D, E, and F are constant and have appropriate dimensions. It is assumed that (C, A) is an observable pair and the matrix E is of full column rank.

Problem of unstable invariant zeros

Consider the robust fault detection filter described in Subsection 2.6.1 applied to the system (5.1). Tan et al. (2006*a*) observed that the invariant zeros of the system (A, E_i, C) are unobservable modes of the pair (C', A'), cf. (2.69). As a result, if the invariant zero is unstable, the pair (C', A') is not detectable. Consequently, in order to ensure stability of the fault detection filter (2.54) in the case, when the triple (A, E_i, C) has an unstable invariant zero, the design procedure needs to be altered, which is proposed in Subsections 5.2.2, 5.2.3, and 5.2.4.

Lemma 5.1. Denote invariant zeros of (A, E_i, C) as $z_1, z_2, \cdots, z_{q_i}$. Then zeros of (A, E_i, C) fulfil the following recursive set of equations:

$$\begin{bmatrix} z_j I - A & -v_{j-1} \\ C & 0 \end{bmatrix} \begin{bmatrix} v_j \\ g_j \end{bmatrix} = 0 \tag{5.2}$$

where v_0 denotes E_i, $v_j, j = 1, \cdots, q_i$ are vectors and $g_j, j = 1, \cdots, g_i$ are scalar values.

Proof. Equation (5.2) can be reformulated as:

$$\begin{aligned} A \begin{bmatrix} v_1 & v_2 & \cdots & v_{q_i} \end{bmatrix} - \begin{bmatrix} v_1 & v_2 & \cdots & v_{q_i} \end{bmatrix} \begin{bmatrix} z_1 & -g_2 & 0 & \cdots & 0 \\ 0 & z_2 & -g_3 & \cdots & 0 \\ \vdots & \vdots & \vdots & \ddots & \vdots \\ 0 & 0 & 0 & \cdots & z_{q_i} \end{bmatrix} \\ + E_i \begin{bmatrix} g_1 & 0 & \cdots & 0 \end{bmatrix} = 0 \end{aligned} \tag{5.3}$$

which is equivalent to (2.35). ∎

Lemma 5.2. If the pair (A, C) is observable, scalars g_j, $j = 1, \cdots, q_i$ in (5.2) are non-zero.

Proof. If $g_j = 0$ then (5.2) becomes:

$$\begin{bmatrix} z_j I - A \\ C \end{bmatrix} v_j = 0 \tag{5.4}$$

which means that z_j is an unobservable mode of the system (A, E_i, C). However, the pair (C, A) is observable, hence it does not have unobservable modes. Consequently, $g_j \neq 0$. ∎

Rank condition

A certain case when the rank condition:

$$\text{rank}(CE) = \text{rank}(\begin{bmatrix} A_\lambda \\ CE \end{bmatrix}) \tag{5.5}$$

is not fulfilled is considered here and a solution is proposed, which allows to relax the strict rank condition and, consequently, apply the robust fault detection filter presented in Subsection 2.6.1. Denote $\delta_i, i = 1, \cdots, q$ the lowest number for which:

$$CA^{\delta_i} E_i \neq 0 \tag{5.6}$$

Consider the situation when $\delta_i = 0$ for $i = 1, \cdots, q_0$, where $q_0 < q$, whilst $\delta_i \neq 0$ for $i = q_0 + 1, \cdots, q$. Then $CE_i = 0$ for $i = q_0 + 1, \cdots, q$, whilst the i^{th} column of A_λ is:

$$(A - \lambda_i I) E_i \tag{5.7}$$

The rank condition (5.5) is fulfilled if and only if the i^{th} column of A_λ, $i = q_0 + 1, \cdots, q$, is zero. This occurs if and only if E_i is a right eigenvector of A corresponding to the eigenvalue λ_i. This would, however, mean that E_i belongs to the unobservable subspace of the pair (C, A). Thus, as it has been assumed that (C, A) is observable, i.e. (C, A) does not have any unobservable subspace, E_i is not a right eigenvector of A and the rank condition (5.5) is not fulfilled. In order to relax this condition it is proposed to slightly alter the robust fault detection filter design presented in Subsection 2.6.1, by replacing E with the following matrix:

$$e = \begin{bmatrix} e_1 & e_2 & \cdots & e_q \end{bmatrix} \tag{5.8}$$

where:

$$e_i = A^{\delta_i} E_i \tag{5.9}$$

From the definition of δ_i, cf. (5.6), it holds that $Ce_i \neq 0$ for $i = 1, \cdots, q$. Therefore, columns of A_λ do not require to be equal to zero.

Theorem 5.1. Invariant zeros of the triple (A, e_i, C) are equal to the invariant zeros of (A, E_i, C) plus δ_i zero-valued invariant zeros.

Proof. For $j = 1, 2, \cdots, \delta_i$ it holds, that

$$\begin{bmatrix} -A & -A^j E_i \\ C & 0 \end{bmatrix} \begin{bmatrix} A^{j-1} E_i \\ -1 \end{bmatrix} = 0 \tag{5.10}$$

Therefore, from Lemma 5.1 it follows, that invariant zeros of (A, e_i, C) are $z_1 = z_2 = \cdots = z_{\delta_i} = 0$, whilst the corresponding vectors $v_0 = A^{\delta_i} E_i = e_i$, $v_1 = A^{\delta_i - 1} E_i, \cdots, v_{\delta_i} = E_i$, and $g_1 = g_2 = \cdots = g_{\delta_i} = -1$. ∎

Consequently, replacing the matrix E with e in the filter described in Subsection 2.6.1 results in the pair (C', A') having zero-valued unobservable modes. It may be, however, desired to set the eigenvalues of $(A - KC)$ to different numbers that zero. In such a situation the algorithms presented in the following subsections may be used.

Positive values of δ_i indicate a delay between the disturbance and the system output. Thus, the system (5.1) can be reformulated as:

$$\begin{aligned} x(t+1) &= Ax(t) + Bu(t) + F\mu(t) + ed^*(t) \\ y(t) &= Cx(t) + Du(t) \end{aligned} \tag{5.11}$$

where elements of $d^*(t)$ are respective elements of $d(t)$ delayed by δ_i, i.e.:

$$d^*(t) = \begin{bmatrix} d_1(t-\delta_1) & d_2(t-\delta_2) & \cdots & d_q(t-\delta_q) \end{bmatrix}^T \tag{5.12}$$

5.2.2 Solution for $q = 1$ with a single invariant zero

In this subsection the algorithm of Chen & Patton (1999) is extended to the system, where the invariant zero of (A, e, C) is unstable. For sake of simplicity it is assumed that $q = 1$ and the triple (A, e, C) has only one invariant zero denoted as z_e. Hence, from the definition of an invariant zero, cf. (2.9), it follows that:

$$\begin{bmatrix} z_e I - A & -e \\ C & 0 \end{bmatrix} \begin{bmatrix} v \\ g \end{bmatrix} = 0 \tag{5.13}$$

where v and g are the invariant zero state and input directions, respectively. Utilising a similar solution to that in (Massoumnia 1986) a vector $\bar{e}$ is created, such that:

$$\bar{e} = \begin{bmatrix} e & v \end{bmatrix} \tag{5.14}$$

The aim of the scheme is to create such a filter that the state trajectory yielded by the disturbance $d(t)$ remains in the subspace $\mathrm{Im}\{\bar{e}\}$, as opposed to the algorithm presented in (Chen & Patton 1999), where the state trajectory of the disturbance $d(t)$ remains in the one-dimensional subspace $\mathrm{Im}\{e\}$. In order for the solution to this problem to exist the subspace $\mathrm{Im}\{\bar{e}\}$ must be (C, A)-invariant, i.e. there must exist such a gain matrix K that $\mathrm{Im}\{(A - KC)\bar{e}\} \subseteq \mathrm{Im}\{\bar{e}\}$, see (Halmos 1958, Basile & Marro 2002). This means that there exists such a matrix X, that, cf. (2.19):

$$(A - KC)\bar{e} = \bar{e}X \tag{5.15}$$

Note that, if (A, e, C) has no invariant zeros, then $v = \varnothing$, and, consequently, $\bar{e} = E$ and $X = \lambda_1$, where λ_1 is the desired eigenvalue of $(A - KC)$ corresponding to the vector E. The necessary and sufficient conditions for disturbance decoupling are:

1. The subspace $\mathrm{Im}\{\bar{e}\}$ is an invariant subspace of $(A - KC)$

2. $QCe = 0$

From (5.15) it holds that the columns of $\bar{e}$ are linear combinations of eigenvectors of the matrix $(A - KC)$:

$$\bar{e} = V_e \Psi \tag{5.16}$$

where columns of V_e are the first two eigenvectors of $(A - KC)$ and Ψ is an appropriate matrix. Because $(A - KC)$ is allocated distinct eigenvalues, $\text{rank}\{V_e\} = 2$, i.e. columns of V_e are linearly independent. Also columns of $\bar{e}$ are linearly independent (El-Ghezawi et al. 1983). Consequently, matrix Ψ is of full rank. Furthermore:

$$(A - KC)V_e = V_e \Lambda_e \tag{5.17}$$

where Λ_e is a diagonal matrix, whose diagonal elements are user defined eigenvalues corresponding to the columns of V_e. By postmultiplying both sides of (5.17) by Ψ, the following equation is obtained:

$$(A - KC)V_e \Psi = V_e \Lambda_e \Psi \tag{5.18}$$

Incorporating (5.15) and (5.16) into (5.18):

$$V_e \Lambda_e \Psi = V_e \Psi X \tag{5.19}$$

This yields:

$$\Lambda_e \Psi = \Psi X \tag{5.20}$$

Therefore, recalling that Ψ is of full rank, the matrix X can be defined as:

$$X = \Psi^{-1} \Lambda_e \Psi \tag{5.21}$$

where columns of Ψ^{-1} are right eigenvectors of X, whilst diagonal elements of Λ_e are its corresponding eigenvalues. Consequently, it can be noted that the eigenvalues of X are equal to the eigenvalues of $(A - KC)$ corresponding to the columns of V_e, i.e. the linear combinations of columns of $\bar{e}$.

From (5.15) it follows that:

$$KC\bar{e} = A\bar{e} - \bar{e}X \tag{5.22}$$

Denote $A\bar{e} - \bar{e}X$ as A_e. The necessary and sufficient conditions to assign all columns of $\bar{e}$ as linear combinations of the right eigenvectors of $(A - KC)$ are:

(i) $\text{rank}(C\bar{e}) = \text{rank}\left(\begin{bmatrix} A_e \\ C\bar{e} \end{bmatrix}\right)$

(ii) (C', A') is a detectable pair, where:

$$\begin{aligned} A' &= A - A_e(C\bar{e})\ C \\ C' &= \left(I - C\bar{e}(C\bar{e})\ \right)C \end{aligned} \tag{5.23}$$

Theorem 5.2. Diagonal elements of Λ_e are unobservable modes of the pair (C', A').

Proof. Diagonal elements of Λ_e, denoted as λ_1 and λ_2, correspond to the right eigenvectors of $(A' - K'C')$ denoted as w_1 and w_2:

$$\left(A - A_e(Ce)\ C - K'\left(I - Ce(Ce)\ \right)C\right)w_i = \lambda_i w_i \tag{5.24}$$

which holds for any arbitrary K', therefore if $K' = 0$:

$$\left(\lambda_i I - \left(A - A_e(Ce)\ C\right)\right)w_i = (\lambda_i I - A')w_i = 0 \tag{5.25}$$

Consequently:

$$K'\left(I - Ce(Ce)\ \right)Ce = K'C'w_i = 0 \tag{5.26}$$

which is valid for any K', hence:

$$C'w_i = 0 \tag{5.27}$$

As a result it holds that:

$$\begin{bmatrix} \lambda_i I - A' \\ C' \end{bmatrix} w_i = 0 \tag{5.28}$$

which means that the diagonal elements of Λ_e are unobservable modes of the pair (C', A') and only remaining $n-2$ eigenvalues can be allocated by K'. ∎

Calculation of the matrix X

From (5.13) it follows that:

$$Av = z_e v - ge \tag{5.29a}$$

$$Cv = 0 \tag{5.29b}$$

Therefore, from (5.29b) it follows that:

$$(A - KC)v = Av \tag{5.30}$$

Consider (5.15), then:

$$(A - KC)\begin{bmatrix} e & v \end{bmatrix} = \begin{bmatrix} e & v \end{bmatrix} X \tag{5.31}$$

Denote elements of X as x_{ij}. Incorporating (5.30) into (5.31) it holds that:

$$\begin{bmatrix} (A - KC)e & Av \end{bmatrix} = \begin{bmatrix} x_{11}e + x_{21}v & x_{12}e + x_{22}v \end{bmatrix} \tag{5.32}$$

Consequently, from (5.29a) it can be deduced that $x_{12} = -g$ and $x_{22} = z_e$. Knowing that X has the same eigenvalues as Λ_e, x_{11} and x_{21} are calculated as:

$$x_{11} = \lambda_1 + \lambda_2 - z_e \tag{5.33a}$$

$$x_{21} = -\frac{(z_e - \lambda_1)(z_e - \lambda_2)}{g} \tag{5.33b}$$

Rank condition

Recall the rank condition (i) in Subsection 5.2.1 and (5.29b). It can be deduced that:

$$\operatorname{rank}(C\bar{e}) = \operatorname{rank}(\begin{bmatrix} Ce & Cv \end{bmatrix}) = \operatorname{rank}(Ce) \tag{5.34}$$

and:

$$A_e = \begin{bmatrix} Ae - x_{11}e - x_{21}v & Av - z_e v + ge \end{bmatrix} \tag{5.35}$$

From (5.29a), it holds that the second column of A_e is equal to zero. Therefore, using the notation:

$$A_e^* = Ae - x_{11}e - x_{21}v \tag{5.36}$$

it holds that:

$$\operatorname{rank}(\begin{bmatrix} A_e \\ C\bar{e} \end{bmatrix}) = \operatorname{rank}(\begin{bmatrix} A_e^* \\ Ce \end{bmatrix}) \tag{5.37}$$

Hence, the assignability condition can be reformulated as:

(i) $\operatorname{rank}(Ce) = \operatorname{rank}(\begin{bmatrix} A_e^* \\ Ce \end{bmatrix})$

(ii) (C', A') is a detectable pair, where:

$$\begin{aligned} A' &= A - A_e^*(Ce)^{\dagger} C \\ C' &= \left(I - Ce(Ce)^{\dagger}\right) C \end{aligned} \tag{5.38}$$

The algorithm for the design of a robust fault detection filter (RFDF) using right eigenstructure assignment is summarised below.

Algorithm 5.1 (RFDF via right eigenstructure assignment, $q = 1, q_1 = 1$).

1. Obtain disturbance direction matrix e using (5.6), (5.8) and (5.9)
2. Calculate Q such that $QCe = 0$
3. Select eigenvalues λ_1 and λ_2

4. Calculate invariant zero state and input directions v and g from

$$\begin{bmatrix} z_e I - A & -e \\ C & 0 \end{bmatrix} \begin{bmatrix} v \\ g \end{bmatrix} = 0 \tag{5.39a}$$

5. Calculate coefficients x_{11} and x_{21} via:

$$x_{11} = \lambda_1 + \lambda_2 - z_e \tag{5.39b}$$

$$x_{21} = -\frac{(z_e - \lambda_1)(z_e - \lambda_2)}{g} \tag{5.39c}$$

6. Obtain matrix A_e as:

$$A_e^* = (A - x_{11} I)e - x_{21} v \tag{5.39d}$$

7. Obtain:

$$A' = A - A_e^*(Ce)\ C \tag{5.39e}$$

$$C' = \big(I - Ce(Ce)\ \big)C \tag{5.39f}$$

8. Using any eigenstructure assignment method allocate remaining $n-2$ eigenvalues of $(A' - K'C')$

9. Calculate the gain matrix K:

$$K = A_e^*(Ce)\ + K'\big(I - Ce(Ce)\ \big) \tag{5.39g}$$

5.2.3 Solution for $q = 1$ with multiple invariant zeros

Consider the system (5.1) where $q = 1$ and the triple (A, e, C) has q_1 ($q_1 < n$) invariant zeros denoted as $z_1, \cdots, z_{q_1}$. One can assign a vector v_i and a scalar g_i to each invariant zero z_i such that:

$$\begin{bmatrix} z_i I - A & -v_{i-1} \\ C & 0 \end{bmatrix} \begin{bmatrix} v_i \\ g_i \end{bmatrix} = 0 \tag{5.40}$$

where v_0 refers to the vector e. It follows from Lemma 5.2 that g_i are non-zero, hence, vectors v_i, $i = 1, 2, \cdots, q_1$ can be scaled such that $g_i = -1$ for $i = 1, 2, \cdots, q_1$. The aim of the algorithm is to force the state trajectory governed by the disturbance $d(t)$ to remain within the subspace $\mathrm{Im}\{\bar{e}\}$ defined as:

$$\bar{e} = \begin{bmatrix} e & v_1 & \cdots & v_{q_1} \end{bmatrix} \tag{5.41}$$

which requires $\bar{e}$ to be a (C, A)-invariant subspace, i.e. there exist such a gain matrix K that, cf. (5.15):

$$KC\bar{e} = A\bar{e} - \bar{e}X \tag{5.42}$$

Due to the fact that $Cv_i = 0$ for $i = 1, \cdots, q_1$, all columns of $A_e = A\bar{e} - \bar{e}X$, except of the first one, must be equal to zero for the solution of (5.42) to exist. Denote the elements of X as x_{ij}, then the i^{th} column of A_e is given by:

$$Av_{i-1} - (x_{1i}v_0 + x_{2i}v_1 + \cdots + x_{q_1+1}v_{q_1}) = 0 \tag{5.43}$$

From (5.40) it follows that (recall that $g_i = -1$ for $i = 1, 2, \cdots, q_1$):

$$Av_{i-1} = z_{i-1}v_{i-1} + v_{i-2} \tag{5.44}$$

Incorporating (5.44) into (5.43) the following equation is obtained:

$$x_{1i}v_0 + x_{2i}v_1 + \cdots + (x_{i-1,i} - 1)v_{i-2} + (x_{i,i} - z_{i-1})v_{i-1} + \cdots + x_{q_1+1}v_{q_1} = 0 \tag{5.45}$$

Due to the fact that $v_1, \cdots, v_{q_1}$ are linearly independent:

$$x_{i-1,i} = 1 \text{ for } i = 2, \cdots, q_1 + 1 \tag{5.46a}$$

$$x_{i,i} = z_{i-1} \text{ for } i = 2, \cdots, q_1 + 1 \tag{5.46b}$$

$$x_{j,i} = 0 \text{ for } j \neq i \text{ and } j \neq i - 1 \tag{5.46c}$$

Consequently the matrix X is given by:

$$X = \begin{bmatrix} x_{11} & 1 & 0 & 0 & \cdots & 0 & 0 \\ x_{21} & z_1 & 1 & 0 & \cdots & 0 & 0 \\ x_{31} & 0 & z_2 & 1 & \cdots & 0 & 0 \\ \vdots & \vdots & \vdots & \vdots & \ddots & \vdots & \vdots \\ x_{q_1 1,1} & 0 & 0 & 0 & \cdots & z_{q_1-1} & 1 \\ x_{q_1+1,1} & 0 & 0 & 0 & \cdots & 0 & z_{q_1} \end{bmatrix} \tag{5.47}$$

The first column of X is chosen such that the eigenvalues of X are equal to the desired eigenvalues of $(A - KC)$ corresponding to the linear combinations of columns of $\bar{e}$, cf. (5.20). Consequently, (for derivation details see Appendix A) the first column of X given by:

$$\begin{bmatrix} x_{11} \\ x_{12} \\ \vdots \\ x_{q_1+1,1} \end{bmatrix} = \tilde{\tilde{A}}^{-1}\tilde{\tilde{B}} \tag{5.48}$$

where an element of $\tilde{\tilde{A}} \in \mathbb{R}^{(q_1+1)\times(q_1+1)}$, denoted as $\tilde{\tilde{A}}_{j,k}$ is:

$$\tilde{\tilde{A}}_{j,k} = (-1)^{k-1} \prod_{l=k}^{q_i} (z_l - \lambda_j) \tag{5.49}$$

whilst the j^{th} element of the vector $\tilde{\tilde{B}} \in \mathbb{R}^{q_1+1}$, denoted as $\tilde{\tilde{B}}_j$ is:

$$\tilde{\tilde{B}}_j = \lambda_j \prod_{l=1}^{q_i} (z_l - \lambda_j) \tag{5.50}$$

Algorithm 5.2 (RFDF via right eigenstructure assignment, $q = 1, q_1 \geq 1$).

1. Obtain disturbance direction matrix e using (5.6), (5.8) and (5.9)
2. Obtain Q such that $QCe = 0$
3. Denote e as v_0 and obtain invariant zeros of the pair (A, e, C) and corresponding vectors v_i, for $i = 1, \cdots, q_1$

$$\begin{bmatrix} z_i I - A & -v_{i-1} \\ C & 0 \end{bmatrix} \begin{bmatrix} v_i \\ -1 \end{bmatrix} = 0 \tag{5.51a}$$

4. Select eigenvalues $\lambda_1, \cdots, \lambda_{q_1+1}$
5. Calculate coefficients $x_{11}, \cdots, x_{q_1+1,1}$ using (5.48), (5.49), and (5.50)
6. Obtain matrix A_e^* as:

$$A_e^* = (A - x_{11} I)e - x_{21} v_1 - x_{31} v_2 - \cdots - x_{q_1+1,1} v_{q_1} \tag{5.51b}$$

7. Obtain:

$$A' = A - A_e^* (Ce)\ C \tag{5.51c}$$

$$C' = \left(I - Ce(Ce)\ \right) C \tag{5.51d}$$

8. Allocate remaining $n - q_1 - 1$ eigenvalues of $(A' - K'C')$
9. Calculate K

$$K = A_e^* (Ce)\ + K' \left(I - Ce(Ce)\ \right) \tag{5.51e}$$

5.2.4 General solution for $q \geq 1$

In this section a general solution for the robust fault detection filter when $q \geq 1$ is presented. It is assumed that the triple (A, e, C) has invariant zeros. The invariant zeros of (A, e_i, C), where e_i refers to the i^{th} column of e, are denoted as $z_1^{(i)}, \cdots, z_{q_i}^{(i)}$. It is assumed that the invariant zeros fulfil the condition:

$$\Omega = \biguplus_{i=1}^{q} \Omega_i \tag{5.52}$$

where Ω is the set of all invariant zeros of (A, e, C), whilst Ω_i denotes the set of the invariant zeros of (A, e_i, C), see (Massoumnia 1986). The aim of the algorithm is to ensure that the state trajectory driven by $d_i(t)$ remains in the subspace $\mathrm{Im}\{\bar{e}_i\}$, where:

$$\bar{e}_i = \begin{bmatrix} e_i & v_1^{(i)} & \cdots & v_{q_i}^{(i)} \end{bmatrix} \tag{5.53}$$

Therefore, the necessary and sufficient conditions for the robust fault detection are:

1. For each column of the matrix e it holds that $\mathrm{Im}\{\bar{e}_i\}$ is an invariant subspace of $(A - KC)$
2. $QCe = 0$

Analogously to the case where e is a column vector, cf. Subsection 5.2.2, the matrix A_e^* is built, such that:

$$A_e^* = \begin{bmatrix} A_e^{*(1)} & A_e^{*(2)} & \cdots & A_e^{*(q)} \end{bmatrix} \tag{5.54}$$

where:

$$A_e^{*(i)} = (A - x_{11}^{(i)} I)e_i - x_{21}^{(i)} v_1^{(i)} - x_{31}^{(i)} v_2^{(i)} - \cdots - x_{q_i+1,1}^{(i)} v_{q_i}^{(i)} \tag{5.55}$$

The matrices A' and C' are built as in (5.51c) and (5.51d). Note that if the (A, e_i, C) has no invariant zeros then it holds that $\delta_i = 0$ and $e_i = E_i$, see Lemma 5.2, and:

$$A_e^{*(i)} = (A - \lambda_i I)e_i \tag{5.56}$$

Hence, if the system has no invariant zeros and $\delta_i = 0$ for $i = 1, \cdots, q$ the algorithm presented here is equivalent to that of Chen & Patton (1999). The necessary conditions for the solution of the robust fault detection filter to exist are:

(i) $\mathrm{rank}(Ce) = \mathrm{rank}\left(\begin{bmatrix} A_e^* \\ Ce \end{bmatrix}\right)$

(ii) (C', A') is a detectable pair, where:

$$\begin{aligned} A' &= A - A_e^*(Ce)\ C \\ C' &= \left(I - Ce(Ce)\ \right)C \end{aligned} \tag{5.57}$$

Similarly as in the previous case the matrix $X^{(i)}$ is given by:

$$X^{(i)} = \begin{bmatrix} x_{11}^{(i)} & 1 & 0 & 0 & \cdots & 0 & 0 \\ x_{21}^{(i)} & z_1^{(i)} & 1 & 0 & \cdots & 0 & 0 \\ x_{31^{(i)}} & 0 & z_2^{(i)} & 1 & \cdots & 0 & 0 \\ \vdots & \vdots & \vdots & \vdots & \ddots & \vdots & \vdots \\ x_{q_1 1,1}^{(i)} & 0 & 0 & 0 & \cdots & z_{q_1-1}^{(i)} & 1 \\ x_{q_1+1,1}^{(i)} & 0 & 0 & 0 & \cdots & 0 & z_{q_1}^{(i)} \end{bmatrix} \tag{5.58}$$

and its first column is calculated via:

$$\begin{bmatrix} x_{11}^{(i)} \\ x_{12}^{(i)} \\ \vdots \\ x_{q_1+1,1}^{(i)} \end{bmatrix} = (\tilde{\tilde{A}}^{(i)})^{-1} \tilde{\tilde{B}}^{(i)} \tag{5.59}$$

where an element of $\tilde{\tilde{A}}^{(i)} \in \mathbb{R}^{(q_i+1)\times(q_i+1)}$, denoted as $\tilde{\tilde{A}}_{j,k}^{(i)}$ is:

$$\tilde{\tilde{A}}_{j,k}^{(i)} = (-1)^{k-1} \prod_{l=k}^{q_i} (z_l^{(i)} - \lambda_j^{(i)}) \tag{5.60}$$

whilst the j^{th} element of the vector $\tilde{\tilde{B}} \in \mathbb{R}^{q_1+1}$, denoted as $\tilde{\tilde{B}}_j$ is:

$$\tilde{\tilde{B}}_j^{(i)} = \lambda_j^{(i)} \prod_{l=1}^{q_i} \left(z_l^{(i)} - \lambda_j^{(i)} \right) \tag{5.61}$$

The generalised form of the algorithm for disturbance decoupled fault detection filter is given below.

Algorithm 5.3 (RFDF via right eigenstructure assignment, $q \geq 1, q_i \geq 0$).

1. Calculate disturbance direction matrix e using (5.6), (5.8) and (5.9)
2. Obtain Q such that $QCe = 0$
3. For each column of e obtain invariant zeros of the triple (A, e_i, C), denoted as $z_j^{(i)}$, and corresponding vectors $v_j^{(i)}$, for $j = 1, \cdots, q_i$

$$\begin{bmatrix} z_j^{(i)} I - A & -v_{j-1}^{(i)} \\ C & 0 \end{bmatrix} \begin{bmatrix} v_j^{(i)} \\ -1 \end{bmatrix} = 0 \tag{5.62a}$$

where $v_0^{(i)}$ denotes e_i.

4. Select eigenvalues $\lambda_1^{(i)}, \cdots, \lambda_{q_i+1}^{(i)}$ corresponding to linear combinations of $v_j^{(i)}$, $j = 1, 2, \cdots, q_i + 1$

5. Calculate coefficients $x_{11}^{(i)}, \cdots, x_{q_i+1,1}^{(i)}$ using (5.59–5.61)

6. Obtain matrix A_e^* as:

$$A_e^* = \begin{bmatrix} A_e^{*(1)} & A_e^{*(2)} & \cdots & A_e^{*(q)} \end{bmatrix} \tag{5.62b}$$

where

$$A_e^{*(i)} = (A - x_{11}^{(i)} I)e_i - x_{21}^{(i)} v_1^{(i)} - x_{31}^{(i)} v_2^{(i)} - \cdots - x_{q_i+1,1}^{(i)} v_k^{(i)} \tag{5.62c}$$

7. Obtain:

$$A' = A - A_e^*(Ce)\ C \tag{5.62d}$$

$$C' = \left(I - Ce(Ce)\ \right)C \tag{5.62e}$$

8. Allocate remaining eigenvalues of $(A' - K'C')$

9. Calculate K

$$K = A_e^*(Ce)\ + K'\left(I - Ce(Ce)\ \right) \tag{5.62f}$$

5.2.5 Consideration of residual response to fault

In this subsection some remarks considering the residual response to a fault and its dependency on the choice of the gain matrix K are discussed.

Zero-pole cancellation in the residual response to fault

Remark 5.1. Unobservable modes of (C', A') are unobservable modes of $(QC, (A - KC))$.

Demonstration. Consider unobservable modes of (C', A'), i.e. the eigenvalues of $(A - KC)$ corresponding to linear combinations of e_i. Denote the eigenvectors of $(A - KC)$ corresponding to the unobservable modes of (C', A') as $w_j^{(i)}, i = 1, \cdots, q; j = 1, \cdots, q_i$. Recall that $w_j^{(i)} \in \mathrm{Im}\{\begin{bmatrix} e_i & v_1^{(i)} & \cdots & v_{q_i}^{(i)} \end{bmatrix}\}$. It is known that:

$$Cv_j^{(i)} = 0 \tag{5.63a}$$

$$QCe_i = 0 \tag{5.63b}$$

Therefore, it holds that:

$$QCw_j^{(i)} = 0 \tag{5.64a}$$

$$\left(I\lambda_j^{(i)} - A + KC\right) w_j^{(i)} = 0 \tag{5.64b}$$

where $\lambda_j^{(i)}$ is the eigenvalue of $(A - KC)$ corresponding to the eigenvector $\lambda_j^{(i)}$. Consequently, the unobservable modes of (C', A') are the unobservable modes of $(QC, (A - KC))$. ∎

This results in a zero-pole cancellation of the unobservable modes of (C', A') in the transfer function of $(A - KC, F, QC)$. Consequently, the observable modes of $(A - KC, F, QC)$ are only those eigenvalues of $(A - KC)$ which are assigned by the choice of the matrix K'. This information may be useful for designing the residual response to faults.

Note that the necessary condition for the fault to be detected by the filter is:

$$QC(zI - A + KC)^{-1}F \neq 0 \tag{5.65}$$

Without loss of generality assume that F is a column vector. Using the notation $\bar{e} = \begin{bmatrix} \bar{e}_1 & \bar{e}_2 & \cdots & \bar{e}_q \end{bmatrix}$, the matrix F can be expressed as a sum of its orthogonal projections on $\mathrm{Im}\{\bar{e}\}$ and the orthogonal completion of $\mathrm{Im}\{\bar{e}\}$

$$F = F(\bar{e}) + F(\bar{e}^{\perp}) \tag{5.66}$$

where $F(\bar{e})$ is an orthogonal projection of F on $\mathrm{Im}\{\bar{e}\}$, whereas $F(\bar{e}^{\perp})$ denotes an orthogonal projection of F on the orthogonal completion on $\mathrm{Im}\{\bar{e}\}$. Due to the fact that $F(\bar{e})$ belongs to the unobservable subspace of the fault detection filter, the fault to residual transfer function, denoted as $G_{fr}(z)$, is given by:

$$G_{fr}(z) = QC(zI - A + KC)^{-1}F(\bar{e}^{\perp}) \tag{5.67}$$

This means that the necessary condition for the robust fault detection filter to exist is that the dimension of the unobservable subspace of $(QC, A - KC)$ is lower that n (otherwise no fault can be detected as the whole state space is unobservable for the fault detection filter).

Invariant zeros in the residual response to fault

Invariant zeros shape the response of the residual to a fault. In some situations, e.g. fault identification, it may be desirable to influence not only its poles, but also zeros.

Remark 5.2. If $\mathrm{rank}(Q) = n - \mathrm{rank}(Ce)$, then the selection of eigenvalues of $(A - KC)$ has no influence on the invariant zeros of the residual response to a fault.

DEMONSTRATION. Without loss of generality it is assumed that $\dim\{F\} = 1$. Then the invariant zero of the residual response to a fault, denoted z_f, fulfils the condition:

$$\begin{bmatrix} A' - K'C' - z_f I & F \\ QC & 0 \end{bmatrix} \begin{bmatrix} v_f \\ g_f \end{bmatrix} = 0 \tag{5.68}$$

where v_f and g_f are the invariant zero state and input directions, respectively. Note that $\mathrm{Im}\{v_f\} \subset \mathrm{Ker}\{QC\}$, i.e. the state direction v_f belongs to the right nullspace of QC. The matrix Q which fulfils the condition $QCe = 0$ can be defined as (Basilevsky 1983):

$$Q = Q_0 \left(I - Ce(Ce) \right) \tag{5.69}$$

where Q_0 is an arbitrary matrix. Note that rows of Q are linear combinations of rows of $\left(I - Ce(Ce) \right)$. Therefore, if $\mathrm{rank}(Q_0) = \mathrm{rank}\left(I - Ce(Ce) \right) = n - \mathrm{rank}(Ce)$, then $\mathrm{rank}(Q) = n - \mathrm{rank}(Ce)$. Hence, it follows, that if $\mathrm{rank}(Q_0) = \mathrm{rank}\left(I - Ce(Ce) \right)$, then the subspace spanned by the rows of Q is the subspace spanned by the rows of $\left(I - Ce(Ce) \right)$. Furthermore, it holds that:

$$QC = Q_0 \left(I - Ce(Ce) \right) C = Q_0 C' \tag{5.70}$$

Hence, $\mathrm{Ker}\{QC\} = \mathrm{Ker}\{Q_0 C'\}$. This means that, if $\mathrm{rank}(Q) = n - \mathrm{rank}(Ce)$ then $\mathrm{Ker}\{QC\} = \mathrm{Ker}\{Q_0 C'\} = \mathrm{Ker}\{C'\}$. Recall that $v_f \subset \mathrm{Ker}\{QC\}$, then, if $\mathrm{rank}(Q) = n - \mathrm{rank}(Ce)$, it holds that:

$$QCv_f = C'v_f = 0 \tag{5.71}$$

This shows that the invariant zero of the residual response to fault, defined by (5.68), does not depend on choice of K', i.e. z_f does not depend on the choice of the eigenvalues of $(A - KC)$, which are not corresponding to the linear combinations of $\bar{e}_i, i = 1, \cdots, q$. As a result (5.68) can be rewritten as:

$$A'v_f - z_f v_f + F g_f = 0 \tag{5.72a}$$

$$QCv_f = 0 \tag{5.72b}$$

Now it will be demonstrated that the invariant zeros of the residual response to a fault do not depend on the choice of eigenvalues of $(A - KC)$ corresponding to the linear combinations of $\bar{e}_i, i = 1, \cdots, q$. Consider the following change of basis using the following orthonormal matrix:

$$T = \begin{bmatrix} T_1 & T_2 \end{bmatrix} \tag{5.73}$$

where:

$$\mathrm{Im}\{T_1\} = \mathrm{Im}\{\begin{bmatrix} \bar{e}_1 & \bar{e}_2 & \cdots & \bar{e}_q \end{bmatrix}\} \tag{5.74}$$

and $\mathrm{Im}\{T_2\}$ is an orthogonal completion of $\mathrm{Im}\{T_1\}$. Equation (5.72) is reformulated using the similarity transformation T:

$$T^T A' T T^T v_f - z_f T^T v_f + g_f T^T F = 0 \tag{5.75a}$$

$$QCTT^T v_f = 0 \tag{5.75b}$$

which furthermore can be rewritten as:

$$\begin{bmatrix} A_1 & A_2 \\ 0 & A_3 \end{bmatrix} \begin{bmatrix} T_1^T v_f \\ T_2^T v_f \end{bmatrix} - z_f \begin{bmatrix} T_1^T v_f \\ T_2^T v_f \end{bmatrix} + g_f \begin{bmatrix} T_1^T F \\ T_2^T F \end{bmatrix} = 0 \tag{5.76a}$$

$$\begin{bmatrix} 0 & QCT_2 \end{bmatrix} \begin{bmatrix} T_1^T v_f \\ T_2^T v_f \end{bmatrix} = 0 \tag{5.76b}$$

where A_1, A_2, and A_3 are the appropriate submatrices of $T^T A' T$. The first element in the left hand side matrix of (5.76b) is equal zero because $QCe = 0$. Using the notation $v'_f = T_2^T v_f$, if the invariant zero of the residual response to a fault exists, then it conforms the following equation:

$$A_3 v'_f - z_f v'_f + F g_f = 0 \tag{5.77a}$$

$$QCv'_f = 0 \tag{5.77b}$$

Knowing v'_f one can calculate v_f which fulfils $v'_f = T_2^T v_f$ by solving $\dim\{T_2\}$ equations with n unknowns. Hence the obtained solution has $n - \dim\{T_2\}$ parameters. The second part of (5.76), i.e.

$$\left(A_1 T_1^T + A_2 T_2^T - z_f T_1^T + g_f T_1^T\right) v_f = 0 \tag{5.78a}$$

consists of $n - \dim\{T_2\}$ equations, from which remaining parameters can be found and the vector v_f calculated. Therefore, the existence of z_f depends on $A_3 = T_2^T A' T_2$. Recall (5.62b) and (5.62c):

$$\begin{aligned} A_e^* &= \begin{bmatrix} Ae_1 & Ae_2 & \cdots & Ae_q \end{bmatrix} + \begin{bmatrix} \sum_{i=0}^{q_1} v_i^{(1)} & \sum_{i=0}^{q_2} v_i^{(2)} & \cdots & \sum_{i=0}^{q_q} v_i^{(q)} \end{bmatrix} \\ &= Ae + \Omega \end{aligned} \tag{5.79}$$

where:

$$\Omega = \begin{bmatrix} \sum_{i=0}^{q_1} v_i^{(1)} & \sum_{i=0}^{q_2} v_i^{(2)} & \cdots & \sum_{i=0}^{q_q} v_i^{(q)} \end{bmatrix} \tag{5.80}$$

Recall that:

$$A' = A - Ae(Ce)\ C + \Omega(Ce)\ C \tag{5.81}$$

Due to the fact that $T_2^T \Omega = 0$:

$$A_3 = T_2^T A' T_2 = T_2^T (A - Ae(Ce)\ C) T_2 \tag{5.82}$$

Therefore, the matrix A_3 and hence the invariant zeros of the residual response to a fault do not depend on the choice of the eigenvalues of $(A-KC)$. ∎

5.2.6 Differences and similarities with fault isolation filter of Chen and Speyer (2006*a*)

Although Algorithm 5.3 is designed for a robust fault detection, whilst Algorithm presented in Subsection 2.7.1, cf. (Chen & Speyer 2006*a*), is for a fault isolation, their eigenstructures are the same, i.e. the eigenstructure of $(A-KC,E,C)$ using Algorithm 5.3 and eigenstructure of $(A-KC,F,C)$ using the algorithm of Chen & Speyer (2006*b*) are the same. The idea of both schemes is to find such a gain matrix K that the following conditions are fulfilled:

(i) Eigenvalues of $(A-KC)$ can be arbitrarily chosen (with constraint to no repeated eigenvalues and conjugate symmetry)

(ii) Eigenvectors of $(A-KC)$ are linear combinations of columns of e (f) and their invariant zeros state directions.

Note that the condition (ii) in (Chen & Speyer 2006*a*) has been specified as:

$$w_j^{(i)} = \bar{\Theta}^{(i)}\bar{\beta}_j^{(i)} + f_i = \Theta^{(i)}\beta_j^{(i)} \tag{5.83}$$

where $w_j^{(i)}$ is an eigenvector of $(A-KC)$ and $\bar{\beta}^{(i)}$ is an appropriate coefficient vector. Columns of $\bar{\Theta}^{(i)}$ span the following subspace:

$$\mathrm{Im}\{\bar{\Theta}^{(i)}\} = \mathrm{Im}\{\begin{bmatrix} F_i & AF_i & \cdots & A^{\delta_i-1}F_i \end{bmatrix}\} \oplus \mathcal{V}_i \tag{5.84}$$

where $\mathcal{V}_i$ is the subspace spanned by invariant zero state directions of (A,F_i,C).

Chen & Speyer (2006*a*) explicitly indicate that each eigenvector of $(A-KC)$ corresponding to f_i contains the vector f_i. Although it is not explicitly said Algorithm 5.3 is characterised by the same property.

Lemma 5.3. Each eigenvector of $(A-KC)$ obtained using Algorithm 5.3 corresponding to linear combination of $\bar{e}_i$ contains e_i.

Proof. Denote an eigenvector of $(A-KC)$ corresponding to a linear combination of columns of $\bar{e}_i$ as:

$$w_j^{(i)} = \alpha_0^{(i)}e_i + \alpha_1^{(i)}v_1 + \alpha_2^{(i)}v_2^{(i)} + \cdots + \alpha_{q_i}^{(i)}v_{q_i}^{(i)} \tag{5.85}$$

Consider the situation when $\alpha_0^{(i)} = 0$, i.e. the j^{th} eigenvector of $(A-KC)$ corresponding to linear combination of $\bar{e}$, denoted as $w_j'^{(i)}$, is a linear combination of vectors $v_k^{(i)}, k = 1,2,\cdots,q_i$ but not e_i:

$$w_j'^{(i)} = \alpha_1^{(i)}v_1 + \alpha_2^{(i)}v_2^{(i)} + \cdots + \alpha_{q_i}^{(i)}v_{q_i}^{(i)} \tag{5.86}$$

Then it holds that:

$$(A - KC)w_j'^{(i)} = \lambda_j^{(i)} w'^{(i)} \tag{5.87}$$

As $w_j'^{(i)}$ is a linear combination of $v_k^{(i)}, k = 1, \cdots, q_i$, it holds that $Cw_j'^{(i)} = 0$, cf. (5.40). Consequently:

$$Aw_j'^{(i)} = \lambda_j^{(i)} w_j'^{(i)} \tag{5.88}$$

i.e. $w_j'^{(i)}$ a right eigenvector of A corresponding to eigenvalue $\lambda_j'^{(i)}$. Then, it holds that:

$$\alpha_1^{(i)} A v_1^{(i)} + \alpha_2^{(i)} A v_2^{(i)} + \cdots + \alpha_{q_i}^{(i)} A v_{q_i}^{(i)} = \lambda_j^{(i)} v_1^{(i)} + \lambda_j^{(i)} v_2^{(i)} + \cdots + \lambda_j^{(i)} v_{q_i}^{(i)} \tag{5.89}$$

Incorporating (5.40) into (5.89):

$$\begin{aligned} &-\alpha_1^{(i)} g_1^{(i)} e_i + \left(\alpha_1^{(i)} z_1^{(i)} - \alpha_2^{(i)} g_2 - \lambda_j^{(i)}\right) v_1^{(i)} + \left(\alpha_2^{(i)} z_2^{(i)} - \alpha_3^{(i)} g_3 - \lambda_j^{(i)}\right) v_2^{(i)} + \cdots + \\ &\left(\alpha_{q_i-1}^{(i)} z_{q_i-1}^{(i)} - \alpha_{q_i}^{(i)} g_{q_i} - \lambda_j^{(i)}\right) v_{q_i-1}^{(i)} + \left(\alpha_{q_i}^{(i)} z_{q_i}^{(i)} - \lambda_j^{(i)}\right) v_{q_i}^{(i)} = 0 \end{aligned} \tag{5.90}$$

Because columns of $\bar{e}_i$ are linearly independent, the above equation holds if and only if:

(i) $g_i = 0$

(or)

(ii) $\alpha_1^{(i)} = \alpha_2^{(i)} = \cdots = \alpha_{q_i}^{(i)} = 0$

Assumption (i) does not hold as the system is observable, see Lemma 5.2. Assumption (ii) would mean that the eigenvector of $(A - KC)$ corresponding to a linear combination of columns of $\bar{e}_i$ is equal zero. Consequently, eigenvectors of $(A - KC)$ corresponding to linear combination of $\bar{e}_i$ must contain e_i. Due to the fact that eigenvectors can be arbitrarily scaled, the coefficient $\alpha_0^{(i)}$ can be set to unity and the rest of the coefficients can be scaled accordingly. ∎

The solution to Algorithm 5.3 is such a matrix K that:

$$KCe = A_e^* \tag{5.91}$$

whilst the solution to the algorithm of Chen & Speyer (2006*a*) is:

$$KCf = A_w \tag{5.92}$$

where

$$A_w = \begin{bmatrix} (A - \lambda_1^{(1)} I) w_1^{(1)} & (A - \lambda_1^{(2)} I) w_1^{(2)} & \cdots & (A - \lambda_1^{(q)} I) w_1^{(q)} \end{bmatrix} \tag{5.93}$$

and $w_1^{(i)}$, $i = 1, 2, \cdots, q$, are eigenvectors of $(A - KC)$ corresponding to $\lambda_j^{(i)}$.

Lemma 5.4. Matrices A_e^* and A_w are equal.

PROOF. See Appendix B. ∎

The main difference between both algorithms is the calculation of the coefficients needed to obtain columns of A_e^* (A_w). The algorithm presented in Subsection 2.7.1 requires to calculate $q_i(q_i+1)$ of $\bar{\beta}_j$ coefficients in order to calculate one column of A_w. This is done by a pseudoinverse of a matrix of the dimension $nq_i \times q_i(q_i+1)$. Furthermore, the $\bar{\beta}_j$ coefficients are linearly dependent, cf. (B.9), and not all of them are needed to compute a column of A_w. On the other hand, Algorithm 5.3 requires q_i+1 coefficients to obtain any column of A_e^*, which are calculated by solving a set of q_i+1 linear equations, which requires an inverse of a matrix of the dimension $(q_i+1)\times(q_i+1)$, which is computationally less demanding compared to the algorithm of Chen & Speyer (2006*a*).

5.2.7 Tutorial examples

Example 5.1. $q = 1$**, single invariant zero**
Consider the system (5.1), whose A, C, D, E, and F matrices are given by:

$$A = \begin{bmatrix} 0 & 1 & 0 & 0 \\ 0 & 0 & 1 & 0 \\ 0 & 0 & 0 & 1 \\ -0.1155 & -0.7985 & -2.06 & -2.35 \end{bmatrix} \quad E = \begin{bmatrix} -0.8000 \\ 1.4000 \\ 1.2000 \\ 3.7725 \end{bmatrix} \quad F = \begin{bmatrix} 1 \\ 1.1 \\ 0 \\ 0 \end{bmatrix}$$
$$C = \begin{bmatrix} -0.8165 & 0.5266 & -0.2367 & 0 \\ -0.4082 & -0.2367 & 0.8816 & 0 \end{bmatrix} \tag{5.94}$$

The triple (A, E, C) has one invariant zero at $z_e = 1.2$, whose input direction is $g = 1$ and the zero state direction is given by:

$$v = \begin{bmatrix} 1 & 2 & 1 & 0 \end{bmatrix}^T \tag{5.95}$$

Also $CE \neq 0$, thus $\delta_1 = 0$ and $e = E$. The aim of the algorithm is to limit the state trajectory governed by $d(t)$ to the subspace $\mathrm{Im}\{\begin{bmatrix} E & v \end{bmatrix}\}$. Eigenvalues of $(A - KC)$ corresponding to linear combinations of E and v are selected to be 0.45 and 0.65. This corresponds to $x_{11} = -0.1$, cf. (5.39b), and $x_{21} = 0.4125$, cf. (5.39c). Consequently, the matrix A_e^* is calculated as, cf. (5.39d):

$$A_e^* = \begin{bmatrix} 0.9075 \\ 0.5150 \\ 3.4800 \\ -11.9856 \end{bmatrix} \tag{5.96}$$

Matrices A' and C' are given by, cf. (5.39e) and (5.39f):

$$A' = \begin{bmatrix} 0.5186 & 0.8704 & -0.2593 & 0 \\ 0.2943 & -0.0736 & 0.8529 & 0 \\ 1.9886 & -0.4971 & -0.9943 & 1 \\ -6.9644 & 0.9137 & 1.3645 & -2.35 \end{bmatrix}$$
$$C' = \begin{bmatrix} -0.1843 & 0.3685 & -0.5528 & 0 \\ 0.1936 & -0.3872 & 0.5807 & 0 \end{bmatrix} \tag{5.97}$$

It is noted that:

$$\operatorname{rank}(CE) = \operatorname{rank}(\begin{bmatrix} A_e^* \\ CE \end{bmatrix}) = 1 \tag{5.98}$$

and (C', A') is a detectable pair, i.e. its unobservable modes, 0.45 and 0.65, lie within the unit circle. Therefore, the solution for the stable filter design exists. The remaining eigenvalues of $(A - KC)$ are chosen to be 0.35 and 0.4 and consequently the matrix K' is given by:

$$K' = \begin{bmatrix} -0.5936 & 4.0532 \\ 0.7442 & 2.6206 \\ 0.6739 & -7.8011 \\ -0.9526 & 2.0485 \end{bmatrix} \tag{5.99}$$

Finally, the gain matrix K is obtained as:

$$K = \begin{bmatrix} -1.8760 & 2.8324 \\ -0.7107 & 1.2356 \\ 5.8663 & -2.8584 \\ -7.1590 & -3.8596 \end{bmatrix} \tag{5.100}$$

Note that the fault distribution matrix F can be represented as a sum of:

$$F(\bar{E}^{\perp}) = \begin{bmatrix} 0.3889 \\ 0.0528 \\ -0.4944 \\ 0.2201 \end{bmatrix} \text{ and } F(\bar{E}) = \begin{bmatrix} 0.6111 \\ 1.0472 \\ 0.4944 \\ -0.2201 \end{bmatrix} \tag{5.101}$$

where $F(\bar{E}) \in \operatorname{Im}\{\bar{E}\}$, whilst the vector $F(\bar{E}^{\perp})$ is orthogonal to the subspace $\operatorname{Im}\{\bar{E}\}$. Furthermore, the generalised angle between and F and the subspace $\operatorname{Im}\{\bar{E}\}$ is given by:

$$\arccos\left(\frac{F^T F(\bar{E})}{\|F\|_2 \|F(\bar{E})\|_2}\right)\frac{180^o}{\pi} = 26.7^o \tag{5.102}$$

Consequently, as the fault input direction $F \notin \operatorname{Im}\{\bar{E}\}$, the fault occurrence can be detected by the robust fault detection filter. The simulation results are presented in Fig. 5.1. As expected the fault detection filter is insensitive to disturbances, whereas

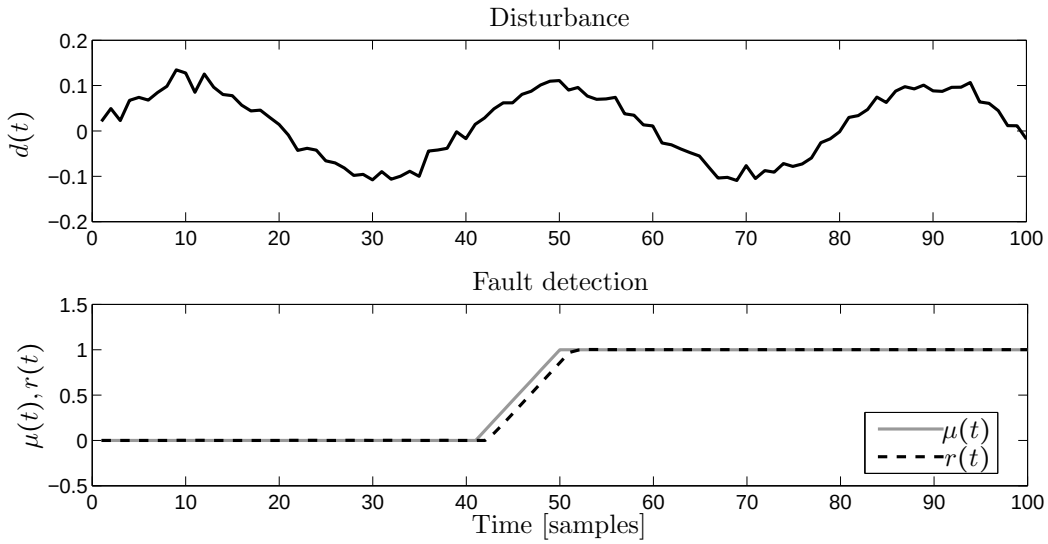

Figure 5.1: Robust fault detection, $q = 1$, the triple (A, E, C) has single invariant zero. Upper subfigure presents disturbances, whilst lower subfigure demonstrates robust fault detection process. It can be noted that residual, $r(t)$, is insensitive to disturbances.

it is sensitive to fault.

Example 5.2. $q = 1$**, multiple invariant zeros**

In this example $q = 1$ and the triple (A, E, C) has two invariant zeros. Matrices of the state-space system (5.1) are given by:

$$A = \begin{bmatrix} 0 & 1 & 0 & 0 & 0 \\ 0 & 0 & 1 & 0 & 0 \\ 0 & 0 & 0 & 1 & 0 \\ 0 & 0 & 0 & 0 & 1 \\ -0.0751 & -0.6345 & -2.1375 & -3.5875 & -3 \end{bmatrix} \quad E = \begin{bmatrix} -2.4400 \\ 0.6200 \\ 1.5600 \\ -3.4816 \\ 18.3643 \end{bmatrix}$$
$$C = \begin{bmatrix} 0.0948 & -0.4811 & 0.8675 & 0 & -0.0837 \\ -0 & 0 & 0 & 1 & 0 \end{bmatrix} \quad F = \begin{bmatrix} 1 & -1 & 1 & 1 & 0.3 \\ 2 & 3.4 & 2 & 0 & 0 \end{bmatrix}^T \tag{5.103}$$

The triple (A, E, C) has two invariant zeros, namely $z_1 = 1.3$ and $z_2 = 1.2$, and:

$$v_1 = \begin{bmatrix} 0.8000 \\ -1.4000 \\ -1.2000 \\ 0.0000 \\ -3.4816 \end{bmatrix} \quad v_2 = \begin{bmatrix} 1 \\ 2 \\ 1 \\ 0 \\ 0 \end{bmatrix} \tag{5.104}$$

Poles of $(A - KC)$ corresponding to linear combinations of E, v_1, and v_2 are selected to be 0.35, 0.3, and 0.25. Consequently, matrices $\tilde{\tilde{A}}$ and $\tilde{\tilde{B}}$ are, cf. (5.49) and (5.50):

$$\tilde{\tilde{A}} = \begin{bmatrix} 0.9975 & -0.95 & 1 \\ 0.9000 & -0.90 & 1 \\ 0.8075 & -0.85 & 1 \end{bmatrix} \qquad \tilde{\tilde{B}} = \begin{bmatrix} 0.2494 \\ 0.2700 \\ 0.2826 \end{bmatrix} \tag{5.105}$$

Thus, the first column of the matrix X is given by, see (5.48):

$$X = \begin{bmatrix} -1.6000 \\ -2.7075 \\ -0.7268 \end{bmatrix} \tag{5.106}$$

Then, the matrix A_e^* is calculated as, cf. (5.51b):

$$A_e^* = \begin{bmatrix} -0.3912 \\ 0.2150 \\ -3.5079 \\ 12.7937 \\ -26.1909 \end{bmatrix}^T \tag{5.107}$$

Furthermore, matrices A' and C' are obtained using (5.51c) and (5.51d):

$$A' = \begin{bmatrix} -0.0021 & 1.0106 & -0.0192 & -0.1078 & 0.0019 \\ 0.0012 & -0.0058 & 1.0105 & 0.0593 & -0.0010 \\ -0.0188 & 0.0954 & -0.1720 & 0.0331 & 0.0166 \\ 0.0686 & -0.3480 & 0.6275 & 3.5263 & 0.9394 \\ -0.2154 & 0.0779 & -3.4220 & -10.8064 & -2.8760 \end{bmatrix} \tag{5.108}$$

$$C' = \begin{bmatrix} 0.0910 & -0.4617 & 0.8324 & -0.1968 & -0.0804 \\ -0.0187 & 0.0947 & -0.1708 & 0.0404 & 0.0165 \end{bmatrix}$$

Similarly, as in the previous example:

$$\operatorname{rank}(CE) = \operatorname{rank}\left(\begin{bmatrix} A_e^* \\ CE \end{bmatrix}\right) = 1 \tag{5.109}$$

and (C', A') is a detectable pair, hence the solution to the robust fault detection problem exists. The remaining eigenvalues of $(A - KC)$ are selected to be 0.45 and 0.4 and,

consequently, the gain matrix K is given by, cf. (5.51e):

$$K = \begin{bmatrix} 2.6891 & -0.4392 \\ 3.1731 & -0.7126 \\ 0.1983 & 0.9669 \\ -0.7233 & -3.5263 \\ 1.4808 & 7.2189 \end{bmatrix} \tag{5.110}$$

The orthogonal projections of F on the subspace $\mathrm{Im}\{\bar{E}\}$ and the orthogonal completion of $\mathrm{Im}\{\bar{E}\}$ are given by:

$$F(\bar{E}^{\perp}) = \begin{bmatrix} 0.9687 & 0.1092 \\ -0.9910 & -0.1749 \\ 1.0133 & 0.2406 \\ 1.0324 & 0.0660 \\ 0.2718 & 0.0125 \end{bmatrix} \qquad F(\bar{E}) = \begin{bmatrix} 0.0313 & 1.8908 \\ -0.0090 & 3.5749 \\ -0.0133 & 1.7594 \\ -0.0324 & -0.0660 \\ 0.0282 & -0.0125 \end{bmatrix} \tag{5.111}$$

One can calculate the generalised angles between, respectively, F_1 and F_2 and their projections on the subspace $\mathrm{Im}\{\bar{E}\}$, cf. (5.102), which are, respectively, 88.4264^o and 4.2009^o. Note that the F_1 is 'almost orthogonal' to the subspace $\mathrm{Im}\{\bar{E}\}$, whilst F_2 'almost lies' in the subspace $\mathrm{Im}\{\bar{E}\}$, i.e. the angle between F_2 and $\mathrm{Im}\{\bar{E}\}$ is low. Since the norm of $F_1(\bar{E}^{\perp})$, i.e. 2.02, is significantly larger than the norm of $F_2(\bar{E}^{\perp})$, i.e. 0.32, it is expected that the steady state gain of the residual response to the fault $\mu_1(t)$ will be larger than the one of $\mu_2(t)$. The responses of the residual to both faults in the z-domain are given by:

$$\begin{aligned} \frac{r(z)}{\mu_1(z)} &= \frac{0.39613(z-0.0221)}{(z-0.45)(z-0.4)} \\ \frac{r(z)}{\mu_2(z)} &= \frac{0.094264(z-0.08207)}{(z-0.45)(z-0.4)} \end{aligned} \tag{5.112}$$

where $r(z)$, $\mu_1(z)$, and $\mu_2(z)$ are, respectively, z-domain representations of $r(t)$, $\mu_1(t)$, and $\mu_2(t)$. The responses of the residual to both faults are presented in Fig. 5.2. It can be noted that the residual is insensitive to disturbances. The steady state gain of the residual response to fault $\mu_1(t)$ is larger than the one of the residual response to fault $\mu_2(t)$.

Example 5.3. $q = 2$**, two invariant zeros**
In this example $q = 2$ and there are two invariant zeros of the triple (A, E, C). The

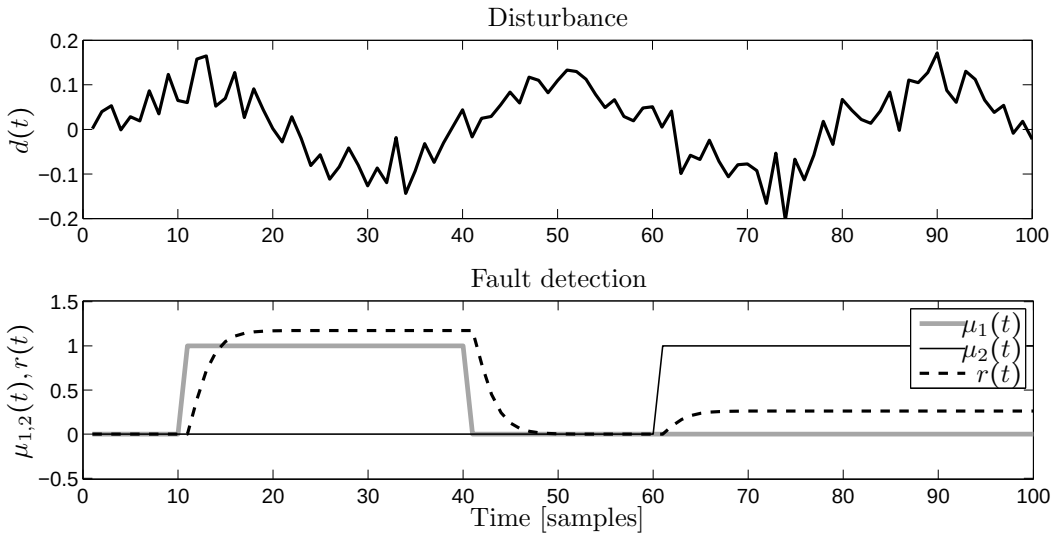

Figure 5.2: Robust fault detection, $q = 1$, the triple (A, E, C) has two invariant zeros at 1.2 and 1.3. Upper subfigure presents disturbances, whilst lower subfigure demonstrates robust fault detection process, i.e. residual, $r(t)$, is insensitive to disturbances.

system is described by equation (5.1), whose matrices are:

$$A = \begin{bmatrix} 0 & 1 & 0 & 0 & 0 \\ 0 & 0 & 1 & 0 & 0 \\ 0 & 0 & 0 & 1 & 0 \\ 0 & 0 & 0 & 0 & 1 \\ -0.0751 & -0.6345 & -2.1375 & -3.5875 & -3 \end{bmatrix} \quad E = \begin{bmatrix} -0.8 & 0 \\ 1.4 & 1 \\ 1.2 & 0 \\ 0 & 1 \\ 3.4816 & 1 \end{bmatrix}$$
$$C = \begin{bmatrix} 0.0948 & -0.4811 & 0.8675 & 0 & -0.0837 \\ 0 & 0 & 0 & 1 & 0 \\ 0.8375 & -0.3069 & -0.2238 & 0 & 0.3929 \end{bmatrix} \quad F = \begin{bmatrix} 1 & 1 & 0 & 0 & 0 \\ 0 & 0 & 1 & 1 & 0 \end{bmatrix}^T \tag{5.113}$$

Note that $CE_1 = 0$ and $\delta_1 = 1$, whilst $\delta_2 = 0$. The invariant zero of (A, E_1, C) is 1.2 and e_1 is given by:

$$e_1 = AE = \begin{bmatrix} 1.4 & 1.2 & 0 & 3.4816 & -13.8381 \end{bmatrix}^T \tag{5.114}$$

whilst $e_2 = E_2$. Note that the triple (A, e_1, C) has two invariant zeros $z_1 = 0$ and $z_2 = 1.2$ and the corresponding $v_0^{(1)} = e_1$, $v_1^{(1)} = E_1$ and $v_2^{(1)} = -\begin{bmatrix} 1 & 2 & 1 & 0 & 0 \end{bmatrix}$. Eigenvalues of $X^{(1)}$ are selected to be 0.4, 0.5, and 0.6, whilst the eigenvalue corresponding to E_2 is 0.7. Then matrices $\tilde{\tilde{A}}^{(1)}$ and $\tilde{\tilde{B}}^{(1)}$ are calculated as:

$$\tilde{\tilde{A}} = \begin{bmatrix} -0.32 & -0.8 & 1 \\ -0.35 & -0.7 & 1 \\ -0.36 & -0.6 & 1 \end{bmatrix} \qquad \tilde{\tilde{B}} = \begin{bmatrix} -0.128 \\ -0.175 \\ -0.216 \end{bmatrix} \tag{5.115}$$

Thus, the first column of the matrix X is given by:

$$X^{(1)} = \begin{bmatrix} 0.300 \\ -0.380 \\ 0.336 \end{bmatrix} \tag{5.116}$$

Subsequently, the matrix A_e^* is obtained using (5.62b) and (5.62c):

$$A_e^* = \begin{bmatrix} 0.1400 & 1 \\ -0.5000 & -0.7 \\ 3.6016 & 1 \\ -14.8826 & 0.3 \\ 33.6320 & -7.922 \end{bmatrix} \tag{5.117}$$

Note that:

$$\operatorname{rank}(CE) = \operatorname{rank}(\begin{bmatrix} A_e^* \\ CE \end{bmatrix}) = 2 \tag{5.118}$$

and (C', A') is a detectable pair, hence the solution to the robust fault detection problem exists. The remaining eigenvalue of $(A - KC)$ is chosen to be 0.3. As a result the gain matrix K is obtained as:

$$K = \begin{bmatrix} -0.7707 & 0.5424 & 0.2586 \\ 0.6203 & -0.3448 & -0.0556 \\ -0.6264 & 0.6775 & -0.3647 \\ -1.3397 & -0.6720 & 2.5006 \\ 6.5303 & -3.4705 & -8.8598 \end{bmatrix} \tag{5.119}$$

Note that the unobservable subspace of $(QC, A - KC)$ is 4-dimensional, therefore its observable subspace is only one-dimensional. This means that $F_1(\bar{E}^\perp)$ and $F_2(\bar{E}^\perp)$ are colinear and are given by:

$$F_1(\bar{E}^\perp) = -0.4143 \begin{bmatrix} 0.4397 \\ -0.5181 \\ 0.5965 \\ 0.4143 \\ 0.1038 \end{bmatrix} \quad F_2(\bar{E}^\perp) = 1.0108 \begin{bmatrix} 0.4397 \\ -0.5181 \\ 0.5965 \\ 0.4143 \\ 0.1038 \end{bmatrix} \tag{5.120}$$

As a result the transfer functions between, respectively, $\mu_1(t)$ and $\mu_2(t)$ and the residual

differ only by the steady state gain:

$$\begin{aligned}\frac{r(z)}{\mu_1(z)} &= \frac{-0.29}{(z-0.3)}\\ \frac{r(z)}{\mu_2(z)} &= \frac{0.70}{(z-0.3)}\end{aligned} \tag{5.121}$$

The results of the simulation are presented in Fig. 5.3. It can be seen that transient

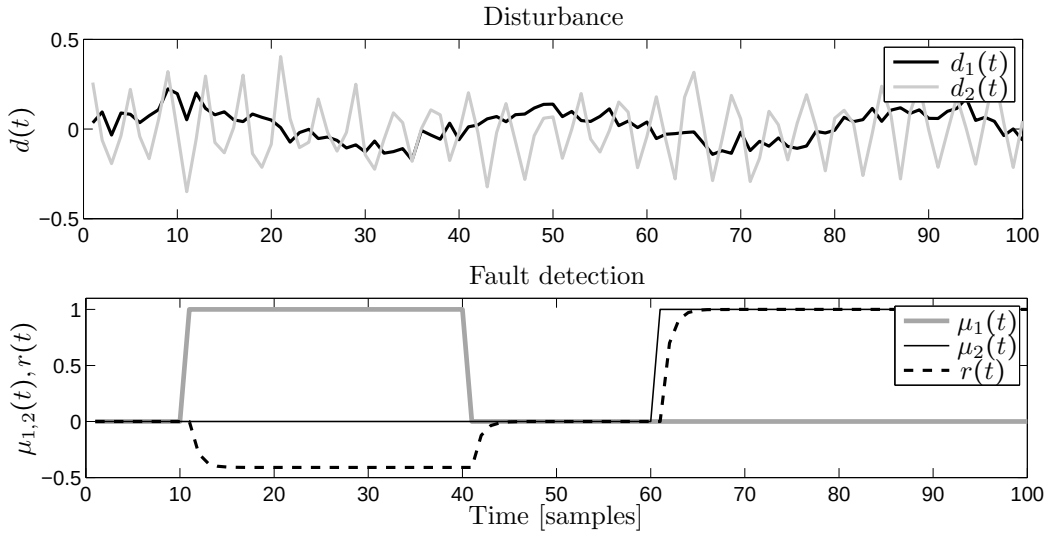

Figure 5.3: Robust fault detection, $q = 2$, the triple (A, E, C) has two invariant zeros. Upper subfigure presents disturbances, whilst lower subfigure demonstrates robust fault detection process. Trajectory of disturbances remains within a 4-dimensional subspace of 5-dimensional state space of fault detection filter, thus only one-dimensional subspace is left for fault detection. As a result the responses of residual to different faults differ only by steady state gain, cf. Remarks 5.1 and 5.2.

behaviour of the residual responses to both faults is the same, but their steady state gains differ.

5.3 Design of robust parity equations using right eigenstructure assignment

In this section a novel design of robust PE is proposed. An illustration of the proposed scheme is presented in Fig. 5.4. The method utilises a finite-time convergent observer in order to obtain the state estimate. Then, by multiplying the estimated state vector, $\hat{x}(t)$, by the system output matrix C and adding $Du(t)$ an output estimate, $\hat{y}(t)$, is constructed and compared with the measured output. Note that the difference between the robust residual generator described in the previous section and the scheme proposed in this section is that the algorithm proposed here utilises a finite-time convergent

state observer. This means that the state estimate converges within a finite time (as opposed to the asymptotic observer in Subsection 2.6.1 and in the previous section). Consequently, due to a finite impulse response of the state observer, the proposed scheme is equivalent to PE. The material presented in this section is extension to (Sumisławska, Larkowski & Burnham 2011*b*), where a design of robust PE for systems, which do not contain any invariant zeros, has been proposed.

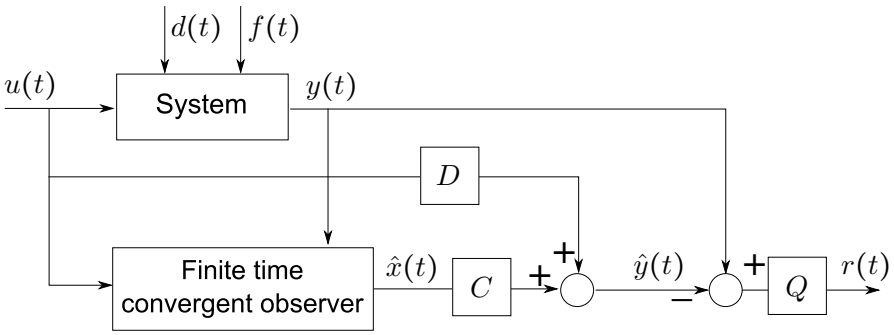

Figure 5.4: Schematic illustration of the proposed residual generator

The finite-time convergent observer is presented in Subsection 5.3.1. Then in Subsection 5.3.2 the robust fault detection filter, which has been proposed in Section 5.2, is combined with the finite-time convergent observer. In Subsection 5.3.3 it is demonstrated that the proposed method is equivalent to PE. Finally, the design scheme is explained using a numerical example in Subsection 5.3.4.

5.3.1 Finite-time convergent observer

A finite time convergent observer was originally developed by Engel & Kreisselmeier (2002) for continuous-time systems. The scheme proposed here utilises an equivalent observer in a discrete-time domain, which converges in a predefined time of τ samples. For sake of completeness, the discrete-time form of the observer described by Engel & Kreisselmeier (2002) is given in this subsection.

The system (5.1) in a fault-free, disturbance-free condition is described by:

$$\begin{aligned} x(t+1) &= Ax(t) + Bu(t) \\ y(t) &= Cx(t) + Du(t) \end{aligned} \tag{5.122}$$

Consider two Luenberger-type full-order state observers in the form of:

$$z_i(t+1) = A_{c_i} z_i(t) + K_i y(t) + (B - K_i D)u(t) \text{ for } i = 1, 2 \tag{5.123}$$

where:

$$A_{c_i} = A - K_i C \tag{5.124}$$

The i^{th} state estimation error $\xi_i(t) = z_i(t) - x(t)$ is then governed by:

$$\xi_i(t+1) = A_{c_i}\xi_i(t) \tag{5.125}$$

Therefore, the state estimation error as a function of time and initial conditions is defined by:

$$\xi_i(t) = A_{c_i}^t \xi_i(0) \tag{5.126}$$

The estimation error delayed by τ samples is then:

$$\xi_i(t-\tau) = A_{c_i}^{t-\tau} \xi_i(0) \tag{5.127}$$

Subsequently, using (5.126) and (5.127), it holds that:

$$\xi_i(t) - A_{c_i}^{\tau}\xi_i(t-\tau) = A_{c_i}^t \xi_i(0) - A_{c_i}^t \xi_i(0) = 0 \tag{5.128}$$

thus $\xi_i(t)$ can be eliminated from the state estimation $z_i(t)$:

$$z_i(t) - A_{c_i}^{\tau} z_i(t-\tau) = x(t) - A_{c_i}^{\tau} x(t-\tau) \tag{5.129}$$

In order to obtain the correct state estimate the term $A_{c_i}^{\tau} x(t-\tau)$ needs to be eliminated from the expression (5.129). Note that there are two unknowns in (5.129), namely, $x(t)$ and $x(t-\tau)$, and two equations, i.e. two Luenberger-type observers, therefore an explicit solution to the set of equations can be found. By combining the two observer, the following is obtained, cf. (Engel & Kreisselmeier 2002):

$$z(t+1) = A_c z(t) + Ky(t) + Gu(t) \tag{5.130a}$$

$$\hat{x}(t) = J\left(z(t) - A_c{}^{\tau} z(t-\tau)\right) \tag{5.130b}$$

where:

$$A_c = \begin{bmatrix} A_{c_1} & 0 \\ 0 & A_{c_2} \end{bmatrix} \quad K = \begin{bmatrix} K_1 \\ K_2 \end{bmatrix} \quad G = \begin{bmatrix} B - K_1 D \\ B - K_2 D \end{bmatrix} \quad z = \begin{bmatrix} z_1 \\ z_2 \end{bmatrix} \tag{5.131}$$

The gain matrix J should be chosen in such a way, the the terms $A_{c_i}^{\tau} x(t-\tau), i = 1, 2$ are eliminated from (5.130b), i.e.

$$J\left(z(t) - A_c^{\tau} z(t-\tau)\right) = J\begin{bmatrix} x(t) - A_{c_1}^{\tau} x(t-\tau) \\ x(t) - A_{c_2}^{\tau} x(t-\tau) \end{bmatrix} = x(t) \tag{5.132}$$

Therefore, J should fulfil the following condition:

$$J\begin{bmatrix} I & A_{c_1}^{\tau} \\ I & A_{c_2}^{\tau} \end{bmatrix} = \begin{bmatrix} I & 0 \end{bmatrix} \tag{5.133}$$

Consequently, the gain matrix J is calculated as, cf. (Engel & Kreisselmeier 2002, Raff, Menold, Ebenbauer & Allgöwer 2005):

$$J = \begin{bmatrix} I & 0 \end{bmatrix} \begin{bmatrix} I & A_{c_1}^{\tau} \\ I & A_{c_2}^{\tau} \end{bmatrix}^{-1} \tag{5.134}$$

Note that the solution of the expression (5.134) exists if the observer transition matrices A_{c_1} and A_{c_2} have distinct eigenvalues. Therefore, if the system (A, E, C) contains an invariant zero, Algorithm 5.3 should be used in order to ensure distinct eigenvalues of A_{c_1} and A_{c_2}.

5.3.2 Proposed scheme

The necessary and sufficient conditions for a disturbance decoupling in the proposed scheme are:

1. $QCe = 0$
2. For each column of the matrix E it holds that $\mathrm{Im}\{\bar{e}_i\}$ is an invariant subspace of A_{c_1} and A_{c_2}
3. A_{c_1} and A_{c_2} have distinct eigenvalues and no common eigenvalues

Conditions 1 and 2 ensure disturbance decoupling, whilst the condition 3 is essential for an existence of a finite time convergent observer (Engel & Kreisselmeier 2002).

If the disturbance and fault vectors are present in the system (5.1), the state estimation term of the i^{th} observer, $\xi_i(t) = z_i(t) - x(t)$, see (5.127), is driven by, cf. (5.11) and (5.12):

$$\xi_i(t+1) = A_{c_i}\xi_i(t) + F\mu(t) + Ed(t) = A_{c_i}\xi_i(t) + F\mu(t) + ed^*(t) \tag{5.135}$$

Therefore, $e_i(t)$ can be defined by:

$$\xi_i(t) = A_{c_i}^t \xi_i(0) + \sum_{j=0}^{t-1} A_{c_i}^j F\mu(t-j) + \sum_{j=0}^{t-1} A_{c_i}^j ed^*(t-j) \tag{5.136}$$

Hence, the term $z_i(t) - A_{c_i}^{\tau} z(t-\tau)$ can be expanded as:

$$\begin{aligned}
&z_i(t) - A_{c_i}^{\tau} z(t-\tau) = x(t) + A_{c_i}^{t}\xi_i(0) + \sum_{j=0}^{t-1} A_{c_i}^{j} F\mu(t-j) + \sum_{j=0}^{t-1} A_{c_i}^{j} ed^*(t-j) - \\
&A_{c_i}^{\tau} x(t-\tau) - A_{c_i}^{\tau} A_{c_i}^{t-\tau}\xi_i(0) - A_{c_i}^{\tau} \sum_{j=0}^{t-\tau-1} A_{c_i}^{j} F\mu(t-\tau-j) - A_{c_i}^{\tau} \sum_{j=0}^{t-\tau-1} A_{c_i}^{j} ed^*(t-\tau-j) \\
&= x(t) - A_{c_i}^{\tau} x(t-\tau) + \sum_{j=0}^{t-1} A_{c_i}^{j} F\mu(t-j) + \sum_{j=0}^{t-1} A_{c_i}^{j} ed^*(t-j) - \sum_{j=\tau}^{t-1} A_{c_i}^{j} F\mu(t-j) - \\
&\sum_{j=\tau}^{t-1} A_{c_i}^{j} ed^*(t-j) = x(t) - A_{c_i}^{\tau} x(t-\tau) + \sum_{j=0}^{\tau-1} A_{c_i}^{j} F\mu(t-j) + \sum_{j=0}^{\tau-1} A_{c_i}^{j} ed^*(t-j)
\end{aligned} \tag{5.137}$$

Therefore, one can obtain the state estimate $\hat{x}(t)$, see (5.133):

$$\hat{x}(t) = x(t) + J\begin{bmatrix} \sum_{j=0}^{\tau-1} A_{c_1}^{j} F\mu(t-j) \\ \sum_{j=0}^{\tau-1} A_{c_2}^{j} F\mu(t-j) \end{bmatrix} + J\begin{bmatrix} \sum_{j=0}^{\tau-1} A_{c_1}^{j} ed^*(t-j) \\ \sum_{j=0}^{\tau-1} A_{c_2}^{j} ed^*(t-j) \end{bmatrix} \tag{5.138}$$

Hence, the residual in the fault-free case is given by:

$$r(t) = QCJ\begin{bmatrix} \sum_{j=0}^{\tau-1} A_{c_1}^{j} ed^*(t-j) \\ \sum_{j=0}^{\tau-1} A_{c_2}^{j} ed^*(t-j) \end{bmatrix} \tag{5.139}$$

The matrix J can be expressed as:

$$J = \begin{bmatrix} J_1 & J_2 \end{bmatrix} \tag{5.140}$$

where $J_1, J_2 \in \mathbb{R}^{n\times n}$. Incorporating (5.140) into (5.134), the following relationships are obtained:

$$\begin{aligned}
J_1 &= -A_{c_2}^{\tau}\left[A_{c_1}^{\tau} - A_{c_2}^{\tau}\right]^{-1} \\
J_2 &= I - J_1
\end{aligned} \tag{5.141}$$

Consequently, the residual in the fault-free case is:

$$\begin{aligned}
r(t) &= QC\begin{bmatrix} J_1 & J_2 \end{bmatrix}\begin{bmatrix} \sum_{j=0}^{\tau-1} A_{c_1}^{j} ed^*(t-j) \\ \sum_{j=0}^{\tau-1} A_{c_2}^{j} ed^*(t-j) \end{bmatrix} \\
&= QCJ_1 \sum_{j=0}^{\tau-1} A_{c_1}^{j} ed^*(t-j) + QCJ_2 \sum_{j=0}^{\tau-1} A_{c_2}^{j} ed^*(t-j)
\end{aligned} \tag{5.142}$$

Denote a subspace spanned by columns of an arbitrary matrix V as $\mathcal{V}$. Assume that there exist two matrices P and R, such that $\mathcal{V}$ is P-invariant and R-invariant. From

the definition of invariance it holds that (Halmos 1958):

$$\begin{aligned} P\mathcal{V} &\subseteq \mathcal{V} \\ R\mathcal{V} &\subseteq \mathcal{V} \end{aligned} \tag{5.143}$$

Therefore:

$$P\mathcal{V} + R\mathcal{V} = (P+R)\mathcal{V} \subseteq \mathcal{V} \tag{5.144}$$

This means that $\mathcal{V}$ is $(P+R)$-invariant. Furthermore, $\mathcal{V}$ is a P^i-invariant subspace, where $i \in \mathbb{Z}$. This leads to the conclusion that $\mathrm{Im}\{\bar{e}\}$ is J_1- and J_2-invariant, cf. (5.141). Due to the fact that $\mathrm{Im}\{e\} \subseteq \mathrm{Im}\{\bar{e}\}$, it holds that:

$$A_{c_i}^j \mathrm{Im}\{e\} \subseteq \mathrm{Im}\{\bar{e}\} \text{ for } i = 1,2; j = 0,\cdots,\tau-1 \tag{5.145}$$

because $\mathrm{Im}\{\bar{e}\}$ is $A_{c_i}^j$-invariant and $\mathrm{Im}\{e\} \subseteq \mathrm{Im}\{\bar{e}\}$. Hence:

$$J_i A_{c_i}^j \mathrm{Im}\{e\} \subseteq \mathrm{Im}\{\bar{e}\} \text{ for } i = 1,2; j = 0,\cdots,\tau-1 \tag{5.146}$$

because $\mathrm{Im}\{\bar{e}\}$ is J_i-invariant and $\mathrm{Im}\{e\} \subseteq \mathrm{Im}\{\bar{e}\}$. Consequently:

$$QCJ_i A_{c_i}^j \mathrm{Im}\{e\} \subseteq QC\mathrm{Im}\{\bar{e}\} = \mathrm{Im}\{QC\bar{e}\} = 0 \text{ for } i = 1,2; j = 0,\cdots,\tau-1 \tag{5.147}$$

Thus in the fault-free case the residual, cf. (5.139), is equal to zero.

5.3.3 Design of robust PE

A state estimation using the finite time convergent observer described in Subsection 5.3.1 can be expressed as a function of the last τ past values of the system input and output:

$$\hat{x}(t) = \sum_{i=1}^{2} J_i \sum_{j=0}^{\tau-1} A_{c_i}^j (B - K_i D) u(t-j-1) + \sum_{i=1}^{2} J_i \sum_{j=0}^{\tau-1} A_{c_i}^j K_i y(t-j-1) \tag{5.148}$$

(The derivation of the above equation is analogous to (5.137).) Therefore, the residual generator can be described by the following parity relation:

$$r(t) = Qy(t) - Q(C\hat{x}(t) + Du(t)) = W_y Y(t) - W_u U(t) \tag{5.149}$$

where:

$$\begin{aligned} Y(t) &= \begin{bmatrix} y^T(t-\tau) & y^T(t-\tau+1) & \cdots & y^T(t) \end{bmatrix}^T \\ U(t) &= \begin{bmatrix} u^T(t-\tau) & u^T(t-\tau+1) & \cdots & u^T(t) \end{bmatrix}^T \end{aligned} \tag{5.150}$$

and:

$$W_u = -\Big[\; QC(J_1 A_{c_1}^{\tau-1}(B - K_1 D) + J_2 A_{c_2}^{\tau-1}(B - K_2 D)) \quad \cdots \\ QC(J_1 A_{c_1}^{2}(B - K_1 D) + J_2 A_{c_2}^{2}(B - K_2 D)) \\ QC(J_1 A_{c_1}(B - K_1 D) + J_2 A_{c_2}(B - K_2 D))B \quad QCB \quad -QD \;\Big] \tag{5.151}$$

$$W_y = \Big[\; QC(J_1 A_{c_1}^{\tau-1} K_1 + J_2 A_{c_2}^{\tau-1} K_2) \quad \cdots \quad QC(J_1 A_{c_1}^{2} K_1 + J_2 A_{c_2}^{2} K_2) \\ QC(J_1 A_{c_1}^{1} K_1 + J_2 A_{c_2}^{1} K_2) \quad QC(J_1 K_1 + J_2 K_2) \quad -Q \;\Big]$$

The algorithm for obtaining vectors W_u and W_y is given below:

Algorithm 5.4 (Robust PE via right eigenstructure assignment).

1. Obtain the disturbance direction matrix $e = \Big[\; e_1 \quad e_2 \quad \cdots \quad e_q \;\Big]$, where

$$e_i = A^{\delta_i} E_i \tag{5.152a}$$

   and δ_i is the smallest number for which $CA^{\delta_i} E_i \neq 0$

2. Obtain Q such that $QCe = 0$

3. Select eigenvalues for $A_{c_1} = A - K_1 C$

4. For each column of E obtain invariant zeros of the triple (A, e_i, C), denoted as $z_j^{(i)}$, and corresponding vectors $v_j^{(i)}$, for $j = 1, \cdots, q_i$, such that:

$$\begin{bmatrix} z_j^{(i)} I - A & v_{j-1}^{(i)} \\ C & 0 \end{bmatrix} \begin{bmatrix} v_j^{(i)} \\ -1 \end{bmatrix} = 0 \tag{5.152b}$$

   where $v_0^{(i)}$ denotes e_i.

5. Calculate coefficients $x_{11}^{(i)}, \cdots, x_{q_i+1,1}^{(i)}$ using (5.59–5.61)

6. Obtain matrix A_e^* as:

$$A_e^* = \Big[\; A_e^{*(1)} \quad A_e^{*(2)} \quad \cdots \quad A_e^{*(q)} \;\Big] \tag{5.152c}$$

   where

$$A_e^{*(i)} = (A - x_{11}^{(i)} I)e_i - x_{21}^{(i)} v_1^{(i)} - x_{31}^{(i)} v_2^{(i)} - \cdots - x_{q_i+1,1}^{(i)} v_k^{(i)} \tag{5.152d}$$

7. Obtain:

$$A' = A - A_e^*(CE)\ C \tag{5.152e}$$
$$C' = \left(I - CE(CE)\ \right)C \tag{5.152f}$$

8. Using any eigenstructure assignment method allocate remaining eigenvalues of $A_{c_1} = (A' - K_1'C')$

9. Calculate K_1

$$K_1 = A_e^*(CE)\ + K_1'[I - CE(CE)\ ] \tag{5.152g}$$

10. Repeat steps 3 to 9 for $A_{c_2} = A - K_2C$

11. Choose τ and calculate J_1 and J_2 using

$$J_1 = -A_{c_2}^{\tau}\left[A_{c_1}^{\tau} - A_{c_2}^{\tau}\right]^{-1} \tag{5.152h}$$
$$J_2 = I - J_1 \tag{5.152i}$$

12. Obtain W_u and W_y using (5.151)

13. Calculate residual via

$$r(t) = W_yY(t) - W_uU(t) \tag{5.152j}$$

5.3.4 Numerical example

In this example Algorithm 5.4 is used in order to design robust PE. The influence of the selection of eigenvalues of A_{c_1} and A_{c_2} and the convergence time τ on step and impulse response of the residual to the fault is examined.

Example 5.4. Design of robust PE using right eigenstructure assignment
Consider the system (5.1), where:

$$A = \begin{bmatrix} 0 & 3 & 4 \\ 1 & 2 & 3 \\ 0 & 2 & 5 \end{bmatrix} B = \begin{bmatrix} 1 & 0 \\ 0 & 0 \\ 0 & 1 \end{bmatrix} E = \begin{bmatrix} 1 \\ 2 \\ -1 \end{bmatrix} F = \begin{bmatrix} 1 \\ -0.5 \\ 0.5 \end{bmatrix} C = \begin{bmatrix} 0 & 1 & 0 \\ 0 & 0 & 1 \end{bmatrix} \tag{5.153}$$

and the matrix D is null. The eigenvalues of the matrix A_{c_1} are chosen to be $\lambda_{A_{c_1}} = \{0.9, 0.925, 0.95\}$, whereas the eigenvalues of A_{c_2} are $\lambda_{A_{c_2}} = \{0.965, 0.975, 0.995\}$. (Note that eigenvalues of A_{c_1} and A_{c_2} are close to unity.) Gain matrices K_1' and K_2' have

been selected to minimise Frobenius norms of K_1 and K_2 and are given by:

$$K_1 = \begin{bmatrix} 3.6306 & 6.1612 \\ -0.3713 & -0.9425 \\ 2.2481 & 4.5963 \end{bmatrix} \quad K_2 = \begin{bmatrix} 3.7124 & 6.3899 \\ -0.4854 & -1.0407 \\ 2.2577 & 4.5504 \end{bmatrix} \tag{5.154}$$

Algorithm 5.4 is used to calculate W_u and W_y for parity space orders equal to $\tau = 5$ and $\tau = 15$ samples. The impulse and step responses of the residual $r(t)$ to the fault $\mu(t)$ for the two aforementioned parity space orders are compared in Fig. 5.5. It is worth noting that the response of the residual to fault is strongly dependent on the chosen parity space order. This is due to the fact that the eigenvalues of A_{c_1} and A_{c_2} are selected to be close to unity, therefore the two asymptotic state observers which are combined to create the finite time convergent observers are relatively slow in comparison to the chosen parity space orders.

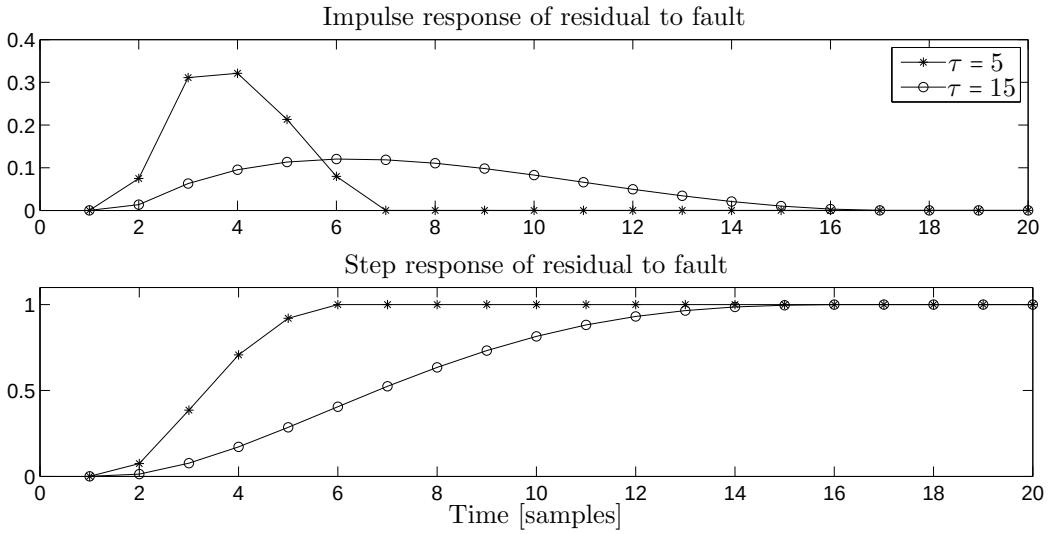

Figure 5.5: Comparison of step and impulse responses of the residual to fault for different cases of τ. Eigenvalues of $(A - K_1C)$ and $(A - K_2C)$ are, respectively, $\lambda_{A_{c_1}} = \{0.9, 0.925, 0.95\}$ and $\lambda_{A_{c_2}} = \{0.965, 0.975, 0.995\}$.

In the second simulation 'fast' eigenvalues are taken into consideration, i.e. $\lambda^*_{A_{c_1}} = \{0.33, 0.25, 0.3\}$ and $\lambda^*_{A_{c_2}} = \{0.15, 0.20, 0.35\}$, and compared with 'slow' eigenvalues from the previous experiment for parity space $\tau = 15$. The gain matrices K_1^* and K_2^* are:

$$K_1^* = \begin{bmatrix} 2.7472 & 3.8243 \\ 0.7943 & 0.2487 \\ 2.3278 & 5.3257 \end{bmatrix} \quad K_2^* = \begin{bmatrix} 2.7472 & 3.8243 \\ 0.7943 & 0.2487 \\ 2.3278 & 5.3257 \end{bmatrix} \tag{5.155}$$

Step and impulse responses of the residual to the fault for two different sets of eigen-

values ('slow', i.e. $\lambda_{A_{c_1}}$ and $\lambda_{A_{c_2}}$, versus 'fast', i.e. $\lambda^*_{A_{c_1}}$ and $\lambda^*_{A_{c_2}}$) are compared in Fig. 5.6. As expected, the response of the residual to the fault is faster when the eigenvalues of A_{c_1} and A_{c_2} are closer to the origin. The experiment also revealed that, in the case of 'fast' eigenvalues, the increase of the parity space order has a negligible influence on the residual response to the fault.

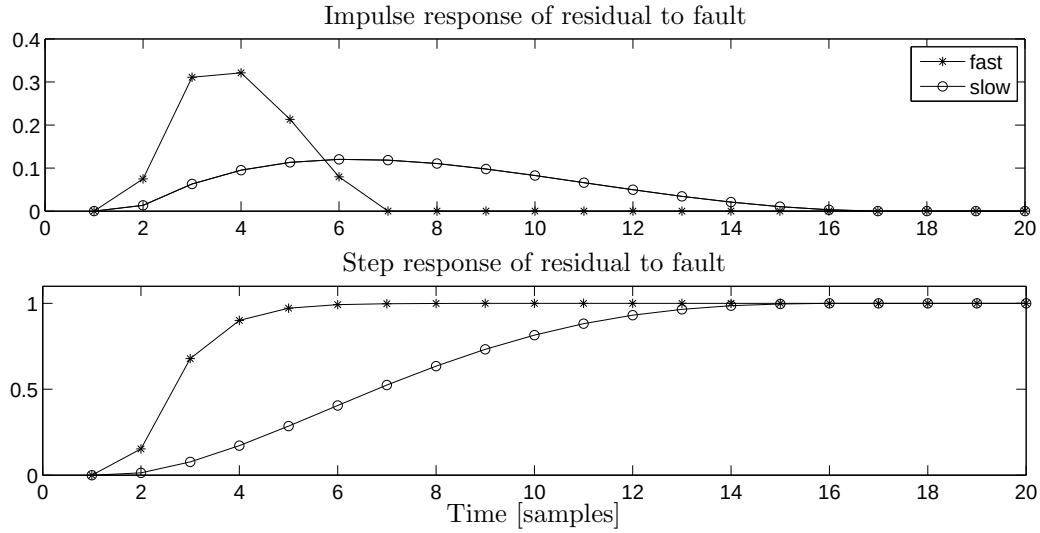

Figure 5.6: Comparison of step and impulse responses of the residual to fault for different choices of eigenvalues of A_{c_1} and A_{c_2}. Slow eigenvalues: $\lambda_{A_{c_1}} = \{0.9, 0.925, 0.95\}$ and $\lambda_{A_{c_2}} = \{0.965, 0.975, 0.995\}$. Fast eigenvalues: $\lambda^*_{A_{c_1}} = \{0.33, 0.25, 0.3\}$ and $\lambda^*_{A_{c_2}} = \{0.15, 0.20, 0.35\}$.

5.4 Design of robust parity equations using left eigenstructure assignment

The basic idea of the fault detection filter presented in this Section is similar to that described in Section 5.3. The state estimate is obtained using the finite time convergent observer (see Subsection 5.3.1). Then, based on the state estimate, an output estimate is calculated an compared with the measured output. The difference between the measured and estimated output is then multiplied by the matrix Q, see Fig. 5.4. The difference between the filter designed in this section and that presented in Section 5.3 is that the state observer gains K_1 and K_2 are obtained using the left eigenstructure assignment, see Subsection 2.6.3.

5.4.1 Design of robust PE

Decoupling conditions of the proposed scheme are:

1. $QCE = 0$
2. All rows of QC are left eigenvectors of A_{c_1} and A_{c_2}
3. A_{c_1} and A_{c_2} have distinct eigenvalues and no common eigenvalues

Condition 2. is achieved by the left eigenstructure assignment algorithm presented in Subsection 2.6.3. Analogously, to the case presented in Section 5.3, the fault detection filter can be reformulated as a parity equation (5.149), whose matrices W_u and W_y are given by (5.151). Consequently, the algorithm for the design of robust PE is summarised as follows:

Algorithm 5.5 (Robust PE via left eigenstructure assignment).

1. Calculate the matrix Q, which fulfils the condition $QCE = 0$
2. Select the desired eigenvalues of the matrix A_{c_1}, $\lambda_i, i = 1, 2, \cdots, n$
3. Compute $P(\lambda_i)$ as
$$P(\lambda_i) = (\lambda_i I - A^T)^{-1} C^T \tag{5.156a}$$
4. Calculate l_i^* and w_i^*, $i = 1, \cdots, q$ using
$$l_i^* = P(\lambda_i) w_i^* \tag{5.156b}$$
$$w_i^* = [P(\lambda_i)^T P(\lambda_i)]^{-1} P(\lambda_i)^T l_i \tag{5.156c}$$
and check the assignability condition $l_i^* = l_i$.
5. Select arbitrary w_i, $i = q+1, \cdots, n$ and obtain l_i, $i = q+1, \cdots, n$ using
$$l_i = -(\lambda_i I - A^T)^{-1} C^T w_i \tag{5.156d}$$
6. Obtain L and W as
$$L = \begin{bmatrix} l_1^* & \cdots & l_q^* & l_{q+1} & \cdots & l_n \end{bmatrix} \tag{5.156e}$$
$$W = \begin{bmatrix} w_1^* & \cdots & w_q^* & w_{q+1} & \cdots & w_n \end{bmatrix} \tag{5.156f}$$
7. Calculate K_1 via
$$K = -(L^{-1})^T W^T \tag{5.156g}$$
8. Repeat steps (2-7) for the matrix A_{c_2} and obtain K_2

9. Choose τ and calculate J_1 and J_2 using

$$J_1 = -A_{c_2}^{\tau}\left[A_{c_1}^{\tau} - A_{c_2}^{\tau}\right]^{-1} \tag{5.156h}$$

$$J_2 = I - J_1 \tag{5.156i}$$

10. Construct W_u and W_y as given by (5.151)

11. Calculate residual via

$$r(t) = W_y Y(t) - W_u U(t) \tag{5.156j}$$

Theorem 5.3. Algorithm 5.5 ensures disturbance decoupling.

Proof. Assume that two arbitrary matrices P and R have a common eigenvector x corresponding to eigenvalues λ_p and λ_r, respectively:

$$Px = \lambda_p x \quad Rx = \lambda_r x \tag{5.157}$$

then x is also an eigenvector of their sum or difference:

$$(P \pm R)x = (\lambda_p \pm \lambda_r)x \tag{5.158}$$

Furthermore, P can be expressed in a Jordan form as:

$$P = V\Lambda V^{-1} \tag{5.159}$$

where diagonal elements of Λ are eigenvalues of P, whereas eigenvectors of P are appropriate columns of V. Then it is known that:

$$P^i = V\Lambda^i V^{-1} \tag{5.160}$$

which means that P and its i^{th} power have common eigenvectors. Consequently, if all rows of QC are left eigenvectors of A_{c_1} and A_{c_2}, then all rows of QC are also left eigenvectors of J_1 and J_2.

The residual in the fault-free case can be described by, see (5.142):

$$r(t) = \sum_{l=1}^{2}\sum_{k=1}^{\tau} P_{l,k} d(t-k) \tag{5.161}$$

where:

$$P_{l,k} = QCJ_l A_{c_l}^{k-1} E \tag{5.162}$$

Denote the i^{th} left eigenvector, right eigenvector, and the corresponding eigenvalue of the matrix $A_{c_l}^{k-1}$ as, respectively, $(l_i^{A_c})^T$, $v_i^{A_c}$, and $\lambda_i^{A_c}$. Analogously, use the notation $(l_i^J)^T$, v_i^J, and λ_i^J for the left eigenvector, right eigenvector, and the corresponding eigenvalue of the matrix J_l. The first r_q left eigenvectors of $A_{c_1}^{k-1}$, $A_{c_2}^{k-1}$, J_1, and J_2 are rows of QC. Then $P_{l,k}$ can be expressed as:

$$P_{l,k} = QC \sum_{i=1}^{r_q} \lambda_i^J v_i^J (l_i^J)^T A_{c_l}^{k-1} E + QC \sum_{i=r_q+1}^{n} \lambda_i^J v_i^J (l_i^J)^T A_{c_l}^{k-1} E \tag{5.163}$$

The second element of the above expression is equal to zero because $QCv_i^J = 0$, for $i = r_q + 1, \cdots, n$ (because rows of QC are first left eigenvectors of J_l). Subsequently:

$$\begin{aligned} P_{l,k} = QC \sum_{i=1}^{r_q} \sum_{j=1}^{r_q} \lambda_i^{A_c} \lambda_j^J v_j^J (l_j^J)^T v_i^{A_c} (l_i^{A_c})^T E \\ + QC \sum_{i=r_q+1}^{n} \sum_{j=1}^{r_q} \lambda_i^{A_c} \lambda_j^J v_j^J (l_j^J)^T v_i^{A_c} (l_i^{A_c})^T E \end{aligned} \tag{5.164}$$

The first element of the above expression is zero because $(l_i^{A_c})^T$ is equal to i^{th} row of QC and $QCE = 0$. The second element is equal to zero because $(l_j^J)^T v_i^{A_c} = (l_j^J)^T v_i^J = 0$, for $i = r_q + 1, \cdots, n$, $j = 1, \cdots, r_q$. This shows, therefore, that the residual is null if there is no fault present in the system. ∎

5.4.2 Numerical example

In the following example, the design of robust PE using left eigenstructure assignment is presented. The influence of the choice of τ as well as eigenvalues of A_{c_1} and A_{c_2} on step and impulse responses of the residual to fault is examined. Furthermore, the proposed scheme is compared with the DRFDF, i.e. a first order parity equation presented in Subsection 2.6.4.

Example 5.5. Design of robust PE using left eigenstructure assignment
Consider system (5.1), whose matrices A, B, C, E, and F matrices are, cf. (Chen & Patton 1999):

$$A = \begin{bmatrix} 0.25 & 0 & 0 \\ 0 & 0.5 & 0 \\ 0 & 0 & 0.375 \end{bmatrix} B = \begin{bmatrix} 0 \\ 0 \\ 1 \end{bmatrix} E = \begin{bmatrix} 1 \\ 1 \\ 0 \end{bmatrix} F = \begin{bmatrix} 1.0 \\ 0.1 \\ 1.0 \end{bmatrix} C = \begin{bmatrix} 1 & 1 & 0 \\ 0 & 1 & 1 \end{bmatrix} \tag{5.165}$$

whilst the feedthrough matrix is null.

Eigenvalues of the matrix A_{c_1} are selected to be $\lambda_{A_{c_1}} = \{0.975, 0.985, 0.995\}$, whilst eigenvalues of A_{c_2} are $\lambda_{A_{c_2}} = \{0.9, 0.925, 0.95\}$. The matrix Q, such that $QCE = 0$ is given by:

$$Q = \begin{bmatrix} 1 & -2 \end{bmatrix} \tag{5.166}$$

Thus $QC = l_1^T = \begin{bmatrix} 1 & -1 & -2 \end{bmatrix}$. The eigenvalue corresponding to l_1^T is $\lambda_1 = 0.975$ and hence $P(\lambda_1)$ is calculated via (5.156a) as:

$$P(\lambda_1) = \begin{bmatrix} 1.3793 & 0 \\ 2.1053 & 2.1053 \\ 0 & 1.6667 \end{bmatrix} \tag{5.167}$$

and corresponding $w_1^* = \begin{bmatrix} 0.7250 & -1.2 \end{bmatrix}^T$, cf. (5.156c). It holds that $P(\lambda_1)w_1^* = l_1$, hence a complete decoupling can be achieved. The remaining eigenvalues of A_{c_1} are $\lambda_2 = 0.985$ and $\lambda_3 = 0.995$ and the corresponding matrices $P(\lambda_2)$ and $P(\lambda_3)$ are obtained using (5.156a):

$$P(\lambda_2) = \begin{bmatrix} 1.3605 & 0 \\ 2.0619 & 2.0619 \\ 0 & 1.6393 \end{bmatrix} \quad P(\lambda_3) = \begin{bmatrix} 1.3423 & 0 \\ 2.0202 & 2.0202 \\ 0 & 1.6129 \end{bmatrix} \tag{5.168}$$

Vectors w_2 and w_3 can be freely chosen and they are selected to be $w_2 = \begin{bmatrix} 1 & 0 \end{bmatrix}^T$ and $w_2 = \begin{bmatrix} 0 & 1 \end{bmatrix}^T$. Then, the corresponding l_2 and l_3 are computed using (5.156d):

$$l_2 = \begin{bmatrix} 1.3605 \\ 2.0619 \\ 0 \end{bmatrix} \quad l_3 = \begin{bmatrix} 0 \\ 2.0202 \\ 1.6129 \end{bmatrix} \tag{5.169}$$

Consequently, matrices L and W are obtained via, respectively, (5.156e) and (5.156e) as:

$$L = \begin{bmatrix} 1 & 1.3605 & 0 \\ -1 & 2.0619 & 2.0202 \\ -2 & 0 & 1.6129 \end{bmatrix} \quad W = \begin{bmatrix} 0.725 & 1 & 0 \\ -1.200 & 0 & 1 \end{bmatrix} \tag{5.170}$$

and the gain matrix K_1 calculated using (5.156g) is:

$$K_1 = \begin{bmatrix} 0.7203 & -5.8212 \\ -0.9603 & 3.8412 \\ 1.2028 & -5.4312 \end{bmatrix} \tag{5.171}$$

Analogously, the gain matrix K_2 is calculated. Vectors w_2 and w_3 are selected such that the Frobenius norm of K_2 is minimised and K_2 is given by:

$$K_2 = \begin{bmatrix} -1.6037 & -0.5727 \\ 0.7037 & 0.1227 \\ -0.8287 & -0.8727 \end{bmatrix} \tag{5.172}$$

Then, the matrices J_1 and J_2 and the PE coefficient vectors W_u and W_y are cal-

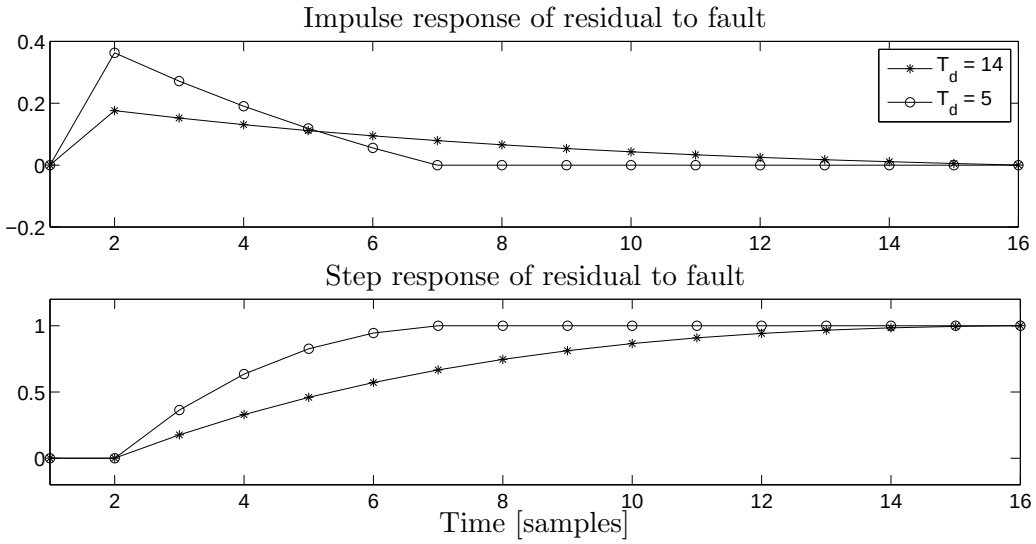

Figure 5.7: Comparison of responses of residual to fault for different cases of parity space order. Eigenvalues of A_{c_1} and A_{c_2} are, respectively, $\lambda_{A_{c_1}} = \{0.9, 0.925, 0.95\}$ and $\lambda_{A_{c_2}} = \{0.965, 0.975, 0.995\}$.

culated using, respectively, (5.156h), (5.156i), and (5.151) for the parity space orders equal to $\tau = 5$ and $\tau = 14$ samples. Impulse and step responses of the residual $r(t)$ to the fault $\mu(t)$ for the two aforementioned values of τ are compared in Fig. 5.7. Similarly, as in Example 5.4 a strong influence of the parity space order τ on the residual response to fault can be observed (due to the fact that the eigenvalues of A_{c_1} and A_{c_2} are close to unity). Also the impulse response of the residual to the fault decays almost linearly. In the second simulation 'fast' eigenvalues are taken into consideration, i.e. $\lambda^*_{A_{c_1}} = \{0.2, 0.3, 0.4\}$ and $\lambda^*_{A_{c_2}} = \{0.8, 0.7, 0.6\}$, and compared with 'slow' eigenvalues from the previous experiment for the parity space order $\tau = 8$. The gain matrices K_1^* and K_2^* of the 'fast' filter are:

$$K_1^* = \begin{bmatrix} 0.0010 & -0.0620 \\ 0.0390 & 0.0820 \\ -0.0440 & 0.1030 \end{bmatrix} \qquad K_2^* = \begin{bmatrix} -0.5790 & -0.1020 \\ 0.1390 & -0.1180 \\ -0.0840 & -0.4170 \end{bmatrix} \tag{5.173}$$

Step and impulse responses of the residual to the fault for two different sets of eigenvalues ('slow', i.e. $\lambda_{A_{c_1}}$ and $\lambda_{A_{c_2}}$, versus 'fast', i.e. $\lambda^*_{A_{c_1}}$ and $\lambda^*_{A_{c_2}}$) are compared in Fig. 5.8. Similarly to the experiment in Example 5.4, the response of the residual to the fault is faster when the eigenvalues of A_{c_1} and A_{c_2} are closer to the origin. Also in the case of 'fast' eigenvalues, the increase of the parity space order has negligible influence on the residual response to the fault.

Choice of a low parity space order or selection of eigenvalues close to the origin leads to a fast reaction of the residual to a fault. However, in practice there is always noise present in the system. Therefore, it may be required to increase the parity space order

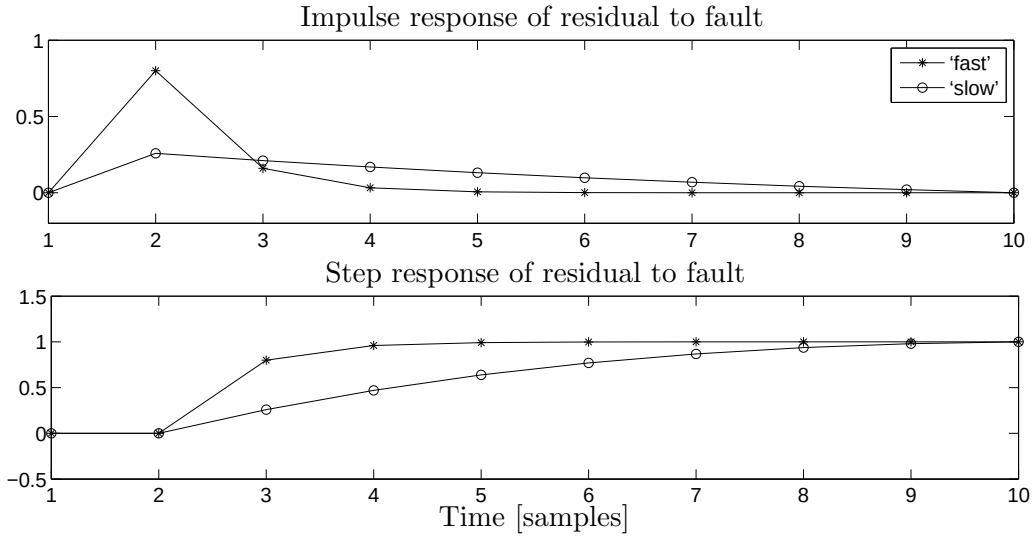

Figure 5.8: Influence of eigenvalues of matrices A_{c_1} and A_{c_2} on step and impulse response of residual to fault for $\tau = 8$. Slow eigenvalues: $\lambda_{A_{c_1}} = \{0.975, 0.985, 0.995\}$ and $\lambda_{A_{c_2}} = \{0.9, 0.925, 0.95\}$. Fast eigenvalues: $\lambda^*_{A_{c_1}} = \{0.2, 0.3, 0.4\}$ and $\lambda^*_{A_{c_2}} = \{0.8, 0.7, 0.6\}$.

for the purpose of minimising the effects of noise on the residual generator. In this experiment the scheme proposed here is compared with the DRFDF, see Subsection 2.6.4, which is equivalent to the PE, whose W_u and W_y coefficients are:

$$\begin{aligned} W_u &= \begin{bmatrix} 0 & 2 \end{bmatrix} \\ W_y &= \begin{bmatrix} 1 & -2 & -0.25 & 0.75 \end{bmatrix} \end{aligned} \tag{5.174}$$

Algorithm 5.5 has been designed using the 'slow' eigenvalues set, i.e. $\lambda_{A_{c_1}}$ and $\lambda_{A_{c_2}}$ for two cases of the time delay, $\tau = 3$ and $\tau = 8$. The PE coefficient vectors for $\tau = 3$ are:

$$\begin{aligned} W_u &= \begin{bmatrix} 0.28 & 0.60 & 0.95 & 0 \end{bmatrix} \\ W_y &= \begin{bmatrix} -0.03 & 0.10 & 0.06 & -0.06 & 0.18 & -0.24 & 0.47 & -0.95 \end{bmatrix} \end{aligned} \tag{5.175}$$

whilst those coefficients for $\tau = 8$ are:

$$\begin{aligned} W_u &= \begin{bmatrix} 0.04 & 0.8 & 0.13 & 0.18 & 0.24 & 0.31 & 0.39 & 0.47 & 0 \end{bmatrix} \\ W_y &= \begin{bmatrix} -0.005 & 0.014 & 0.009 & -0.008 & 0.023 & -0.031 & 0.04 & -0.058 \\ & & 0.06 & -0.089 & 0.081 & -0.124 & 0.106 & -0.163 & 0.133 \end{bmatrix} \end{aligned} \tag{5.176}$$

Fig. 5.9 shows the efficacy of the developed algorithm and the DRFDF, when the system output is affected by an additive, white, Gaussian, zero-mean measurement noise with variance equal to 0.01. The DRFDF yields a fast reaction of the residual to a fault,

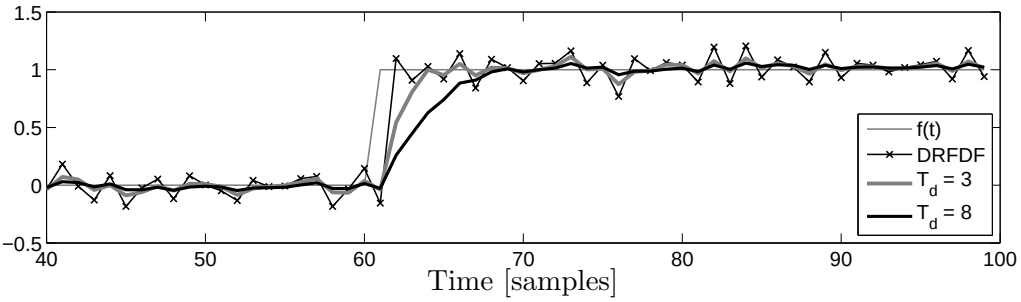

Figure 5.9: Fault detection in the case when the output is subjected to measurement noise

however it is relatively sensitive to noise. The filter obtained using Algorithm 5.5 allows for an increase of the parity space order, hence a reduction of the residual sensitivity to noise. Nevertheless, a high parity space order results in slow response of the residual to the fault.

5.5 Concluding remarks

The drawback of the robust fault detection filter of Chen & Patton (1999) is its inapplicability to systems with unstable invariant zeros. In such a case the design of a stable filter was infeasible. In this chapter an extension to the aforementioned robust fault detection filter has been presented which ensures stability of the scheme in the case when the system has unstable invariant zeros. It has been demonstrated that the eigenstructure of the developed scheme is equivalent that of the fault isolation filter proposed in (Chen & Speyer 2006*a*). However, the algorithm presented in this chapter is computationally simpler.

Furthermore, a novel design of robust PE of a user defined order has been presented. In the proposed fault detection scheme the traditional asymptotically convergent observer is replaced by a state observer, which converges within a finite, user predefined time. By selecting the time (the number of samples) after which the state observer converges, the order of the parity space can be arbitrarily chosen. This is an extension to (Patton & Chen 1991*b*), where the left eigenstructure assignment method has been used to design a first order PE. The method proposed in this chapter utilises both the left and right eigenstructure assignment to design PE and is applicable to systems with unstable invariant zeros.

Design freedom of the novel algorithms has been demonstrated on numerical examples. The residual response to faults can be shaped by a selection of the parity space order as well as the eigenvalues of the component state observers, which form the finite time convergent (open-loop) state observer. Advantages of the proposed scheme in a noisy environment have also been shown. By selecting the order of the parity space the

residual sensitivity to noise can be adjusted.

As further work an optimisation algorithm for minimisation of the influence of noise on residual is considered. It may also be worth exploring the applicability of the scheme when equation (5.52) is not fulfilled, i.e. the disturbance direction vectors e_i combine with each other to create new invariant zeros.

Chapter 6

Fault isolation via diagonal PE

Nomenclature

A	state transition matrix in state-space model
A_{c_1}, A_{c_2}	filter state transition matrices
$A_\lambda, A_e^*, A_e^{*(i)}, A_w$ ...	auxiliary matrices
$\tilde{\tilde{A}}, \tilde{A}$	auxiliary matrices
A'	auxiliary matrix
B	input matrix of the input in state-space model
$\tilde{\tilde{B}}$	auxiliary matrix
C	output matrix in state-space model
C'	auxiliary matrix
D	feedforward matrix of known input in state-space model
f	matrix of directions of elements of $\mu(t)$
f_i	direction of μ_i
$\bar{f}$	matrix built from matrices f_i
$\bar{f}_i$	matrix whose image is sum of image of f_i and images of invariant zero directions of (A, f_i, C)
F	input matrix of fault signal in state-space model
F_i	i^{th} column of F
g, g_i	auxiliary scalar
I	identity matrix
J, J_1, J_2	gain matrices
K, K_1, K_2, K'	gain matrices
l_j, l_j^*	transposes of left eigenvectors of filter state transition matrix
m	number of system outputs
$M(t)$	stacked vector of last $\tau + 1$ values of $\mu(t)$
n	number of states in a state-space model
p	number of system inputs
$P(\lambda_i)$	auxiliary function of λ_i
P, R	auxiliary matrices
q	number of disturbance signals
Q	gain matrix
r	number of fault signals
$r(t)$	residual
$r_i(t)$	i^{th} element of $r(t)$

T	similarity transformation matrix
$u(t)$	measured system input
$U(t)$	stacked vector of last $\tau+1$ values of $u(t)$
$v, v_j, v_j^{(i)}$	auxiliary vectors
V_e	matrix whose columns are eigenvectors of filter state transition matrix
$w_j, w_j^{(i)}, w_j'^{(i)}$	right eigenvectors of filter state transition matrix
w_j^*	auxiliary vector
W	auxiliary matrix
$W_u, W_y, \mathring{W}_u, \mathring{W}_y, W_\mu$	parity matrices
$x(t)$	state vector instate space model
$\hat{x}(t)$	state estimate
$x_{i,j}$	auxiliary scalars
X	auxiliary matrix
$y(t)$	measured system output
$Y(t)$	stacked vector of last $\tau+1$ values of $y(t)$
z_i	system zero
$z_i(t)$	state estimate
α_i	auxiliary parameter
$\beta_i, \bar{\beta}_i$	auxiliary parameter vector
δ_i	auxiliary term
$\lambda_j, \lambda_j^{(i)}$	eigenvalue of filter state transition matrix
Λ_e	diagonal matrix whose diagonal elements are eigenvalues of filter state transition matrix
$\mu(t)$	fault signal
$\mu_i(t)$	i^{th} element of fault signal
$\hat{\mu}(t)$	estimate of fault signal
$\Theta^{(i)}, \bar{\Theta}^{(i)}$	auxiliary matrices
Ω	set of all invariant zeros of (A, e, C) or auxiliary matrix
Ω_i	set of all invariant zeros of (A, e_i, C)
τ	convergence time of finite time-convergent state observer, order of parity space
$\Xi(t)$	auxiliary matrix
Ψ	auxiliary matrix

Preliminary reading: Sections 2.2, 2.6, 2.7, 5.2, and 5.3.

6.1 Introduction

Directional residuals have been used in various industrial applications, such as induction motor drives (Campos-Delgado 2011), a class of linear networked control systems (Chabir, Sauter & Keller 2009), neuro-fuzzy diagnosis of AC motors (Alexandru 2003, Alexandru & Popescu 2004), and engine fault detection and isolation (Dutka, Javaherian & Grimble 2009). Also a structured residual set has been applied for fault diagnosis of many industrial systems, such as: a two non-interacting tank system (Bhattacharjee & Roy 2010), a heat exchanger (Fagarasan & St. Iliescu 2008), an aircraft (Fravolini, Brunori, Campa, Napolitano & La Cava 2009), and a Tennessee Eastman process example (Xie, Zhang & Wang 2006, Ye, Shi & Liang 2011).

Furthermore, Patton & Chen (1997) proposed a scheme for condition monitoring and fault diagnoisis of a seawater pumping system in operation at the Nuclear Electric Heysham 2 power station. Simultaneous sensor and actuator fault diagnosis on a water treatment system has been presented in (Fragkoulis, Roux & Dahhou 2009). Lia & Jengb (2010) demonstrated a fault detection isolation and identification filter for a nonisothermal continuous stirred tank reactor.

This chapter is an extension of the Algorithm 5.4 to a fault diagnosis scheme. In Section 6.3 a fault isolation algorithm utilising a directional residual set is devised, whilst in Section 6.4 the scheme is extended to fault identification.

6.2 Problem statement

It is assumed that a linear, dynamic, discrete-time, time-invariant system can be represented by the following equations:

$$\begin{aligned} x(t+1) &= Ax(t) + Bu(t) + F\mu(t) \\ y(t) &= Cx(t) + Du(t) \end{aligned} \tag{6.1}$$

where $x(t) \in \mathbb{R}^n$ is the system state vector, $u(t) \in \mathbb{R}^p$ and $y(t) \in \mathbb{R}^m$ are, respectively, the system input and output, and $\mu(t) \in \mathbb{R}^r$ is a fault signal. Matrices A, B, C, D, and F are constant and have appropriate dimensions. It is assumed that (C, A) is observable and F is of full column rank. The aim of this chapter is to provide algorithms for fault isolation an identification.

6.3 Design of fault isolation filter

A schematic illustration of the proposed fault isolation and identification filter is presented in Fig. 6.1. Analogously to the filter presented in Chapter 5, the method utilises a finite-time convergent observer in order to obtain the state estimate. Then, using the estimated state vector an output estimate is calculated and compared with the measured output. The difference between the measured and the estimated output is a directional residual (used for fault isolation). The residual is then evaluated in order to identify the fault, see Section 6.4.

Design of the fault isolation filter is analogous to that proposed in Section 5.3, i.e. the fault isolation filter is designed using Algorithm 5.4 by replacing the matrix E by F and setting Q to an identity matrix. The necessary conditions for the fault isolation filter to exist are:

1. (C,A) is an observable pair
2. $\text{rank}(\begin{bmatrix} Cf_1 & Cf_2 & \cdots & Cf_r \end{bmatrix}) = r$

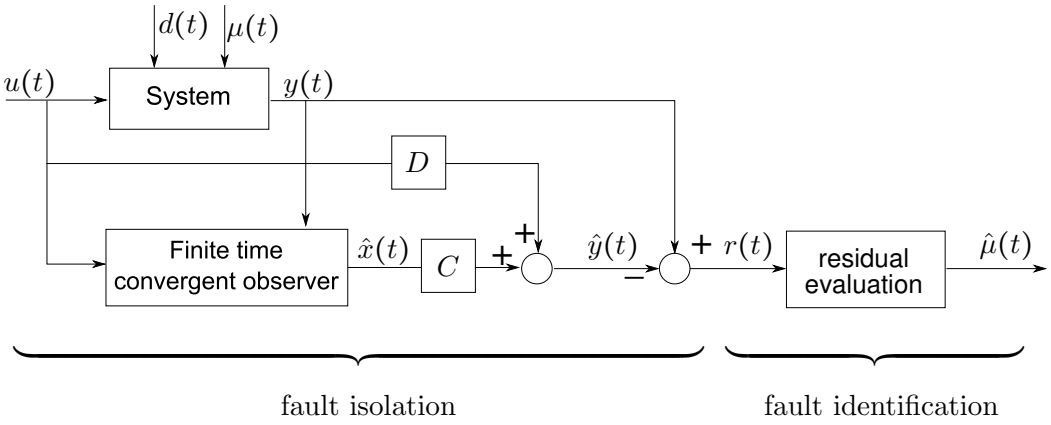

Figure 6.1: Schematic illustration of the proposed residual generator

where $f_i = A^{\delta_i} F_i$ and δ_i is the smallest number for which $CA^{\delta_i} F_i \neq 0$. Condition 1 allows all eigenvalues of $(A - K_1 C)$ and $(A - K_2 C)$ to be arbitrarily specified, whilst condition 2 ensures that residual vectors yielded by different faults lie in different directions.

Algorithm 6.1 (Fault isolation using directional PE).

1. For each column of F obtain δ_i, which is the smallest number for which $CA^{\delta_i} F_i \neq 0$ and compute zero directions $f_i = A^{\delta_i} F_i$
2. Select eigenvalues for $A_{c_1} = (A - K_1 C)$
3. For $f_i, i = 1, \cdots, r$ obtain invariant zeros of the triple (A, f_i, C), denoted as $z_j^{(i)}$, and corresponding directions $v_j^{(i)}$, for $j = 1, \cdots, r_i$, where r_i is the number of invariant zeros of the triple (A, f_i, C), such that

$$\begin{bmatrix} z_j^{(i)} I - A & v_{j-1}^{(i)} \\ C & 0 \end{bmatrix} \begin{bmatrix} v_j^{(i)} \\ -1 \end{bmatrix} = 0 \tag{6.2a}$$

   where $v_0^{(i)}$ denotes f_i.
4. Obtain matrix $\tilde{\tilde{A}}^{(i)}$ and vector $\tilde{\tilde{B}}^{(i)}$ whose elements are given by

$$\tilde{\tilde{A}}_{j,k}^{(i)} = (-1)^{k-1} \prod_{l=k}^{r_i} (z_l^{(i)} - \lambda_j^{(i)}) \tag{6.2b}$$

$$\tilde{\tilde{B}}_j^{(i)} = \lambda_j \prod_{l=1}^{r_i} \left(z_l^{(i)} - \lambda_j^{(i)} \right) \tag{6.2c}$$

5. For $i = 1, \cdots, r$ calculate coefficients $x_{11}^{(i)}, \cdots, x_{r_i+1,1}^{(i)}$ which fulfil the condition

$$\begin{bmatrix} x_{11}^{(i)} & x_{12}^{(i)} & \cdots & x_{r_i+1,1}^{(i)} \end{bmatrix}^T = (\tilde{\tilde{A}}^{(i)})^{-1} \tilde{\tilde{B}}^{(i)} \tag{6.2d}$$

6. Obtain matrix A_e^* as:

$$A_e^* = \begin{bmatrix} A_e^{*(1)} & A_e^{*(2)} & \cdots & A_e^{*(r)} \end{bmatrix} \tag{6.2e}$$

where

$$A_e^{*(i)} = (A - x_{11}^{(i)} I) f_i - x_{21}^{(i)} v_1^{(i)} - x_{31}^{(i)} v_2^{(i)} - \cdots - x_{r_i+1,1}^{(i)} v_{r_i}^{(i)} \tag{6.2f}$$

7. Obtain:

$$A' = A - A_e^* (CE)\ C \tag{6.2g}$$
$$C' = \left(I - CE(CE)\ \right) C \tag{6.2h}$$

8. Using any eigenstructure assignment methods allocate remaining eigenvalues of $A_{c_1} = (A' - K_1' C')$

9. Calculate K_1 as

$$K_1 = A_e^* (CE)\ + K_1' \left(I - CE(CE)\ \right) \tag{6.2i}$$

10. Repeat steps 2 to 9 for the gain matrix K_2 and obtain $A_{c_1} = A - K_2 C$

11. Choose τ and calculate J_1 and J_2 using

$$J_1 = -A_{c_2}^{\tau} \left[A_{c_1}^{\tau} - A_{c_2}^{\tau}\right]^{-1} \tag{6.2j}$$
$$J_2 = I - J_1 \tag{6.2k}$$

12. Calculate W_u and W_y via

$$\begin{aligned} W_u = -\Big[\ & C(J_1 A_{c_1}^{\tau-1}(B - K_1 D) + J_2 A_{c_2}^{\tau-1}(B - K_2 D)) \quad \cdots \\ & C(J_1 A_{c_1}^{2}(B - K_1 D) + J_2 A_{c_2}^{2}(B - K_2 D)) \\ & C(J_1 A_{c_1}(B - K_1 D) + J_2 A_{c_2}(B - K_2 D))B \quad CB \quad -D\ \Big] \end{aligned} \tag{6.2l}$$

$$\begin{aligned} W_y = \Big[\ & C(J_1 A_{c_1}^{\tau-1} K_1 + J_2 A_{c_2}^{\tau-1} K_2) \quad \cdots \quad C(J_1 A_{c_1}^{2} K_1 + J_2 A_{c_2}^{2} K_2) \\ & C(J_1 A_{c_1}^{1} K_1 + J_2 A_{c_2}^{1} K_2) \quad C(J_1 K_1 + J_2 K_2) \quad -I\ \Big] \end{aligned} \tag{6.2m}$$

13. Calculate residual via

$$r(t) = W_y Y(t) - W_u U(t) \tag{6.2n}$$

Remark 6.1. The residual $r_i(t)$ obtained using Algorithm 6.1 lies in the direction Cf_i.

Demonstration. The residual calculated using Algorithm (6.1) is, cf. (5.139):

$$\begin{aligned} r(t) &= C \begin{bmatrix} J_1 & J_2 \end{bmatrix} \begin{bmatrix} \sum_{j=0}^{\tau-1} A_{c_1}^j F\mu(t-j) \\ \sum_{j=0}^{\tau-1} A_{c_2}^j F\mu(t-j) \end{bmatrix} \\ &= CJ_1 \sum_{j=0}^{\tau-1} A_{c_1}^j F\mu(t-j) + QCJ_2 \sum_{j=0}^{\tau-1} A_{c_2}^j F\mu(t-j) \end{aligned} \tag{6.3}$$

Consider a matrix $\bar{f}_i = \begin{bmatrix} f_i & v_1^{(i)} & \cdots & v_{r_i}^{(i)} \end{bmatrix}$. It has been shown in Subsection 5.3.2, that $\mathrm{Im}\{\bar{f}_i\}$ is an invariant subspace of A_{c_1}, A_{c_2}, J_1, and J_2. Hence, it holds that, cf. Subsection 5.3.2:

$$CJ_k A_{c_k}^j \mathrm{Im}\{\bar{f}_i\} \subseteq C\mathrm{Im}\{\bar{f}_i\} \text{ for } k = 1,2; j = 0,\cdots,\tau-1, i = 1,\cdots,r \tag{6.4}$$

Recall that $Cv_j^{(i)} = 0$ for $j = 1,\cdots,r_l, i = 1,\cdots,r$. Consequently:

$$\mathrm{Im}\{C\bar{f}_i\} = \mathrm{Im}\{Cf_i\} \text{ for } i = 1,\cdots,r \tag{6.5}$$

Thus, a design of the fault isolation filter using Algorithm 6.1 ensures that the residual driven by the fault signal $\mu_i(t)$ lies in the direction Cf_i. ∎

6.4 Fault identification

6.4.1 Change of coordinates

The presence of the i^{th} fault yields residual direction Cf_i. Thus, it is useful to represent the residual vector $r(t)$ as a linear combination of residual directions $Cf_i, i = 1,2,\cdots,r$, i.e.

$$r(t) = \gamma_1 Cf_1 + \gamma_2 Cf_2 + \cdots + \gamma_r Cf_r \tag{6.6}$$

where $\gamma_1, \gamma_2, \cdots, \gamma_r$ are scalar coefficients. The parameter γ_i deviating from zero indicates a presence of the fault $\mu_i(t)$ and its value depends on the magnitude of the fault. Consequently, a change of coordinates is defined as:

$$T = \begin{bmatrix} T_1 & T_2 \end{bmatrix} \tag{6.7}$$

where $T_1 = \begin{bmatrix} Cf_1 & Cf_2 & \cdots & Cf_r \end{bmatrix}$ and $\mathrm{Im}\{T_2\}$ is an orthogonal completion of $\mathrm{Im}\{T_1\}$. Applying the above similarity transformation to $r(t)$ a variable $\mathring{r}(t)$ is obtained:

$$\mathring{r}(t) = T^{-1} r(t) \tag{6.8}$$

Remark 6.2. An occurrence of $\mu_i(t)$ causes $\mathring{r}_i(t)$ deviate from zero, whilst the remaining components of $\mathring{r}(t)$ are zero.

Demonstration. The term $\mathring{r}(t)$ is given by:

$$\mathring{r}(t) = \begin{bmatrix} Cf_1 & Cf_2 & \cdots & Cf_r & T2 \end{bmatrix}^{-1} (\gamma_1 Cf_1 + \gamma_2 Cf_2 + \cdots + \gamma_r Cf_r) \tag{6.9}$$

which can be reformulated as:

$$\begin{bmatrix} Cf_1 & Cf_2 & \cdots & Cf_r & T2 \end{bmatrix} \mathring{r}(t) = \gamma_1 Cf_1 + \gamma_2 Cf_2 + \cdots + \gamma_r Cf_r \tag{6.10}$$

which it true if and only if:

$$\mathring{r}(t) = \begin{bmatrix} \gamma_1 & \gamma_2 & \cdots & \gamma_r & 0 & \cdots & 0 \end{bmatrix}^T \tag{6.11}$$

Thus $\mathring{r}_i(t)$ deviates from zero only when the fault $\mu_i(t)$ occurs. ∎

6.4.2 Steady state gain calculation

From (6.3) it follows that the directional residual as a function of a fault signal can be represented by:

$$r(t) = W_\mu M(t) \tag{6.12}$$

where:

$$W_\mu = \begin{bmatrix} C(L_1 A_{c_1}^{\tau-1} + L_2 A_{c_2}^{\tau-1})F & \cdots & C(L_1 A_{c_1}^2 + L_2 A_{c_2}^2)F \\ & & C(L_1 A_{c_1} + L_2 A_{c_2})F \quad QCF \quad 0 \end{bmatrix} \tag{6.13}$$

and:

$$M(t) = \begin{bmatrix} \mu^T(t-\tau) & \mu^T(t-\tau+1) & \cdots & \mu^T(t) \end{bmatrix}^T \tag{6.14}$$

It has been shown that the fault direction driven by $\mu_i(t)$ is Cf_i. Consequently, the directional residual, $r(t)$, can be formulated as:

$$r(t) = \sum_{j=0}^{\tau} \sum_{i=1}^{r} \alpha_j^{(i)} Cf_i \mu_i(t-j) \tag{6.15}$$

where $\alpha_j^{(i)}$ are scalar coefficients. Then, the term $\mathring{r}(t)$ can be reformulated as:

$$\mathring{r}(t) = T^{-1}W_\mu M(t) = \Omega M(t) \tag{6.16}$$

where $\Omega \in \mathbb{R}^{m\times k(\tau+1)}$ is given by $\Omega = T^{-1}W_\mu$.

Remark 6.3. The term Ω is in the form of:

$$\Omega = \begin{bmatrix} \alpha_\tau^{(1)} & 0 & \cdots & 0 & \alpha_{\tau-1}^{(1)} & 0 & \cdots & 0 & \cdots & \alpha_0^{(1)} & 0 & \cdots & 0 \\ 0 & \alpha_\tau^{(2)} & \cdots & 0 & 0 & \alpha_{\tau-1}^{(2)} & \cdots & 0 & \cdots & 0 & \alpha_0^{(2)} & \cdots & 0 \\ \vdots & \vdots & \ddots & \vdots & \vdots & \vdots & \ddots & \vdots & \ddots & \vdots & \vdots & \ddots & \vdots \\ 0 & 0 & \cdots & \alpha_\tau^{(k)} & 0 & 0 & \cdots & \alpha_{\tau-1}^{(k)} & \cdots & 0 & 0 & \cdots & \alpha_0^{(k)} \\ 0 & 0 & \cdots & 0 & 0 & 0 & \cdots & 0 & \cdots & 0 & 0 & \cdots & 0 \\ \vdots & \vdots & \ddots & \vdots & \vdots & \vdots & \ddots & \vdots & \ddots & \vdots & \vdots & \ddots & \vdots \\ 0 & 0 & \cdots & 0 & 0 & 0 & \cdots & 0 & \cdots & 0 & 0 & \cdots & 0 \end{bmatrix} \tag{6.17}$$

Demonstration. See Appendix C ∎

Note that $\mathring{r}_i(t)$ is the residual vector $r(t)$ represented by the basis T, and, consequently, $\mathring{r}_i(t)$ can be reformulated as, cf. (6.15):

$$\mathring{r}_i(t) = \alpha_0^{(i)}\mu_i(t) + \alpha_1^{(i)}\mu_i(t-1) + \cdots + \alpha_\tau^{(i)}\mu_i(t-\tau) \tag{6.18}$$

Therefore, the steady state gain of the response of $\mathring{r}_i(t)$ to the fault $\mu_i(t)$ is equal to $\sum_{j=0}^{\tau}\alpha_j^{(i)}$, which is the sum of elements of the i^{th} row of Ω. Consider a diagonal matrix:

$$\Xi = \operatorname{diag}\begin{bmatrix} \sum_{i=1}^{\tau}\alpha_i^{(1)} & \sum_{i=1}^{\tau}\alpha_i^{(2)} & \cdots & \sum_{i=1}^{\tau}\alpha_i^{(k)} & 1 & \cdots & 1 \end{bmatrix} \tag{6.19}$$

and the variable:

$$\hat{\mu}(t) = \Xi^{-1}\mathring{r}(t) \tag{6.20}$$

The first r elements of the vector $\hat{\mu}(t)$ are estimates of $\mu(t)$, whereas remaining $m-r$ elements of $\hat{\mu}(t)$ should be equal zero and may be treated as control variables (if they deviate from zero it indicates there is a fault or a disturbance that is not covered by the model). Consequently, the PE for fault isolation and identification is given by:

$$\hat{\mu}(t) = \mathring{W}_y Y(t) + \mathring{W}_u U(t) \tag{6.21}$$

where

$$\mathring{W}_u = \Xi^{-1}T^{-1}W_u \text{ and } \mathring{W}_y = \Xi^{-1}T^{-1}W_y \tag{6.22}$$

The algorithm for fault isolation and identification via diagonal PE is summarised below.

Algorithm 6.2 (Fault isolation and identification via diagonal PE).

1. Compute $r(t)$ using Algorithm 6.1
2. Obtain T using (6.7)
3. Obtain W_μ using (6.13) and obtain Ω as:

$$\Omega = T^{-1} W_\mu \tag{6.23a}$$

4. Compute Ξ using (6.19)
5. Calculate $\mathring{W}_u$ and $\mathring{W}_y$ as:

$$\mathring{W}_u = \Xi^{-1} T^{-1} W_u \tag{6.23b}$$
$$\mathring{W}_y = \Xi^{-1} T^{-1} W_y \tag{6.23c}$$

6. Compute reconstructed fault vector as:

$$\hat{\mu}(t) = \mathring{W}_y Y(t) + \mathring{W}_u U(t) \tag{6.23d}$$

6.5 Consideration of measurement noise

In practice there is noise present in the system. Consequently, the residual is rarely equal to zero, and a decision must me made, whereas the residual deviating from zero indicates presence of a fault or is a result of noise. A fault presence is sensed if a residual exceeds a certain threshold (Ding 2008). An appropriate choice of the threshold allows minimisation of the number of false alarms as well as missed fault occurrences. In this subsection a simple method for calculating thresholds is presented.

Consider the system (6.1) in the EIV framework:

$$\begin{aligned} x(t+1) &= Ax(t) + Bu_0(t) + F\mu(t) \\ y_0(t) &= Cx(t) + Du(t) \\ u(t) &= u_0(t) + \tilde{u}(t) \\ y(t) &= y_0(t) + \tilde{y}(t) \end{aligned} \tag{6.24}$$

where noise-free input and output, $u_0(t)$ and $y_0(t)$ are affected by white, Gaussian, zero-mean, mutually uncorrelated noise sequences $\tilde{u}(t)$ and $\tilde{y}(t)$, respectively. The terms $u(t)$ and $y(t)$ are measured values of the input and output. The term $\hat{\mu}(t)$ is

calculated as:

$$\hat{\mu}(t) = \mathring{W}_y Y(t) + \mathring{W}_u U(t) = \mathring{W}_y(Y_0(t) + \tilde{Y}(t)) + \mathring{W}_u(U_0(t) + \tilde{U}(t)) \tag{6.25}$$

which in a fault-free case is:

$$\hat{\mu} = \mathring{W}_y \tilde{Y}(t) + \mathring{W}_u \tilde{U}(t) \tag{6.26}$$

It should be noted that each column of $\hat{\mu}(t)$ is affected by the measurement noise in different level. Therefore, thresholds calculation should be based on the expected values of the variance each element of $\hat{\mu}(t)$ in the fault-free case. The covariance matrix of $\hat{\mu}(t)$, denoted as $\Sigma_{\hat{\mu}}$, in fault-free case is given by:

$$\Sigma_{\hat{\mu}} = \mathring{W}_y \Sigma_{\tilde{y}} \mathring{W}_y^T + \mathring{W}_u \Sigma_{\tilde{u}} \mathring{W}_u^T \tag{6.27}$$

where $\Sigma_{\tilde{y}} = \mathrm{E}\{\tilde{Y}(t)\tilde{Y}^T(t)\}$ and $\Sigma_{\tilde{u}} = \mathrm{E}\{\tilde{U}(t)\tilde{U}^T(t)\}$. In the EIV framework with no process noise, cf. (6.24), $\Sigma_{\tilde{y}}$ and $\Sigma_{\tilde{u}}$ are diagonal matrices. Based on the assumption that the measurement noise sequences are white, Gaussian, zero-mean, and mutually uncorrelated, the threshold which $\hat{\mu}_i(t)$ needs to violate for the fault to be noticed should be calculated as an appropriate multiplicity of the standard deviation of $\hat{\mu}_i(t)$ in a fault-free case, i.e. an appropriate multiplicity of the square root of the i^{th} diagonal element of $\Sigma_{\hat{\mu}}$.

6.6 Numerical example

Example 6.1. Design of diagonal PE for fault isolation and identification
It is assumed that a linear discrete-time time-invariant system is described by (6.24) where the system matrices are:

$$A = \begin{bmatrix} 0 & 1 & 0 & 0 & 0 \\ 0 & 0 & 1 & 0 & 0 \\ 0 & 0 & 0 & 1 & 0 \\ 0 & 0 & 0 & 0 & 1 \\ 0.1512 & -1.1274 & 3.325 & -4.85 & 3.5 \end{bmatrix} \quad B = \begin{bmatrix} 0 \\ 0 \\ 0 \\ 0 \\ 1 \end{bmatrix} \quad F = \begin{bmatrix} 1 & 1 & 0 \\ 1 & 0 & 0 \\ 0 & -1 & 0 \\ 0 & 2 & 1 \\ 0 & 0 & 2 \end{bmatrix}$$
$$C = \begin{bmatrix} 1 & -1 & 0 & 0 & 0 \\ 0 & 0 & 1 & 1 & 0 \\ 0 & 0 & 1 & 0 & 1 \\ 0 & 0 & 0 & 0 & 1 \end{bmatrix} \quad D = \begin{bmatrix} 0 \\ 0 \\ 0 \\ 0 \end{bmatrix} \tag{6.28}$$

The first output is affected by white, Gaussian, zero-mean noise with the variance equal to $\sigma^2_{y_1} = 0.01$, whilst the remaining three are subjected to white, Gaussian, zero-mean noise sequences with the variances of $\sigma^2_{y_2} = \sigma^2_{y_3} = \sigma^2_{y_4} = 0.0001$. Output measurement

noise sequences are mutually uncorrelated.

Note that $CF_1 = 0$ and:

$$f_1 = AF_1 = \begin{bmatrix} 1 & 0 & 0 & 0 & -0.9762 \end{bmatrix}^T \tag{6.29}$$

Therefore, $\delta_1 = 1$. Due to the fact that $CF_2 \neq 0$ and $CF_3 \neq 0$, $f_2 = F_2$ and $f_3 = F_3$. Consequently, residual directions are:

$$Cf_1 = \begin{bmatrix} 1 \\ 0 \\ -0.9762 \\ -0.9762 \end{bmatrix} \quad Cf_2 = \begin{bmatrix} 1 \\ 1 \\ -1 \\ 0 \end{bmatrix} \quad Cf_3 = \begin{bmatrix} 0 \\ 1 \\ 2 \\ 2 \end{bmatrix} \tag{6.30}$$

Note that $\text{rank}(\begin{bmatrix} Cf_1 & Cf_2 & Cf_3 \end{bmatrix}) = 3$, hence the possibility for a complete fault isolation exists.

Eigenvalues of $(A - K_1C)$ are chosen to be 0.22, 0.77, 0.66, 0.55, 0.44. Note that the triple (A, f_1, C) has an invariant zero at $z_1^{(1)} = 0$, whilst the state and input zero directions are, respectively, $v_1^{(1)} = F_1$ and $g_1^{(1)} = -1$. Eigenvalues of $(A - K_1C)$ corresponding to a linear combination of columns of $\bar{f}_1 = \begin{bmatrix} f_1 & F_1 \end{bmatrix}$ are 0.22 and 0.44. As a result, the first column of the matrix $X^{(1)}$ is given by, cf. (6.2b), (6.2c), (6.2d):

$$X^{(1)} = \begin{bmatrix} 0.6600 \\ -0.0968 \end{bmatrix} \tag{6.31}$$

Hence, $A^{*(1)}$ is calculated as, cf. (6.2f):

$$A^{*(1)} = (A - 0.66I)f_1 + 0.0968v_1^{(1)} = \begin{bmatrix} -0.5632 & 0 & 0 & -0.9762 & -2.2157 \end{bmatrix}^T \tag{6.32}$$

whereas $A^{*(2)}$ and $A^{*(3)}$ are:

$$A^{*(2)} = (A - 0.55I)f_2 \quad A^{*(3)} = (A - 0.66I)f_2 \tag{6.33}$$

Subsequently, the matrix A^* is obtained as, cf. (6.2e):

$$A^* = \begin{bmatrix} -0.5632 & -0.5500 & 0 \\ 0 & -1 & 0 \\ 0 & 2.5500 & 1 \\ -0.9762 & -1.1000 & 1.34 \\ -2.7157 & -12.8738 & 0.83 \end{bmatrix} \tag{6.34}$$

The remaining eigenvalue of $(A' - K_1'C')$ is chosen to be 0.77. Subsequently, the gain

matrix K_1 is computed as:

$$K_1 = \begin{bmatrix} -0.4196 & -0.2943 & -0.1639 & 0.3110 \\ 0.2175 & -0.2472 & 0.9702 & -0.8466 \\ -0.3623 & 1.7423 & -1.1700 & 0.7988 \\ 0.0020 & -0.6641 & 0.4379 & 0.5642 \\ -1.0702 & -2.3477 & 9.4559 & -7.8671 \end{bmatrix} \tag{6.35}$$

The eigenvalues of $(A - K_2C)$ are selected to be 0.95, 0.85, 0.18, 0.33, 0.47 and, as a consequence, K_2 is calculated as:

$$K_2 = \begin{bmatrix} -0.9584 & -0.0699 & -0.5583 & 0.5932 \\ 1.0705 & -0.5388 & 1.5317 & -1.2623 \\ -0.3388 & 1.6940 & -1.1147 & 0.7677 \\ 0.1891 & -0.5675 & 0.5616 & 0.6321 \\ 1.1636 & -3.6841 & 10.3533 & -7.6162 \end{bmatrix} \tag{6.36}$$

The order of the parity space is chosen as $\tau = 8$ and matrices W_u and W_y are calculated using (6.2l) and (6.2m), respectively. Then T is obtained using (6.7):

$$T = \begin{bmatrix} 1 & 1 & 0 & 0.3072 \\ 0 & 1 & 1 & -0.6294 \\ -0.9762 & -1 & 2 & -0.3222 \\ -0.9762 & 0 & 2 & 0.6369 \end{bmatrix} \tag{6.37}$$

The matrix Ω is then computed as, cf. (6.23a):

$$\Omega = T^{-1}W_\mu = \begin{bmatrix} 0 & 0 & 0 & 2.3e-2 & 0 & 0 \\ 0 & 3.2e-2 & 0 & 0 & 1.3e-1 & 0 \\ 0 & 0 & 4.3e-3 & 0 & 0 & 3e-2 \\ 0 & 0 & 0 & 0 & 0 & 0 \end{bmatrix} \tag{6.38}$$

$$\begin{bmatrix} 1.8e-1 & 0 & 0 & 1 & 0 & 0 & 0 & 0 & 0 \\ 0 & 3.8e-1 & 0 & 0 & 1 & 0 & 0 & 0 & 0 \\ 0 & 0 & 1.8e-1 & 0 & 0 & 1 & 0 & 0 & 0 \\ 0 & 0 & 0 & 0 & 0 & 0 & 0 & 0 & 0 \end{bmatrix}$$

The first three diagonal elements of Ξ are equal to sum of appropriate rows of Ω. The

last diagonal element of Ξ is unity, see (6.19):

$$\Xi = \begin{bmatrix} 1.2004 & 0 & 0 & 0 \\ 0 & 1.5386 & 0 & 0 \\ 0 & 0 & 1.2118 & 0 \\ 0 & 0 & 0 & 1 \end{bmatrix} \tag{6.39}$$

Consequently, $\mathring{W}_u$ and $\mathring{W}_y$ are calculated using, respectively, (6.23b) and (6.23c) and the fault estimate is obtained using (6.23d).

Measurement noise

Recall that output measurements are affected by white, zero-mean, Gaussian, and mutually uncorrelated noise sequences with variances of $\sigma^2_{y_1} = 0.01$ and $\sigma^2_{y_2} = \sigma^2_{y_3} = \sigma^2_{y_4} = 0.0001$, whilst $\tau = 8$. Hence, the output measurement covariance matrix is a 36^{th} order ($(\tau+1)m = 9 \times 4 = 36$) diagonal matrix, whose diagonal is the vector $\begin{bmatrix} \sigma^2_{y_1} & \sigma^2_{y_2} & \sigma^2_{y_3} & \sigma^2_{y_4} \end{bmatrix}$ repeated $\tau + 1 = 9$ times. Consequently, $\Sigma_{\hat{\mu}}$ is calculated as, cf. (6.27):

$$\Sigma_{\hat{\mu}} = \begin{bmatrix} 0.0190 & -0.0119 & 0.0129 & 0.0048 \\ -0.0119 & 0.0190 & -0.0118 & -0.0034 \\ 0.0129 & -0.0118 & 0.0118 & 0.0045 \\ 0.0048 & -0.0034 & 0.0045 & 0.0038 \end{bmatrix} \tag{6.40}$$

Thus, the variances of the consecutive elements of $\hat{\mu}(t)$ in a fault-free case are, respectively, 0.0190, 0.0190, 0.0118, and 0.0038. The threshold of each element of $\hat{\mu}(t)$ is selected as its standard deviation in a fault-free case multiplied by 3.1 (which results in the confidence bound of 0.999, assuming a Gaussian distribution of the measurement noise) and are given by, respectively, 0.4272, 0.3557, 0.3363, and 0.1915. Results of the simulation are presented in Fig. 6.2. The filter identifies abrupt faults $\mu_1(t)$ and $\mu_2(t)$, as well as an incipient fault $\mu_3(t)$. After the 100^{th} sample an unmodelled fault occurs. This is indicated by $\hat{\mu}_4(t)$ violating the threshold.

6.7 Conclusions

The fault isolation and identification filter devised in this chapter utilises a diagonal residual set. Therefore, multiple faults can be isolated and identified. Furthermore, if the number of linearly independent outputs exceeds the number of modelled faults, a new variable has been introduced, which indicates occurrence of an unmodelled fault. This provides a signal to stop the process and investigate the source of a possibly dangerous fault. Also a straightforward method to calculate residual thresholds, whose violation indicates a fault, has been proposed for the EIV framework. A simulation study has demonstrated promising results for both diagnosis of abrupt and incipient

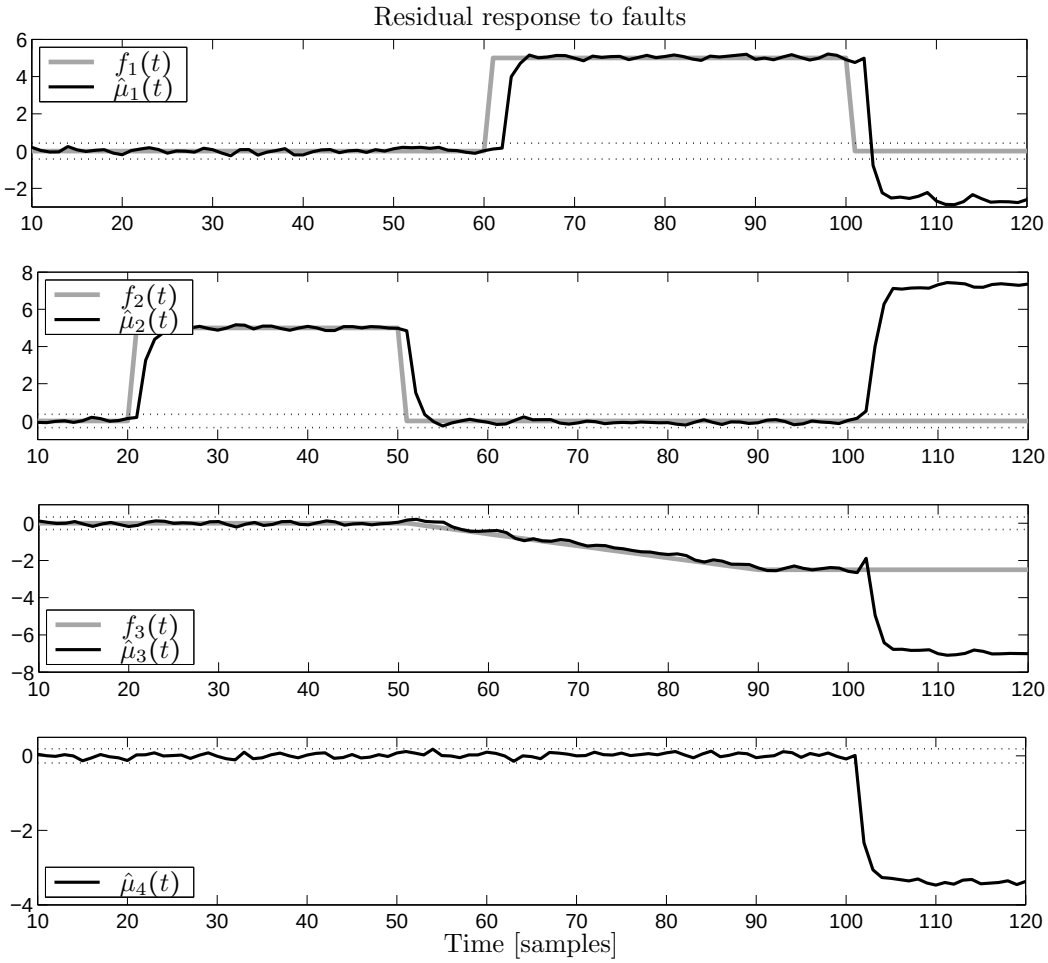

Figure 6.2: Fault identification using diagonal PE. At the 100^{th} time sample unmodelled fault occurs causing $\hat{\mu}_4(t)$ deviate from zero.

faults.

Further work aims to extend the scheme to fault isolation and identification of multidimensional faults.

Chapter 7

Potential applications

Nomenclature

A_p	piston area
C	compensation variable
d_1, d_2, d_2	damping coefficients
$F_c(t)$	Coulomb friction
$F_{fric}(t)$	total friction force
$F_h(t)$	hydraulic force
$F_r(t)$	roll force
$F_s(t)$	Stribeck friction (stiction)
$F_v(t)$	viscous friction
G_1, G_2	controller gains
$G_v(z)$	transfer function
k_1	spring constant
k_2	spring constant
k_3	steel strip spring constant
K_c	hydraulic oil compressibility coefficient
K_p	proportional gain of hydraulic piston controller
l	stroke length of the piston
$h(t)$	exit gauge
$\hat{h}(t)$	estimate of exit gauge
$h_{ref}(t)$	exit gauge reference signal
$H(t)$	input gauge
m_1	mass of hydraulic piston
m_2	mass of backup roll
m_3	mass of work roll
M	mill modulus (spring constant)
$\hat{M}$	estimated mill modulus
$p(t)$	hydraulic pressure
$q_f(t)$	fluid flow to hydraulic capsule
$v(t)$	unknown input
$\hat{v}(t)$	unknown input estimate
v_c, v_1, v_2	auxiliary coefficients
$y(t)$	system output
$z(t)$	position of the hydraulic piston

$z_{ref}(t)$ ..... hydraulic piston position reference signal
μ_c ..... Coulomb friction level
μ_s ..... Stribeck friction coefficient
μ_v ..... viscous friction coefficient

Preliminary reading: Sections 3.2, 3.3, and 3.5

7.1 Introduction

Algorithms developed in Chapter 3 are evaluated using two practical examples. In Section 7.2 the PE-UIO (see Algorithm 3.1) is used to improve control performance of a steel rolling mill. Furthermore, the two stage PE-UIO (Algorithm 3.4) is used to estimate the concentration of river pollutant. Conclusions and a critical appraisal of practical use of the developed algorithms are presented in Section 7.4.

7.2 Steel rolling mill

In this Section Algorithm 3.1 is applied to a model of a single stand hot strip finishing rolling mill. Rolling is a process of shaping a metal piece by a reduction of its thickness, i.e. gauge. The metal is compressed by being progressed between rollers rotating with the same velocity but in the opposite direction. The final stage of the rolling process is the finishing mill, where the main goal is to maintain the exit gauge, i.e. the thickness of the steel strip emerging from the mill, within increasingly tight specifications. The finishing mill consists of several stands, which consecutively reduce the thickness of the steel strip. Each of the finishing mill stands is controlled separately.

For the purpose of control, the force acting on the strip (further denoted as 'roll force') is required to be inferred via measurement of a hydraulic actuator force. The roll force is obtained via measurements of the fluid pressure in a hydraulic actuator mounted on the top of the stand. However, a problem, which occasionally arises is an oscillation of the exit gauge. It is believed that this is due to limit cycles, which result from the nonlinearities in the plant, caused mainly by friction. The contacting surfaces of the mill are many and the friction forces acting on the elements can be large hence their impact on the plant behaviour is significant. The friction force is a strongly non-linear phenomenon, difficult to model and dependent on many operating environment conditions, such as temperature, properties of lubricant, wear of surfaces, etc., see, for example, (Papadopoulos & Chasparis 2002, Putra 2004). The non-stationarity of these conditions cause the friction to be difficult to parametrise.

Algorithm 3.1 is applied to the plant in order to estimate the value of the force measurement error, which is assumed to be mainly caused by the friction and constitutes on the unknown input. Based on the estimated value of the error, a correction is made to the measured value of the force, which is then fed back to the plant.

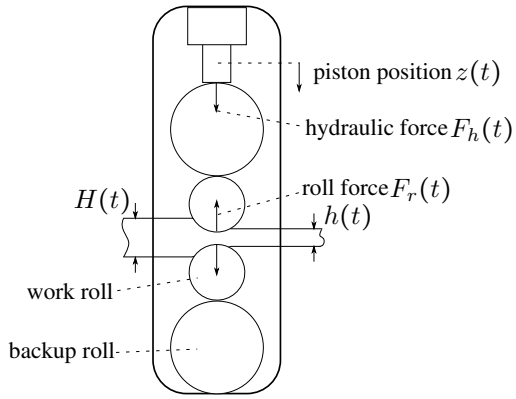

Figure 7.1: Schematic illustration of controlled plant

A PE-based friction compensator applied to a deterministic model of a rolling mill has been previously investigated by the author in (Sumisławska, Burnham, Hearns, Larkowski & Reeve 2010). Furthermore, in (Sumisławska, Larkowski & Burnham 2010*a*) an additive measurement noise on the piston position and hydraulic force has been considered.

7.2.1 Description of the plant

A white-box model of the plant has been originally developed in (Sumisławska 2009). Furthermore, it has been reported in (Sumisławska, Reeve, Burnham, Pozniak-Koszałka & Hearns 2009) and (Sumisławska, Burnham, Hearns, Larkowski & Reeve 2010). A schematic illustration of the plant is presented in Fig. 7.1. The steel strip remains constantly in a contact with a pair of working rolls, which are supported by the backup rolls. The entry gauge and the exit gauge of the strip are denoted as $H(t)$ and $h(t)$, respectively. The hydraulic actuator mounted at the top of the stack changes the position of the backup, hence the work rolls, and ultimately controls the exit gauge of the strip (Yildiz, Forbes, Huang, Zhang, Wang, Vaculik & Dudzic 2009).

Control scheme

Harsh temperature conditions close to the rolling mill stand render direct measurement of the exit gauge impossible (Yildiz et al. 2009), hence a need arises to estimate the exit gauge from the measured value of the roll force and the mill modulus, i.e. mill sensitivity to force, see (Yildiz et al. 2009). Due to the fact that the roll force is inaccessible for measurements, the force in the hydraulic actuator capsule is measured. Therefore the exit gauge is estimated via:

$$\hat{h}(t) = z(t) + \frac{C}{\hat{M}} F_h(t) \tag{7.1}$$

where $\hat{h}(t)$ denotes the estimated exit gauge, $\hat{M}$ is the estimated value of the mill modulus M (i.e. mill sensitivity to force), $z(t)$ denotes the hydraulic piston position and $F_h(t)$ corresponds to the value of the force measured in the hydraulic actuator capsule, noting that $F_h(t) \approx F_r(t)$, where $F_r(t)$ denotes the roll force. In fact it is the difference between the measured $F_h(t)$ and the actual $F_r(t)$ which constitutes the unknown input. The actual exit gauge, denoted $h(t)$, is is given by:

$$h(t) = z(t) + \frac{C}{M} F_r(t) \tag{7.2}$$

In order to improve the robustness of the control loop a compensation variable $C < 1$ is introduced.

The control scheme of the rolling mill is presented in Fig. 7.2. The controller gains G_1 and G_2 are given by:

$$G_1 = 1 + (1 - C)\frac{k_3}{\hat{M}}, \qquad G_2 = \frac{\hat{M} + k_3}{\hat{M} + k_3 + Ck_3} \tag{7.3}$$

where k_3 denotes the steel strip sensitivity to force (strip modulus). The term K_p denotes the proportional gain of the hydraulic piston position controller and defines a relation between the piston position error and the fluid flow, denoted $q_f(t)$, to the hydraulic actuator capsule.

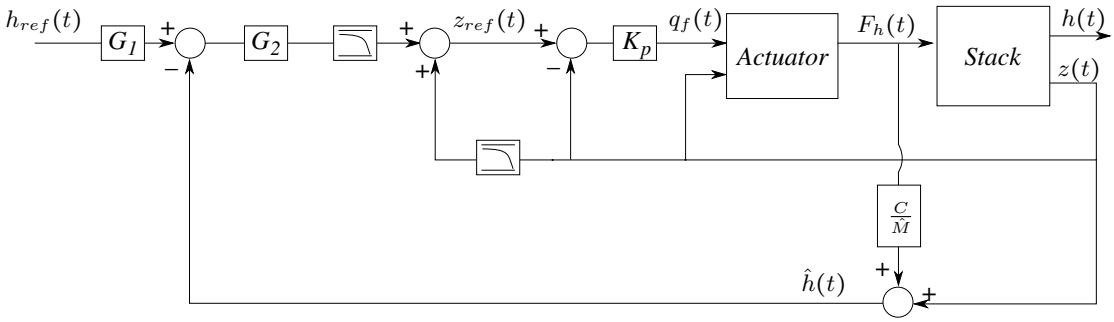

Figure 7.2: Control loop, $h_{ref}(t)$ – exit gauge reference signal, $z_{ref}(t)$ – piston position reference signal, $F_h(t)$ – hydraulic force, $q_f(t)$ – flow of hydraulic fluid

7.2.2 Plant model

Stack model

The stack of rolls (i.e. backup and work rolls with a steel strip between them, further referred to as the stack) is modelled by making use of a classical mass-spring-damper model representation, see Fig. 7.3. Due to the symmetrical construction of the stack, only the upper backup and work rolls are taken into consideration. The values of the model parameters are given in Table 7.1. In the further analysis the damper denoted

d_1 is replaced by a friction model, which introduces a nonlinear dependency between the piston velocity and the friction force.

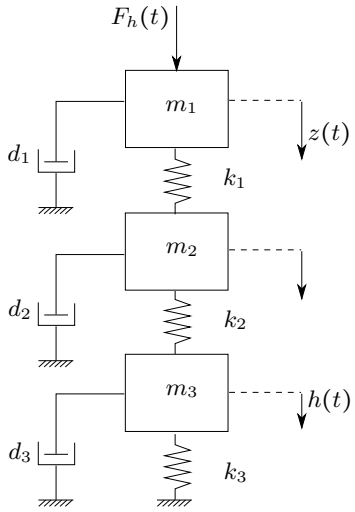

Figure 7.3: Mass-spring-damper representation of the stack, m_1 - hydraulic piston mass, m_2 - backup roll mass, m_3 - work roll mass, k_1 - spring coefficient between piston and backup roll, k_2 - spring coefficient between backup and work roll, k_3 - spring coefficient of the strip

Parameter	Value	Unit
m_1	$1 \cdot 10^2$	kg
m_2	$5 \cdot 10^4$	kg
m_3	$6 \cdot 10^3$	kg
k_1	$1 \cdot 10^{10}$	$\frac{N}{m}$
k_2	$1 \cdot 10^{10}$	$\frac{N}{m}$
k_3	$3 \cdot 10^9$	$\frac{N}{m}$
d_1	$1 \cdot 10^7$	$\frac{kg}{s}$
d_2	$5 \cdot 10^6$	$\frac{kg}{s}$
d_3	$5 \cdot 10^6$	$\frac{kg}{s}$
M	$5 \cdot 10^9$	$\frac{N}{m}$

Table 7.1: Parameters of rolling mill model

Friction model

The friction is modelled as a sum of three components: Coulomb friction, viscous friction and Stribeck friction. The latter is also named stiction (Putra 2004):

$$F_{fric}(t) = F_c(t) + F_v(t) + F_s(t) \tag{7.4}$$

where the term $F_{fric}(t)$ denotes the total frictional force, whilst $F_c(t)$, $F_v(t)$ and $F_s(t)$ refer to the Coulomb, viscous and Stribeck friction, respectively. The Coulomb friction is modelled as:

$$F_c(t) = -\mu_c \text{sign}(\dot{z}(t))(1 - e^{|\frac{\dot{z}(t)}{v_c}|}) \tag{7.5}$$

where the term μ_c denotes the Coulomb friction level, whilst the exponential term is introduced in order to avoid a zero-crossing discontinuity. The element related to the viscous friction is modelled as a linear function of the hydraulic piston velocity, denoted $\dot{z}(t)$:

$$F_v(t) = -\mu_v \dot{z}(t) \tag{7.6}$$

where the term μ_v denotes the viscous damping of the frictional force. The Stribeck friction (stiction) model is given by:

$$F_s(t) = -\mu_s \text{sign}(\dot{z}(t))(1 - e^{|\frac{\dot{z}(t)}{v_1}|})e^{|\frac{\dot{z}(t)}{v_2}|} \tag{7.7}$$

where the term μ_s determines the magnitude of the static friction, whilst v_1 and v_2 are utilised to shape the stiction model.

Hydraulic servo system model

Dependency between the fluid flow, denoted $q_f(t)$, into the capsule and the pressure denoted p(t) acting on the piston area denoted A_p is represented by the following linear relation, see e.g. (Jelali & Kroll 2003):

$$p(t) = K_c \frac{\int q_f(t)dt - A_p l}{A_p l} \tag{7.8}$$

where l denotes the stroke length of the piston, and the term K_c corresponds to the hydraulic oil compressibility coefficient. Therefore, the force denoted $F_h(t)$ acting on the hydraulic piston is given by:

$$F_h(t) = A_p p(t) \tag{7.9}$$

The values of the hydraulic actuator model parameters are given in Table 7.2.

Parameter	Value	Unit
A_p	0.331	m^2
l	0.1	m
K_p	7.0	$\frac{N}{m}$
K_c	$3.32 \cdot 10^9$	Pa

Table 7.2: Parameters of hydraulic actuator model

7.2.3 Simulation results

To simulate the plant the full nonlinear model is used, however to generate the PE-UIO a linear model is required. The nonlinear model of the system has been linearised by replacing the damping coefficient d_1 (i.e. the ratio of the friction force to the piston velocity) by its nominal value equal to $10^7 \frac{kg}{s}$. The white-box model described in Subsection 7.2.2 is discretised using a sampling interval of 10 ms, which corresponds to the sampling interval of the controller. The minimal state-space representation of the model is a one-input two-output 7^{th} order system, which is conveniently obtained using the MATLAB *linmod* function.

The resulting discretised form of the linearised closed-loop system has then been used for friction force estimator design. The reference signal is considered to be the input to the system. The two measured outputs of the system are the roll force (i.e. the force acting on the strip) and the piston position, given by, respectively, the first and the second elements of the output vector $y(t)$, see (7.10). It is convenient to scale the roll force by $\frac{C}{\hat{M}}$ to ensure numerical scalability.

$$y(t) = \begin{bmatrix} \frac{C}{\hat{M}} F_r(t) & z(t) \end{bmatrix}^T \tag{7.10}$$

Recall that due to the fact that the roll force $F_r(t)$ is inaccessible, the hydraulic force $F_h(t)$ is measured. Subsequently, the force measurement is affected by the friction force and the parasitic dynamics of the stack. Due to the fact that the bandwidth of the parasitic dynamics of the stack exceeds the sampling frequency, it can be assumed that the frictional force has the most significant contribution to the roll force measurement error. Therefore, the difference between the roll force $F_r(t)$ and the force measured in the hydraulic capsule $F_h(t)$ is considered to be the unknown input to the system, further referred to as $v(t)$, where $v(t) = \frac{C}{\hat{M}}(F_r(t) - F_h(t))$. (The factor $\frac{C}{\hat{M}}$ is used to ensure to ensure numerical scalability.) Hence, the matrices G and H of the system (3.1) are:

$$G = 0, \qquad H = \begin{bmatrix} 1 & 0 \end{bmatrix}^T \tag{7.11}$$

Subsequently, the exit gauge change is estimated via:

$$\hat{h}(t) = z(t) + \frac{C}{\hat{M}} F_h(t) - \hat{v}(t) \tag{7.12}$$

where $\hat{v}(t)$ is the correction term (i.e. the estimated force the measurement error $v(t)$, corresponding to the unknown input obtained from the PE-UIO).

Engineering knowledge and past experience of technicians with the plant indicate that it is reasonable to assume that the piston position and hydraulic force measurements are affected by white, zero-mean, Gaussian, mutually uncorrelated noise sequences, whose standard deviations are, respectively, 0.1μm and 1000N. The PE-UIO algorithm with $s = 4$ samples is used to obtain $\hat{v}(t)$.

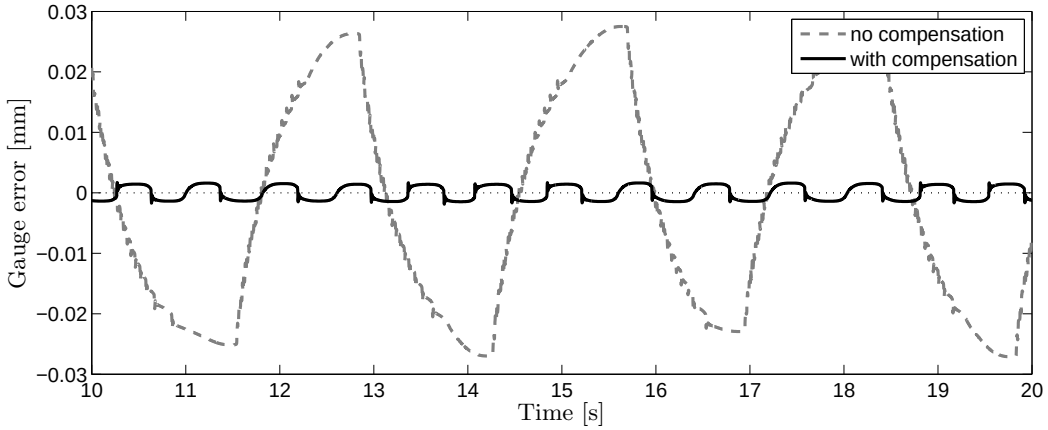

Figure 7.4: Friction compensation effect on the exit gauge error

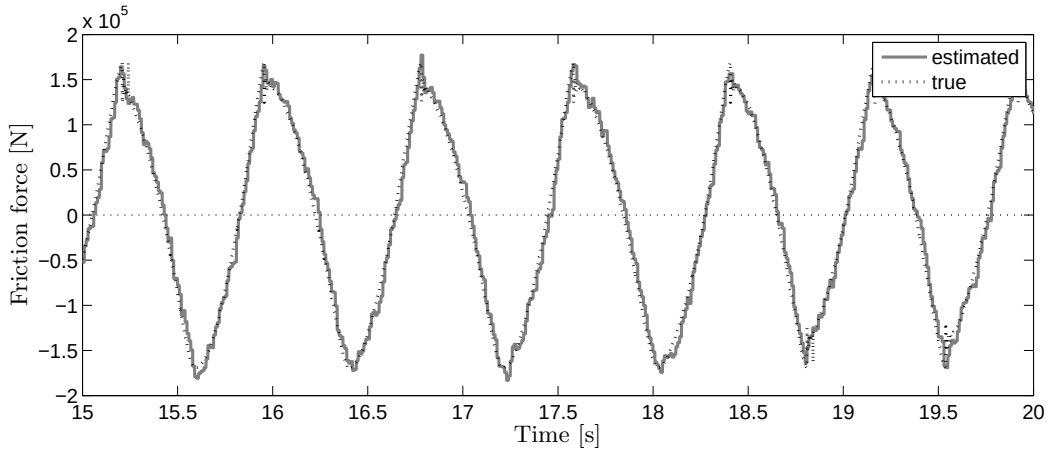

Figure 7.5: Friction force estimation

Fig. 7.4 presents the simulated results for the cases of no compensation and with the unknown input compensation applied. The grey dashed line corresponds to a simulated reconstruction of a typical limit cycle condition found in practice. The black solid line corresponds to the compensated case and clearly indicates that the limit cycle amplitude is significantly reduced, implying potential for improved product quality. Fig. 7.5 shows the actual unknown input and the estimated unknown input corresponding to the simulated condition in Fig. 7.4. The PE-UIO accurately estimates the friction force affecting the exit gauge and a subsequent feedback compensation that utilises the estimated unknown input results in a significant improvement in control.

7.3 Hydrological application

The second example is based on the data collected during a potassium bromide (KBr) tracer experiment carried out in a wetland area by Martinez & Wise (2003). A

schematic illustration of the experiment is depicted in Fig. 7.6. A tracer has been poured into the river at the point (1). Two tracer concentration sensors have been placed downstream, at points (2) and (3), whose readings are denoted, respectively, as $v(t)$ and $y(t)$. A linear model of the relation between $v(t)$ and $y(t)$, where $v(t)$ is the input to the system, whilst $y(t)$ is the output, has been developed in (Young & Sumisławska 2012). The input $v(t)$, further referred to as upstream tracer concentra-

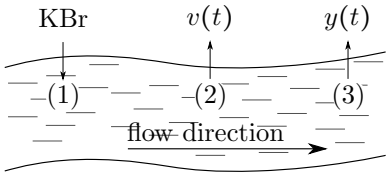

Figure 7.6: Tracer experiment

tion, and the output $y(t)$, the tracer concentration measured downstream, are plotted as the grey line and black line, respectively, in Fig. 7.7. The aim of this simulation is to use the two stage PE-UIO (Algorithm 3.4) scheme to estimate the input $v(t)$ based on output measurements and the knowledge of the system model. The system can be

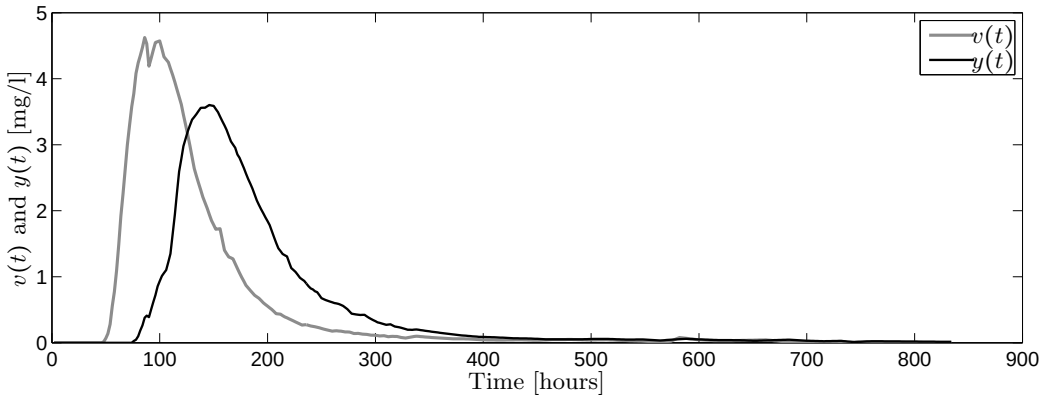

Figure 7.7: Input and output signals in tracer experiment

approximated by a linear second order model, with time constants of 17.4 and 83.7 hours, i.e. a stiff system. The discrete time model of the two-hourly sampled system is given by (Young & Sumisławska 2012):

$$G_v(z) = \frac{0.017591(z + 4.302)(z - 0.9735)}{(z - 0.9764)(z - 0.8916)} \tag{7.13}$$

Note that the same model has been used in Example 3.7 to obtain the unknown input of the simulated system (in contrast to this example, where real input and output measurements are used). The model is nonminimum-phase. Although the standard PE-UIO can cope with the zero at -4.302, the zero at 0.9735 requires the two stage

PE-UIO to be used. For the design of the unknown input reconstruction it has been assumed that the measurements are affected by white, zero-mean, Gaussian, mutually uncorrelated measurement noise. The parity space order has been set to 15 samples, which leads to an estimation time lag of 7 samples. The result of an unknown input estimation using the two stage PE-UIO is compared with the input reconstructed using the INPEST, see Fig. 7.8. The parameters of the INPEST method are $\mathring{\tau} = 7$ and $\mathring{q}_e = 0.8$ obtained for $\lambda = 0.001$, see (Young & Sumisławska 2012). It is noted that both

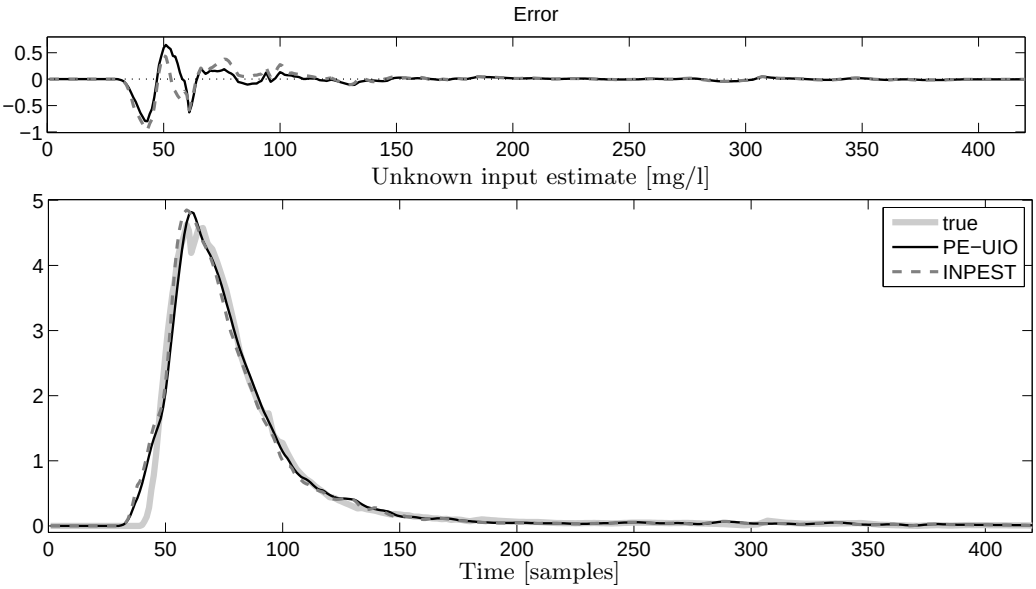

Figure 7.8: Result of unknown input estimation

methods give similar results. Both methods detect a rise of $v(t)$ in approximately the 33^{th} sample, whereas the measured input starts rising at approximately the 42^{th} sample. Furthermore, after the 200^{th} sample the estimation errors of the PE-UIO and the INPEST are virtually the same. It is believed that the input reconstruction discrepancies are caused mainly by the modelling inaccuracy, presumably caused by system nonlinearities. This hypothesis is supported by Fig. 7.9, which compares the measured output with the model output. The simulated output starts rising approximately 10 samples after the rise of the measured output. Furthermore, the observed characteristic 'bumps' of the measured output between 100 and 150 samples result in the input reconstruction error pattern visible in the upper subfigure of Fig. 7.8.

7.4 Critical appraisal of practical application of developed methods

A simulation study of a single finishing stand of a steel rolling mill has demonstrated promising results. The force measurement error has been estimated quite accurately,

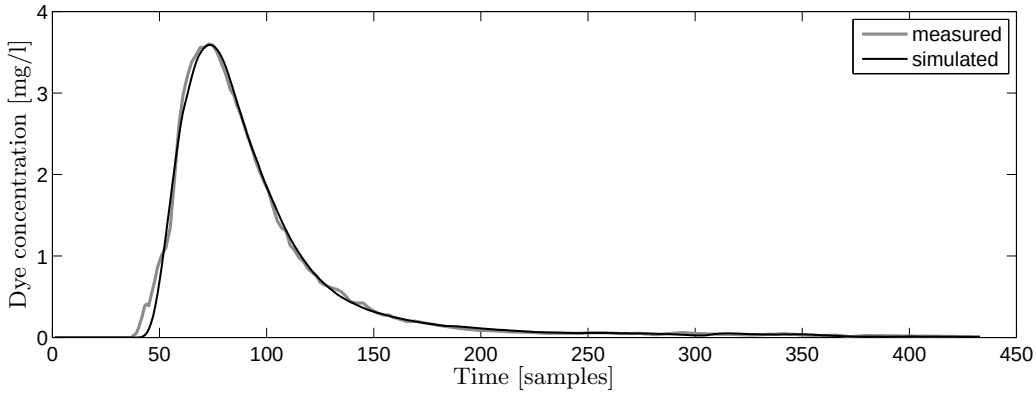

Figure 7.9: Model output vs. measured output

and the compensation significantly reduced the amplitude of limit cycles. The high frequency and low amplitude oscillations, which may be observed after enhancement of the control, are probably the result of unknown input estimation delay. In the industrial plant, however, unmeasured variations of the input gauge H occur, which should be treated as a disturbance. Thus, before application to an actual plant, the possibility of disturbance decoupling in the PE-UIO needs to be explored.

The two stage PE-UIO has estimated the tracer concentration in the river accurately. Further improvement could possibly be achieved, if, instead of the assumption of a white measurement noise, a coloured process noise model, which can explain discrepancy between modelled and simulated output (model mismatch), is assumed.

Chapter 8

Conclusions & further work

8.1 Conclusions

This thesis presents novel developments in the fields of unknown input reconstruction and fault detection, isolation and identification. The developed algorithms are applicable to time-invariant, discrete-time systems. Most of the research is devoted to linear systems, except for the unknown input reconstruction method presented in Chapter 4, which has been designed for a class of nonlinear systems, namely, Hammerstein-Wiener systems. Two potential applications for the algorithms developed in Chapter 3 have been proposed and promising results demonstrated via simulation studies.

This section is divided into three logical parts. Subsection 8.1.1 summarises the development of unknown input reconstruction schemes. In Subsection 8.1.2 fault detection and diagnosis algorithms are concluded. The main contributions of this thesis are summarised in Subsection 8.1.3.

8.1.1 Unknown input reconstruction

In Chapter 3 a novel scheme combining PE and the Lagrange multiplier optimisation method for unknown input reconstruction of MIMO stochastic systems has been devised. Due to that fact that the PE-UIO utilises parity equations, i.e. both input and output signals are filtered in an analogous manner, the method is suitable for systems in the EIV framework. It is assumed that the system input is affected by white, Gaussian, zero-mean measurement noise, whilst the output is subjected to coloured noise, which may represent a combination of measurement and process noise sequences. In particular, the methods can be applied to systems with well known noise models, such as ARX, ARMAX or OE. The PE-UIO requires the knowledge of the system model and, if the input is subjected to measurement noise (EIV framework), at least the ratio between the variances of the input and output noise sequences. Otherwise, if the input can be measured directly (i.e. there is no noise affecting the input), the knowledge of the noise variance is not required to be known explicitly for the design of the input

reconstruction filter (it is, however, required to know the noise model). In the case of OE systems the design procedure can be simplified, which has also been demonstrated. The only tuning parameter for the PE-UIO is the parity space order. By increasing it, the bandwidth of the filter is reduced, and, consequently, noise filtering properties are improved. On the other hand, reduced bandwidth causes an estimation lag. Thus, the trade-off between noise filtering and estimation lag as well as an a'priori knowledge of the bandwidth of the reconstructed signal needs to be taken into consideration. The algorithm is applicable to both minimum-phase and nonminimum-phase systems.

The drawback of the PE-UIO is that it may produce a distorted unknown input estimate, if a zero of the system transfer function to an unknown input is unity (a system with a derivative term) or lies close to unity. To tackle this problem an extension to the PE-UIO, i.e. a two stage PE-UIO, has been proposed. The two stage PE-UIO is applicable to systems, whose minimum-phase zeros lie close to unity or its zeros are equal unity. It has been demonstrated that the two stage algorithm has superior noise filtering properties compared to the standard PE-UIO, however, it may introduce larger estimation lag. Both, the standard and the two stage input reconstruction algorithms, are computationally simple. The filter parameters need to be calculated only once before the filter is applied to the system.

Both, the standard (single stage) PE-UIO and the two stage PE-UIO, have been compared with two other methods found in the literature: a Kalman filter-based MVU and the INPEST method, based on linear quadratic control. A simulation study has revealed superior noise filtering properties of the PE-UIO compared to the MVU. This is due to the adjustable bandwidth of the PE-UIO (which, however, causes the trade-off between the noise filtering and estimation delay). Furthermore, the MVU in the case of a single output system resembles a naive inversion, thus it cannot be used for unknown input reconstruction of single output nonminimum-phase systems. The INPEST method has shown comparable results to those of the PE-UIO (both single stage and the two stage).

Potential industrial applications of the proposed unknown input reconstruction schemes have been demonstrated via simulation studies in Chapter 7. The PE-UIO has been used to improve the control performance of a steel rolling mill, by reconstruction of a parasitic friction force. The two stage PE-UIO has been proposed in a hydrological application in order to estimate the level of pollutant in a river.

In Chapter 4 the PE-UIO has been extended to Hammerstein-Wiener systems, i.e. systems which can be modelled as a linear dynamic block preceded and followed by a static nonlinearity. The algorithm has been developed for a system with a single measurable input, single output, and a single unknown input to be reconstructed in an EIV framework, where both measured input and output are subjected to white, Gaussian, zero-mean mutually uncorrelated noise sequences. As the system operating point changes, the influence of the input and output noise on the unknown input es-

timate varies. Thus, the algorithm needs to adapt to these changes. Two versions of the scheme are proposed. In the first version the parity space order remains constant, whilst the filter parameters vary at each time sample. In the second version the parity space order varies according to the system operating point. Furthermore, assuming a Gaussian distribution of the measurement noise, a method for computation of the confidence bounds has been proposed. The simulation study has demonstrated applicability of proposed algorithms to the particular class of nonlinear systems. It has also been shown that for relatively mild nonlinearities a linear algorithm can be used in order to reduce the computational effort.

8.1.2 Fault detection and diagnosis

A robust fault detection filter of (Chen & Patton 1999) has been extended to system with unstable invariant zeros, which improved the applicability of the scheme. Furthermore, a modification has been proposed which allowed relaxation of a strict rank condition. The robust fault isolation filter proposed in Chapter 5 has an equivalent eigenstructure to the fault isolation filter proposed in (Chen & Speyer 2006*a*), however, it has been demonstrated that the design procedure presented in Chapter 5 is computationally simpler. It has been shown that the devised robust fault detection filter is completely decoupled from disturbances. The user can influence the transient behaviour of the residual response to faults via assignment of poles of the filter.

Furthermore, by building on the finite time convergent state observer of Engel & Kreisselmeier (2002), the proposed robust fault detection filter has been used to design robust PE of an arbitrary order. Analogously, left eigenstructure assignment has been used to design the PE of any user defined order. It has been demonstrated that both algorithms provide complete disturbance decoupling.

In Chapter 6 the robust PE via right eigenstructure assignment have been extended to the fault isolation and identification filter case. Decoupling properties of the robust PE presented in Chapter 5 have been used to design a directional residual set. Furthermore, by application of a similarity transformation and by setting to unity the steady state gain of the residual response of the filter to a given fault, a filter has been obtained, which provides an estimate of the fault vector, i.e. reconstructs the fault vector. In the case when the number of outputs exceeds the number of possible faults, the design freedom has been used to devise a control variable, which remains zero when any of the modelled faults occurs. Deviation of the control variable from zero indicates an occurrence of a fault which has not been covered by the model. Applicability of the novel PE design for fault identification to stochastic systems in the EIV framework has been considered and a simple method for calculation of thresholds, whose violation indicates a fault, has been proposed. Efficacy of the method has been demonstrated using a numerical example.

8.1.3 Contributions

The main contributions of this thesis are briefly summarised in order of importance as follows:

1. Incorporation of the Lagrange multiplier optimisation method into PE design in order to minimise the noise effect on the unknown input estimate (Chapter 3).
2. Extension of the proposed unknown input estimator to Hammersten-Wiener systems (Chapter 4).
3. Application of the novel PE-based unknown input reconstruction method for enhancement of a control loop in a single stand of a rolling mill and for a hydrological application (Chapter 7).
4. Use of right and left eigenstructure assignment to develop robust fault detection PE of user defined order (Chapter 5).
5. Extension of the robust fault detection filter via right eigenstructure assignment to systems with unstable invariant zeros (Chapter 5).
6. Use of right eigenstructure assignment to develop PE of arbitrary order for the purpose of fault isolation and identification (Chapter 6).

8.2 Further work

The following aspects are considered as further work regarding the PE-UIO for linear stochastic systems:

- Up to date the PE-UIO can be applied to systems where a single unknown input needs to be reconstructed. Thus, an extension of the algorithm to systems with multiple unmeasurable inputs could be considered.
- Application of a disturbance decoupling scheme to the PE-UIO could improve applicability of the algorithm.
- The single stage PE-UIO produces a distorted unknown input estimate when a zero of the system response to an unknown input lies close to unity. The two stage PE-UIO copes with such a situation if the problematic zero lies inside the unit circle. However, the problem remains open for the cases when a system nonminimum-phase zero lies close to unity.

The following aspects of the input reconstruction scheme for Hammerstein-Wiener systems could be taken into consideration:

- Extension of the algorithm to the multivariable case, with multiple measured inputs and outputs as well as multiple unknown inputs to be reconstructed.

- Algorithms presented in Chapter 4 require calculation of filter parameters at each time sample, thus they need a computational power which is not negligible. Consequently, an optimisation of the procedure is considered as an interesting aspect of future work.
- The scheme utilises a direct inversion of the output transforming nonlinearity, hence it is not applicable to systems where the output nonlinearity is not invertible. It would be interesting to consider e.g. adaptive learning methods to reconstruct the input to the noninvertible block and hence improve the applicability of the method.

Additional research on the topic of fault detection and diagnosis could include:

- Robust fault detection for stochastic systems. Design freedom of both robust PE and a robust asymptotic filter could be used to minimise the influence of the noise of the residual. Also calculation of thresholds, whose violation indicates the presence of faults has not been discussed for the robust fault detection filter (it has been discussed only for the fault isolation and identification filter in Chapter 6).
- Exploring applicability of the robust fault detection scheme to systems where the disturbance direction vectors e_i combine with each other to create new invariant zeros.
- Extension the fault isolation and identification scheme to multidimensional faults.

Furthermore, the following future research directions could also be considered:

- Extension of the proposed schemes to time-varying and uncertain systems.
- Extension of the proposed robust fault detection and diagnosis methods to nonlinear systems; particularly, Hammerstein-Wiener and bilinear systems could be considered.
- Whilst two of the developed algorithms have been applied to practical applications, it would be desirable to evaluate the other methods developed within this thesis to real world applications to assess their potential benefits.

References

Alexandru, M. (2003), 'Analysis of induction motor fault diagnosis with fuzzy neural network', *Applied Artificial Intelligence: An International Journal* **17**(2), 105–133.

Alexandru, M. & Popescu, D. (2004), Neuro-fuzzy diagnosis in final control elements of AC motors, *in* 'Proceedings of the 2004 American Control Conference', Boston, MA, USA.

Anbumani, K., Patnaik, L. & Sarma, I. (1981), 'Self-tuning minimum-variance control of nonlinear systems of the Hammerstein model', *IEEE Transactions on Automatic Control* **26**(4), 959–961.

Antsaklis, P. (1978), 'Stable proper nth-order inverses', *IEEE Transactions on Automatic Control* **23**(6), 1104–1106.

Ashari, A., Sedigh, A. & Yazdanpanah, M. (2005*a*), Output feedback reconfigurable controller design using eigenstructure assignment: post fault order change, *in* 'Proceedings of the International Conference on Control and Automation, 2005. ICCA '05', Vol. 1, Budapest, Hungary, pp. 474–479.

Ashari, A., Sedigh, A. & Yazdanpanah, M. (2005*b*), 'Reconfigurable control system design using eigenstructure assignment: static, dynamic and robust approaches', *International Journal of Control* **78**(13), 1005–1016.

Basile, G. & Marro, G. (1969), 'Controlled and conditioned invariant subspaces in linear system theory', *Journal of Optimisation Theory and Applications* **33**(5), 305–315.

Basile, G. & Marro, G. (2002), *Controlled and Conditioned Invariants in Linear Systems Theory*, Department of Electronics, Systems and Computer Science, University of Bologna, Italy.

Basile, G. & Marro, G. (2010), 'The geometric approach toolbox', `http://www3.deis.unibo.it/Staff/FullProf/GiovanniMarro/geometric.htm\#reftools`.

Basilevsky, A. (1983), *Applied Matrix Algebra in the Statistical Sciences*, North-Holland, New York/Amsterdam/Oxford.

Beard, R. V. (1971), Failure Accommodation in Linear Systems through Self-reorganisation, PhD thesis, Massachusetts Institute of Technology, USA.

Berriri, H., Naouar, M. W. & Slama-Belkhodja, I. (2011), Parity space approach for current sensor fault detection and isolation in electrical systems, *in* 'Proceedings of the 8th International Multi-Conference on Systems, Signals & Devices', Sousse, Tunisia.

Bertsekas, D. P. (1982), *Constrained Optimisation and Lagrange Multiplier Methods*, Academic press, Inc., London.

Bhattacharjee, A., Sengupta, A. & Sutradhar, A. (2010), Nonparametric modeling of glucose-insulin process in IDDM patient using Hammerstein-Wiener model, *in* 'Proceedings of 11th International Conference on Control Automation Robotics & Vision (ICARCV),', Singapore.

Bhattacharjee, N. & Roy, B. (2010), Fault detection and isolation of a two non-interacting tanks system using partial PCA, *in* 'Proceedings of 2010 International Conference on Industrial Electronics, Control & Robotics (IECR)', Rourkela, India.

Campos-Delgado, D. (2011), 'An observer-based diagnosis scheme for single and simultaneous open-switch faults in induction motor drives', *IEEE Transactions on Industrial Electronics* **58**(2), 671–679.

Celka, P. & Colditz, P. (2002), 'Nonlinear nonstationary Wiener model of infant EEG seizures', *IEEE Transactions on Biomedical Engineering* **49**(6), 556–564.

Chabir, K., Sauter, D. & Keller, J. (2009), Design of fault isolation filter under network induced delay, *in* 'Proceedings of 2009 IEEE Conference on Control Applications, (CCA) & Intelligent Control, (ISIC)'.

Chan, C., Hua, S. & Hong-Yue, Z. (2006), 'Application of fully decoupled parity equation in fault detection and identification of dc motors', *IEEE Transactions on Industrial Electronics* **53**(4), 1277–1284.

Chen, B. & Nagarajaiah, S. (2007), 'Linear-matrix-inequality-based robust fault detection and isolation using the eigenstructure assignment method', *Journal of Guidance, Control, and Dynamics* **30**(6), 1831–1835.

Chen, J. & Patton, R. J. (1999), *Robust Model-Based Fault Diagnosis for Dynamic Systems*, Kluver Academic Publishers, Boston.

Chen, R. H. & Speyer, J. L. (2006*a*), Detection filter analysis and design using eigenstructure assignment, *in* 'Proceedings of the American Control Conference (ACC'06)', Minneapolis, Minnesota USA.

Chen, R. & Speyer, J. (2006*b*), Generalization of the detection filter using spectral theory, *in* 'Proceedings of the American Control Conference (ACC'06)', Minneapolis, Minnesota USA.

Chen, R. & Speyer, J. (2007), Spectral analysis and design of detection filter for multiple-dimensional faults, *in* 'Proceedings of the American Control Conference (ACC'07)', New York City, USA.

Chow, E. & Willsky, A. (1984), 'Analytical redundancy and the design of robust failure detection systems', *IEEE Transactions on Automatic Control* **29**(7), 603–614.

Craddock, R. V. (1962), 'Take-off monitoring apparatus for aircraft', United States Patent, No. 3,034,096, 8 May.

Crama, P. & Rolain, Y. (2002), Broadband measurement and identification of a Wiener-Hammerstein model for an RF amplifier, *in* 'Proceedings of 60th ARFTG Conference Digest'.

Crama, P. & Schoukens, J. (2004), 'Hammerstein-Wiener system estimator initialization', *Automatica* **40**(9), 1543–1551.

Czop, P. (2011), 'Application of inverse data-driven parametric models in the reconstruction of passenger vehicle wheel vertical movement under ride conditions', *Journal of Vibration and Control* **18**(8), 1133–1140.

Darouach, M. & Zasadzinski, M. (1997), 'Unbiased minimum variance estimation for systems with unknown exogenous inputs', *Automatica* **33**(4), 717–719.

De-Feng, H., Li, Y. & Guo-Shi, Y. (2010), A pole placement-based NMPC algorithm of constrained Hammerstein systems, *in* 'Proceedings of 29th Chinese Control Conference (CCC 2010)', Beijing, China.

Dever, J. A. (1960), 'Control apparatus', United States Patent, No. 2,931,763, 5 May.

Ding, S. X. (2008), *Model-based Fault Diagnosis Techniques: Design Schemes, Algorithms and Tools*, Springer Verlag, Berlin.

Ding, S. X., Zhong, M., Bingyong, T. & Zhang, P. (2001), An LMI approach to the design of fault detection filter for time-delay LTI systems with unknown inputs, *in* 'Proceedings of the American Control Conference (ACC'01)', Arlington, VA, USA.

Dobrowiecki, T. & Schoukens, J. (2002), Cascading Wiener-Hammerstein systems, *in* 'Proceedings of the IEEE Instrumentation and Measurement Technology Conference', Anchorage, AK, USA.

Dorato, P. (1969), 'On the inverse of linear dynamical systems', *IEEE Transactions on Systems Science and Cybernetics* **5**(1), 43–48.

Douglas, R. K., Speyer, J. L., Mingori, D. L., Chen, R. H., Malladi, D. P. & Chung, W. H. (1996), 'Fault detection and identification with application to advanced vehicle control systems: Final report', Research Reports, California Partners for Advanced Transit and Highways (PATH), Institute of Transportation Studies (UCB), UC Berkeley.

Douglas, R. & Speyer, J. (1995), Robust fault detection filter design, *in* 'Proceedings of the American Control Conference (ACC'95)', Vol. 1, Seattle, WA, USA, pp. 91–96.

Duan, G. & Patton, R. J. (2001), 'Robust fault detection using Luenberger-type unknown input observers – a parametric approach', *International Journal of Systems Science* **32**(4), 533–540.

Dutka, A., Javaherian, H. & Grimble, M. J. (2009), Model-based engine fault detection and isolation, *in* 'Proceedings of the American Control Conference (ACC'09)', St. Louis, MO, USA.

Edelmayer, A. (2005), *Fault Detection in Dynamic Systems: From State Estimation to Direct Input Reconstruction Methods*, D.Sc. thesis, Hungarian Academy of Sciences, Budapest, Hungary.

El-Ghezawi, O., Billings, S. & Zinober, A. (1983), Variable-structure systems and system zeros, *in* 'IEE Proceedings Control Theory and Applications', Vol. 130, pp. 1–5.

Engel, R. & Kreisselmeier, G. (2002), 'A continuous-time observer which converges in finite time', *IEEE Transactions on Automatic Control* **47**(7), 1202–1204.

Fagarasan, I. & St. Iliescu, S. (2008), Parity equations for fault detection and isolation, *in* 'Proceedings of IEEE International Conference on Automation, Quality and Testing, Robotics, (AQTR 2008)', Cluj-Napoca, Romania.

Fantuzzi, C., Simani, S. & Beghelli, S. (2001), Robust fault diagnosis of dynamic processes using parametric identification with eigenstructure assignment approach, *in* 'Proceedings of the 40th IEEE Conference on Decision and Control', Orlando, FL, USA.

Fernando, T. & Trinh, H. (2006), Design of reduced-order state/unknown input observers: A descriptor system approach, *in* 'Proceedings of the 2006 IEEE International Conference on Control Applications', Munich, Germany.

Floquet, T. & Barbot, J. (2006), 'State and unknown input estimation for linear discrete-time systems', *Automatica* **42**(11), 1883–1889.

Fragkoulis, D., Roux, G. & Dahhou, B. (2009), A global scheme for multiple and simultaneous faults in system actuators and sensors, *in* 'Proceedings of the 6th International Multi-Conference on Systems, Signals and Devices (SSD '09)', Djerba, Tunisia.

Frank, P. M. & Wünnenberg, J. (1989), *Fault Diagnosis in Dynamic Systems: Theory and Application*, Prentice Hall, chapter Robust Fault Diagnosis Using Unknown Input Schemes, pp. 47–98.

Fravolini, M., Brunori, V., Campa, G., Napolitano, M. & La Cava, M. (2009), 'Structural analysis approach for the generation of structured residuals for aircraft FDI', *IEEE Transactions on Aerospace and Electronic Systems* **45**(4), 1466–1482.

Fruzzetti, K., Palazoglu, A. & McDonald, K. (1997), 'Nonlinear model predictive control using Hammerstein models', *Journal of ProcessControl* **7**(1), 31–44.

Fu, H., Kirtikar, S., Zattoni, E., Palanthandalam-Madapusi, H. & Bernstein, D. (2009), Approximate input reconstruction for diagnosing aircraft control surfaces, *in* 'Proceedings of the AIAA Guidance, Navigation, and Control Conference', Chicago, Illinois.

Fu, H., Yan, J., Santillo, M. A., Palanthandalam-Madapusi, H. & Bernstein, D. (2009), Fault detection for aircraft control surfaces using approximate input reconstruction, *in* 'Proceedings of the American Control Conference (ACC'09)', St. Louis, MO, USA.

Gao, Z., Breikin, T. & Wang, H. (2007), 'High-gain estimator and fault-tolerant design with application to a gas turbine dynamic system', *IEEE Transactions on Control Systems Technology* **15**(4), 740–753.

Garrick, B. J., Gekler, W. C., Goldfisher, L., Karcher, R. H., Shimizu, B. & Wilson, J. H. (1967), Reliability analysis of nuclear power plant protective system, Technical Report HN-190 AEC Research & Development Report, Holmes & Narver, Inc., Nuclear Division.

Gertler, J. & Kunver, M. (1995), 'Optimal residual decoupling for fault diagnosis', *International Journal of Control* **61**(2), 395–421.

Gertler, J. & Singer, D. (1990), 'A new structurel framework for parity equation-based failure detection and isolation', *Automatica* **26**(2), 381–388.

Ghahremani, E. & Kamwa, I. (2011), Simultaneous state and input estimation of a synchronous machine using the extended Kalman filter with unknown inputs, *in* 'Proceedings of the 2011 IEEE International Electric Machines & Drives Conference (IEMDC)', pp. 1468– 473.

Gillijns, S. & De Moor, B. (2007*a*), 'Unbiased minimum variance input and state estimation for linear discrete-time systems', *Automatica* **43**(1), 111–116.

Gillijns, S. & De Moor, B. (2007*b*), 'Unbiased minimum variance input and state estimation for linear discrete-time systems with direct feedthrough', *Automatica* **43**(5), 934–937.

Gu, D. & Poon, F. W. (2003), 'A robust fault-detection approach with application in a rolling-mill process', *IEEE Transactions on Control Systems Technology* **11**(3), 408–414.

Halmos, P. R. (1958), *Finite-dimensional vector spaces*, Springer.

Halton, H. (1963), 'Design philosophy of an automatic checkout and launch system for a drone', *IEEE Transactions on Aerospace* **1**(2), 538–546.

Hou, M. & Müller, P. (1992), 'Design of observers for linear systems with unknown inputs', *IEEE Transactions on Automatic Control* **37**(6), 871–875.

Hsieh, C. (2000), 'Robust two-stage Kalman filters for systems with unknown inputs', *IEEE Transactions on Automatic Control* **45**(12), 2374–2378.

Ibaraki, S., Suryanarayanan, S. & Tomizuka, M. (2005), 'Design of Luenberger state observers using fixed-structure H_∞ optimization and its application to fault detection in lane-keeping control of automated vehicles', *IEEE/ASME Transactions on Mechatronics* **10**(1), 34–42.

Ibnkahla, M. (2002), 'Natural gradient learning neural networks for adaptive inversion of Hammerstein systems', *IEEE Signal Processing Letters* **9**(10), 315–317.

Isermann, R. (2005), 'Model-based fault-detection and diagnosis–status and applications', *Annual Reviews in Control* **29**, 71–85.

Isermann, R. & Balle, P. (1997), 'Trends in the application of model-based fault detection and diagnosis of technical processes', *Control Engineering Practice* **5**(5), 709–719.

Janis, J. P. (1963), 'Checkout methods for space vehicle subsystems', *IEEE Transactions on Aerospace* **1**(2), 547–549.

Jelali, M. & Kroll, A. (2003), *Hydraulic servo-systems: modelling, identification and control*, Springer-Verlag, London.

Jirauch, D. H. (1967), 'Software design techniques for automatic checkout', *IEEE Transaction on Aerospace and Electronic Systems* **AES-3**(6), 934–940.

Jones, H. L. (1973), Failure Detection in Linear Systems, PhD thesis, Massachusetts Institute of Technology, USA.

Kaufmann, R. H. & Finison, H. J. (1952), *D-C Power Systems for Aircrafts*, John Wiley & Sons, Inc., New York.

Keller, J. & Sauter, D. (2010), A variable geometric state filtering for stochastic linear systems subject to intermittent unknown inputs, *in* 'Proceedings of the Conference on Control and Fault-Tolerant Systems (SysTol)', pp. 558–563.

Kennedy, J. J. (1970), 'Fault detection monitor circuit provides "self-heal capability" in electronic modules: A concept', NASA Tech. Brief 70-10515.

Kirtikar, S., Palanthandalam-Madapusi, H., Zattoni, E. & Bernstein, D. S. (2009), l-delay input recontruction for discrete-time linear systems, *in* 'Proc. of the Conference on Decision and Control', Shanghai, China, pp. 1848–1853.

Korbicz, J., Koscielny, J. M., Kowalczuk, Z. & Cholewa, W., eds (2003), *Fault Diagnosis: Models, Artificial Intelligence, Applications*, Springer.

Kowalczuk, Z. & Suchomski, P. (2005), Entirely left eigenstructure-assignment for fault diagnosis observers, *in* 'Proceedings of the 16th IFAC World Congress, 2005', Vol. 16.

Lajic, Z., Blanke, M. & Nielsen, U. D. (2009), Fault detection for shipboard monitoring Volterra kernel and Hammerstein model approaches, *in* 'Proceedings of IFAC Symposium on Fault Detection, Supervision and Safety of Technical Processes', pp. 24–29.

Lee, F. (1962), 'An automatic self-checking and fault-locating method', *IRE Transactions on Electronic Computers* **EC-11**(5), 649–654.

Li, W. & Shah, S. (2002), 'Structured residual vector-based approach to sensor fault detection and isolation', *Journal of Process Control* **12**, 429–443.

Lia, C.-C. & Jengb, J.-C. (2010), 'Multiple sensor fault diagnosis for dynamic processes', *ISA Transactions* **48**(4), 415–432.

Ljung, L. (1999), *System Identification - Theory for the User*, PTR Prentice Hall Information and System Sciences Series, 2nd edn, Prentice Hall, New Jersey.

Luenberger, D. G. (1964), 'Observing the state of linear systems', *IEEE Trans. Mil. Electr.* **MIL-8**, 70–80.

MacFarlane, A. & Karcanias, N. (1976), 'Poles and zeros of linear multivariable systems: A survey of the algebraic, geometric and complex variable theory', *International Journal of Control* **24**, 33–74.

Marro, G. & Zattoni, E. (2010), 'Unknown-state, unknown-input reconstruction in discrete-time nonminimum-phase systems: Geometric approach', *Automatica* **46**, 815–822.

Martinez, C. J. & Wise, W. R. (2003), 'Analysis of constructed treatment wetland hydraulics with the transient storage model OTIS', *Ecological Engineering* **20**(3), 211–222.

Massoumnia, M. A. (1986), 'A geometric approach to the synthesis of failure detection filters', *IEEE Transaction on Automatic Control* **AC-31**, 839–846.

Mast, L. T., Mayper, V. & Pilnick, C. (1966), 'Survey of Saturn/Apollo checkout automation, spring 1965: Detailed description', Memorandum RM-4785-NASA.

Mironovski, L. A. (1979), 'Functional diagnosis of linear dynamic systems', *Automn Remote Control* **40**, 1198–1205.

Moylan, P. (1977), 'Stable inversion of linear systems', *IEEE Transactions on Automatic Control* **22**(1), 74–78.

Ng, H., Chen, R. & Speyer, J. (2006), 'A vehicle health monitoring system evaluated experimentally on a passenger vehicle', *IEEE Transactions on Control Systems Technology* **14**(5), 854–870.

Palanthandalam-Madapusi, H. & Bernstein, D. (2007), Unbiased minimum-variance filtering for input reconstruction, *in* 'Proceedings of the American Control Conference (ACC'07)', pp. New York City, USA.

Palanthandalam-Madapusi, H., Ridley, A. & Bernstein, D. (2005), Identification and prediction of ionospheric dynamics using a Hammerstein-Wiener model with radial basis functions, *in* 'Proceedings of the American Control Conference (ACC'05)', Portland, OR, USA.

Papadopoulos, E. G. & Chasparis, G. C. (2002), Analysis and model-based control of servomechanisms with friction, *in* 'Proceedings of the International Conference on Intelligent Robots and Systems (IROS 2002)', Lausanne, Switzerland.

Park, J. & Rizzoni, G. (1994), 'An eigenstructure assignment algorithm for the design of fault detection filters', *IEEE Transactions on Automatic Control* **39**(7), 1521–1524.

Patel, R. V. (1985), On blocking zeros in linear multivariable systems, *in* 'Proceedings of 24th Conference on Decision and Control'.

Patel, R. V. & Munro, N. (1982), *Multivariable System Theory and Design*, Pergamon Press, Inc.

Patton, R. & Chen, J. (1997), 'Observer-based fault detection and isolation: Robustness and applications', *Control Engineering Practice* **5**(5), 671–682.

Patton, R. J. (1997), 'Robustness in model-based fault diagnosis: The 1995 situation', *Annual Reviews of Control* **21**, 103–120.

Patton, R. J. & Chen, J. (1991*a*), A parity space approach to robust fault detection using eigenstructure assignment, *in* 'Proceedings of European Control Conference ECC91', Grenoble, France.

Patton, R. J. & Chen, J. (1991*b*), Robust fault diagnosis using eigenstructure assignment: A tutorial consideration and some new results, *in* 'Proceedings of the 30th Conference on Decision and Control', pp. 2242–2247.

Patton, R. J. & Chen, J. (1991*c*), A robust parity space approach to fault diagnosis based on optimal eigenstructure assignment, *in* 'International Conference on Control 1991. Control '91', Edinburgh , UK, pp. 1056–1061.

Patton, R. J. & Chen, J. (1992), 'Robust fault detection of jet engine sensor systems using eigenstructure assignment', *Journal of Guidance, Control, and Dynamics* **15**(6), 1491–1497.

Patton, R. & Liu, G. (1994), Robust control design via eigenstructure assignment, genetic algorithms and gradient-based optimisation, *in* 'IEE Proceedings on Control Theory and Applications', Vol. 141, pp. 202–208.

Pearson, R. K. (1995), 'Nonlinear input/output modelling', *Journal of Process Control* **5**(4), 197–211.

Pearson, R. K. (2003), 'Selecting nonlinear model structures for computer control', *Journal of Process Control* **13**(1), 1–26.

Pearson, R. K. & Pottmann, M. (2000), 'Gray-box identification of block-oriented nonlinear models', *Journal of Process Control* **10**, 301–315.

Pierria, F., Paviglianiti, G., Caccavale, F. & Mattei, M. (2008), 'Observer-based sensor fault detection and isolation for chemical batch reactors', *Engineering Applications of Artificial Intelligence* **21**, 1204–1216.

Pottmann, M. & Pearson, R. K. (2006), 'Block-oriented NARMAX models with output multiplicities', *AIChE journal* **44**(1), 131–140.

Putra, D. (2004), Control of Limit Cycling in Frictional Mechanical Systems, PhD thesis, Technische Universiteit Eindhoven, Eindhoven.

Raff, T., Menold, P., Ebenbauer, C. & Allgöwer, F. (2005), A finite time functional observer for linear systems, *in* 'Procedings of the 44th IEEE Conference on Decision and Control and the European Control Conference 2005', Seville, Spain.

Reliability, Availability, and Maintainability Dictionary (1988), ASQC Quality Press, Milwaukee.

Rocha-Cozatl, E., Moreno, J. A. & Vande Wouwer, A. (2012), Application of a continuous-discrete unknown input observer to estimation in phytoplanktonic cultures, *in* 'Preprints of the 8th IFAC Symposium on Advanced Control of Chemical Processes', Singapore.

Sain, M. & Massey, J. (1969), 'Invertibility of linear time-invariant dynamical systems', *IEEE Transactions on Automatic Control* **14**(2), 141–149.

Shen, L. & Hsu, P. (1998), 'Robust design of fault isolation observers', *Automatica* **34**(11), 1421–1429.

Siahi, M., Sadrnia, M. A. & Darabi, A. (2009), 'A new method for observer design using eigenstructure assignment and its application on fault detection and isolation', *World Applied Sciences Journal* **6**(1), 100–104.

Simani, S., Fantuzzi, C. & Patton, R. J. (2002), *Model-based fault diagnosis in dynamic systems using identification techniques*, Springer-Verlag, London, UK.

Söderström (2007), 'Errors-in-variables methods in system identification', *Automatica* **43**(6), 939–958.

Sumisławska, M. (2009), *Prediction of Limit Cycles in Hot Strip Mill Gauge Control*, M.Sc. thesis, Control Theory and Applications Centre, Coventry University, Coventry, UK.

Sumisławska, M., Burnham, K. J., Hearns, G., Larkowski, T. M. & Reeve, P. J. (2010), Parity equation-based friction compensation applied to a rolling mill, *in* 'Proceedings of the UKACC International Conference on Control 2010', Coventry, UK, pp. 1043–1048.

Sumisławska, M., Burnham, K. J. & Larkowski, T. M. (2010), Design of unknown input estimator of a linear system based on parity equations, *in* 'Procedings of the XVII International Conference on Systems Science', Wrocław, Poland, pp. 81–90.

Sumisławska, M., Larkowski, T. & Burnham, K. J. (2010*a*), 'Parity equations-based unknown input estimator for multiple-input multiple-output linear systems', *Systems Science* **36**(3), 49–56.

Sumisławska, M., Larkowski, T. & Burnham, K. J. (2011*a*), Design of unknown input reconstruction filter based on parity equations for errors-in-variables case, *in* 'Proceedings of the 18th IFAC World Congress', Milan, Italy, pp. 4272–4277.

Sumisławska, M., Larkowski, T. & Burnham, K. J. (2012), Unknown input reconstruction observer for Hammerstein-Wiener systems in the errors-in-variables framework, *in* 'Proceedings of the 16th IFAC Symposium on System Identification', Brussels, Belgium, pp. 1377–1382.

Sumisławska, M., Larkowski, T. M. & Burnham, K. J. (2010*b*), Design of unknown input reconstruction algorithm in presence of measurement noise, *in* 'Procedings of the 8th European ACD2010 Workshop on Advanced Control and Diagnosis', Ferrara, Italy, pp. 213–216.

Sumisławska, M., Larkowski, T. M. & Burnham, K. J. (2011*b*), Design of parity equations using right eigenstructure assignment, *in* 'Proceedings of International Conference on Systems Engineering', Las Vegas, USA, pp. 367–370.

Sumisławska, M., Reeve, P. J., Burnham, K. J., Pozniak-Koszałka, I. & Hearns, G. (2009), Computer control simulation and development with industrial applications, *in* 'Procedings of the 9th Polish-British Workshop', Sienna, Poland, pp. 230–239.

Szabo, Z., Gaspar, P. & Bokor, J. (2005), Reference tracking for Wiener systems using dynamic inversion, *in* 'Proceedings of the 2005 IEEE International Symposium on, Mediterrean Conference on Control and Automation Intelligent Control', Limassol, Cyprus.

Tan, C. P., Edwards, C. & Kuang, Y. C. (2006*a*), Robust sensor fault reconstruction using a reduced order linear observer, *in* '9th International Conference on Control, Automation, Robotics and Vision (ICARCV '06)', Singapore.

Tan, C. P., Edwards, C. & Kuang, Y. C. (2006*b*), Robust sensor fault reconstruction using right eigenstructure assignment, *in* 'Third IEEE International Workshop on Electronic Design, Test and Applications (DELTA 2006)', Kuala Lumpur, Malaysia.

Tan, C. P. & Habib, M. K. (2004), Robust sensor fault reconstruction for an inverted pendulum using right eigenstructure assignment, *in* 'Proceedings of the 2004 IEEE International Conference on Control Applications', Taipei, Taiwan.

Tan, C. P. & Habib, M. K. (2006), Fault tolerance of a flexible manipulator, *in* '9th International Conference on Control, Automation, Robotics and Vision (ICARCV '06)', Singapore, pp. 1–5.

Tervo, K. & Manninen, A. (2010), Analysis of model orders in human dynamics identification using linear polynomial and Hammerstein-Wiener structures, *in* 'Proceedings of 2010 International Conference on Networking, Sensing and Control (ICNSC)', Chicago, IL, USA.

Wang, J., Jiang, B. & Shi, P. (2008), 'Adaptive observer-based fault diagnosis for satellite attitude control system', *International Journal of Innovative Computing, Information and Control* **4**(8), 1921–1929.

White, J. E. & Speyer, J. L. (1986), Detection filter design: Spectral theory and algorithms, *in* 'Proceedings of the American Control Conference (ACC'86)', Seattle, WA, USA.

Wohnam, W. M. & Morse, A. (1970), 'Decoupling and pole assignment in linear multivariable systems: A geometric approach', *SIAM Journal of Control* **8**(1), 1–18.

Xie, L., Zhang, J. & Wang, S. (2006), 'Investigation of dynamic multivariate chemical process monitoring', *Chinese Journal of Chemical Engineering* **14**(5), 559–568.

Ye, L., Shi, X. & Liang, J. (2011), 'A multi-level approach for complex fault isolation based on structured residuals', *Chinese Journal of Chemical Engineering* **19**(3), 462–472.

Yildiz, S. K., Forbes, J. F., Huang, B., Zhang, J., Wang, F., Vaculik, V. & Dudzic, M. (2009), 'Dynamic modelling and simulation of a hot strip finishing mill', *Applied Mathematical Modelling* **33**, 3208 – 3225.

Yiua, J. C. & Wang, S. (2007), 'Multiple ARMAX modeling scheme for forecasting air conditioning system performance', *Energy Conversion and Management* **48**(8), 2276–2285.

Young, P. C. (2011), *Recursive Estimation and Time Series Analysis: An Introduction for the Student and Practitioner*, Springer.

Young, P. C., Behzadi, M. A., Wang, C. L. & Chotai, A. (1987), 'Direct digital and adaptive control by input-output state variable feedback', *International Journal of Control* **46**, 1861–1881.

Young, P. C. & Sumisławska, M. (2012), A control systems approach to input estimation with hydrological applications, *in* 'Proceedings of the 16th IFAC Symposium on System Identification', Brussels, Belgium, pp. 1043–1048.

Zhong, M., Ding, S. X., Lam, J. & Wang, H. (2003), 'An LMI approach to design robust fault detection filter for uncertain LTI systems', *Automatica* **39**(3), 543–550.

Appendices

Appendix A

Calculation of parameters x_{ij}

The matrix X is given by:

$$X = \begin{bmatrix} x_{11} & 1 & 0 & 0 & \cdots & 0 & 0 \\ x_{21} & z_1 & 1 & 0 & \cdots & 0 & 0 \\ x_{31} & 0 & z_2 & 1 & \cdots & 0 & 0 \\ \vdots & \vdots & \vdots & \vdots & \ddots & \vdots & \vdots \\ x_{q_1 1,1} & 0 & 0 & 0 & \cdots & z_{q_1-1} & 1 \\ x_{q_1+1,1} & 0 & 0 & 0 & \cdots & 0 & z_{q_1} \end{bmatrix} \tag{A.1}$$

Eigenvalues corresponding to the linear combinations of columns of $\bar{e}$, λ_j, $j = 1, \cdots, q_1$, must fulfil the equation:

$$\det(\lambda_j I - X) = 0 \tag{A.2}$$

i.e.

$$\begin{aligned} &\det \begin{bmatrix} x_{11} - \lambda_j & 1 & 0 & 0 & \cdots & 0 & 0 \\ x_{21} & z_1 - \lambda_j & 1 & 0 & \cdots & 0 & 0 \\ x_{31} & 0 & z_2 - \lambda_j & 1 & \cdots & 0 & 0 \\ \vdots & \vdots & \vdots & \vdots & \ddots & \vdots & \vdots \\ x_{q_1 1,1} & 0 & 0 & 0 & \cdots & z_{q_1-1} - \lambda_j & 1 \\ x_{q_1+1,1} & 0 & 0 & 0 & \cdots & 0 & z_{q_1} - \lambda_j \end{bmatrix} \\ &= \det \begin{bmatrix} x_{11} - \lambda_j & x_{21} & x_{31} & \cdots & x_{q_1 1,1} & x_{q_1+1,1} \\ 1 & z_1 - \lambda_j & 0 & \cdots & 0 & 0 \\ 0 & 1 & z_2 - \lambda_j & \cdots & 0 & 0 \\ 0 & 0 & 1 & \cdots & 0 & 0 \\ \vdots & \vdots & \vdots & \ddots & \vdots & \vdots \\ 0 & 0 & 0 & \cdots & z_{q_1-1} - \lambda_j & 0 \\ 0 & 0 & 0 & \cdots & 1 & z_{q_1} - \lambda_j \end{bmatrix} = 0 \end{aligned} \tag{A.3}$$

Using a determinant expansion by minors, the following recursive expression is obtained:

$$\begin{aligned}\det(\lambda_j I - X) = (x_{11} - \lambda_j)\det\begin{bmatrix} z_1 - \lambda_j & 0 & \cdots & 0 & 0 \\ 1 & z_2 - \lambda_j & \cdots & 0 & 0 \\ 0 & 1 & \cdots & 0 & 0 \\ \vdots & \vdots & \ddots & \vdots & \vdots \\ 0 & 0 & \cdots & z_{q_1-1} - \lambda_j & 0 \\ 0 & 0 & \cdots & 1 & z_{q_1} - \lambda_j \end{bmatrix} \\ - \det\begin{bmatrix} x_{21} & x_{31} & \cdots & x_{q_1 1,1} & x_{q_1+1,1} \\ 1 z_2 - \lambda_j & \cdots & 0 & 0 & \\ 0 & 1 & \cdots & 0 & 0 \\ \vdots & \vdots & \ddots & \vdots & \vdots \\ 0 & 0 & \cdots & z_{q_1-1} - \lambda_j & 0 \\ 0 & 0 & \cdots & 1 & z_{q_1} - \lambda_j \end{bmatrix}\end{aligned} \tag{A.4}$$

The determinant of a lower triangular matrix is equal to the product of its diagonal elements, hence the first element of (A.4) is calculated via:

$$\begin{aligned}&(x_{11} - \lambda_j)\det\begin{bmatrix} z_1 - \lambda_j & 0 & \cdots & 0 & 0 \\ 1 & z_2 - \lambda_j & \cdots & 0 & 0 \\ 0 & 1 & \cdots & 0 & 0 \\ \vdots & \vdots & \ddots & \vdots & \vdots \\ 0 & 0 & \cdots & z_{q_1-1} - \lambda_j & 0 \\ 0 & 0 & \cdots & 1 & z_{q_1} - \lambda_j \end{bmatrix} \\ &= (x_{11} - \lambda_j)(z_1 - \lambda_j)(z_2 - \lambda_j)\cdots(z_{q_1} - \lambda_j)\end{aligned} \tag{A.5}$$

The second element of (A.4) is developed as:

$$- \det\begin{bmatrix} x_{21} & x_{31} & \cdots & x_{q_1 1,1} & x_{q_1+1,1} \\ 1 & z_2 - \lambda_j & \cdots & 0 & 0 \\ 0 & 1 & \cdots & 0 & 0 \\ \vdots & \vdots & \ddots & \vdots & \vdots \\ 0 & 0 & \cdots & z_{q_1-1} - \lambda_j & 0 \\ 0 & 0 & \cdots & 1 & z_{q_1} - \lambda_j \end{bmatrix} = \tag{A.6}$$

$$= -x_{12}\det\begin{bmatrix} z_2-\lambda_j & 0 & \cdots & 0 & 0 \\ 1 & z_3-\lambda_j & \cdots & 0 & 0 \\ 0 & 1 & \cdots & 0 & 0 \\ \vdots & \vdots & \ddots & \vdots & \vdots \\ 0 & 0 & \cdots & z_{q_1-1}-\lambda_j & 0 \\ 0 & 0 & \cdots & 1 & z_{q_1}-\lambda_j \end{bmatrix}$$

$$+\det\begin{bmatrix} x_{31} & x_{41} & \cdots & x_{q_1,1} & x_{q_1+1,1} \\ 1 & z_3-\lambda_j & \cdots & 0 & 0 \\ 0 & 1 & \cdots & 0 & 0 \\ \vdots & \vdots & \ddots & \vdots & \vdots \\ 0 & 0 & \cdots & z_{q_1-1}-\lambda_j & 0 \\ 0 & 0 & \cdots & 1 & z_{q_1}-\lambda_j \end{bmatrix}$$

Following this recursive procedure equation (A.2) is reformulated as:

$$\begin{aligned} &x_{11}(z_1-\lambda_j)(z_2-\lambda_j)\cdots(z_{q_1}-\lambda_j)+(-1)x_{21}(z_2-\lambda_j)(z_3-\lambda_j)\cdots(z_{q_1}-\lambda_j)+ \\ &(-1)^2x_{31}(z_3-\lambda_j)(z_4-\lambda_j)\cdots(z_{q_1}-\lambda_j)+\cdots+(-1)^{q_1}x_{q_1,1}(z_{q_1}-\lambda_j)+ \\ &(-1)^{q_1+1}x_{q_1+1,1}=\lambda_j(z_1-\lambda_j)(z_2-\lambda_j)\cdots(z_{q_1}-\lambda_j) \end{aligned} \tag{A.7}$$

The above equation needs to be fulfilled for λ_j, $j=1,w,\cdots,q_1+1$, i.e.

$$\begin{bmatrix} \prod_{k=1}^{q_1}(z_k-\lambda_1) & -\prod_{k=2}^{q_1}(z_k-\lambda_1) & \cdots & (-1)^{q_1-1}(z_{q_1}-\lambda_1) & (-1)^{q_1} \\ \prod_{k=1}^{q_1}(z_k-\lambda_2) & -\prod_{k=2}^{q_1}(z_k-\lambda_2) & \cdots & (-1)^{q_1-1}(z_{q_1}-\lambda_2) & (-1)^{q_1} \\ \vdots & \vdots & \ddots & \vdots & \vdots \\ \prod_{k=1}^{q_1}(z_k-\lambda_{q_1}) & -\prod_{k=2}^{q_1}(z_k-\lambda_{q_1}) & \cdots & (-1)^{q_1-1}(z_{q_1}-\lambda_{q_1}) & (-1)^{q_1} \end{bmatrix}$$
$$\begin{bmatrix} x_{11} \\ x_{21} \\ \vdots \\ x_{q_1+1,1} \end{bmatrix} = \begin{bmatrix} \lambda_1\prod_{k=1}^{q_1}(z_k-\lambda_1) \\ \lambda_2\prod_{k=1}^{q_1}(z_k-\lambda_2) \\ \vdots \\ \lambda_{q_1}\prod_{k=1}^{q_1}(z_k-\lambda_{q_1}) \end{bmatrix} \tag{A.8}$$

Consequently, the first column of X is given by:

$$\begin{bmatrix} x_{11} \\ x_{12} \\ \vdots \\ x_{q_1+1,1} \end{bmatrix} = (\tilde{\tilde{A}})^{-1}\tilde{\tilde{B}} \tag{A.9}$$

where an element of $\tilde{\tilde{A}}^{(i)} \in \mathbb{R}^{(q_1+1)\times(q_1+1)}$, denoted as $\tilde{\tilde{A}}_{j,k}$ is:

$$\tilde{\tilde{A}}_{j,k} = (-1)^{k-1}\prod_{l=k}^{q_1}(z_l-\lambda_j) \tag{A.10}$$

whilst the j^{th} element of the vector $\tilde{\tilde{B}} \in \mathbb{R}^{q_1+1}$, denoted as $\tilde{\tilde{B}}_j$ is:

$$\tilde{\tilde{B}}_j = \lambda_j \prod_{l=1}^{q_1} (z_l - \lambda_j) \tag{A.11}$$

Appendix B

Proof of Lemma 5.4

For the sake of brevity, the superscript $^{(i)}$ is omitted. Matrices A_e^* and A_w are equal if their appropriate columns are equal. From equation (2.103) it holds that eigenvectors of $(A - KC)$ are given by:

$$w_j^{(i)} = f_i + \begin{bmatrix} v_1^{(i)} & v_2^{(i)} & \cdots & v_{q_i}^{(i)} \end{bmatrix} \bar{\beta}_j^{(i)} \tag{B.1}$$

where $\bar{\beta}_j^{(i)}$ is a column vector of q_i parameters. The parameters $\bar{\beta}_j^{(i)}$ conform to (2.107), which can be reformulated as:

$$\begin{aligned} (A - \lambda_k^{(i)} I) \begin{bmatrix} v_1^{(i)} & v_2^{(i)} & \cdots & v_{q_i}^{(i)} \end{bmatrix} \bar{\beta}_k^{(i)} \\ - (A - \lambda_{q_i}^{(i)} I) \begin{bmatrix} v_1^{(i)} & v_2^{(i)} & \cdots & v_{q_i}^{(i)} \end{bmatrix} \bar{\beta}_{q_i}^{(i)} = (\lambda_k^{(i)} - \lambda_{q_i}^{(i)}) e_i \end{aligned} \tag{B.2}$$

for $k = 1, \cdots, q_i - 1$. Using the notation:

$$\bar{\beta}_j^{(i)} = \begin{bmatrix} \beta_{j,1}^{(i)} & \beta_{j,2}^{(i)} & \cdots & \beta_{j,q_i}^{(i)} \end{bmatrix} \tag{B.3}$$

it follows that:

$$\begin{aligned} &\beta_{k,1} A v_1 + \beta_{k,2} A v_2 + \cdots + \beta_{k,q_i} A v_{q_i} - \lambda_k \beta_{k,1} v_1 - \lambda_k \beta_{k,2} v_2 - \cdots - \lambda_k \beta_{k,q_i} v_{q_i} - \\ &\beta_{q_i,1} A v_1 - \beta_{q_i,2} A v_2 - \cdots - \beta_{q_i,q_i} A v_{q_i} + \lambda_{q_i+1} \beta_{q_i,1} v_1 + \lambda_{q_i+1} \beta_{q_i,2} v_2 + \cdots + \lambda_{q_i+1} \beta_{q_i,q_i} v_{q_i} \\ &= (\lambda_k - \lambda_{q_i+1}) e_i \end{aligned} \tag{B.4}$$

$k = 1, \cdots, q_i$. From (5.62a), it follows that:

$$A v_j = z_j v_j + v_{j-1} \tag{B.5}$$

Recalling that $v_0 = e_i$, (B.4) can be reformulated as:

$$\begin{aligned}
&\beta_{k,1}z_1v_1 + \beta_{k,1}e_i + \beta_{k,2}z_2v_2 + \beta_{k,2}v_1 + \cdots + \beta_{k,q_i}z_{q_i}v_{q_i} + \beta_{k,q_i}v_{q_i-1} \\
&- \lambda_k\beta_{k,1}v_1 - \lambda_k\beta_{k,2}v_2 - \cdots - \lambda_k\beta_{k,q_i}v_{q_i} - \beta_{q_i,1}z_1v_1 + \beta_{q_i,1}e_i + \beta_{q_i,2}z_2v_2 \\
&+ \beta_{q_i,2}v_1 + \cdots + \beta_{q_i,q_i}z_{q_i}v_{q_i} + \beta_{q_i,q_i}v_{q_i-1} - \lambda_{q_i+1}\beta_{q_i,1}v_1 - \lambda_{q_i+1}\beta_{q_i,2}v_2 \\
&- \cdots - \lambda_{q_i+1}\beta_{q_i,q_i}v_{q_i} = (\lambda_k - \lambda_{q_i+1})e_i
\end{aligned} \tag{B.6}$$

Then:

$$\begin{aligned}
&-(\lambda_k - \beta_{k,1})e_i + (\beta_{k,1}z_1 + \beta_{k,2} - \lambda_k\beta_{k,1})v_1 + (\beta_{k,2}z_2v_2 + \beta_{k,3} - \lambda_k\beta_{k,2})v_2 \\
&+ \cdots + (\beta_{k,q_i-1}z_{q_i-1} + \beta_{k,q_i} - \lambda_k\beta_{k,q_i-1})v_{q_i-1} + (\beta_{k,q_i}z_{q_i} - \lambda_k\beta_{k,q_i})v_{q_i} = \\
&-(\lambda_{q_i+1} - \beta_{q_i,1})e_i + (\beta_{q_i,1}z_1 + \beta_{q_i,2} - \lambda_{q_i+1}\beta_{q_i,1})v_1 + (\beta_{q_i,2}z_2 + \beta_{q_i,3} - \lambda_{q_i+1}\beta_{q_i,2})v_2 \\
&+ \cdots + (\beta_{q_i,q_i-1}z_{q_i-1} + \beta_{q_i,q_i} - \lambda_{q_i+1}\beta_{q_i,q_i-1})v_{q_i-1} + (\beta_{q_i,q_i}z_{q_i} - \lambda_{q_i+1}\beta_{k,q_i})v_{q_i}
\end{aligned} \tag{B.7}$$

Due to the fact that $e_i, v_1, v_2, \cdots, v_{q_i}$ are linearly independent, it holds that:

$$\begin{aligned}
\lambda_k - \beta_{k,1} &= \lambda_{q_i+1} - \beta_{q_i,1} \\
\beta_{k,1}z_1 + \beta_{k,2} - \lambda_k\beta_{k,1} &= \beta_{q_i,1}z_1 + \beta_{q_i,2} - \lambda_{q_i+1}\beta_{q_i,1} \\
\beta_{k,2}z_2v_2 + \beta_{k,3} - \lambda_k\beta_{k,2} &= \beta_{q_i,2}z_2 + \beta_{q_i,3} - \lambda_{q_i+1}\beta_{q_i,2} \\
&\vdots \\
\beta_{k,q_i-1}z_{q_i-1} + \beta_{k,q_i} - \lambda_k\beta_{k,q_i-1} &= \beta_{q_i,q_i-1}z_{q_i-1} + \beta_{q_i,q_i} - \lambda_{q_i+1}\beta_{q_i,q_i-1} \\
\beta_{k,q_i}z_{q_i} - \lambda_k\beta_{k,q_i} &= \beta_{q_i,q_i}z_{q_i} - \lambda_{q_i+1}\beta_{k,q_i}
\end{aligned} \tag{B.8}$$

for $k = 1, \cdots, q_i$. Consequently, for any $j, k = 1, \cdots, q_i + 1$ it holds that:

$$\begin{aligned}
\lambda_k - \beta_{k,1} &= \lambda_j - \beta_{j,1} \\
\beta_{k,1}z_1 + \beta_{k,2} - \lambda_k\beta_{k,1} &= \beta_{j,1}z_1 + \beta_{j,2} - \lambda_j\beta_{j,1} \\
\beta_{k,2}z_2v_2 + \beta_{k,3} - \lambda_k\beta_{k,2} &= \beta_{j,2}z_2 + \beta_{j,3} - \lambda_j\beta_{j,2} \\
&\vdots \\
\beta_{k,q_i-1}z_{q_i-1} + \beta_{k,q_i} - \lambda_k\beta_{k,q_i-1} &= \beta_{j,q_i-1}z_{q_i-1} + \beta_{j,q_i} - \lambda_j\beta_{j,q_i-1} \\
\beta_{k,q_i}z_{q_i} - \lambda_k\beta_{k,q_i} &= \beta_{j,q_i}z_{q_i} - \lambda_j\beta_{k,q_i}
\end{aligned} \tag{B.9}$$

The following notation is proposed:

$$\begin{aligned}
x_{11} &= \lambda_j - \beta_{j,1} \\
x_{21} &= -\beta_{j,1}z_1 - \beta_{j,2} + \lambda_j\beta_{j,1} \\
x_{31} &= -\beta_{j,2}z_2 - \beta_{j,3} + \lambda_j\beta_{j,2} \\
&\vdots \\
x_{q_i,1} &= -\beta_{j,q_i-1}z_{q_i-1} - \beta_{j,q_i} + \lambda_j\beta_{j,q_i-1} \\
x_{q_i+1,1} &= -\beta_{j,q_i}z_{q_i} + \lambda_j\beta_{j,q_i}
\end{aligned} \tag{B.10}$$

Now consider the i^{th} column of A_w, cf. (5.93):

$$\begin{aligned}(A-\lambda_1 I)w_1 = Ae_i + Av_1 + Av_2 + \cdots + Av_{q_i} - \lambda_1 e_i - \lambda_1 v_1 - \\ \lambda_1 v_2 - \cdots - \lambda_1 v_{q_i}\end{aligned} \tag{B.11}$$

Incorporating (B.5) into (B.11) and reorganising, the following is obtained:

$$\begin{aligned}(A-\lambda_1 I)w_1 = Ae - (\lambda_1 - \beta_{1,1})e_i + (\beta_{1,1}z_1 + \beta_{1,2} - \lambda_1\beta_{1,1})v_1 + \\ (\beta_{1,2}z_2 + \beta_{1,3} - \lambda_1\beta_{1,2})v_2 + \cdots + (\beta_{1,q_i}z_{q_i} - \lambda_1\beta_{k,q_i})v_{q_i}\end{aligned} \tag{B.12}$$

Incorporating (B.10) into (B.12)

$$(A-\lambda_1^{(i)} I)w_1 = Ae - x_{11}e_i - x_{21}v_1 - x_{31}v_2 - \cdots - x_{q_i+1,1}v_{q_i} \tag{B.13}$$

which is equal to the i^{th} column of $A_e^\star$.

Appendix C

Demonstration of Remark 6.3

From (6.16) it follows that:

$$r(t) = T\mathring{r}(t) = T\Omega M(t) \tag{C.1}$$

where the product term $T\Omega$ can be formulated as:

$$\begin{aligned} T\Omega = &\begin{bmatrix} Cf_1 & Cf_2 & \cdots Cf_r & T_2 \end{bmatrix} \\ &\begin{bmatrix} \alpha_\tau^{(1)} & 0 & \cdots & 0 & \alpha_{\tau-1}^{(1)} & 0 & \cdots & 0 & \alpha_0^{(1)} & 0 & \cdots & 0 \\ 0 & \alpha_\tau^{(2)} & \cdots & 0 & 0 & \alpha_{\tau-1}^{(2)} & \cdots & 0 & 0 & \alpha_0^{(2)} & \cdots & 0 \\ \vdots & \vdots & \ddots & \vdots & \vdots & \vdots & \ddots & \vdots & \vdots & \vdots & \ddots & \vdots \\ 0 & 0 & \cdots & \alpha_\tau^{(k)} & 0 & 0 & \cdots & \alpha_{\tau-1}^{(k)} & 0 & 0 & \cdots & \alpha_0^{(k)} \\ 0 & 0 & \cdots & 0 & 0 & 0 & \cdots & 0 & 0 & 0 & \cdots & 0 \end{bmatrix} \\ = &\begin{bmatrix} Cf_1\alpha_\tau^{(1)} & Cf_2\alpha_\tau^{(2)} & \cdots & Cf_r\alpha_\tau^{(r)} & Cf_1\alpha_{\tau-1}^{(1)} & Cf_2\alpha_{\tau-1}^{(2)} & \cdots & Cf_r\alpha_{\tau-1}^{(r)} \\ & & & & \cdots & Cf_1\alpha_0^{(1)} & Cf_2\alpha_0^{(2)} & \cdots & Cf_r\alpha_0^{(r)} \end{bmatrix} \end{aligned} \tag{C.2}$$

whilst $M(t)$ is expanded as:

$$\begin{aligned} M(t) = \Big[\; & \mu_1(t-\tau) \quad \mu_2(t-\tau) \quad \cdots \quad \mu_k(t-\tau) \quad \mu_1(t-\tau+1) \quad \mu_2(t-\tau+1) \quad \cdots \\ & \mu_k(t-\tau+1) \quad \cdots \quad \mu_1(t) \quad \mu_2(t) \quad \cdots \quad \mu_k(t) \; \Big]^T \end{aligned} \tag{C.3}$$

Recall equation (6.15):

$$r(t) = \sum_{j=0}^{\tau} \sum_{i=1}^{r} \alpha_j^{(i)} Cf_i \mu_i(t-j) \tag{C.4}$$

It follows from (C.1), (C.2), and (C.3) that (C.4) is equivalent to:

$$r(t) = T\Omega M(t) \tag{C.5}$$

Thus:

$$\mathring{r}(t) = \Omega M(t) \tag{C.6}$$